2015

Chlorine Enrichment of Hydrous Minerals in Archean Granulite Facies Ironstone from the Beartooth Mountains, Montana, USA: Implications for High-Grade Metamorphic Fluids

Nicholas Michael Daigle
Louisiana State University and Agricultural and Mechanical College

CHLORINE ENRICHMENT OF HYDROUS MINERALS IN ARCHEAN GRANULITE FACIES IRONSTONES FROM THE BEARTOOTH MOUNTAINS, MONTANA, USA: IMPLICATIONS FOR HIGH-GRADE METAMORPHIC FLUIDS

A Thesis

Submitted to the Graduate Faculty of the
Louisiana State University and
Agricultural and Mechanical College
in partial fulfillment of the
requirements for the degree of
Master of Science

in

The Department of Geology and Geophysics

by
Nicholas M. Daigle
B.S., Louisiana State University, 2013
August 2015

ACKNOWLEDGMENTS

First and foremost I would like to thank my advisor, Dr. Darrell Henry, for his constant guidance and support over the last two years, and also my committee members, Dr. Barbara Dutrow and Dr. Jianwei Wang, for their suggestions and valuable feedback. My fellow classmates are also greatly appreciated for discussions and constructive criticism.

The saintly individuals who aided me in my attempt to keep the microprobe alive and running deserve special recognition: Celina Will, who instructed me on how to run the probe and was always willing to help in any way she could even after leaving LSU; Clayton Loehn, for spending hours of his time away from the SIF to help brainstorm and fix the endless issues with the probe; Rick Young and Wanda Leblanc, for assisting me with maintenance and upkeep for the machines in the probe lab as well as various other tasks I asked of them; and Joe Geller and Chuck Herrington, for being patient and not ignoring the constant barrage of emails I sent them when the probe started acting funny.

Lastly I would like to graciously thank The Red River Desk and Derrick Club, New Orleans Geologic Society, Geologic Society of America, the AAPG LSU student chapter, and the LSU Department of Geology and Geophysics for various monetary support during my research efforts.

TABLE OF CONTENTS

LIST OF TABLES

LIST OF FIGURES

ABSTRACT

The amount of chlorine present in hydrous minerals influences mineral stability and may serve as a monitor of the evolving fluid phase during progressive metamorphism. Chlorine contents of amphibole and biotite vary as a function of temperature, pressure, crystallochemical factors, and fluid composition. The sensitivity of these minerals to serve as a monitor of Cl in aqueous fluids is particularly effective in Fe-rich amphibole and biotite such as those found in iron-formations.

Iron-formations from the eastern Beartooth Mountains, Montana are typified by the dominantly anhydrous mineral assemblages of quartz + magnetite + orthopyroxene + garnet ± clinopyroxene. Thermobarometry suggests equilibration conditions of ~775–800 °C at pressures of ~6–6.5 kbar (granulite facies). These relatively anhydrous iron-formations contain minor amounts of prograde metamorphic amphibole and biotite that occur as inclusions in orthopyroxene and garnet and as matrix minerals. The amphiboles (primarily potassic-hastingsite) and biotites contain high levels of Cl (reaching up to 2.9 wt% and 3.4 wt%, respectively). A positive correlation between Cl and X_{Fe}^{2+}, $Al^{[IV]}$, $K^{[XIII]}$ and $Ba^{[XIII]}$ exists. The biotites also contain up to 10.5 wt% BaO and 6.9 wt% TiO_2. Matrix amphiboles and biotites are more chlorine-rich than amphiboles and biotites present as inclusions in orthopyroxene and garnet in the same sample. Calculated halogen fugacity ratios of $\log(X_F/X_{Cl})$ vs. X_{Mg} in biotite range from -2.7 to -3.9, demonstrating that the metamorphic fluid coexisting with biotite was enriched in Cl.

The variations in chlorine content from pyroxene and garnet inclusions to matrix grains suggest that the fluid evolved to be more chlorine-rich during prograde

metamorphism. These data also provide new evidence for fluid compositions of high-grade brines. High chlorine contents increase the stability field of hydrous minerals and explain their occurrence in granulite facies terranes.

CHAPTER I. INTRODUCTION

Chlorine enrichment of typically hydrous minerals has been observed in a variety of geologic environments, such as skarns, granulites, granofels, volcaniclastics, eclogites and gold-porphyry deposits (e.g. Krutov, 1936; Kamineni et al., 1982; Mora and Valley, 1989; Jiang et al., 1994; Liu et al., 2009; Uher et al., 2014). Two minerals that show this enrichment are amphibole and biotite (Table 1.1). The amount of halogen incorporation in amphibole and biotite is a function of temperature, pressure, fluid composition and crystal chemistry (e.g. Volfinger et al., 1985; Morrison, 1991; Zhu and Sverjensky, 1991, 1992; Manning and Aranovich, 2014). Under high-grade metamorphic conditions, these hydrous minerals tend to either break down to anhydrous minerals (e.g. pyroxene, garnet, feldspar), deprotonate (lose the H in the OH site), and/or incorporate halogens such as F^- and Cl^- into the OH site. Deprotonation and halogen incorporation tends to extend the thermal stability of the nominally "hydrous" minerals (e.g. Volfinger et al., 1985; Morrison, 1991; Makino et al., 1993).

Chlorine-enriched amphibole and biotite are found in iron-rich rocks metamorphosed at granulite facies conditions (Henry, 1988). The iron-rich hydrous silicates found in these rocks have mineral structural features that enhance the incorporation of Cl in the minerals (e.g. Vielzeuf, 1982; Volfinger et al., 1985, Henry, 1988). Of further significance is that Cl is generally partitioned preferentially into aqueous fluids relative to coexisting solid phases (e.g. Yardley, 1985; Mora and Valley, 1989; Zhu and Sverjensky, 1991, 1992; Léger et al., 1996). Partitioning studies between fluids and minerals allow for Cl contents in amphibole and biotite to serve as particularly sensitive indicators of fluid-rock interactions in the Earth's crust.

Table 1.1. Some recorded occurrences of Cl-rich amphibole and biotite in various high-grade metamorphic terranes

Locality	Setting/Rock Type	Am	Bt	Range of Cl	Reference
Transcaucasia, Russia	Skarn	x		Up to 7.24 wt%	Krutov (1936)
Transcaucasia, Russia	Skarn	x		Up to 5.34 wt%	Jacobsen (1975)
St. Pauls Rocks, equatorial Atlantic	Ultrabasic intrusion	x		Up to 6.51 wt%	Jacobsen (1975)
Southern Yukon	Sphalerite skarn	x		1.15 – 3.09 wt%	Dick and Robinson (1979)
Rajastan, NW India	Calcareous meta-sediment	x		Up to 3.6 wt%	Sharma (1981)
Visakpatnam, India	Hypersthene-garnet granulite	x	x	Am: up to 4.18 wt% Bt: up to 2.07 wt%	Kamineni et al. (1982)
Mathematician Ridge, East Pacific Ocean	Oceanic metabasic rocks	x		Up to 4.0 wt%	Vanko (1986)
West Ongul Island, East Antarctica	Amphibolite and carbonate-pegmatite	x		Up to 3.27 wt%	Suwa et al. (1987); Makino et al. (1993)
Sesia-Lanzo, Italy	Marbles	x		Up to 4.21 wt%	Castelli (1988)
Idaho, USA	Carbonate-bearing granofels		x	0.05 – 0.51 wt%	Mora and Valley (1989)
Adirondack Mountains, USA	Marcy anorthosite massif	x		0.05 – 3.0 wt%	Morrison (1991)
Sterling Hill, New Jersey, USA	Skarn in association with Zn-ore		x	0.89 to 7.15 wt%	Tracy (1991)
Salton Sea, California, USA	Metabasic rocks	x		Up to 2.7 wt%	Enami et al. (1992)
Skaergaard intrusion, Greenland	Anorthosites and pegmatites		x	0.15 – 2.02 wt%	Sonnenthal (1992)
Quinling, China	Pb-Zn deposit, volcanoclastic rocks	x	x	Am: 3.55 – 4.37 wt% Bt: 0.3 – 1.2 wt%	Jiang et al. (1994, 1996)

(Table 1.1 continued)

Locality	Setting/Rock Type	Am	Bt	Range of Cl	Reference
Lofoten, Norway	Ductile shear zones in gabbro	x	x	Am: 0.59 – 3.78 wt% Bt: 0.10 – 1.49 wt%	Kullerud (1995, 1996)
Black Rock Forest, New York, USA	Amphibolite to granulite facies gneisses	x	x	Am: up to 5.1 wt% Bt: 1.02 – 4.64 wt%	Léger et al. (1996)
Ramnes Cauldron, Norway	Hydrothermally altered porphyritic alkali granitic rocks	x		0.01 – 2.96 wt%	Sato et al. (1997)
Dronning Maud Land, East Antarctica	Syenites and high-grade marbles	x	x	Am: up to 0.36 apfu Bt: 0 – 0.56 wt%	Markl and Piazolo (1998)
Sudbury, Ontario, Canada	Contact Ni-Cu ore deposits	x		<0.5 – 4.0 wt%	McCormick and McDonald (1999)
North Dabie Shan, China	Felsic granulites	x		0.0 – 4.2 wt%	Xiao et al. (2005)
Tarfala Valley, Northern Swedish Caledonides	Ductile shear zones of the Kebne Dyke Complex	x		0.4 – 0.76 wt%	Baird et al. (2006)
Sulu ultrahigh-pressure metamorphic terrane, Yangkou, China	Eclogites	x		0.05 – 3.0 wt%	Liu et al. (2009)
Northern Central Indian Ridge, Indian Ocean	Mylonitic and altered gabbros	x		0.0 – 0.62 wt%	Ray et al. (2009)
Eastern Dharwar Craton (EDC), Southern India	Crystalline basement rocks below the Deccan trap basalts	x	x	Am: 0.72 – 0.85 wt% Bt: 0.09 – 0.14 wt%	Pandey et al. (2014)
Slovakia	Biely Vrch Au-porphyry deposit	x	x	Am: up to 5 wt% Bt: 0.6–7.45 wt%	Uher et al. (2014)

* Rows colored in green represent the highest recorded chlorine concentrations in amphibole (am) and biotite (bt).

The term ironstone, or iron-formation, is defined as: “a chemical sediment, typically thin bedded or laminated, whose principal chemical characteristic is an anomalously high content of iron (over 15 wt%), commonly but not necessarily containing layers of chert” (e.g. James, 1954; Trendall, 1983; Klein, 2005). The terms ironstone and iron-formation are frequently used interchangeably; however, ironstone typically refers to iron-rich rocks from Phanerozoic time (0.54 Ga to present), and iron-formation encompasses the time span preceding the Phanerozoic. Therefore, the Archean iron-rich rocks examined in this study will be referred to as iron-formation in the remainder of this document. Iron-formations are considered unusual chemical sediments because of their high contents of total Fe and SiO_2. Iron-formations tend to be found in Precambrian terranes over a wide time span (Figure 1.1). They first appear in the rock record at ~3.8 Ga in Archean cratons (e.g. Isua, West Greenland) with their overall volume reaching a maximum at ~2.5 Ga (iron-formations in the Hamersley Basin of Western Australia; Klein, 2005). Around 1.8 Ga the iron-formations disappear from the geologic record for roughly one billion years before briefly reemerging between 0.8–0.6 Ga (Klein, 2005). Although large amounts of dissolved iron were present in the deep oceans of the Archean (likely due to hydrothermal input), the environment was too anoxic for iron-oxides (e.g. magnetite) to readily precipitate from seawater. Large amounts of oxygen in the ocean began appearing at ~2.5 Ga (around the time of the Great Oxidation Event), resulting in large quantities of iron-oxide precipitation, causing greater numbers of banded iron-formations (BIF) to be produced in the Proterozoic as compared to the Archean (Klein, 2005).

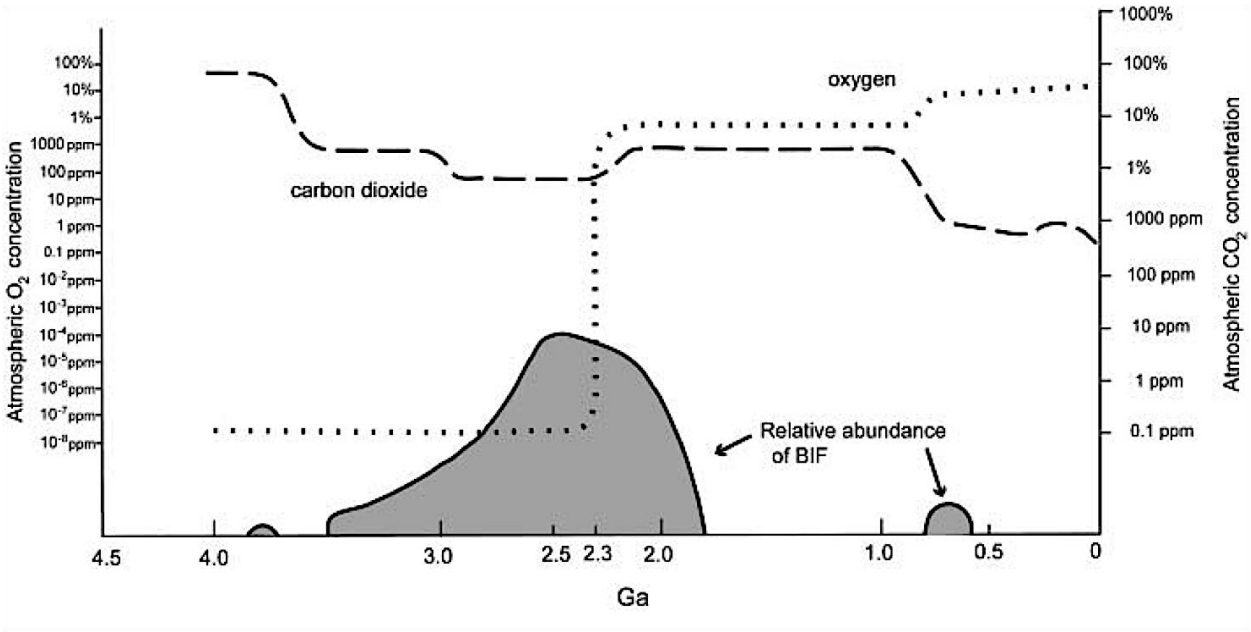

Figure 1.1. Relative abundance of Precambrian BIFs vs. time, with calculated curves for the atmospheric evolution for oxygen and carbon dioxide (Klein, 2005). Abundance of iron-formation is relative to a maximum (at ~2.5 Ga) represented by the total iron-formation volume of the Hamersley Range of Western Australia.

Because of the general association of Cl-enrichment with Fe-rich minerals (Volfinger et al., 1985), a useful petrologic environment to examine enhanced chlorine content in minerals is in high-grade iron-formations such as those found in the Beartooth Mountains of Montana and Wyoming. These lithologies are also useful because iron-formations tend to develop Fe-rich anhydrous assemblages at lower temperatures than the more magnesian minerals. For crystallochemical reasons they contain enhanced chlorine contents in minerals, which can be used as a probe into any aqueous metamorphic fluid. Although studies have been done on Cl-rich amphibole and biotite found in various other lithologies and geologic environments (Table 1.1), the literature is relatively limited in examples of Cl-rich hydrous silicate minerals occurring in high-grade Archean meta-iron-formations (e.g. Henry, 1988).

The purpose of this study is to examine the assemblage and mineral chemistry of the chlorine-rich minerals as well as their coexisting minerals in the iron-formations, to investigate the chemical relationship between the incorporation of Cl^- and other ions, to determine the pressure and temperature conditions of metamorphism using geothermobarometry and phase equilibrium calculations, and to establish the utility of chlorine-rich hydrous silicates to monitor the evolution of the fluid phase during high-grade metamorphism.

CHAPTER II. GEOLOGIC SETTING

2.1 Wyoming Province

Samples used in this study are collected from the Beartooth Mountains, located in the northwestern part of the Wyoming Province (Figure 2.1). The Wyoming Province is a ~500,000 km^2 area encompassing the majority of Wyoming as well as portions of adjacent states (Figure 2.1; e.g. Mueller and Frost, 2006). The Wyoming Province is bounded on three sides by Proterozoic collisional orogens: the Great Falls Tectonic Zone (GFTZ) to the north, Dakota segment of the Trans-Hudson Orogen to the east, and Cheyenne Belt to the south. To the west of the Wyoming Province are various Proterozoic and Archean terranes, which probably extend to the rifted Neoproterozoic margin, now marked by the $^{87}Sr/^{86}Sr = 0.706$ line (Figure 2.1; Mueller and Frost, 2006). This line represents a separation of older cratonic rocks of Laurentia in the east from younger accreted terranes (e.g. flood basalts and volcanics) to the west (e.g. Armstrong et al., 1977). Recent studies by Mueller and Wooden (2012) and Mueller et al. (2014) on Lu-Hf isotopic compositions for 3.3-4.0 Ga detrital zircons in quartzites from the Wyoming Province show decreasing minimum εHf values between 4.0 to ~3.6-3.5 Ga and then a steady increase in minimum εHf values between ~3.6-3.5 to 3.3 Ga suggesting that 4.0 to ~3.6 Ga reflects a more primitive (undepleted) source of material for crustal growth. The sudden change to increasing εHf values from ~3.6 to 3.3 Ga is representative of crustal growth forming from a more juvenile (depleted) source (Mueller and Wooden, 2012; Mueller et al., 2014).

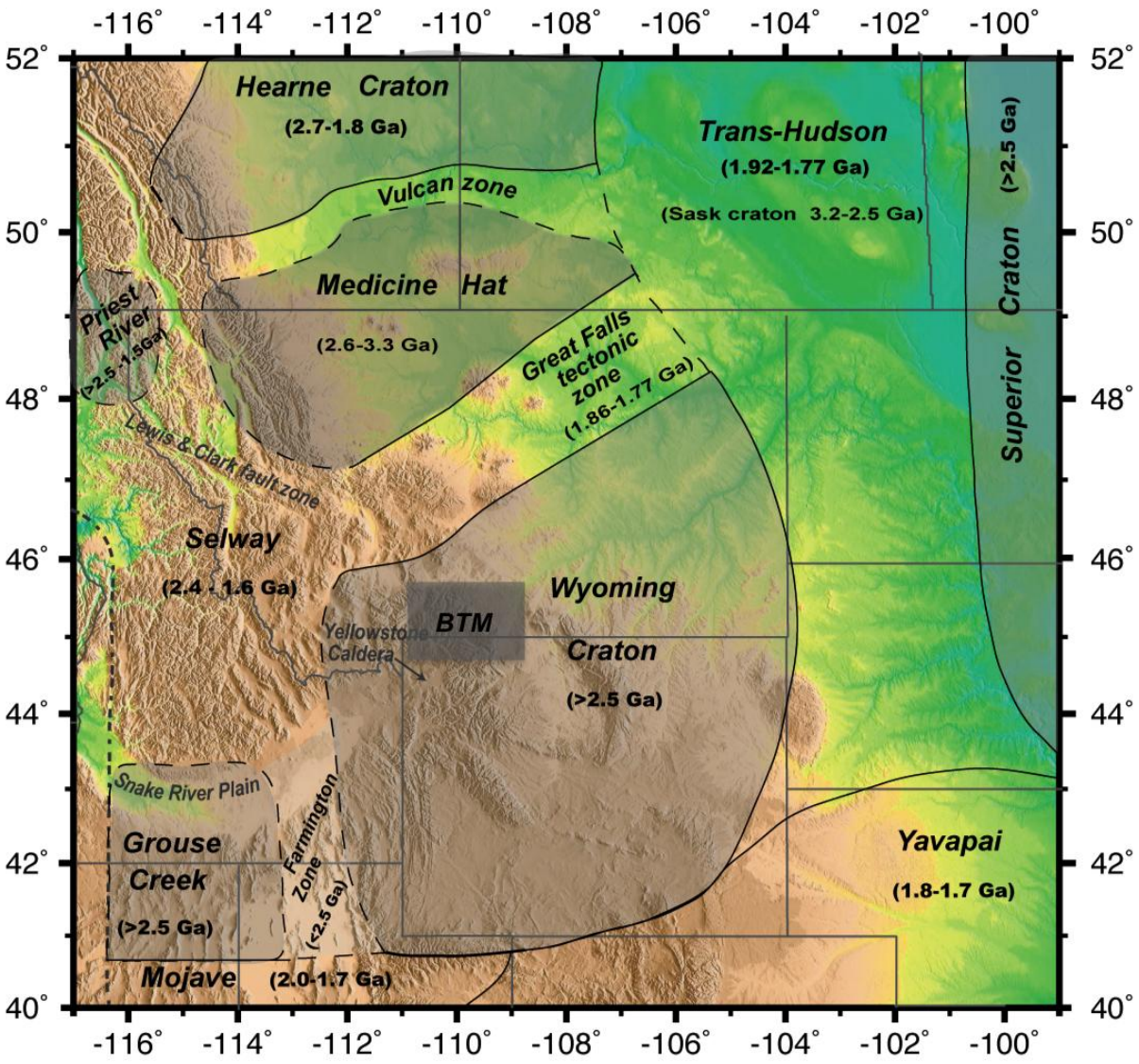

Figure 2.1. Schematic map of Archean and Proterozoic basement terranes of southwest Laurentia (modified from Foster et al., 2006). BTM = Beartooth Mountains, located in the gray box.

The Wyoming Province can be subdivided into three sub-provinces: the Montana Metasedimentary Terrane (MMT), also called the Montana Metasedimentary Province (MMP); the Beartooth-Bighorn Magmatic Zone (BBMZ); and the Southern Accreted Terranes (SAT), otherwise known as the Wyoming Greenstone Province (WGP) (Figure 2.2; e.g. Mueller and Frost, 2006; Mueller et al., 2014). The Montana Metasedimentary

Terrane includes various Neoarchean (2.5–2.8 Ga) metasedimentary lithologies, such as quartzites, pelites and carbonates that have been incorporated within the older Archean (3.2–3.5 Ga) quartzofeldspathic gneisses (e.g. Mueller et al., 1993, 1996, 2004; Krogh et al., 2011; Mueller et al., 2014). The Beartooth-Bighorn Magmatic Zone is primarily composed of Mesoarchean (~2.8–3.0 Ga) metaplutonic rocks of the trondhjemite-tonalite-granodiorite (TTG) association, but also contain enclaves of older lithologies dating as far back as 3.5 Ga (e.g. Mueller et al., 2014). Some of the quartzite

Figure 2.2. Outlines of the major exposures of Archean crystalline basement and generalized approximate sub-province boundaries in the Wyoming Province: Montana Metasedimentary Terrane, Beartooth-Bighorn magmatic zone, and the Wyoming Greenstone Province. The colored blocks represent basement rocks uplifted during the Laramide orogeny (after Mueller et al., 2014).

within the TTG rocks contains detrital zircons dating to 4.0 Ga indicating the presence of early crustal growth (e.g. Mueller et al., 2014). The Mesoarchean TTG gneisses that dominate the BBMZ represent the most voluminous rocks formed during the Hadean-Archean in the northern Wyoming Province (Mueller et al., 2014) although smaller volumes of high-K granodiorites and granites are also present at this time (e.g. Wooden et al., 1988; Frost and Fanning, 2006; Mueller and Frost, 2006). The Southern Accreted Terranes is a mixture of various lithologies (e.g. metavolcanic rocks, metagraywacke, pelitic schist, quartzite, iron-formation) that merged with the southern boundary of the Wyoming Province by ~2.63 Ga (Mueller and Frost, 2006; Mueller et al., 2008).

Numerous exposures of Precambrian rocks throughout the Wyoming Province resulted from the Laramide Orogeny in the Paleocene (66-57 Ma) (e.g. Henry and Mogk, 2003; Mueller et al., 2008). Areas of uplifted Archean basement rocks from the MMT include the North and South Madison Ranges, Ruby Range and the Tobacco Root Mountains. In the BBMZ, Precambrian exposures are found in the Beartooth Mountains, Bighorn Mountains, Granite Mountains, Owl Creek Mountains, Wind River Mountains and the Teton Range. In the SAT, only the northern-most exposures of the Laramie Range, Sierra Madre and Medicine Bow Mountains are Archean in age; exposures in southern region are made of up younger Proterozoic rocks (e.g. Mueller and Frost, 2006; Will, 2013).

2.2 Beartooth Mountains

The Beartooth Mountains are located in south-central Montana and northwestern Wyoming (Figure 2.2). These mountains are part of the northernmost portion of the

Beartooth-Bighorn Magmatic Zone and are dominated by the Late Archean (~2.8 Ga) gneissic and migmatitic rocks of the TTG suite together with a range of older metasupracrustal (meta-igneous and metasedimentary) rocks (e.g. Mueller et al., 2014). The Beartooth Mountains are typically divided into four geographically and geologically distinct domains: the Stillwater Block, the North Snowy Block, the South Snowy Block, and the Beartooth Plateau Block, which is sometimes referred to as the Main Beartooth Massif (Figure 2.3; e.g. Mueller et al., 2014).

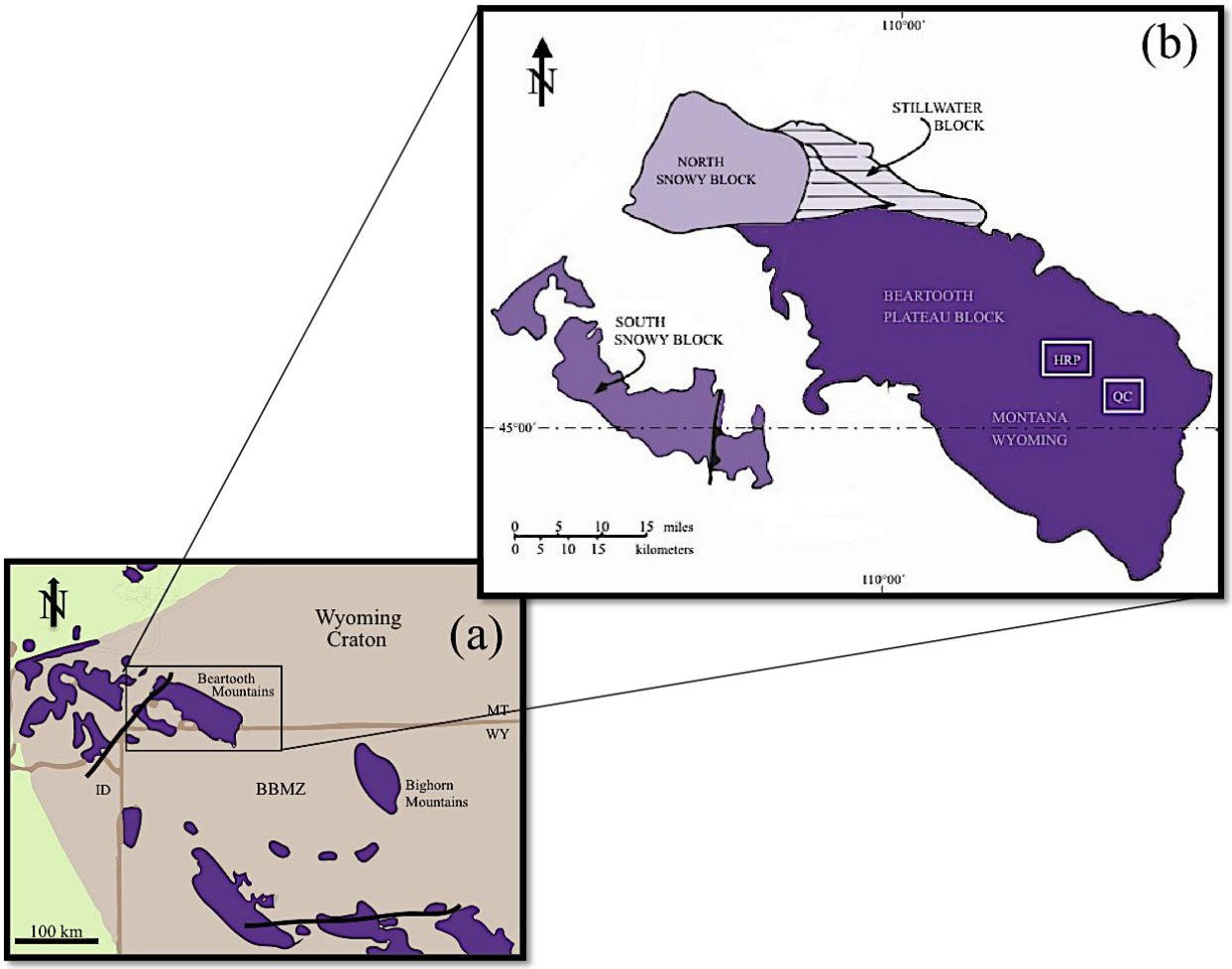

Figure 2.3. (a) The Wyoming Province and its sub-provinces, including the location of the Beartooth Mountains (adapted from Foster et al., 2006); (b) The four geographically and geologically distinct domains of the Beartooth Mountains (adapted from Mueller et al., 2014). BBMZ = Beartooth-Bighorn Magmatic Zone, HRP = Hellroaring Plateau, and QC = Quad Creek.

The Stillwater Block is dominated by the mafic igneous layered Stillwater complex (2.7 Ga) and its contact aureole in older metasediments (e.g. Henry and Mogk, 2003). The North Snowy Block, originally thought to have undergone numerous metamorphic events, was later determined to be comprised of an assortment of lithologic units that were formed elsewhere and tectonically assembled together (e.g. Reid et al., 1975; Wooden et al., 1988; Henry and Mogk, 2003). The South Snowy Block comprises most of the southwestern part of the Beartooth Mountains. This area contains numerous exposures of Late Archean granitic plutonic rocks that were intruded into a thick sequence of metasedimentary rocks (e.g. pelitic schists, quartzites and banded iron formation) known as the Jardine Metasedimentary Sequence (JMS; e.g. Mueller et al., 2014).

The Beartooth Plateau Block is the eastern-most subdivision of the Beartooth Mountains and comprises the majority of the mountain range (Figure 2.3). The samples used in this study are from the Quad Creek (QC), Hellroaring Plateau (HRP) and Rock Creek (RC) localities in the eastern portion of the Beartooth Plateau Block. The area is lithologically dominated by the TTG rocks that characterize the BBMZ, but also contains other meta-igneous and metasedimentary lithologies of varying compositions and metamorphic grade (e.g. Henry and Mogk, 2003; Mueller et al., 2008, 2010). The TTG suite rocks in the eastern Beartooth Plateau Block are typified by an intrusive body called the Long Lake magmatic complex (LLMC). The intrusion of the LLMC occurred over a brief time span (2.79-2.83 Ga), and incorporated older (~3.5 Ga) high-grade rocks into the LLMC lithologies as both xenoliths and tectonically interleaved units. These older xenolithic lithologies in the Beartooth Plateau Block consist of

metabasites, peraluminous gneisses (migmatites), meta-iron-formations, meta-ultramafic rocks, pelitic to psammatic schists, and quartzites, in addition to metaplutonic quartzofeldspathic gneisses (e.g. Henry et al., 1982; Maier et al., 2012; Mueller et al., 2014).

The tectonic setting of the Beartooth Mountains began ~4.0 Ga as a plume-dominated area and later developed into a region of subduction-driven crustal growth at ~3.5–3.4 Ga, which eventually resulted in a tectonic mixing of supracrustal and meta-igneous lithologies along high-grade ductile shear zones (e.g. Mueller et al., 2014). This mixing event led to prograde metamorphism that reached granulite facies conditions of ~775-850 °C and ~6-8 kbar (Figure 2.4; e.g. Mueller et al., 2014). Late Archean intrusions of subsolvus granites and granodiorites associated with the LLMC resulted in an amphibolite-facies overprint of the original granulite facies conditions. This overprint is most easily distinguished by the presence of pyroxene being partially and/or completely replaced by secondary amphibole phases. In some lithologies a second episode of granulite facies metamorphism can be seen locally overprinting the amphibolite facies metamorphic event (e.g. Henry and Mogk, 2003; Mueller et al., 2014).

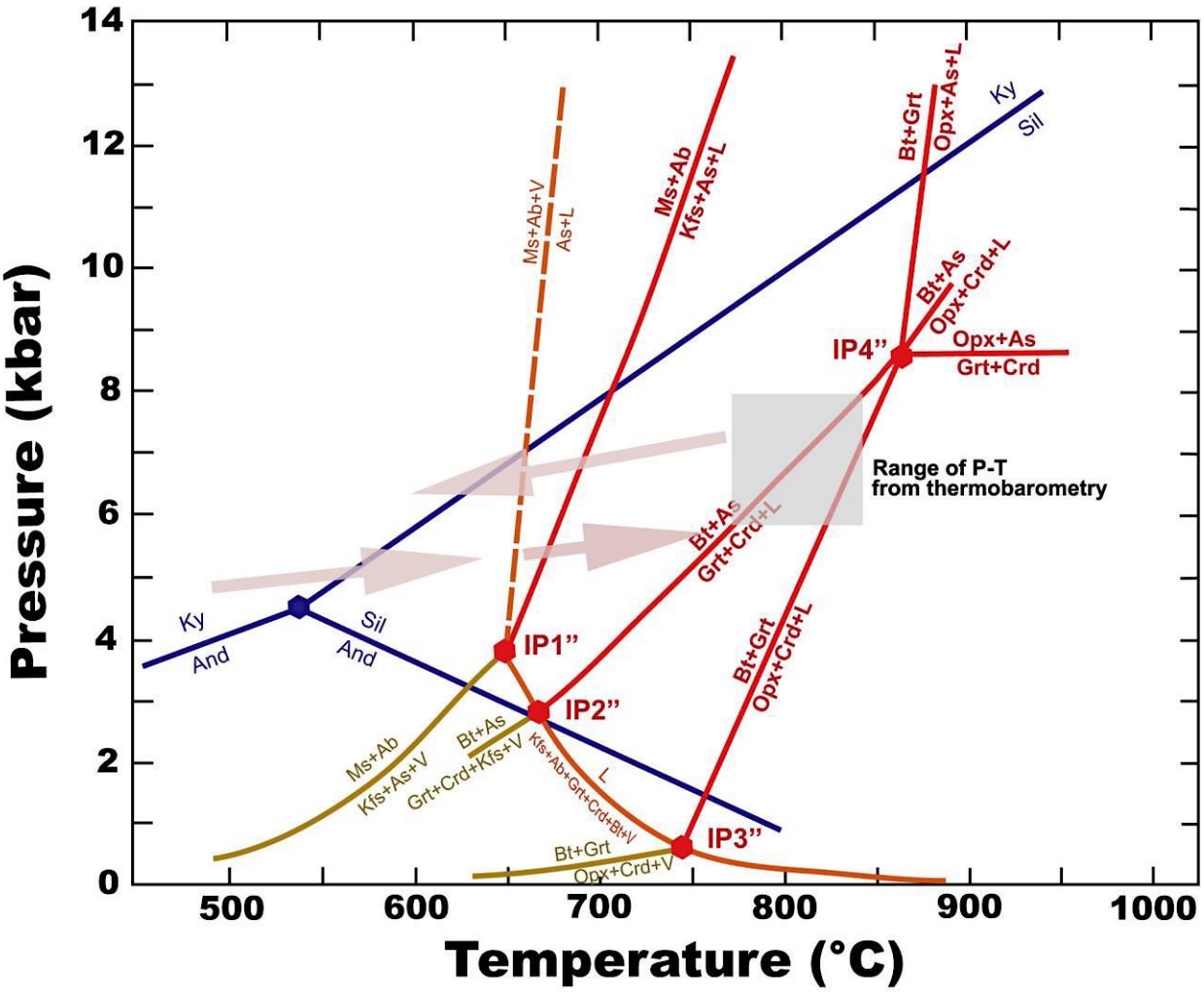

Figure 2.4. Petrogenetic grid adapted from Spear et al. (1999) showing dehydration reactions (gold), H_2O-saturated melting reactions (orange), dehydration-melting reactions (red), and aluminosilicate polymorph boundaries (blue) in pressure-temperature space. The gray-pink arrows suggest the approximate pressure-temperature path experienced by the metamorphic rocks in this area. The gray box indicates the results and standard deviation of the classic geothermobarometry for peak metamorphic conditions (Mueller et al., 2014).

CHAPTER III. METHODS

3.1 Sample Collection and Preparation

Twenty-six meta-iron-formation samples from the eastern portion of the Beartooth Plateau Block are investigated in this study. The majority of these samples were collected by Dr. Darrell Henry between 1981 and 2002. Nineteen of the iron-formations were collected from the Quad Creek area, six from Hellroaring Plateau, and one from Rock Creek.

Samples were labeled with an abbreviation of the locality (e.g. ‘QC’ for Quad Creek; ‘HR’ or ‘HP’ for Hellroaring Plateau; ‘RC’ for Rock Creek) followed by ‘81,’ ‘82’ or ‘02’ to represent the year the sample was collected, and a dash followed by the chronological number of the collected sample in that particular locale. The latitude and longitude for all samples were recorded in the field or later established with Google Earth using the locations established on topographic maps. A Google Earth map with general locations of all samples is shown in Figure 3.1.

3.2 Petrographic and Microanalytical Methods

3.2.1 Petrographic Analysis

Rock chips from each sample were cut using a diamond-embedded rock saw. Billets were made into polished thin sections that are approximately 30 micrometers thick. Petrographic analyses of the thin sections were completed in plane-polarized light (PPL), cross-polarized light (XPL) and reflected light using Olympus BH-2 and Olympus BX50 petrographic microscopes to gather information on minerals, modes and associations, textural features, and alterations. The petrography was used to establish the optimal grains to analyze for mineral chemistry using the electron microprobe.

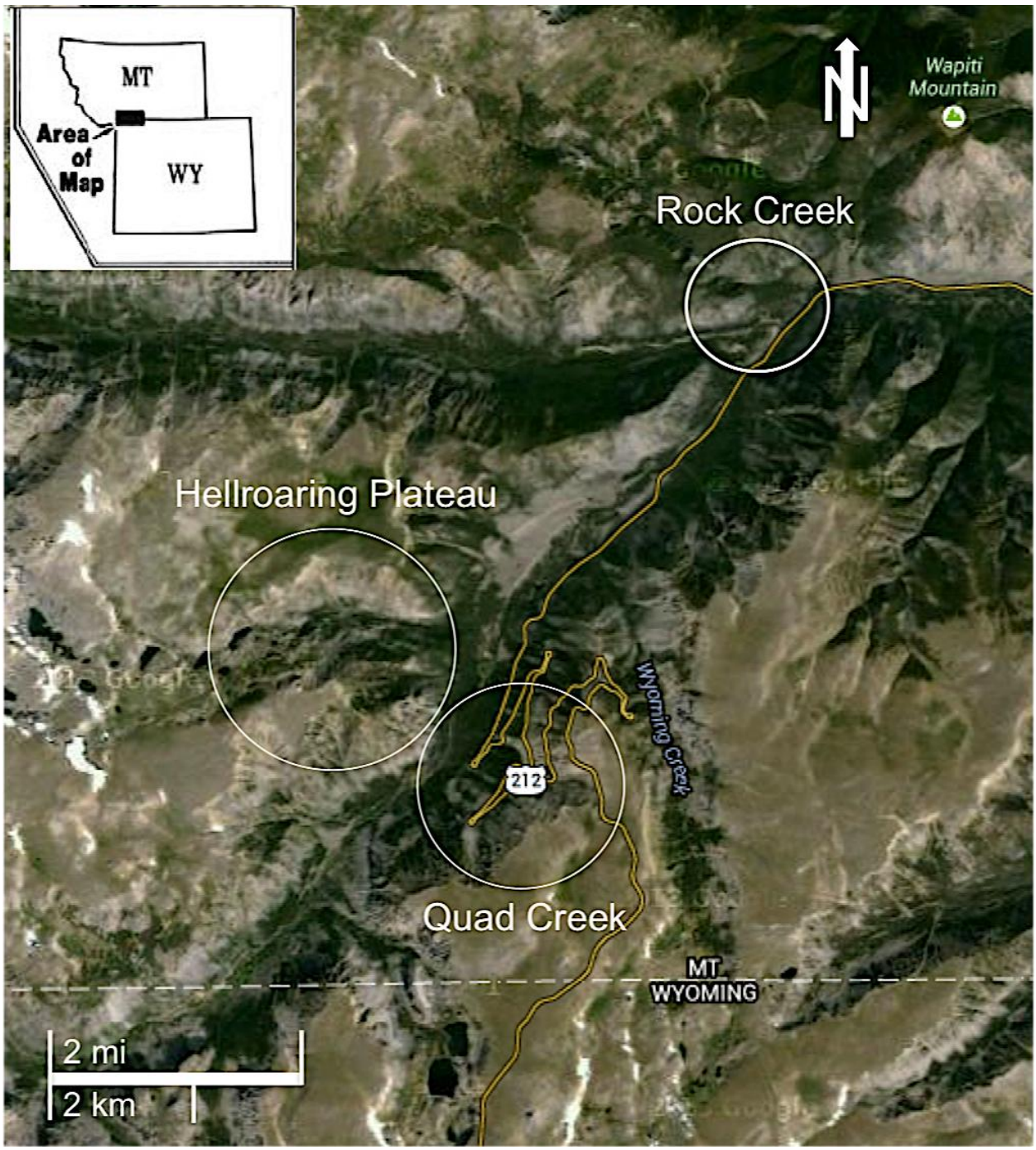

Figure 3.1. Google Earth image showing the three areas from which the iron-formations were collected. MT-WY state line is shown for reference. Yellow line indicates the Beartooth Highway (Highway 212).

Commonly observed minerals (and their abbreviations) in these samples are given in Table 3.1. Whole thin section scans were acquired using a HP Scan Jet G4010 and used as an additional [larger] base map reference for electron microprobe analyses. Thin section photomicrographs were taken at 4-, 10-, 20- and 40-times magnifications using a Nikon Coolpix 995 digital camera.

Table 3.1. List of minerals and their abbreviations (from Whitney and Evans, 2010)

Act	Actinolite	Cum	Cummingtonite	Opx	Orthopyroxene
Amp	Amphibole	Grt	Garnet	Pl	Plagioclase
Ank	Ankerite	Gru	Grunerite	Py	Pyrite
Ap	Apatite	Hst	Hastingsite	Qz	Quartz
Bt	Biotite	Hem	Hematite	Sd	Siderite
Chl	Chlorite	Hbl	Hornblende	Tur	Tourmaline
Cam	Clinoamphibole	Ilm	Ilmenite	Zrn	Zircon
Cpx	Clinopyroxene	Mag	Magnetite		

Backscattered electron (BSE) images were taken using the JEOL 733 electron microprobe (EPMA) at Louisiana State University (LSU). The images were taken under high vacuum conditions of 10^{-7} torr, at an accelerating potential of 15 kV, using a 10–11 nA beam current. The BSE image gray levels are a function of the mean atomic weight of the minerals such that minerals with lower mean atomic weights (e.g. quartz) appear darker than minerals with a higher mean atomic weight (e.g. magnetite). These images

aid in mineral identification and can provide additional information regarding textures (e.g. pyroxene exsolution) and chemical zoning.

Modal amounts of minerals in thin section were determined for many of the iron-formation samples using three different techniques: visual estimates, point counting, and the image analysis software, ImageJ® (Schneider et al., 2012). Visual estimations were done by scanning the samples using a simple petrographic microscope. For point counting, 1000 points were counted across entire thin sections. Point counts were done on two samples (QC-IS and HR02-3) to cross-check the validity of the ImageJ® software and to compare the determined modal amounts with the other two techniques. The ImageJ® software allows a user to assign gray-scale values from BSE images to specific mineral phases. When analyzing non-banded samples with ImageJ, BSE images from three representative areas were averaged together to get the best representative modes for each sample. In banded samples, BSE images from 2-3 representative areas were averaged from both the silicate/oxide-rich bands and the quartz-rich bands. The different bands were treated as separate rock systems and averages from each type of band were calculated to generate the best modal estimates of each mineral in both types of band. For sample HR02-71, modes were determined separately for the amphibole band and for the remainder of the rock. Alteration amphibole was counted as orthopyroxene for all three techniques.

Visually estimating modal amounts of minerals is the least accurate method of determination of modes. The point counting and ImageJ approach are relatively accurate, but also both have room for error. The accuracy of mineral modes determined by point counts is function of the petrographer's ability to adequately distinguish mineral

phases from one another. Thus, a more experienced petrographer may generate different modal amounts than someone less experienced. With ImageJ, the modal amounts may be slightly skewed if certain mineral phases have a similar mean atomic weight, causing the shades of gray to slightly overlap. However, this software makes it easier to distinguish minerals by gray levels if they appear similar under the petrographic microscope. For this reason, the image analysis software is the easier and quicker approach to gathering modal amounts. In this study, BSE images were analyzed in ImageJ® while simultaneously being viewed under a petrographic microscope to help with distinguishing minerals in the case of overlapping gray levels.

3.2.2 Mineral Chemical Analysis

Amphibole, biotite, pyroxene, garnet and plagioclase were quantitatively analyzed by wavelength-dispersive spectrometry (WDS) using the electron probe micro-analyzer (EPMA) at LSU. The WDS analyses were done using a 2 μm electron-beam diameter at high vacuum conditions of 10^{-7} torr, with an accelerating potential of 15 kV, and using a 10–11 nA beam current. For each type of mineral, ~4-6 grains were analyzed in each thin section, with ~2-4 analysis points on each grain. A set of well-characterized natural mineral standards were used as standards and routinely analyzed as unknowns to check for instrument drift (standards are listed in Table 3.2). The empirical method of Bence-Albee (1968) was used for matrix corrections. In addition, correction factors were applied to weight percent oxide data if instrument drift was substantial. This was done by averaging values from each element from the standards that were analyzed as ‘unknowns’ and subtracting those averages from the known values of the elements in the standard. If this difference was larger than two relative

Table 3.2. Mineral standards used for electron microprobe analyses						
Element	Crystal	Feldspar	Garnet	Pyroxene	Amphibole	Biotite
Si	TAP	Toronto albite	Toronto almandine	Johnstown hypersthene	Kakanui hornblende	Kakanui hornblende
Ti	PET	----------	Kakanui hornblende	Kakanui hornblende	Kakanui hornblende	Kakanui hornblende
Al	TAP	Lake County plagioclase	Toronto almandine	Johnstown hypersthene	Kakanui hornblende	Kakanui hornblende
Cr	LIF	----------	Smithsonian chromite	Smithsonian chromite	Smithsonian chromite	Smithsonian chromite
Fe	LIF	Kakanui hornblende	Toronto almandine	Johnstown hypersthene	Kakanui hornblende	Kakanui hornblende
Mn	LIF	----------	Toronto rhodonite	Toronto rhodonite	Toronto rhodonite	Toronto rhodonite
Mg	TAP	Kakanui hornblende	Kakanui pyrope	Johnstown hypersthene	Kakanui hornblende	Kakanui hornblende
Ca	PET	Lake County plagioclase	Grossular 55	Kakanui hornblende	Kakanui hornblende	Kakanui hornblende
Ba	PET	Toronto sanidine	----------	----------	Toronto sanidine	Toronto sanidine
Na	TAP	Toronto albite	----------	Kakanui hornblende	Kakanui hornblende	Kakanui hornblende
K	PET	Toronto sanidine	----------	Kakanui hornblende	Kakanui hornblende	Toronto biotite
F	TAP	----------	----------	Smithsonian fluorapatite	Smithsonian fluorapatite	Smithsonian fluorapatite
Cl	PET	----------	----------	----------	Toronto tugtupite	----------

weight percent, a correction factor [of standard element value/average of 'unknown'] was applied to the data points analyzed in a given sample. Data gathered from EPMA analyses was supplemented by chemical data previously collected by Dr. Darrell Henry (personal communication).

Weight percent oxide analyses from the EPMA were normalized to atoms per formula unit (apfu) based on specified numbers of oxygens or cations. Pyroxene, garnet, feldspar and biotite data were normalized and classified using Excel spreadsheets created by Darrell Henry (personal communication). The amphibole spreadsheet was initially created by Locock (2013) and later modified by Darrell Henry. Pyroxene analyses were normalized on the basis of 6 oxygen atoms, garnet on the basis of 12 oxygen atoms, and feldspar on the basis of 8 oxygen atoms. Biotite was normalized on the basis of 22 oxygens, with the amount of OH calculated to make (OH + F + Cl) = 4. All iron present in the chemical analyses was initially assumed to be FeO (Fe^{2+}); however, these spreadsheets calculate the amount of Fe^{3+} based on charge balance and stoichiometry assuming no vacancies.

Amphibole analyses were normalized and classified on the basis of cation sums using the following [potential] cations: Si, P, Ti, Zr, Al, Sc, V^{3+}, Cr, Mn^{2+}, Mn^{3+}, Fe^{2+}, Fe^{3+}, Co, Ni, Zn, Be, Mg, Ca, Sr, Li, Na, Pb, K. From this list of cations, one or more of the following normalization schemes is used: (1) Sum of cations from Si to Ca, plus Li = 15; (2) Sum of cations from Si to Mg, plus Li = 13; (3) Sum of cations from Si to Na = 15; (4) Sum of cations from Si to K = 16 (Locock, 2013). To account for the more Ba-rich minerals, Darrell Henry modified this spreadsheet using Ba in place of Pb. The amphibole spreadsheet can also be set up to calculate values for Fe^{3+} and OH

assuming no vacancy. Typically, valence states of Fe are not differentiated by EPMA analyses and all iron is assumed to be FeO. The Locock spreadsheet calculates a Fe^{3+} value using the $Fe^{3+}/\Sigma Fe$ ratio (adjusted for charge balance) and the normalized amphibole formula based on the cations sums chosen from the classification schemes mentioned previously. Due to elevated Ti concentrations in some amphibole analyses, the OH calculations are estimated on the basis of Ti content with the assumption that (OH, F, Cl) = 2-2Ti apfu.

3.3 Determination of Pressure-Temperature-Fluid Conditions

To determine the pressure, temperature and fluid conditions during a rock's metamorphic history a variety of thermobarometers, phase equilibrium diagrams and fluid model calculations were done. Each of these approaches is discussed subsequently.

3.3.1 Thermobarometers

Mineral chemical data acquired from the EPMA was used to calculate P-T metamorphic conditions of selected iron-formations using a variety of robust geothermobarometers including a hornblende-plagioclase [net transfer] thermometer (Holland and Blundy, 1994), an orthopyroxene-garnet [Fe-Mg exchange] thermometer (Sen and Bhattacharya, 1984) and a garnet-clinopyroxene [Fe-Mg exchange] thermometer. The temperatures were calculated using assumed pressures of 5.0, 6.0, 6.5 and 7.0 kbar consistent with earlier estimates of peak metamorphic pressures experienced by rocks in the study area (e.g. Henry, 1988; Mueller et al., 2014). One geobarometer (the garnet-amphibole- plagioclase-quartz barometer) was used to gather pressure conditions (e.g. Kohn and Spear, 1990).

The formulation of the hornblende-plagioclase thermometer of Holland and Blundy (1994) includes two separate thermometric expressions based on net-transfer reactions involving components of amphibole and plagioclase. The two geothermometers, known as ‘HB1’ and ‘HB2,’ refer to the following thermometry calibration reactions:

$NaCa_2Mg_5Si_7AlO_{22}(OH)_2 + 4SiO_2 = Ca_2Mg_5Si_8O_{22}(OH)_2 + NaAlSi_3O_8$ (HB1)

Edenite + 4 Quartz = Tremolite + Albite

$NaCa_2Mg_5Si_7AlO_{22}(OH)_2 + 2NaAlSi_3O_8 = Na(CaNa)Mg_5Si_8O_{22}(OH)_2 + CaAl_2Si_2O_8$ (HB2)

Edenite + 2 Albite = Richterite + Anorthite

Both HB1 and HB2 can be used for silica-saturated mineral assemblages, but only HB2 (the quartz-free calibration) can be used on rocks without SiO_2. Although both of these hornblende-plagioclase thermometers perform well (with uncertainties of ±40°C) for equilibrium conditions of 400-1000°C and 1-15 kbar over a broad range of bulk compositions (Holland and Blundy, 1994), temperatures calculated using the HB2 calibration are preferred because HB2 can be used for both silica-saturated and silica-undersaturated rocks. An accompanying Excel spreadsheet was created by Anderson et al. (2008) and later modified by Darrell Henry (personal communication) to calculate peak metamorphic temperature based on weight percent oxide, plagioclase mole fraction, and arbitrary pressure values input by the user.

The orthopyroxene-garnet thermometer (Sen and Bhattacharya, 1984) is an Mg-Fe^{2+} exchange thermometer. This geothermometer is formulated for varying lithologies

that have been metamorphosed at granulite facies conditions and has an uncertainty of ±60°C (Sen and Bhattacharya, 1984).

The garnet-clinopyroxene thermometer formulated by Nakamura (2009) is also an Mg-Fe^{2+} exchange thermometer. This thermometer was formulated using 333 garnet-clinopyroxene pairs from published experimental data (experiments done between 800 and 1820°C). The temperatures calculated for the experimental grt-cpx pairs using Nakamura's thermometer gave comparable results to the experimental data, with an uncertainty of ±74°C.

The garnet-amphibole-plagioclase-quartz geobarometer (Kohn and Spear, 1990) can be applied to a wide range of lithologies that contain garnet, amphibole, plagioclase and quartz in their mineral assemblage. This barometer was calibrated based on 37 natural samples that equilibrated between 2.5–13 kbar and 500–800°C and has an uncertainty of ±0.5 to ±1 kbar.

3.3.2 Equilibrium Assemblage Diagrams (Pseudosections)

An equilibrium assemblage diagram, also called a pseudosection, is a type of phase diagram that plots the stability fields of different equilibrium mineral assemblages in pressure-temperature space for a single bulk-rock composition (e.g. de Capitani and Petrakakis, 2010). The assemblages in these diagrams are calculated from internally consistent thermodynamic databases (e.g. de Capitani and Petrakakis, 2010). Multiple programs have been created to calculate these phase relationships (e.g. THERMOCALC (Powell and Holland, 1988); Perple_X (Connolly, 1987)). The Theriak/Domino (de Capitani and Petrakakis, 2010) program is used for this study. The database used here is a THERMOCALC format file ('tcds55.txt') originally created by

Powell and Holland (2003) that was later converted into a Theriak-Domino format file ('tcd55dt.txt') by Doug Tinkham (2008). Solution models used from this database are: clinoamphibole (Diener et al., 2007), clinopyroxene (Green et al., 2007), orthopyroxene (Holland and Powell, 1996), garnet (White et al., 2007), chlorite (Holland et al., 1998), feldspar (Holland and Powell, 2003), olivine (Holland and Powell, 1998) and melt (Holland and Powell, 1998, plus updates from White et al., 2007). The results from the diagrams generated in this study are compared with thermobarometric calculations.

A user-specified bulk-rock composition, required as input for Theriak/Domino, was determined by the Rock Maker program (Büttner, 2012) using mineral modes and electron microprobe data for the major mineral phases in these samples. The Rock Maker program converts modal amounts of minerals into molar amounts of each element, allowing for the determination of the whole rock's (or one type of band's) bulk composition. Standard pure end-member compositions for quartz and magnetite, as well as representative microprobe compositions for pyroxene(s) and garnet were used as input for these calculations. The quartz was assumed to be 100 wt% SiO_2 and the magnetite was assumed to be 68.97 wt% Fe_2O_3 and 31.03 wt% FeO.

For all samples used for pseudosection calculation, total modes with magnetite and without magnetite (i.e. renormalized modes removing the magnetite contributions) were reported. The magnetite in these iron-formations essentially contains as much iron as possible such that this iron does not interact with any of the surrounding minerals during progressive metamorphism. Therefore, the magnetite acts as an inert phase and can be subtracted from the modal amounts, providing a more accurate "effective bulk composition" of each sample. This "effective bulk composition" (the composition of the

remaining minerals, excluding magnetite) is the preferred method to determine the reactive composition for further calculations.

3.4 Halogen Fugacity Calculations

The replacement of OH by variable amounts of F and Cl in amphibole and biotite can be a potential indicator of the relative activities of HF and HCl in a hydrothermal fluid (e.g. Munoz and Swenson, 1981). Munoz and Swenson developed a quantitative approach for determining relative HF and HCl fugacities of a metamorphic fluid based on Cl and F in biotite. The relative amount of Cl or F in a metamorphic fluid interacting with biotite can is determined using log values of halogen fugacity ratios (calculated from mole fractions of Cl, F and $Mg^{[VI]}$), and the temperature ('T') at which a rock equilibrated. The biotites used in their study were found in molybdenite deposits and porphyry copper deposits, with fugacity ratios ranging from ~0 to -1.5. Log values of halogen fugacity ratios for three of the samples in this study were calculated using mole fractions of Cl, F and Mg (determined from electron microprobe analyses) and specified temperature values chosen based on results from geothermometry calculations. Results are compared to the Munoz and Swenson study.

CHAPTER IV. RESULTS

4.1 Sample Locations

Twenty-six iron-formation samples from the eastern Beartooth Mountains (Montana) were analyzed: nineteen from the Quad Creek area, six from the Hellroaring Plateau area and one from the Rock Creek area. Sample locations are shown in Table 4.1 and general areas in Figure 4.1.

4.2 Sample Descriptions and Petrographic Observations

Based on the macroscopic appearance, the iron-formations can generally be divided into banded and granoblastic varieties. Although some variations exist among and within samples, the mineral assemblages are typically quartz (qz) + magnetite (mag) + orthopyroxene (opx) + garnet (grt) ± clinopyroxene (cpx) ± calcic clino-

Table 4.1. Iron-formation sample locations in the Beartooth Mountains*

Sample	Latitude	Longitude	Sample	Latitude	Longitude
QC-IS	45.028143	-109.415692	QC82-46	45.024602	-109.418431
QC-JW3	45.028143	-109.415692	QC82-47	45.024602	-109.418431
QC81-1	45.028143	-109.415692	QC82-48a	45.024602	-109.418431
QC81-4c	45.028143	-109.415692	QC82-48b	45.024602	-109.418431
QC81-5	45.028143	-109.415692	QC82-49a	45.024602	-109.418431
QC81-6	45.028143	-109.415692	QC82-49b	45.024602	-109.418431
QC81-40a	45.028143	-109.415692	RC81-168a	45.083396	-109.382075
QC81-40b	45.028143	-109.415692	HR02-3	45.045008	-109.446468
QC81-45	45.028143	-109.415692	HR02-71	45.047767	-109.450651
QC81-66	45.028162	-109.415984	HR02-72	45.047767	-109.450651
QC81-113	45.027785	-109.415547	HP81-77	45.040435	-109.451776
QC82-44	45.024602	-109.418431	HP81-82	45.040468	-109.451768
QC82-45	45.024602	-109.418431	HP82-59	45.047778	-109.450744

* Latitude and longitude locations determined by Darrell Henry (personal communication)

Figure 4.1. Google Earth image showing specific sample locations of iron-formation from the Quad Creek and Hellroaring Plateau localities. MT-WY state line is shown for reference. Yellow line indicates the Beartooth Highway (Highway 212). Not pictured is the Rock Creek sample location.

amphibole (cam) ± biotite (bt) ± plagioclase (pl). A variety of trace minerals (e.g. apatite, ilmenite) and alteration minerals (e.g. carbonate in fractures, amphibole altering pyroxene rims) are observed as well. Mineral modes determined based on the three previously mentioned techniques are given in Tables 4.2-4.6.

Table 4.2. Visually Estimated Mineral Modes for Quad Creek Samples																		
																---associated with fractures/rims---		
Sample	B or NB	Qz	Mag	Grt	Opx	Cpx	Cam	Bt	Pl	Ap	Zrn	Tur	Ilm	Hem	Py	Gru-Cum-Act	Sd-Ank	Cpx
QC-IS	NB	25	31	13	20	6	5	tr		tr	tr			x		x	x	
QC-JW3	B	x	x	x	x	x	x					tr	tr	x		x	x	
-----	*Fe*	8	40	8	20	24												
-----	*qz*	85	7		3	3	2											
QC81-1	-----	x	x	x	x	x	x	x										
QC81-4c	NB	27	30	18	21	4					tr			tr		x		
QC81-5	-----	x	x	x	x	x	x	x										
QC81-6	NB	29	26	21	16	4	4				tr					x		
QC81-40a	B	x	x	x	x	x		x	x					x			x	
-----	*Fe*	40	10	25	25	tr		tr						tr				
-----	*qz*	75	3	22				tr	tr					tr				
QC81-40b	NB	30	26	13	29	tr	2											
QC81-45	B	x	x	x	x	x	tr						tr	x		x	x	
-----	*Fe*	19	30	27	18	6	tr											
-----	*qz*	65	18		14	3	tr											
QC81-66	NB	25	18	27	30	tr		tr		tr						x	x	x
QC81-113	NB	23	20	23	34	tr		tr			tr			tr		x		
QC82-44	B	x	x		x		x	tr	x	tr			tr	x			x	
-----	*Fe*	13	44		32		5	tr	4		tr		tr	2				
-----	*qz*	93	3		1		2		1		tr		tr	tr				
QC82-45	NB	13	8	34	38	tr	4	3					tr			x	x	x
QC82-46	-----	x	x	x		x	x		x	tr	tr	tr	tr		tr	tr		
QC82-47	-----	x	x		x	x	x			tr	tr					tr		
QC82-48a	B	x	x	x	x	x	x	tr	x	tr	tr							
-----	*Fe*	10	8	4	2	1	70		5	tr	tr							
-----	*qz*	95	4	tr	tr	tr	tr	tr	1	tr							x	

(Table 4.2 continued)

																---associated with fractures/rims---		
Sample	B or NB	Qz	Mag	Grt	Opx	Cpx	Cam	Bt	Pl	Ap	Zrn	Tur	Ilm	Hem	Py	Gru-Cum-Act	Sd-Ank	Cpx
QC82-48b	-----	x	x	x			x		x	tr	tr							
QC82-49a	-----	x	x		x	x	x		x	tr	tr							
QC82-49b	-----	x	x	x	x	x	x	x	x	tr	tr							

* Abbreviations and symbols in the above table are: B = banded, NB = non-banded, Fe = iron-rich silicate/oxide band, qz = quartz-rich band, tr = trace amounts, X = mineral is present but modal amount not determined/included.

Table 4.3. Visually Estimated Mineral Modes for Rock Creek Samples

						---associated with fractures/rims---	
Sample	B or NB	Qz	Mag	Grt	Opx	Ap	Gru-Cum-Act
RC81-168a	NB	3	tr	1	95	tr	x

* Abbreviations and symbols in the above table are: B = banded, NB = non-banded, Fe = iron-rich silicate/oxide band, qz = quartz-rich band, tr = trace amounts, X = mineral is present but modal amount not determined/included.

Table 4.4. Visually Estimated Mineral Modes for Hellroaring Plateau

													---associated with fractures/rims---		
Sample	B or NB	Qz	Mag	Grt	Opx	Cpx	Cam	Bt	Ap	Zrn	Ilm	Hem	Gru-Cum-Act	Sd-Ank	Chl
HR02-3	NB	32	15	27	26				tr		x		x		
HR02-71	NB	11	19	16	41		13				x	tr	x		
HR02-72	-----	x	x	x			x	x					x		
HP81-77	NB	40	15	7	30		8						x		

(Table 4.4 continued)

HP81-82	NB	10	6	55	10	15		4		tr	tr	tr	x	x	x
HP82-59	B	x	x	x	x			x			tr		x		
-----	*Fe*	11	8	50	28			3					x		
-----	*qz*	95	2	1	2								x		

* Abbreviations and symbols in the above table are: B = banded, NB = non-banded, Fe = iron-rich silicate/oxide band, qz = quartz-rich band, tr = trace amounts, X = mineral is present but modal amount not determined/included.

Table 4.5. Mineral Modes Determined by Point Counts (based on 1000 points)

										---associated with fractures/rims---	
Sample	B or NB	Qz	Mag	Grt	Opx	Cpx	Cam	Ap	Hem	Gru-Cum-Act	Sd-Ank
QC-IS	NB	29.7	30.4	10.2	15.6	4.8	9.2		0.1	x	x
HR02-3	NB	36.8	14.3	23.7	25.2			tr		x	

* Abbreviations and symbols in the above table are: B = banded, NB = non-banded, Fe = iron-rich silicate/oxide band, qz = quartz-rich band, tr = trace amounts, X = mineral is present but modal amount not determined/included.

Table 4.6. Mineral Modes Determined with ImageJ

												---associated with fractures/rims---		
Sample	B or NB	Qz	Mag	Grt	Opx	Cpx	Cam	Bt	Pl	Ilm	Hem	Gru-Cum-Act	Sd-Ank	Other (holes)
QC-IS	NB	25.8	18.7	7.8	28.6	9.56	4.84			2.15		x	1.77	1.41
QC-JW3	*Fe*	12.2	38.0	14.9	7.72	22.95				0.33		x	3.02	1.92
-----	*qz*	86.5	4.71		1.84	3.81	0.87			0.21		x		2.56
QC82-44	*Fe*	24.1	31.8		32.7		4.17		0.71	1.60	0.48		x	4.41
-----	*qz*	93.3	1.50		0.07		1.08							3.92
QC82-45	NB	37.5	2.98	23.6	31.8		0.23			0.62		x	1.95	0.97

(Table 4.6 continued)

HP81-82	NB	23.3	2.26	31.5	27.3			6.18		1.39	0.21			3.27
HP82-59	*Fe*	19.1	12.8	31.4	30.7			1.54		2.70		x		1.76
-----	*qz*	92.9	0.64	1.22	3.63			0.13		0.14		x		1.34
HR02-3	NB	40.1	7.60	25.2	25.3					0.87		x		0.92
HR02-71	NB	38.8	15.7	11.5	24.6					3.84		x	2.39	3.23
-----	*Am*	3.51	10.6	9.19	1.46		71.9			1.88	0.03			1.45

* Abbreviations and symbols in the above table are: B = banded, NB = non-banded, Fe = iron-rich silicate/oxide band, qz = quartz-rich band, tr = trace amounts, X = mineral is present but modal amount not determined/included.

4.2.1 Non-banded Samples

Twelve of the investigated meta-iron-formations are non-banded (Figures 4.2 and 4.3). These are typically fine- to medium-grained rocks with a dark grayish-blue color resulting from the abundance of mafic minerals and iron oxide. The dominant minerals in these samples are quartz, magnetite, garnet and pyroxene, with lesser amounts of amphibole or biotite, and, in some cases, plagioclase. Trace amounts of apatite, zircon and ilmenite are locally present. Tourmaline and pyrite have been rarely observed (Darrell Henry, personal communication). With the exception of a singular sample from

Figure 4.2. A non-banded iron-formation from Hellroaring Plateau of the eastern Beartooth Mountains, MT. The primary mineral assemblage is qz + mag+ grt + opx + bt + ilm. Ruler scale in centimeters. Image credit: Nick Daigle. Photograph of sample HP81-82.

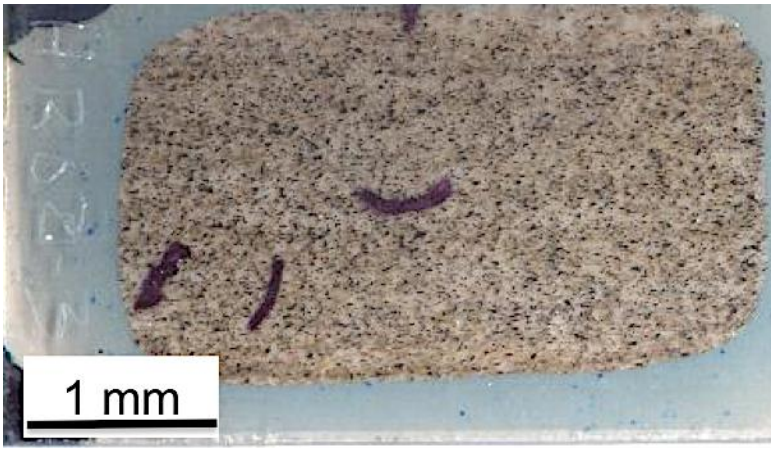

Figure 4.3. A homogeneous non-banded iron-formation from Hellroaring Plateau of the eastern Beartooth Mountains, MT. The primary mineral assemblage is qz + mag + grt + opx + ilm. Image credit: Nick Daigle. Optical scan of a thin section of sample HR02-3.

the Rock Creek locality, there is little variation in the dominant mineral assemblage between the non-banded and banded samples. The sample from Rock Creek is almost entirely comprised of orthopyroxene and is lacking abundant magnetite and quartz. Sample HR02-71, although primarily non-banded, does contain a relatively large, green amphibole-rich band that is easily seen macroscopically.

4.2.2 Banded Samples

The banded meta-iron-formations typically contain similar mineral assemblages as the non-banded samples. Modal amounts of these minerals vary considerably among the Fe-rich silicate and oxide bands and the quartz-rich bands (Table 4.2). Lighter-colored bands are dominated by quartz and darker colored bands are comprised mainly of magnetite and ferromagnesian silicate phases. Distinct banding is easily seen in some samples, whereas others may appear to be non-banded until viewed in thin section. Examples of a well-banded hand sample and thin section are shown in Figures 4.4 and 4.5.

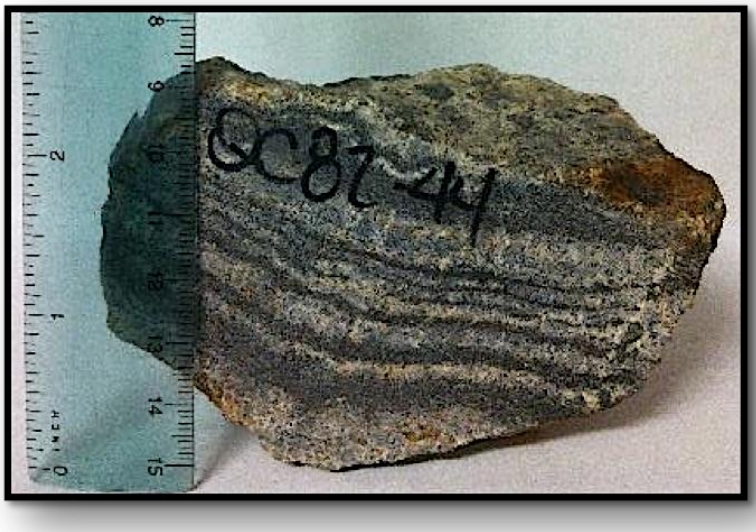

Figure 4.4. A well-banded iron-formation from the Quad Creek locality of the eastern Beartooth Mountains, MT. Bands range in size from ~0.1 to 1 cm. The silicate/oxide-rich bands have a primary mineral assemblage of qz + mag + opx + am + pl + ilm and the quartz-rich bands have a primary mineral assemblage of almost entirely qz, with minor amounts of mag, opx and am. The amphibole in this sample is primary amphibole. Ruler scale in centimeters. Image credit: Nick Daigle. Photograph of sample QC82-44.

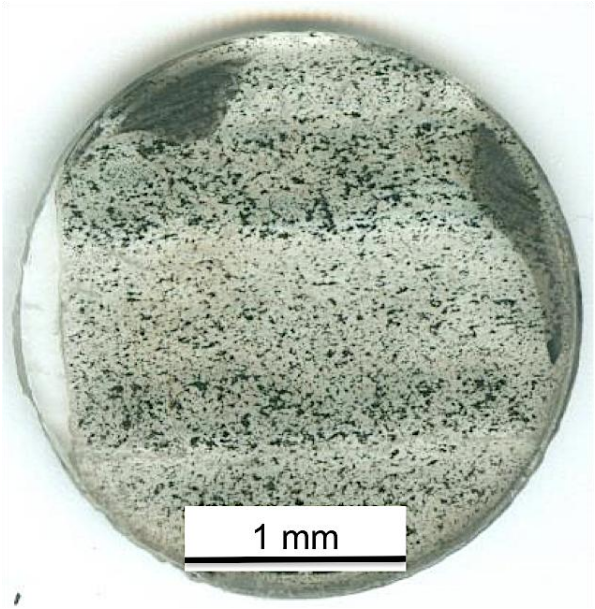

Figure 4.5. A well-banded iron-formation from the Quad Creek locality in the eastern Beartooth Mountains, MT. The silicate/oxide-rich bands have a primary mineral assemblage of qz + mag + grt + opx + cpx + am, and the quartz-rich bands have a primary mineral assemblage of qz + mag + opx + cpx + am. Image credit: Nick Daigle. Optical scan of a thin section of sample QC81-45.

4.2.3 Petrography

Petrographic analyses show the iron-formations contain a general metamorphic mineral assemblage of qz + mag + opx + grt ± cpx ± am ± bt ± pl (Figures 4.6 and 4.7) with some trace amounts of apatite, zircon, ilmenite, and rarely hematite and chlorite alteration. Carbonate minerals are commonly associated with fracture zones (mostly in pyroxenes, but also garnet, plagioclase and magnetite) and quartz veins. Many of the pyroxene grains in the samples are altered to secondary amphibole phases of actinolite, grunerite and cummingtonite.

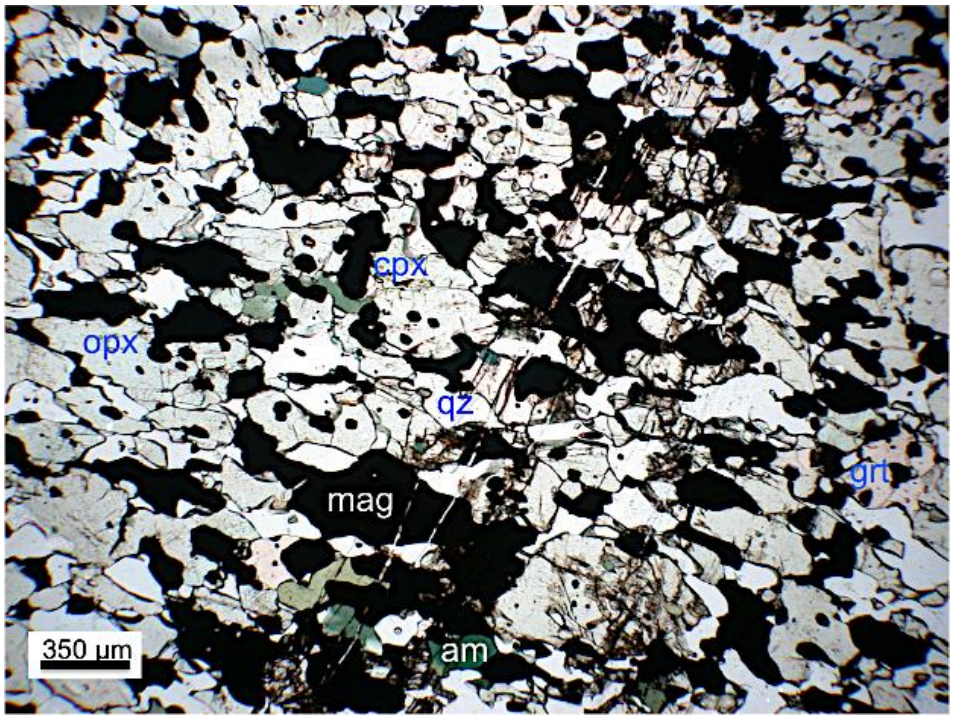

Figure 4.6. A granoblastic iron-formation with the mineral assemblage of qz + mag + grt + opx + cpx + am that is commonly seen in iron-formations from the Quad Creek locality in the eastern Beartooth Mountains, MT. Carbonate-quartz-bearing veins are also seen cross-cutting this area. Image credit: Nick Daigle. Photomicrograph of sample QC-IS taken in PPL.

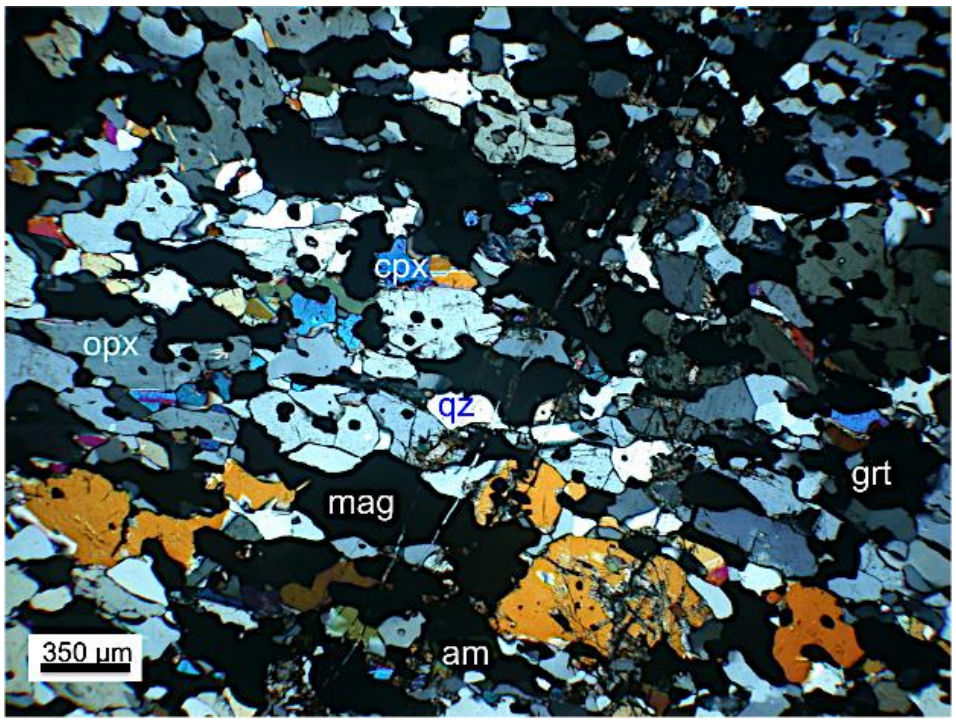

Figure 4.7. View from Figure 4.6 shown in XPL. Image credit: Nick Daigle

Quartz grains vary widely in size from small (~50 µm) to relatively large (~4.25 mm). The largest of quartz grains are typically confined to quartz-rich bands of the banded samples, with the smaller grains more commonly found in more massive samples or the silicate/oxide-rich bands of banded samples. . The quartz in the non-banded samples and the silicate/oxide-rich bands of banded samples are typically equant and granoblastic with sharp, well-defined boundaries. The grains present in quartz-rich bands appear to be recrystallized, with more irregular, lobate grain boundaries. Undulatory extinction is commonly visible in quartz.

Plagioclase grains can typically be distinguished from quartz in these samples due to the well-developed albite twinning present (Figure 4.8), as well as their alteration to ankerite. The grains range in size from ~50 µm to ~750 µm with blocky shapes and

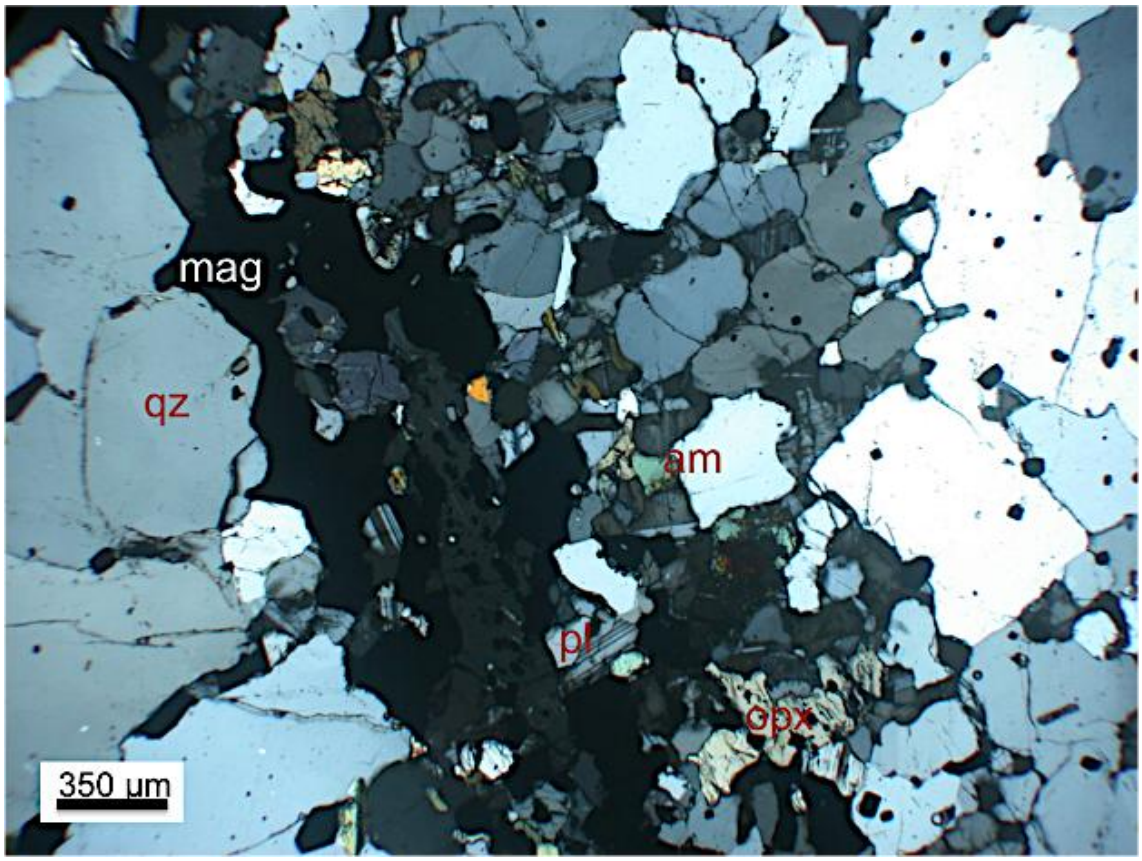

Figure 4.8. A representative area of a banded iron-formation from the Quad Creek locality in the eastern Beartooth Mountains, MT. The primary mineral assemblage in the silicate/oxide-rich band is qz + mag + opx + am + pl. The quartz areas on either side are composed of almost entirely quartz, along with minor amounts of mag/ilm, opx and am. Grain sizes tend to be larger in the qz-rich areas. This sample lacks garnet, but contains plagioclase. Image credit: Nick Daigle. Photomicrograph of sample QC82-44 taken in XPL.

commonly have inclusions of apatite. In plagioclase-bearing samples with abundant garnet or amphibole, the plagioclase will occur adjacent to or near to the garnet or amphibole. In samples that have lesser amounts of garnet or amphibole the plagioclase tends to occur near magnetite, quartz and orthopyroxene.

Magnetite is the dominant iron oxide present. Magnetite ranges in size from ~25 µm to ~1,750 µm. The smaller grains usually have a well-defined cubic shape while the larger grains are more subhedral-to-anhedral and are typically found in the

silicate/oxide-rich layers of well-banded samples. Associated ilmenite appears as separate grain growth cutting many of the magnetite grains in these samples, suggesting high amounts of Ti in the environment and continued Fe-Ti exchange during cooling. Some of the ilmenite exhibits small exsolution of hercynite decorating the magnetite-ilmenite boundary (Darrell Henry, personal communication).

The garnets frequently contain inclusions of quartz, magnetite, orthopyroxene and clinopyroxene, and, less frequently, amphibole and biotite. They range in size from ~50 μm up to ~2.4 mm and are typically euhedral with some showing local fracturing. The garnets are commonly found adjacent to orthopyroxenes.

Orthopyroxene (~50 – 2.1 mm) is the dominant pyroxene present in these samples, but some samples also contain clinopyroxene (~70 – 950 μm) in lesser amounts (Figures 4.6 and 4.7). In plane-polarized light orthopyroxene typically has pleochroism from a light minty green to a light pink, whereas the clinopyroxenes are typically pale lighter green. Opx and cpx are distinguished in XPL by their difference in birefringence (orthopyroxene typically exhibits first order colors and clinopyroxene second order). However, many of the orthopyroxene grains exhibit unusually higher order birefringence colors presumably as a result of their high iron content. The high iron content of the orthopyroxene cause some of the grains to display second order birefringent colors that resemble those of clinopyroxene. The pyroxenes generally have inclusions of magnetite, quartz, ± garnet, and amphibole and biotite (Figure 4.6). Quartz and carbonate minerals are commonly associated with fractures in garnet and orthopyroxene (Figures 4.9 and 4.10). The carbonate phases have been analyzed in some samples and are typically ankerite (if associated with garnet) and magnesio-

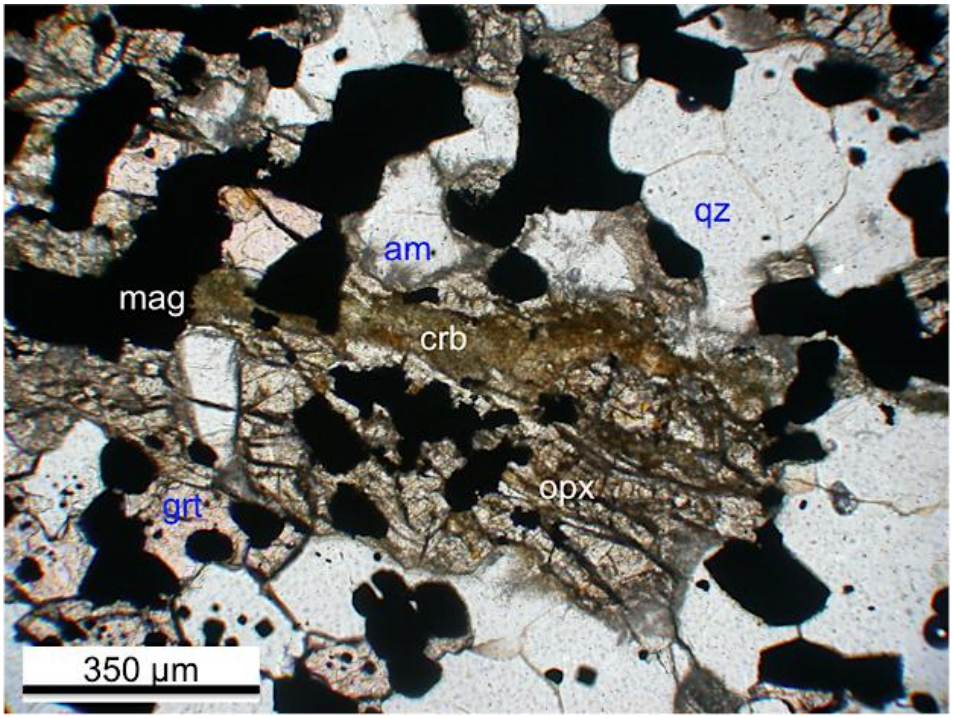

Figure 4.9. Alteration of opx by carbonate minerals (in fracture) and secondary amphibole (grunerite on rims) in an iron-formation from the Hellroaring Plateau locality in the eastern Beartooth Mountains, MT. The primary mineral assemblage in this sample is qz + mag + grt + opx. Image credit: Nick Daigle. Photomicrograph of sample HR02-71 taken in PPL.

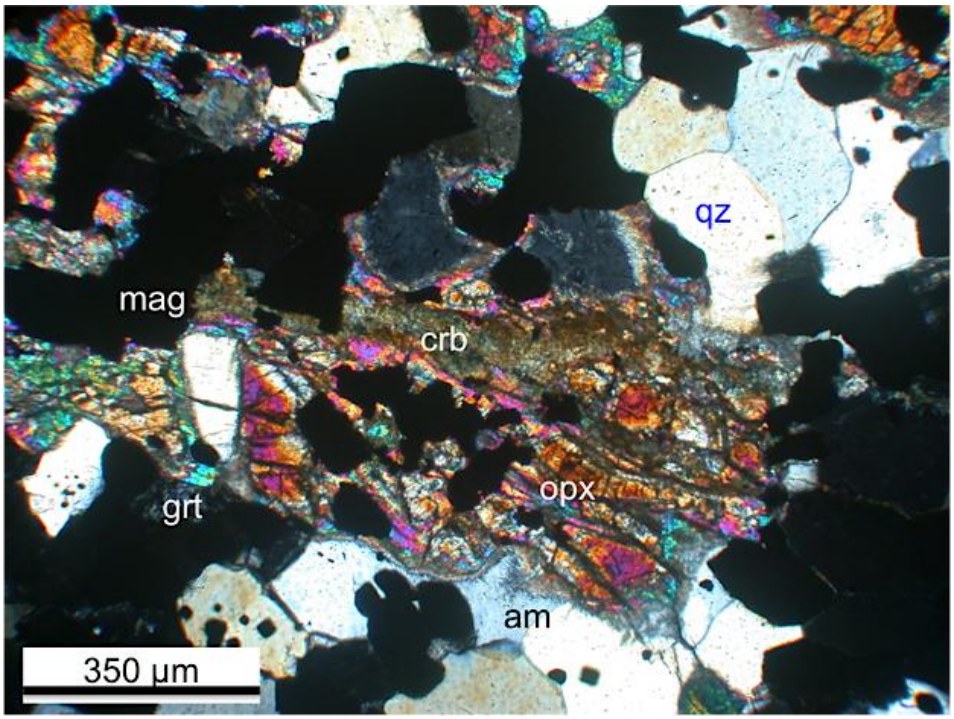

Figure 4.10. View from Figure 4.9 shown in XPL. Image credit: Nick Daigle.

siderite (if associated with orthopyroxene; Darrell Henry, personal communication). In some samples, the pyroxene rims are altered or replaced by secondary amphibole of actinolite, grunerite and/or cummingtonite (Figures 4.11 and 4.12). Additionally, some of the clinopyroxene in the iron-formations contain exsolution lamellae of orthopyroxene, interpreted to result from slow cooling.

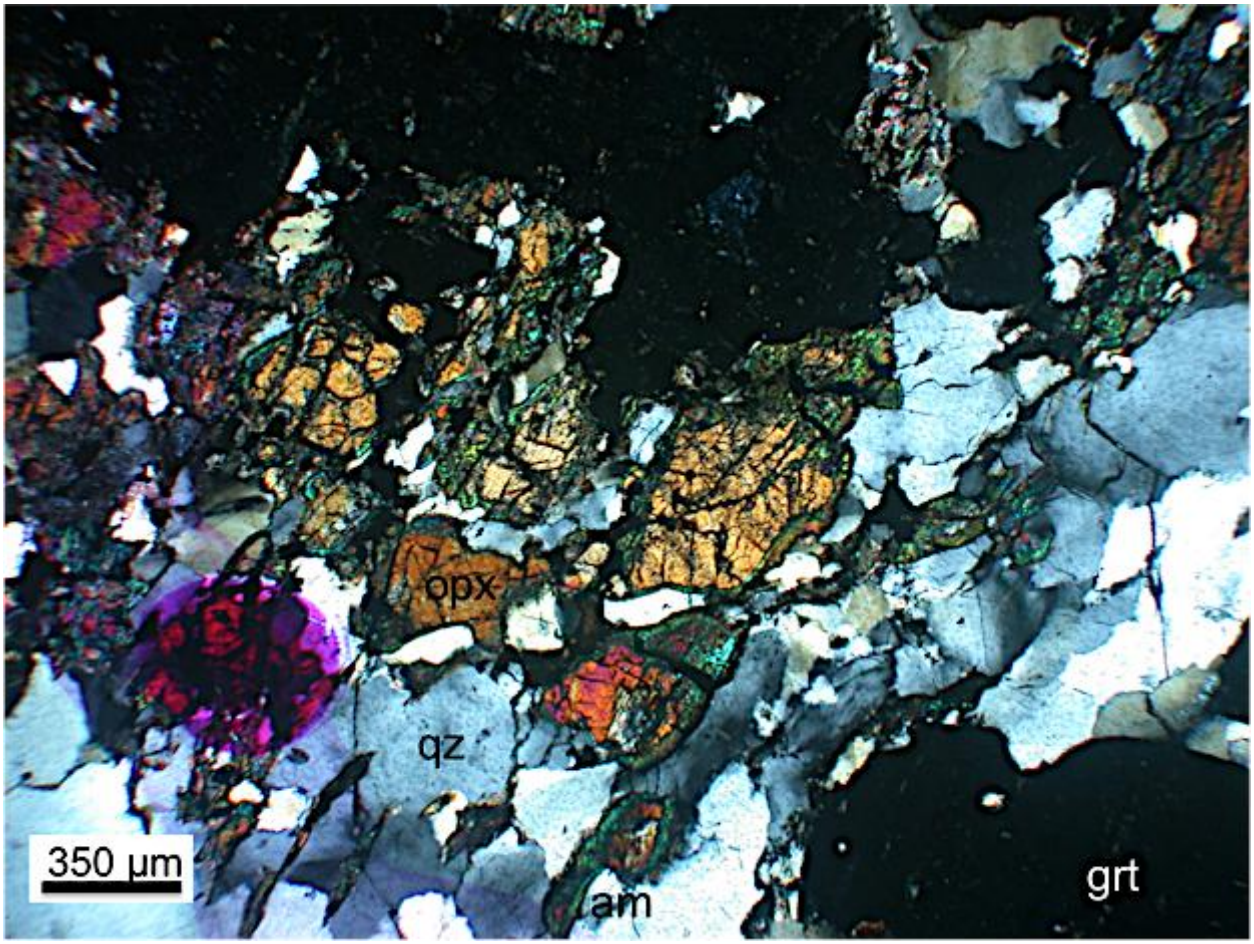

Figure 4.11. A banded iron-formation from Hellroaring Plateau with green-blue secondary amphibole (actinolite) altering the rims of orthopyroxene grains. The purple-pink area in the lower left is a marker. Image credit: Nick Daigle. Photomicrograph of sample HP82-59 taken in XPL.

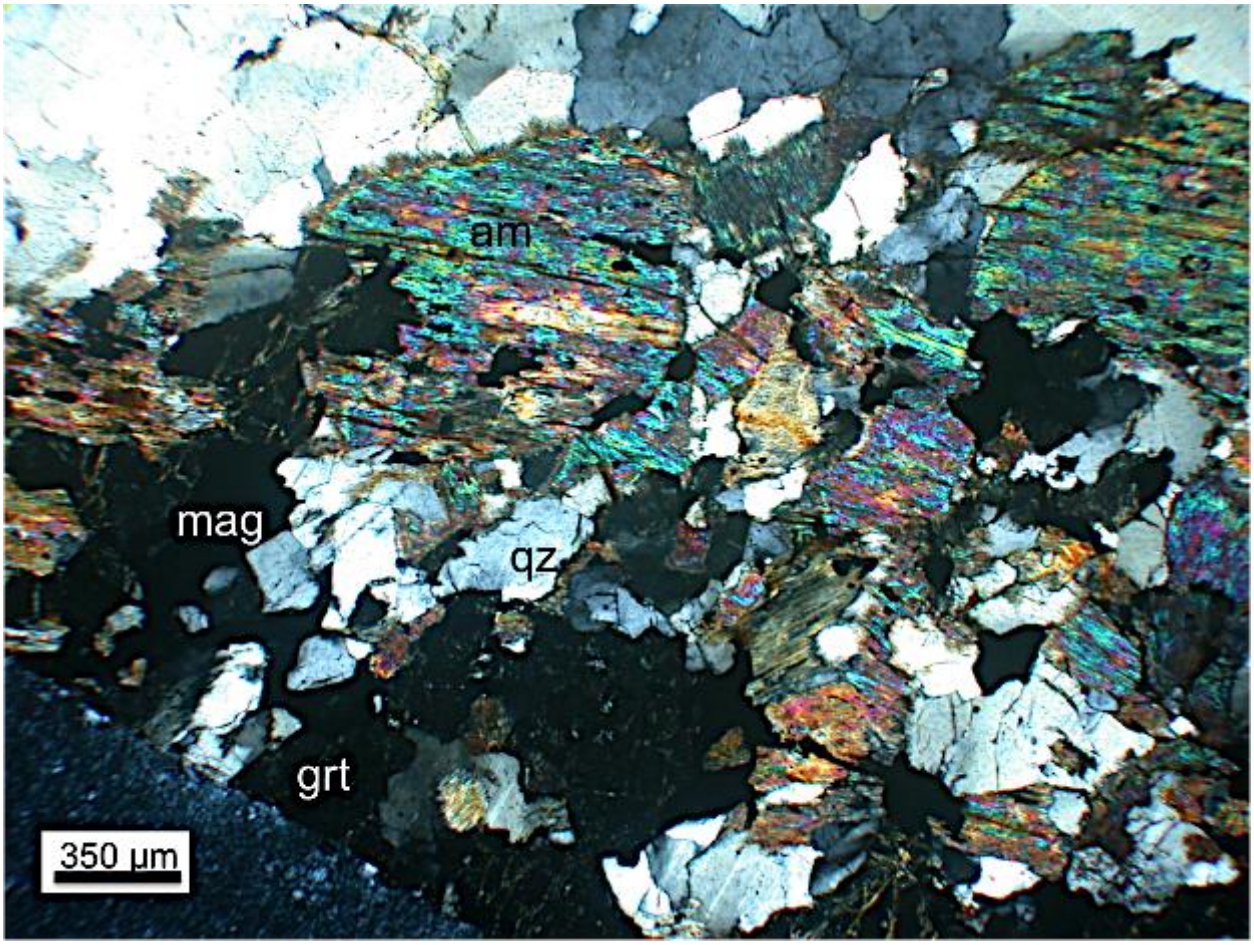

Figure 4.12. A banded iron-formation from Hellroaring Plateau showing complete replacement of pyroxene by secondary amphibole (actinolite and cummingtonite). Note the high birefringent colors and fine, acicular shape of the amphibole on the rims. Image credit: Nick Daigle. Photomicrograph of sample HP82-59 taken in XPL.

Amphiboles in these samples are distinguished by their characteristic 60/120 cleavage angles (when visible) and also the color of the grains in PPL. The pleochroic scheme of the grains ranges from colorless-to-light green to a blue-green teal. In XPL, many of the amphiboles have the same blue-green teal color, but grains with a brownish-yellow color were also common. The amphiboles occur in the matrix and as inclusions in pyroxene and garnet (Figure 4.6). In many samples, a secondary

amphibole (most commonly actinolite or grunerite) alters orthopyroxene rims (Figures 4.10 and 4.11), and in some cases completely replaces the pyroxenes (Figure 4.12). The replacement amphibole typically has an acicular habit and higher XPL birefringence colors than the primary amphibole, and appears essentially colorless in PPL. Some of the primary amphibole grains are also extensively replaced by carbonate minerals. Simple twinning is also observed in some of the primary amphibole grains.

Biotite grains are typically small, ranging from ~50-500 µm, with dark brown to dark brownish-red pleochroism (Figure 4.13). Biotite grains occur as matrix minerals (near pyroxene and garnet) as well as inclusions in both pyroxene and garnet. Small biotite grains are occasionally observed adjacent to magnetite.

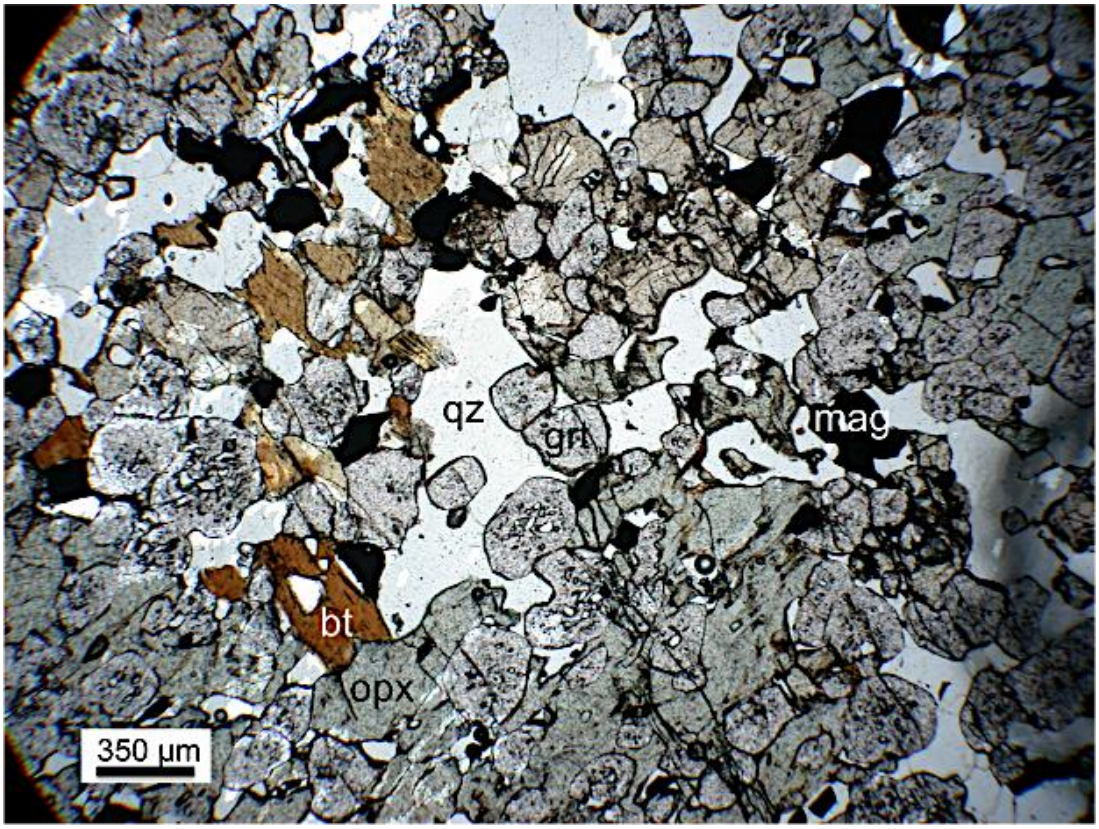

Figure 4.13. A non-banded iron-formation from Hellroaring Plateau showing a cluster of matrix biotite grains interstitial to orthopyroxene, garnet and magnetite. Image credit: Nick Daigle. Photomicrograph of sample HP81-82 taken in PPL.

Apatite, zircon and tourmaline are small, high relief minerals found in minor amounts in some samples. Ilmenite commonly occurs in trace amounts in many of the samples, sometimes with hercynite exsolution. Pyrite has also been observed rarely.

Many of the samples also contain a different suite of minerals associated with fracture zones, most commonly in the form of replacement amphibole or carbonate phases, with chlorite and clinopyroxene occurring less frequently. The amphibole is usually a bright blue-green color altering pyroxene grains and the carbonate phases are present as a yellowish-brown color altering pyroxene, garnet and magnetite grains.

4.3 Backscattered Electron Imaging (BEI)

Backscattered electron images enhance petrographic observations. These images were used for mineral identification and to better observe any significant textures, alteration or chemical zoning that may not be seen with a petrographic microscope. None of the images show signs of identifiable chemical zoning in minerals, but some minerals exhibit fine exsolution and alteration.

Magnetite grains from most samples show laths of ilmenite associated with the magnetite (Figure 4.14). This texture is sometimes observed in reflected light. In some samples, exsolution textures can be seen in pyroxene grains. The darker-gray clinopyroxene grains contain fine, lighter-gray exsolution lamellae of orthopyroxene (Figure 4.15). These lamellae are sometimes visible when using the petrographic microscope, but are much more distinct and easily seen in backscattered images.

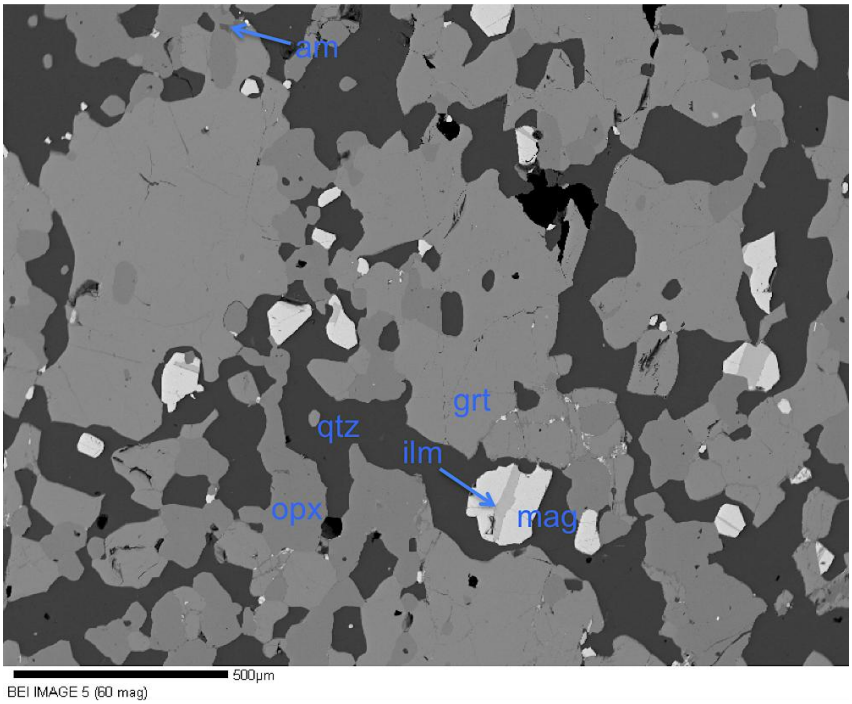

Figure 4.14. A non-banded iron-formation with a primary mineral assemblage of qz + mag + grt + opx + am + ilm. Notice the ilmenite laths growing with associated magnetite grains. Image credit: Nick Daigle. BSE image of sample QC82-45.

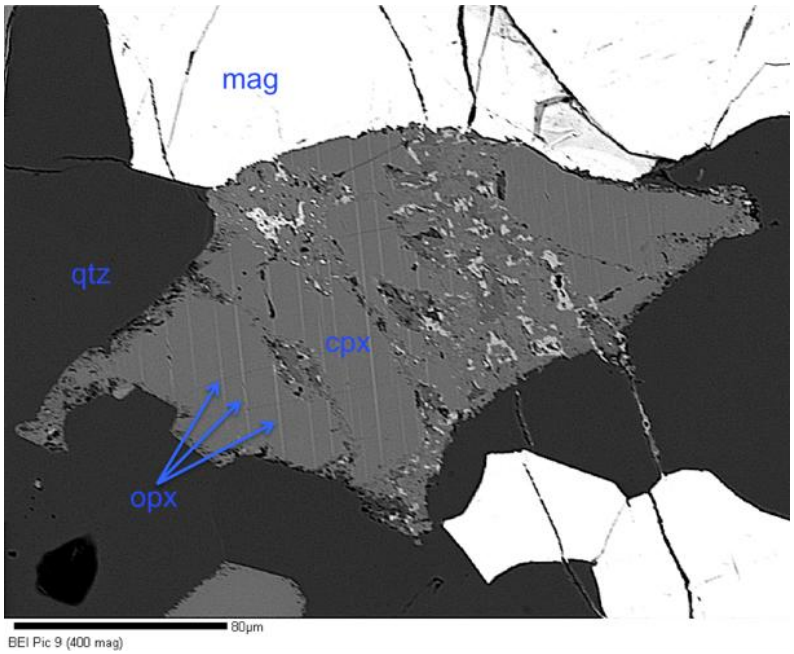

Figure 4.15. A banded iron-formation with pyroxene exsolution. The primary mineral assemblage of the silicate/oxide-rich bands in this sample is qz + mag + grt + opx + cpx + ilm. The darker-gray clinopyroxene grain exhibits distinct thin, lighter-gray exsolution lamellae of orthopyroxene. This grain is also cut by later-stage alteration phases of amphibole/carbonate. Image credit: Nick Daigle. BSE image of sample QC-JW3.

Alteration of pyroxene grains by amphibole phases is readily visible in backscattered images and is a common feature found in many of the meta-iron-formations. The amphibole (mainly actinolite and grunerite) is typically seen forming on the rims and in fracture zones of pyroxenes (Figure 4.16), but in some instances completely replaces the pyroxene (Figure 4.17).

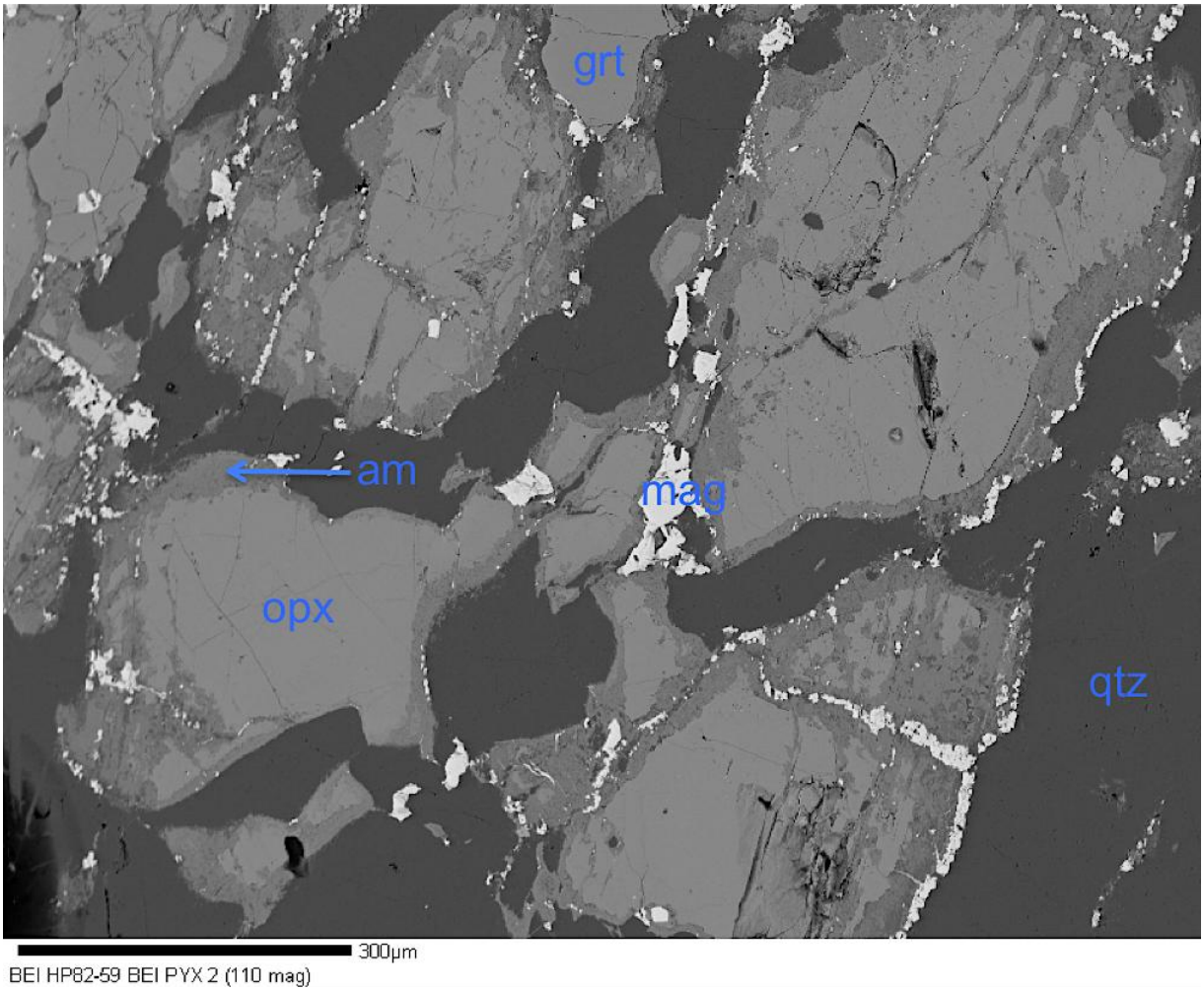

Figure 4.16. A silicate/oxide-rich band from a banded iron-formation with a primary mineral assemblage of qz + mag + grt + opx + bt + ilm. Secondary amphibole (actinolite) is shown altering the rims and fractured areas of the orthopyroxene grains. Magnetite can also be seen forming on the edge of these alteration areas. Image credit: Nick Daigle. BSE image from a silicate/oxide-rich band in sample HP82-59.

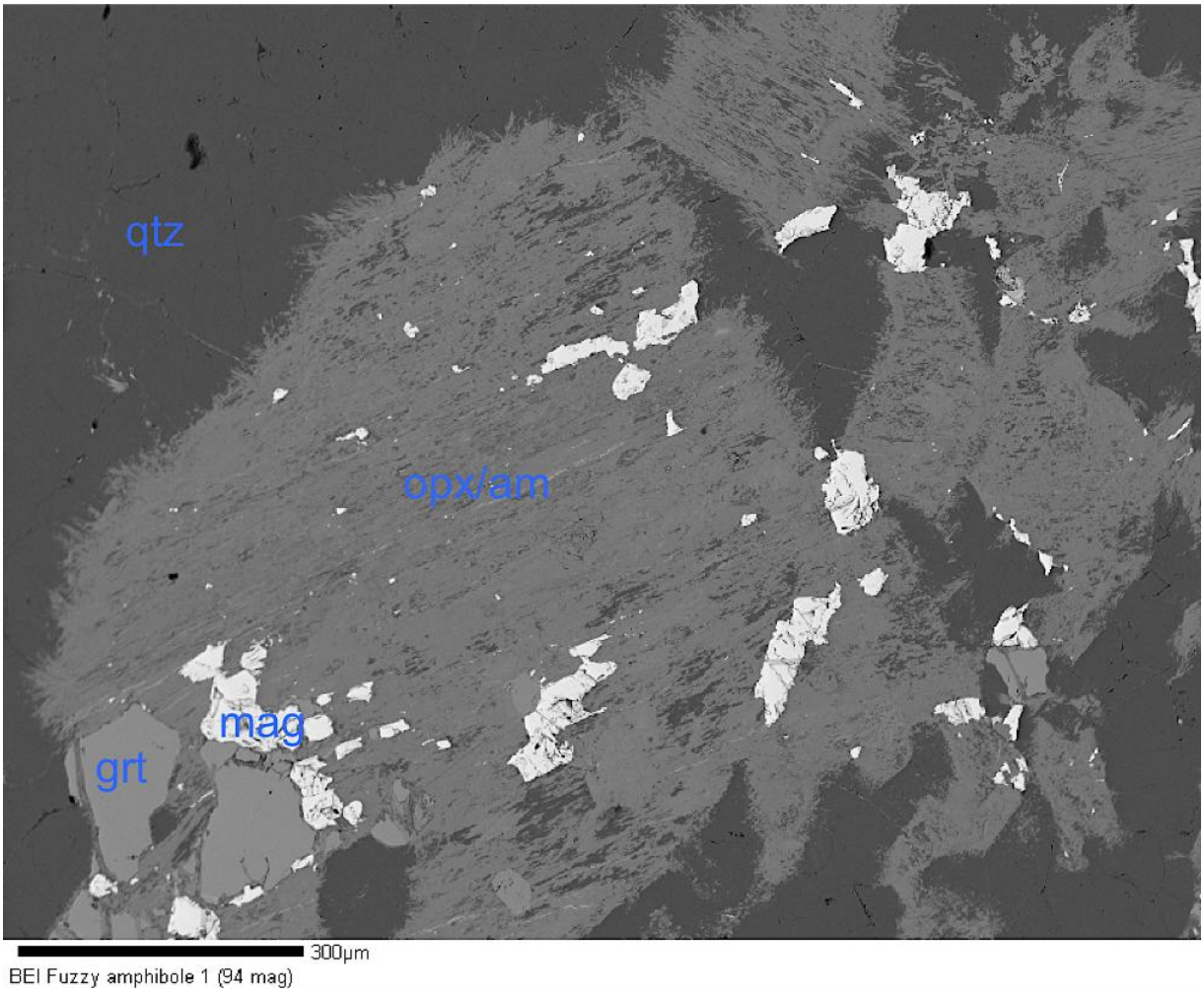

Figure 4.17. A silicate/oxide-rich band from a banded iron-formation with a primary mineral assemblage of qz + mag + grt + opx + bt + ilm. Orthopyroxene is being completely replaced by secondary amphibole (actinolite). Image credit: Nick Daigle. BSE image from a silicate/oxide-rich band in sample HP82-59.

4.4 Mineral Chemistry

Chemical data from EPMA analyses of garnets, pyroxenes, feldspars, amphiboles and biotites are used to characterize the mineral associations and mineral growth histories, and can be used as input for classical geothermobarometric calculations. Ultimately, the chemistry of the analyzed minerals from these meta-iron-formations (particularly amphibole and biotite) will elucidate the possible P-T conditions in the eastern Beartooth Mountains, MT during the time of metamorphism.

4.4.1 Garnet

The chemistry of garnets is a complex solid solution representing endmember components rich in Mg^{2+} (pyrope), Fe^{2+} (almandine), Mn^{2+} (spessartine) and Ca^{2+} (grossular). Mole fractions for Fe^{2+}, Mg^{2+}, Mn^{2+} and Ca^{2+} were calculated using representative compositions of garnets in each sample. Almandine garnets (the iron-rich component) are consistently the dominant endmember component in all samples, ranging from 55.76-79.22. The molecular percentages of pyrope, spessartine and grossular endmember components range from 5.91-13.32, 1.56-14.58 and 2.45-20.22, respectively. X_{Fe} values range from 0.85-0.91, X_{Ca} values ranged from 0.06-0.25, X_{Mg} values ranged from 0.088-0.151 and X_{Mn} values ranged from 0.02-0.18. Minor zoning in garnet rims has been observed in samples from other lithologies in the Beartooth Mountains, MT (Darrell Henry, personal communication). The garnets studied here do not exhibit compositional zoning; therefore, average values from all analyses in each sample are used as representative compositions (Table 4.7). Representative structural formulae for each sample are also given in Table 4.7. Tables of element wt% oxides for analyses in each sample are found in Appendix A.

The relationship between modal amounts of pyroxene and amphibole and the composition of theses coexisting minerals with garnet have compositional effects on garnet chemistry. Two binary plots illustrate these correlations. In the X_{Fe} vs. X_{Ca} plot the garnets with higher values of X_{Ca} (above ~0.15) occur in clinopyroxene-bearing samples (Figure 4.18). QC81-66 falls below 0.15 X_{Ca} even though clinopyroxene is present; however, the modal amount of clinopyroxene is low (Tables 4.2-4.6). The clinopyroxene in sample QC81-1 was most likely rare as well. In the same figure, HR02-

Table 4.7. Representative Garnet Compositions in wt%						
Sample	QC82-45*	QC81-66*	QC81-40b*	HP82-59	HR02-3	QC82-49b*
Analysis #	avg of 68	grt-1	avg of 2	avg of 20	avg of 18	avg of 6
SiO_2	37.36	37.78	37.69	37.09	37.14	37.54
Al_2O_3	20.29	21.31	20.6	20.77	20.82	20.50
TiO_2	0.02	-----	-----	0.02	0.01	0.01
Cr_2O_3	0.05	0.03	0.04	0.03	0.01	0.01
Fe_2O_3 (calculated)	1.14	-----	1.29	1.38	1.48	1.76
FeO (calculated)	29.76	30.63	28.88	33.05	30.59	26.47
MnO	3.22	4.67	4.4	0.69	2.70	3.87
MgO	1.61	2.54	2.57	2.28	3.03	2.64
CaO	6.86	4.08	5.59	5.12	4.45	7.64
Total	100.31	101.04	101.04	100.42	100.24	100.44
Molecular Percent of Components						
Almandine	66.83	67.93	64.07	74.49	68.87	58.96
Pyrope	6.46	10.04	10.17	9.17	12.16	10.50
Spessartine	7.32	10.49	9.89	1.56	6.14	8.74
Grossular	15.71	11.44	12.50	13.72	11.92	18.35
Andradite	3.45	-----	3.27	0.92	0.84	3.41
Schorlomite	0.06	-----	-----	0.06	0.04	0.02
Uvarovite	0.16	0.09	0.11	0.08	0.03	0.03
Structural Formulae for Representative Compositions						
QC82-45	$(Fe^{2+}_2Ca_{0.59}Mn_{0.22}Mg_{0.19})(Al_{1.92}Fe^{3+}_{0.07})Si_3O_{12}$					
QC81-66	$(Fe^{2+}_{2.04}Ca_{0.35}Mn_{0.31}Mg_{0.3})Al_2Si_3O_{12}$					
QC81-40b	$(Fe^{2+}_{1.92}Ca_{0.48}Mg_{0.31}Mn_{0.3})(Al_{1.93}Fe^{3+}_{0.08})Si_3O_{12}$					
HP82-59	$(Fe^{2+}_{2.22}Ca_{0.44}Mg_{0.27}Mn_{0.05})(Al_{1.94}Fe^{3+}_{0.08})(Si_{2.98}Al_{0.02})O_{12}$					
HR02-3	$(Fe^{2+}_{2.05}Ca_{0.38}Mg_{0.36}Mn_{0.18})(Al_{1.94}Fe^{3+}_{0.09})(Si_{2.97}Al_{0.03})O_{12}$					
QC82-49b	$(Fe^{2+}_{1.76}Ca_{0.65}Mg_{0.31}Mn_{0.26})(Al_{1.91}Fe^{3+}_{0.11})(Si_{2.99}Al_{0.01})O_{12}$					

Sample	QC-IS*	QC-JW3*	QC81-1*	QC81-5*	QC81-6*	HR02-71*
Analysis #	avg of 10	avg of 5	grt-2	grt-4	avg of 2	
SiO_2	37.20	37.18	37.17	36.85	37.59	36.94
Al_2O_3	20.72	20.67	20.32	20.44	20.57	20.38
TiO_2	0.01	0.01	0.04	-----	0.01	-----
Cr_2O_3	0.01	0.02	0.07	0.08	0.01	-----
Fe_2O_3 (calculated)	1.91	2.48	0.09	2.76	1.47	1.89
FeO (calculated)	28.00	24.80	34.24	29.82	27.81	26.50

(Table 4.7 continued)

Sample	QC-IS*	QC-JW3*	QC81-1*	QC81-5*	QC81-6*	HR02-71*
Analysis #	avg of 10	avg of 5	grt-2	grt-4	avg of 2	
MnO	3.43	6.40	1.87	1.88	3.78	5.70
MgO	1.87	2.13	3.23	2.96	2.14	1.46
CaO	7.56	7.34	2.02	5.51	7.42	7.25
Total	100.71	101.02	99.05	100.31	100.79	100.12
Molecular Percent of Components						
Almandine	62.93	55.76	79.22	67.68	61.86	59.99
Pyrope	7.49	8.52	13.32	11.97	8.49	5.91
Spessartine	7.81	14.58	4.38	4.32	8.52	13.07
Grossular	20.22	19.38	2.45	14.08	17.84	18.56
Andradite	1.49	1.66	0.27	1.68	3.25	2.47
Schorlomite	0.03	0.03	0.12	-----	0.02	-----
Uvarovite	0.03	0.06	0.23	0.26	0.03	-----
Structural Formulae for Representative Compositions						
QC-IS	$(Fe^{2+}_{1.87}Ca_{0.65}Mn_{0.23}Mg_{0.22})(Al_{1.92}Fe^{3+}_{0.11})(Si_{2.97}Al_{0.03})O_{12}$					
QC-JW3	$(Fe^{2+}_{1.65}Ca_{0.63}Mn_{0.43}Mg_{0.25})(Al_{1.89}Fe^{3+}_{0.15})(Si_{2.96}Al_{0.04})O_{12}$					
QC81-1	$(Fe^{2+}_{2.33}Mg_{0.39}Ca_{0.18}Mn_{0.13})(Al_{1.95}Fe^{3+}_{0.01})Si_{3.02}O_{12}$					
QC81-5	$(Fe^{2+}_{2}Ca_{0.47}Mg_{0.35}Mn_{0.13})(Al_{1.88}Fe^{3+}_{0.17}Cr_{0.01})(Si_{2.95}Al_{0.05})O_{12}$					
QC81-6	$(Fe^{2+}_{1.85}Ca_{0.63}Mn_{0.26}Mg_{0.25})(Al_{1.92}Fe^{3+}_{0.09})(Si_{2.99}Al_{0.01})O_{12}$					
HR02-71	$(Fe^{2+}_{1.79}Ca_{0.63}Mn_{0.39}Mg_{0.18})(Al_{1.91}Fe^{3+}_{0.11})(Si_{2.98}Al_{0.03})O_{12}$					

* Data from Darrell Henry (personal communication)

71, which lacks clinopyroxene, plots as the second most Ca-rich garnet group. While clinopyroxene may be absent, the high X_{Ca} value in these garnets may reflect the presence of another calcic phase: Ca-rich amphibole (Tables 4.2-4.6). In Figure 4.19, the samples with higher amounts of X_{Mn} are those with lower modal amounts of garnet present. Due to the preferential incorporation of Mn into garnet over other minerals, samples with lower amounts of garnet appear to be more enriched in Mn.

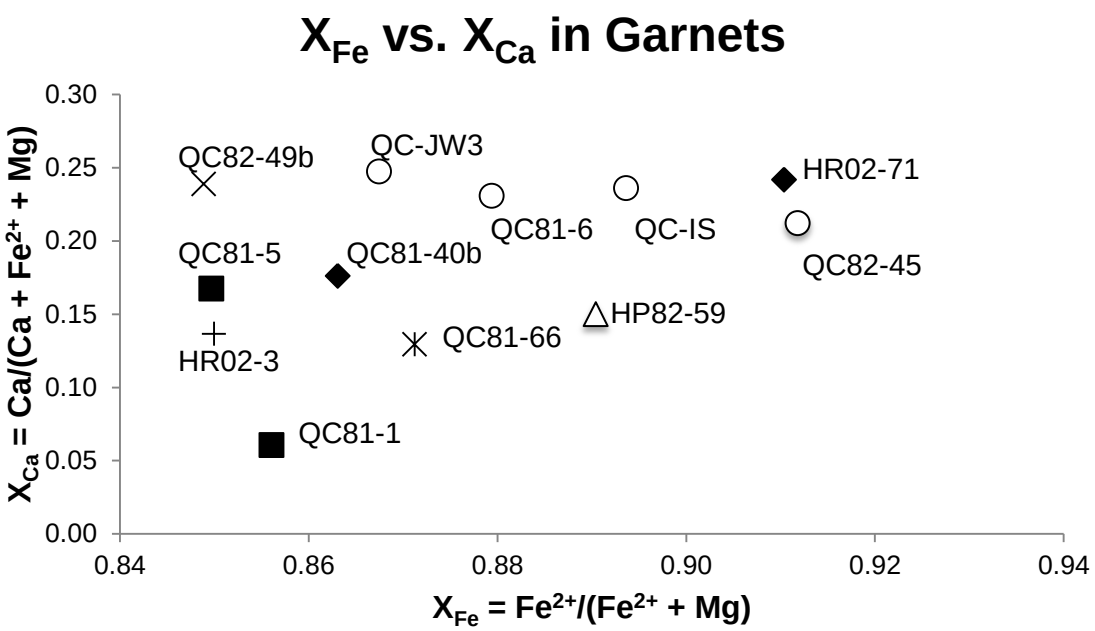

Figure 4.18. Variations in X_{Fe} and X_{Ca} in garnets from each sample. Mole fractions calculated using compositions in Table 4.7. Symbols denote different mineral assemblages: **O** opx + cpx + am; ■ opx + cpx + am + bt; ◆ opx + am; **Δ** opx + bt; □ opx + cpx + am + bt + pl; ◇opx; asterisk = opx + cpx + bt.

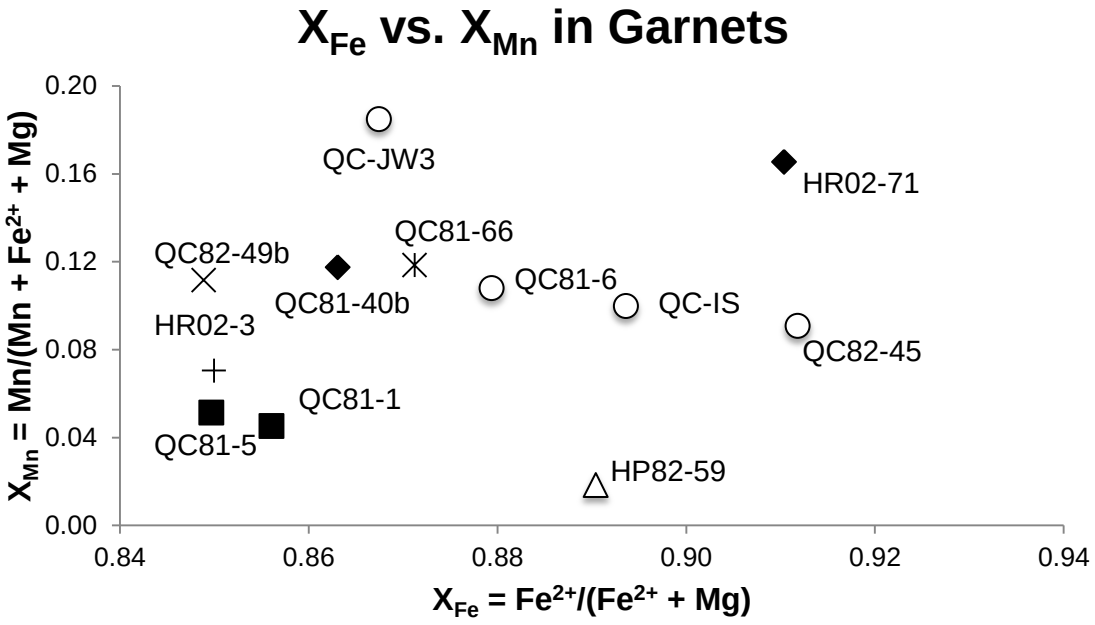

Figure 4.19. Variations in X_{Fe} and X_{Mn} in garnets from each sample. Mole fractions calculated using compositions in Table 4.7. Symbols denote different mineral assemblages: **O** opx + cpx + am; ■ opx + cpx + am + bt; ◆ opx + am; **Δ** opx + bt; □ opx + cpx + am + bt + pl; ◇opx; asterisk = opx + cpx + bt.

4.4.2 Pyroxene

Orthopyroxene is the dominant pyroxene found in all of these samples, however both orthopyroxene and clinopyroxene were analyzed in five of the twenty-six samples. The pyroxenes from these rocks are unzoned, and representative analyses (with structural formulae) of each pyroxene type in each sample are given in Tables 4.8 and 4.9. Tables of element wt% oxides from each analysis point in each sample can be found in Appendix B.

In the orthopyroxenes, X_{Fe} values range from 0.53-0.69, X_{Ca} values ranged from 0.002-0.037, X_{Mg} values ranged from 0.31-0.47 and X_{Mn} values ranged from 0.006-0.052. Ferrosilite is consistently the dominant orthopyroxene endmember component in all samples, with molecular percentages ranging from 53.98 to 71.12. The enstatite and wollastonite endmember components range from 26.99 to 45.13 and 0.24 to 3.99 percent respectively. Other cations like Mn^{2+}, Fe^{3+} and Al^{3+} can be incorporated into the orthopyroxene mineral structure and lead to elevated molecular components such as kanoite and aegerine. All representative orthopyroxene compositions plot within the ferrosilite field of Figure 4.20.

In the clinopyroxenes, X_{Fe} values are 0.46-0.53, X_{Ca} values are 0.45-0.47, X_{Mg} values are 0.47-0.54 and X_{Mn} values are 0.01-0.04. The clinopyroxenes are consistently dominated by the wollastonite endmember component, with molecular percentages ranging from 43.84 to 45.96. The enstatite and ferrosilite endmember components range from 25.23 to 29.85 and 25.25 to 29.42 percent respectively. Other cations like Mn^{2+}, Fe^{3+} and Al^{3+} can be incorporated into the clinopyroxene mineral structure and lead to elevated molecular components such as johannsenite (1.52-3.90), aegerine (0-

Table 4.8. Representative Orthopyroxene Compositions in wt%							
Sample	QC82-45*	QC81-66*	QC81-40b*	HP82-59	HR02-3	QC82-49b*	QC82-44
Analysis #	avg of 15	opx-1	avg of 4	avg of 11	avg of 16	avg of 7	avg of 10
SiO_2	48.54	49.86	50.30	48.86	49.31	49.76	49.28
Al_2O_3	0.40	0.59	0.71	0.75	0.85	0.59	0.78
TiO_2	0.06	0.04	0.01	0.03	0.01	0.01	0.01
Cr_2O_3	0.01	0.02	0.02	0.01	0.01	-----	0.02
Fe_2O_3 (calculated)	1.23	1.38	-----	3.12	2.95	1.26	1.63
FeO (calculated)	37.98	34.14	34.77	37.09	33.09	32.29	30.48
MnO	1.08	1.48	1.48	0.32	0.79	1.49	1.17
MgO	10.11	13.23	12.80	11.35	13.74	13.99	14.97
NiO	-----	-----	-----	-----	-----	0.01	-----
CaO	0.77	0.34	0.45	0.55	0.34	0.59	0.38
Na_2O	-----	-----	0.01	0.02	0.03	-----	0.02
K_2O	-----	-----	-----	0.01	0.01	-----	0.01
Total	100.18	101.08	100.54	102.11	101.12	99.99	98.74
Molecular Percent of Components							
Enstatite	28.04	35.68	34.70	32.42	38.25	37.70	41.26
Ferrosilite	62.91	55.17	56.68	60.43	53.45	52.04	49.38
Aegerine	-----	-----	-----	0.12	0.22	0.01	0.12
Esseneite	-----	-----	-----	-----	-----	-----	-----
Diopside	1.09	0.59	0.76	0.84	0.62	1.10	0.77
Hedenbergite	2.29	0.85	1.16	1.53	0.84	1.42	0.87
Johannsenite	-----	-----	-----	-----	-----	-----	-----
Kanoite	3.74	4.96	4.98	1.10	2.65	5.00	3.93
Molecular Percent of Components (renormalized by subtracting “other” species)							
Wollastonite	1.79	0.78	1.03	1.24	0.78	1.36	0.89
Enstatite	30.30	38.98	37.60	34.49	41.39	41.46	45.13
Ferrosilite	67.91	60.24	61.37	64.27	57.83	57.17	53.98
Structural Formulae for Representative Compositions							
QC82-45	$(Fe^{2+}_{1.29}Mg_{0.61}Mn_{0.04}Ca_{0.03}Fe^{3+}_{0.03})(Si_{1.97}Al_{0.02}Fe^{3+}_{0.01})O_6$						
QC81-66	$(Fe^{2+}_{1.13}Mg_{0.78}Mn_{0.05}Fe^{3+}_{0.03}Ca_{0.01})(Si_{1.96}Al_{0.03}Fe^{3+}_{0.01})O_6$						
QC81-40b	$(Fe^{2+}_{1.15}Mg_{0.76}Mn_{0.05}Al_{0.03}Ca_{0.02})(Si_{1.99}Al_{0.01})O_6$						
HP82-59	$(Fe^{2+}_{1.23}Mg_{0.67}Fe^{3+}_{0.06}Ca_{0.02}Mn_{0.01})(Si_{1.94}Al_{0.04}Fe^{3+}_{0.03})O_6$						
HR02-3	$(Fe^{2+}_{1.09}Mg_{0.81}Fe^{3+}_{0.06}Mn_{0.03}Ca_{0.01})(Si_{1.94}Al_{0.04}Fe^{3+}_{0.02})O_6$						
QC82-49b	$(Fe^{2+}_{1.07}Mg_{0.83}Mn_{0.05}Fe^{3+}_{0.03}Ca_{0.03})(Si_{1.97}Al_{0.03}Fe^{3+}_{0.01})O_6$						
QC82-44	$(Fe^{2+}_{1.01}Mg_{0.89}Fe^{3+}_{0.04}Mn_{0.04}Ca_{0.02})(Si_{1.96}Al_{0.04}Fe^{3+}_{0.01})O_6$						

(Table 4.8 continued)

Sample	QC-IS*	QC-JW3*	QC81-1*	QC81-5*	QC81-6*	HR02-71
Analysis #	avg of 7	avg of 21	opx-3	opx-3	avg of 6	avg of 12
SiO_2	48.96	49.79	49.81	49.15	50.02	47.58
Al_2O_3	0.45	0.46	0.78	0.64	0.53	0.32
TiO_2	-----	0.01	0.02	-----	-----	-----
Cr_2O_3	-----	0.01	0.01	-----	0.03	0.01
Fe_2O_3 (calculated)	1.98	0.74	1.34	1.05	-----	1.81
FeO (calculated)	35.63	31.99	33.29	34.64	36.00	36.65
MnO	1.30	2.96	0.44	0.58	1.43	2.60
MgO	11.65	12.55	14.42	12.80	11.45	9.29
NiO	-----	-----	-----	-----	-----	-----
CaO	0.65	1.64	0.11	0.42	0.76	0.76
Na_2O	-----	0.02	-----	0.04	-----	0.01
K_2O	-----	-----	-----	-----	-----	0.01
Total	100.62	100.17	100.21	99.33	100.21	99.05
Molecular Percent of Components						
Enstatite	31.95	30.30	40.75	36.32	31.21	23.53
Ferrosilite	58.64	50.45	53.69	56.65	59.34	62.23
Aegerine	-----	0.12	-----	0.31	-----	0.11
Esseneite	-----	-----	-----	-----	-----	-----
Diopside	1.04	2.88	0.20	0.72	1.18	1.05
Hedenbergite	1.78	4.12	0.26	1.09	2.09	2.33
Johannsenite	-----	-----	-----	-----	-----	-----
Kanoite	4.45	9.97	1.47	1.97	4.88	9.19
Molecular Percent of Components (renormalized by subtracting “other” species)						
Wollastonite	1.51	3.99	0.24	0.95	1.74	1.89
Enstatite	34.76	36.17	43.04	38.70	33.90	26.99
Ferrosilite	63.73	59.84	56.71	60.34	64.36	71.12
Structural Formulae for Representative Compositions						
QC-IS	$(Fe^{2+}_{1.19}Mg_{0.70}Mn_{0.04}Fe^{3+}_{0.04}Ca_{0.03})(Si_{1.96}Al_{0.02}Fe^{3+}_{0.02})O_6$					
QC-JW3	$(Fe^{2+}_{1.06}Mg_{0.74}Mn_{0.1}Ca_{0.07}Fe^{3+}_{0.02})(Si_{1.98}Al_{0.02})O_6$					
QC81-1	$(Fe^{2+}_{1.10}Mg_{0.85}Fe^{3+}_{0.04}Mn_{0.02}Ca_{0.01})(Si_{1.96}Al_{0.04})O_6$					
QC81-5	$(Fe^{2+}_{1.16}Mg_{0.77}Fe^{3+}_{0.03}Mn_{0.02}Ca_{0.02})(Si_{1.97}Al_{0.03})O_6$					
QC81-6	$(Fe^{2+}_{1.21}Mg_{0.68}Mn_{0.05}Ca_{0.03}Al_{0.03})Si_2O_6$					
HR02-71	$(Fe^{2+}_{1.27}Mg_{0.57}Mn_{0.09}Fe^{3+}_{0.04}Ca_{0.03})(Si_{1.96}Fe^{3+}_{0.02}Al_{0.02})O_6$					

* Data from Darrell Henry (personal communication)

Table 4.9. Representative Clinopyroxene Compositions in wt%					
Sample	QC82-45*	QC82-49b*	QC-IS*	QC-JW3*	QC81-6*
Analysis #	cpx-16	avg of 5	avg of 19	avg of 19	avg of 3
SiO_2	50.53	50.43	51.21	51.02	51.12
Al_2O_3	0.62	0.84	0.76	0.59	0.78
TiO_2	0.08	0.02	-----	-----	-----
Cr_2O_3	0.01	0.01	-----	-----	0.01
Fe_2O_3 (calculated)	0.72	0.94	0.41	1.52	0.84
FeO (calculated)	17.22	16.58	17.28	14.41	16.11
MnO	0.46	0.61	0.66	1.19	0.58
MgO	8.59	8.15	8.81	9.55	8.99
CaO	21.46	21.81	21.06	21.58	21.61
Na_2O	-----	0.14	0.13	-----	0.16
Total	99.69	99.53	100.32	100.02	100.18
Molecular Percent of Components					
Enstatite	4.82	3.55	5.58	5.10	4.66
Ferrosilite	5.42	4.05	6.14	4.31	4.69
Aegerine	-----	1.06	0.98	1.16	1.17
Esseneite	2.12	1.71	0.23	2.70	1.27
Diopside	40.24	40.37	39.66	44.86	42.46
Hedenbergite	45.26	46.09	43.64	37.96	42.69
Johannsenite	1.52	2.01	2.16	3.90	1.90
Kanoite	-----	-----	-----	-----	-----
Molecular Percent of Components (renormalized by subtracting “other” species)					
Wollastonite	44.65	45.96	43.84	44.90	45.05
Enstatite	26.05	25.23	26.74	29.85	27.40
Ferrosilite	29.30	28.81	29.42	25.25	27.55
Structural Formulae for Representative Compositions					
QC82-45	$(Ca_{0.90}Fe^{2+}_{0.56}Mg_{0.50}Fe^{3+}_{0.02}Mn_{0.02})(Si_{1.97}Al_{0.03})O_6$				
QC82-49b	$(Ca_{0.91}Fe^{2+}_{0.54}Mg_{0.48}Fe^{3+}_{0.03}Mn_{0.02}Na_{0.01}Al_{0.01})(Si_{1.97}Al_{0.03})O_6$				
QC-IS	$(Ca_{0.87}Fe^{2+}_{0.56}Mg_{0.51}Mn_{0.02}Al_{0.02}Fe^{3+}_{0.01}Na_{0.01})(Si_{1.98}Al_{0.02})O_6$				
QC-JW3	$(Ca_{0.89}Mg_{0.55}Fe^{2+}_{0.47}Fe^{3+}_{0.04}Mn_{0.04}Na_{0.01})(Si_{1.97}Al_{0.03})O_6$				
QC81-6	$(Ca_{0.90}Fe^{2+}_{0.52}Mg_{0.52}Fe^{3+}_{0.02}Mn_{0.02}Na_{0.01}Al_{0.01})(Si_{1.98}Al_{0.02})O_6$				

* Data from Darrell Henry (personal communication)

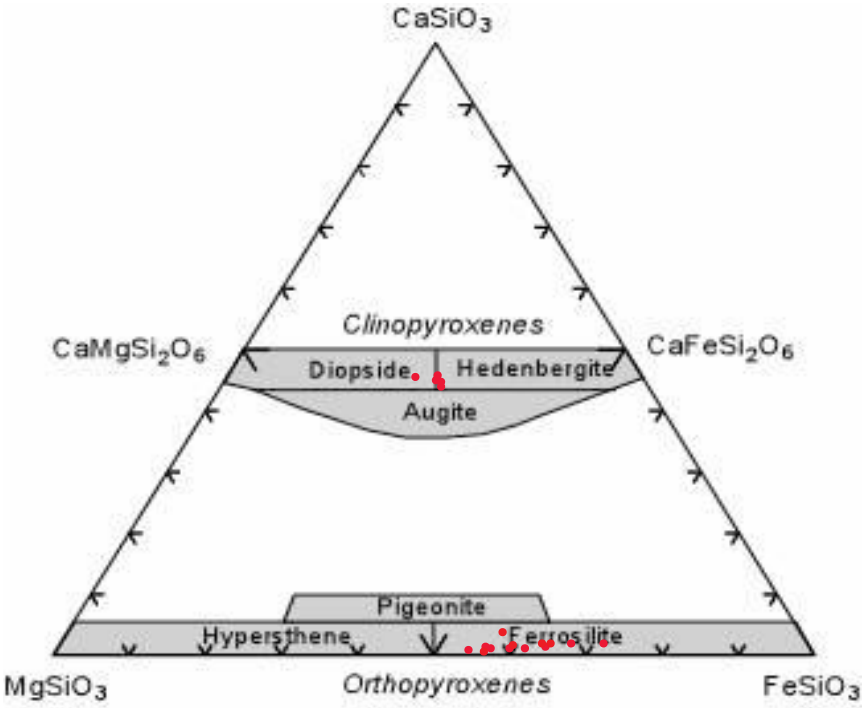

Figure 4.20. Wollastonite-enstatite-ferrosilite diagram showing locations of representative orthopyroxene and clinopyroxene compositions from each sample. Diagram taken from Professor Stephen A. Nelson: (www.tulane.edu/~sanelson/eens211/mineral_chemistry.htm)

1.17) and esseneite (0.23-2.70). Four of the representative clinopyroxene compositions fall within the hedenbergite field, and one falls within the diopside field (Figure 4.20). As with the garnets, there are chemical trends in the pyroxene data that relate to compositional factors associated with coexisting mineral assemblages (Figures 4.21-4.24). High X_{Ca} orthopyroxene values like those shown by QC-JW3 are likely a consequence of a more calcic bulk composition reflected by the abundance of clinopyroxene in that sample (refer to Tables 4.2-4.6). Additionally, lower modal amounts of garnet in some samples (e.g. QC-JW3, HR02-71) are associated with the orthopyroxenes being more enriched in Mn (almost double that of samples with higher garnet modes). Mole fraction values of Fe, Mg and Mn from coexisting orthopyroxenes

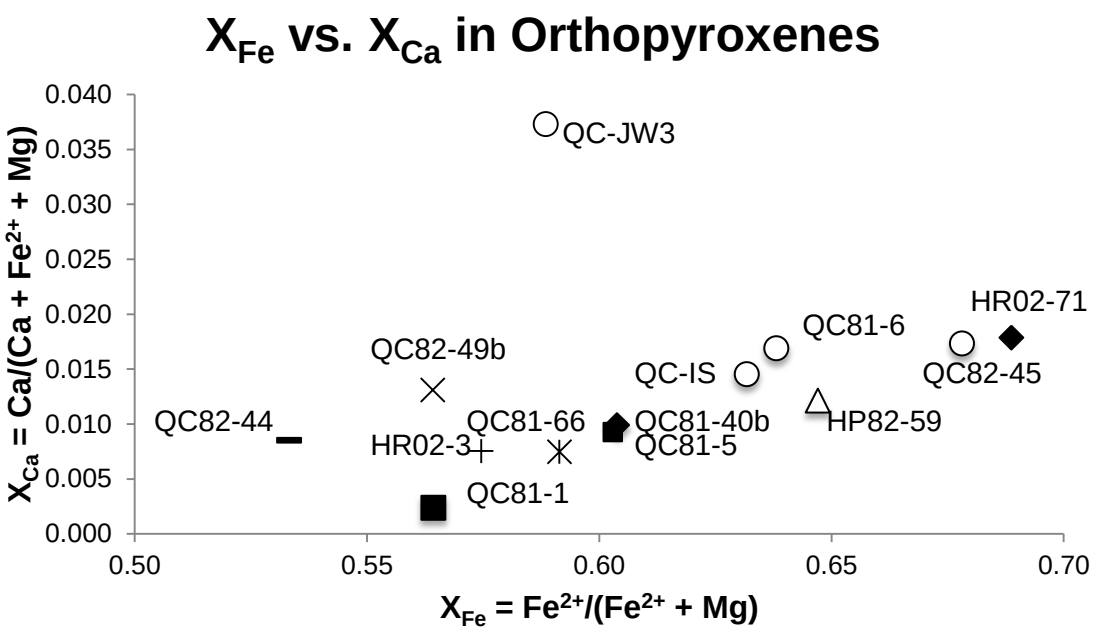

Figure 4.21. Variations in X_{Fe} and X_{Ca} in representative orthopyroxene compositions from each sample. Mole fractions calculated using compositions in Table 4.8. Symbols denote different mineral assemblages: **O** grt + cpx + am; ■ grt + cpx + am + bt; ◆ grt + am; **Δ** grt + bt; ▯ grt + cpx + am + bt + pl; ▯grt; asterisk = grt + cpx + bt; **−** am + pl.

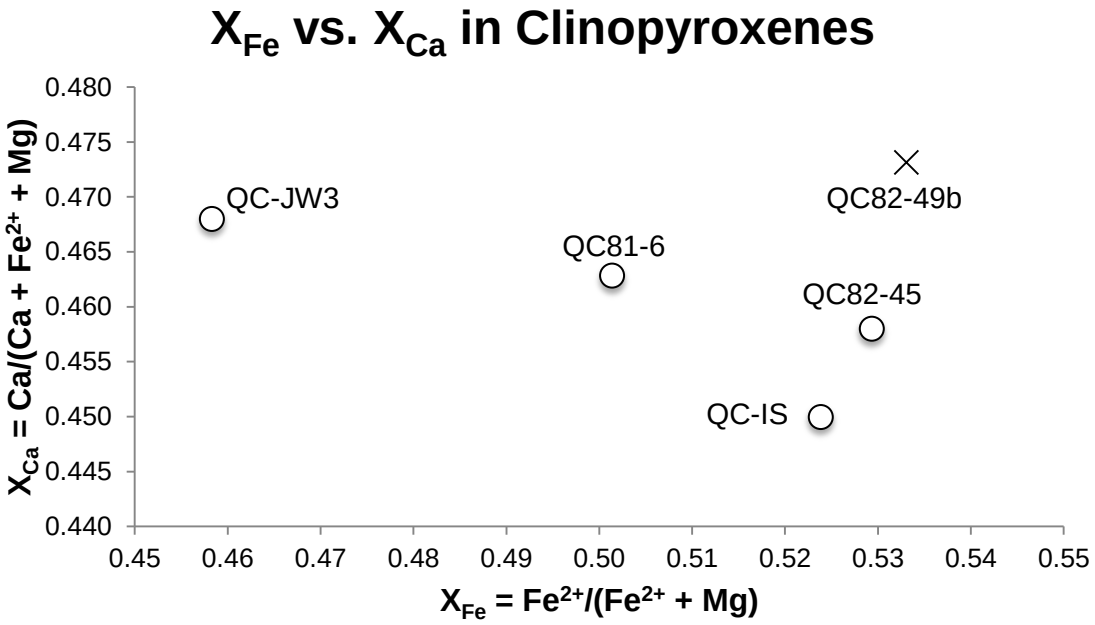

Figure 4.22. Variations in X_{Fe} and X_{Ca} in representative clinopyroxene compositions from each clinopyroxene-bearing sample. Mole fractions calculated using compositions in Table 4.9. Symbols denote different mineral assemblages: **O** grt + opx + am; ▯ grt + opx + am + bt + pl.

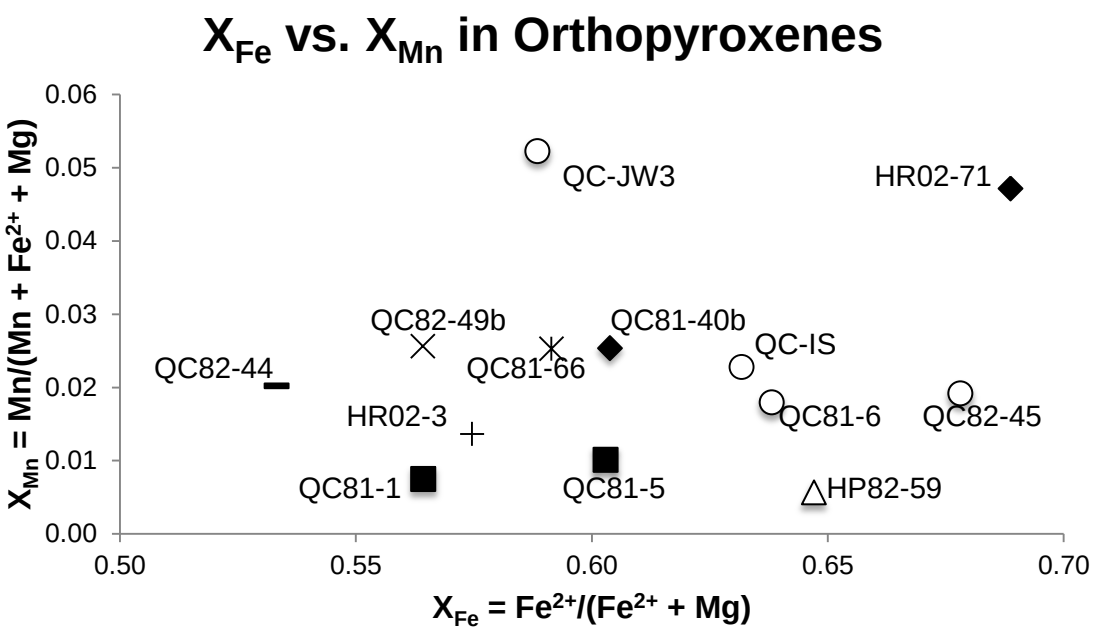

Figure 4.23. Variations in X_{Fe} and X_{Mn} in representative orthopyroxene compositions from each sample. Mole fractions calculated using compositions in Table 4.8. Symbols denote different mineral assemblages: **O** grt + cpx + am; ■ grt + cpx + am + bt; ◆ grt + am; **Δ** grt + bt; ▯ grt + cpx + am + bt + pl; ▯grt; asterisk = grt + cpx + bt; **−** am + pl.

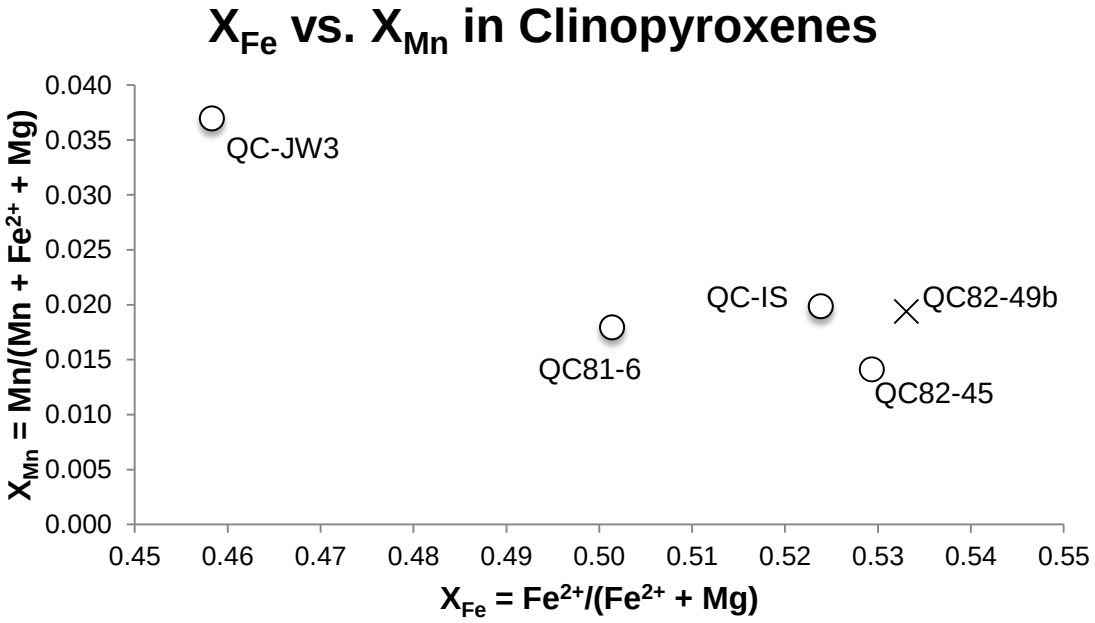

Figure 4.24. Variations in X_{Fe} and X_{Mn} in representative clinopyroxene compositions from each clinopyroxene-bearing sample. Mole fractions calculated using compositions in Table 4.9. Symbols denote different mineral assemblages: **O** grt + opx + am; ▯ grt + opx + am + bt + pl.

and clinopyroxenes in individual samples indicate that orthopyroxene partitions Fe and Mn more effectively than clinopyroxene, and clinopyroxene partitions Mg and Ca more effectively.

4.4.3 Feldspar

Feldspars are a less common occurrence in the iron-formations, but analytical data was determined from two samples: QC82-44 and QC82-49b. Many of the feldspars in these two samples exhibit ‘patchy’ zoning. Feldspars in QC82-44 are plagioclase feldspar with An-content between 43.18 and 53.86. QC82-49b contains both plagioclase (An-content between 64.51 and 85.77) and alkali feldspar (An-content between 0.48 and 5.47). The alkali feldspar in QC82-49b is enriched in barium and has a high celsian component, with the average reaching above ten molecular percent. Ba-rich alkali feldspar with a celsian component >5% is termed “hyalophane” (Deer et al., 2001; Henry et al., 2015). Chemical data from the two samples was normalized without the celsian component and plotted on an albite-anorthite-alkali feldspar ternary diagram (Figure 4.25). Feldspar chemistry from these two samples is summarized in Table 4.10. A table with all analysis points is found in Appendix C.

4.4.4 Amphibole

The amphiboles in these samples occur as matrix minerals, as inclusions in pyroxene and garnet, and, as a later overprint (secondary replacement phases). The chemistry varies depending on which type of amphibole is being considered (i.e. matrix, inclusion or replacement phase). Peak-metamorphic amphibole from Quad Creek samples contain concentrations of Cl ranging from 0.03 to 2.86 wt% (0.007–0.801 apfu) and secondary amphiboles have concentrations from 0 to 0.39 wt% Cl (0–0.117 apfu).

Cl concentrations from Hellroaring Plateau samples range between 0.1 and 0.11 wt% (0.025–0.027 apfu) in primary amphibole and 0 to 0.02 wt% (0–0.005 apfu) in secondary amphibole analyses. For reference, structural formulae for selected calcic amphibole endmembers found in the iron-formations are given in Table 4.11 (from Hawthorne et al., 2012). The chemistry and species classification of representative amphiboles from each sample are given in Tables 4.12 and 4.13. Complete tables of analysis points can be found in Appendix D.

Table 4.10. Representative Feldspar Compositions in wt%

Sample	QC82-44 (plag)	QC82-49b (plag)*	QC82-49b (kspar)*
Analysis #	avg of 18	avg of 13	avg of 7
SiO_2	56.79	47.97	60.81
Al_2O_3	27.40	32.42	19.79
FeO (measured)	0.18	0.16	0.07
MnO	-----	0.01	0.01
CaO	9.60	16.29	0.36
BaO	0.10	0.03	5.56
SrO	-----	0.08	0.07
Na_2O	5.73	2.09	1.05
K_2O	0.19	0.07	12.53
Total	99.98	99.12	100.25
Molecular Percent of Components			
Albite	51.25	18.76	9.90
Anorthite	47.47	80.80	1.89
Orthoclase	1.10	0.39	77.64
Celsian	0.18	0.05	10.57
Structural Formulae for Representative Feldspar Compositions			
QC82-44 (plagioclase)	$(Na_{0.50}Ca_{0.46}K_{0.01}Fe^{2+}_{0.01})(Si_{2.55}Al_{1.45})O_8$		
QC82-49b (plagioclase)	$(Ca_{0.81}Na_{0.19}Fe^{2+}_{0.01})(Si_{2.22}Al_{1.77})O_8$		
QC82-49b (hyalophane)	$(K_{0.76}Ba_{0.10}Na_{0.10}Ca_{0.02})(Si_{2.89}Al_{1.11})O_8$		

* Data from Darrell Henry (personal communication)

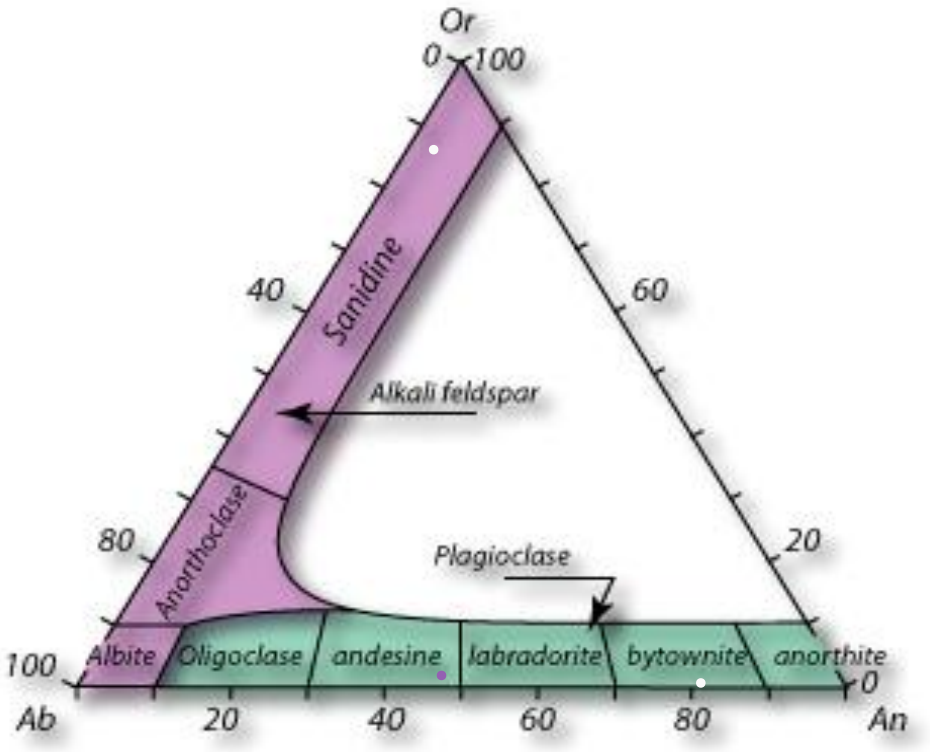

Figure 4.25. Ab-An-Or ternary diagram showing locations of representative plagioclase and alkali feldspar compositions from QC82-44 (purple dot) and QC82-49b (white dots).

Table 4.11. Structural Formulae for Primary Calcium Amphibole Endmembers	
Magnesio-ferri-hornblende	$\square Ca_2(Mg_4Fe^{3+})(Si_7Al)O_{22}(OH)_2$
Ferro-ferri-hornblende	$\square Ca_2(Fe_4^{2+}Fe^{3+})(Si_7Al)O_{22}(OH)_2$
Ferri-tschermakite	$\square Ca_2(Mg_3Fe_2^{3+})(Si_6Al_2)O_{22}(OH)_2$
Hastingsite*	$NaCa_2(Fe_4^{2+}Fe^{3+})(Si_6Al_2)O_{22}(OH)_2$
Ferro-pargasite*	$NaCa_2(Fe_4^{2+}Al)(Si_6Al_2)O_{22}(OH)_2$

* The prefix “Potassic” is used when $^{A}K > {}^{A}Na, {}^{A}Ca, {}^{A}\square$

4.4.4.1 Peak Metamorphic Amphibole

Metamorphic amphiboles found in the matrix or as inclusions in pyroxene and garnet are part of the calcium amphibole subgroup, which is defined as $^{B}Ca/{}^{B}(Ca + Na) \geq 0.75$ and $^{B}Ca/\Sigma B \geq {}^{B}\Sigma M^{2+}/\Sigma B$ where the sum of the small divalent cations in the B site

Table 4.12. Representative Amphibole Compositions in wt%									
Sample	QC-IS*	QC-JW3*	QC-JW3*	QC81-1*	QC81-5*	QC81-5*	QC81-6*	QC81-6*	QC81-45*
Type of Amphibole	matrix	matrix	alteration	alteration	incl. in opx	alteration	matrix	incl. in opx	matrix
Analysis #	avg of 13	avg of 7	am-2	am-4	am-1	am-3	avg of 3	am-3	avg of 3
SiO_2	39.70	41.19	52.37	52.96	37.51	53.02	39.19	39.42	39.34
TiO_2	0.12	0.02	-----	0.01	0.52	0.01	0.09	0.10	0.08
Al_2O_3	11.78	12.17	1.45	0.26	12.81	0.16	11.73	12.12	11.53
Cr_2O_3	0.01	-----	0.02	-----	0.01	-----	-----	-----	-----
MnO	0.26	0.59	0.78	0.24	0.05	0.46	0.25	0.26	0.37
FeO (calculated)	19.74	17.10	15.74	27.66	19.37	29.36	19.53	20.65	18.86
Fe_2O_3 (calculated)	5.80	6.44	3.02	-----	7.02	-----	5.63	4.24	6.44
NiO	0.01	0.01	0.04	-----	-----	-----	0.01	0.01	0.02
MgO	5.70	6.56	12.95	15.27	4.57	13.55	5.47	5.09	5.73
CaO	11.52	11.30	11.57	0.15	11.23	0.07	11.41	11.46	11.41
Na_2O	0.61	0.97	0.07	0.01	1.04	-----	0.71	0.82	0.75
BaO	0.19	0.03	-----	-----	-----	-----	0.11	0.11	0.13
K_2O	2.97	1.22	0.05	-----	2.30	-----	2.57	2.51	2.41
F	0.21	0.04	-----	0.01	-----	-----	0.13	0.12	0.12
Cl	1.34	1.09	0.06	-----	0.98	-----	1.53	1.56	1.69
H_2O^+ (calculated)	1.44	1.65	2.02	2.01	1.52	2.00	1.43	1.42	1.39
Total	101.00	100.13	100.13	98.58	98.71	98.63	99.37	99.50	99.82

* Data from Darrell Henry (personal communication) o Data from Darrel Henry (personal communication) and Nick Daigle

(Table 4.12 continued)

Sample	QC81-45*	QC82-44	QC82-45*	QC82-45*	QC82-45*	QC82-45*	QC82-46*	QC82-46*	QC82-47*
Type of Amphibole	incl. in opx	matrix	matrix	incl. in opx	incl. in grt	alteration	matrix	alteration	matrix
Analysis #	am-1	avg of 12	avg of 12	avg of 7	avg of 4	avg of 5	hbl-2	act-2	avg of 2
SiO_2	40.05	43.40	36.98	36.73	38.18	49.16	46.83	55.04	46.62
TiO_2	0.08	0.27	1.41	1.46	1.92	0.05	0.32	0.02	0.04
Al_2O_3	12.14	12.25	11.35	11.85	10.70	0.99	8.04	0.28	8.44
Cr_2O_3	0.08	0.02	0.04	0.02	0.04	0.01	-----	-----	0.01
MnO	0.46	0.31	0.16	0.19	0.17	0.83	0.36	0.19	0.18
FeO (calculated)	19.28	12.45	20.61	21.48	18.63	33.29	12.58	12.55	12.80
Fe_2O_3 (calculated)	6.55	8.27	6.84	7.21	7.78	1.07	8.11	2.98	6.33
NiO	-----	-----	0.01	-----	0.01	0.01	-----	-----	-----
MgO	5.49	9.48	3.83	3.20	4.94	9.13	11.23	15.84	11.06
CaO	11.46	10.81	11.46	11.48	11.38	0.67	11.32	12.80	11.43
Na_2O	0.74	1.01	0.58	0.61	1.02	0.02	0.67	0.02	0.79
BaO	0.09	-----	0.54	0.91	0.56	-----	-----	0.03	0.03
K_2O	2.31	0.72	3.26	3.25	2.37	0.03	0.50	-----	0.25
F	0.12	-----	0.05	0.11	0.12	0.02	0.04	0.05	-----
Cl	1.81	0.10	2.55	2.58	1.80	011	0.03	0.01	0.05
H_2O^+ (calculated)	1.38	1.93	0.85	0.80	0.92	1.89	1.92	2.04	2.01
Total	101.58	100.99	99.91	101.25	100.08	97.23	101.93	101.83	99.98

(Table 4.12 continued)

Sample	QC82-47*	QC82-48a*	QC82-48b*	QC82-49a*	QC82-49b*	HP82-59	HR02-71*	HR02-71^{o}
Type of Amphibole	incl. in opx	matrix	matrix	matrix	matrix	alteration	matrix	alteration
Analysis #	am-1	am-26	avg of 3	am-2	avg of 3	avg of 18	avg of 2	avg of 5
SiO_2	46.70	43.74	43.63	41.34	41.71	53.47	44.70	53.13
TiO_2	-----	0.12	0.17	0.14	0.18	0.06	0.23	0.01
Al_2O_3	8.59	10.82	10.57	12.42	12.50	1.44	8.23	0.29
Cr_2O_3	-----	0.01	0.01	0.01	0.01	0.01	0.05	-----
MnO	0.15	0.72	0.65	0.68	0.48	0.25	0.53	2.55
FeO (calculated)	13.51	11.89	13.20	14.96	15.64	20.15	17.84	32.47
Fe_2O_3 (calculated)	5.39	7.21	7.53	7.50	5.95	0.60	6.29	-----
NiO	-----	-----	-----	-----	-----	0.01	-----	-----
MgO	11.12	10.08	9.52	7.75	7.73	11.98	7.71	10.15
CaO	12.03	11.23	11.60	11.60	11.33	10.93	11.34	0.51
Na_2O	0.88	1.12	1.06	1.07	1.02	0.13	0.89	0.03
BaO	-----	0.02	0.03	0.08	0.02	0.02	0.03	0.02
K_2O	0.37	0.50	0.74	1.28	1.41	0.14	0.78	0.02
F	-----	-----	-----	-----	0.02	-----	-----	0.04
Cl	0.05	0.09	0.14	0.33	0.37	0.06	0.10	0.01
H_2O^+ (calculated)	2.01	1.97	1.92	1.85	1.83	1.99	1.89	1.93
Total	100.79	99.50	100.74	100.94	100.11	101.23	100.59	101.14

Table 4.13. Species and Representative Formulae from Amphiboles in Table 4.12			
Sample	Type of Amphibole	Amphibole Species	Structural Formulae for Representative Compositions
QC-IS	matrix	Potassic-hastingsite	$(K_{0.59}Na_{0.15}Ba_{0.01})(Ca_{1.93}Na_{0.04}Mn_{0.03})(Fe^{2+}_{2.59}Mg_{1.33}Fe^{3+}_{0.68}Al_{0.39}Ti_{0.01})(Si_{6.21}Al_{1.79})O_{22}((OH)_{1.51}Cl_{0.36}F_{0.10}O_{0.03})$
QC-JW3	matrix	Ferro-ferri-hornblende	$(K_{0.24}Na_{0.22})(Ca_{1.86}Na_{0.07}Mn_{0.06})\ (Fe^{2+}_{2.2}\ Mg_{1.5}Fe^{3+}_{0.74}Al_{0.54}Mn_{0.01})(Si_{6.33}Al_{1.67})O_{22}((OH)_{1.69}Cl_{0.29}F_{0.02})$
	alteration	Actinolite	$(Na_{0.01}K_{0.01})(Ca_{1.82}Mn_{0.1}Fe^{2+}_{0.07}Na_{0.01})(Mg_{2.84}Fe^{2+}_{1.87}Fe^{3+}_{0.29}Ni_{0.01})(Si_{7.7}Al_{0.25}Fe^{3+}_{0.05})O_{22}((OH)_{1.98}Cl_{0.02})$
QC81-1	alteration	Grunerite	$(Fe^{2+}_{1.94}Mn_{0.03}Ca_{0.02})(Mg_{3.43}Fe^{2+}_{1.54}Al_{0.03})(Si_{7.98}Al_{0.02})O_{22}((OH)_{1.99}F_{0.01})$
QC81-5	incl. in opx	Potassic-hastingsite	$(K_{0.47}Na_{0.28})(Ca_{1.93}Na_{0.04}Fe^{2+}_{0.03}Mn_{0.01})(Fe^{2+}_{2.57}Mg_{1.09}Fe^{3+}_{0.85}Al_{0.43}\ Ti_{0.06})(Si_{6.01}Al_{1.99})O_{22}((OH)_{1.61}Cl_{0.27}O_{0.13})$
	alteration	Grunerite	$(Fe^{2+}_{1.82}Mn_{0.06}Ca_{0.01})(Mg_{3.07}Fe^{2+}_{1.91}Al_{0.03})(Si_{8.05})O_{22}(OH)_{2.0}$
QC81-6	matrix	Potassic-hastingsite	$(K_{0.52}Na_{0.19}Ba_{0.01})(Ca_{1.94}Na_{0.03}Mn_{0.03})(Fe^{2+}_{2.59}Mg_{1.29}Fe^{3+}_{0.67}Al_{0.42}Ti_{0.01}Mn_{0.01})(Si_{6.22}Al_{1.78})O_{22}((OH)_{1.5}Cl_{0.41}F_{0.06}O_{0.02})$
	incl. in opx	Potassic-ferro-pargasite	$(K_{0.51}Na_{0.23}Ba_{0.01})(Ca_{1.95}Na_{0.03}Mn_{0.02})(Fe^{2+}_{2.74}Mg_{1.2}Al_{0.52}Fe^{3+}_{0.51}Ti_{0.01}\ Mn_{0.01})(Si_{6.26}Al_{1.74})O_{22}((OH)_{1.5}Cl_{0.42}F_{0.06}O_{0.02})$
QC81-45	matrix	Potassic-hastingsite	$(K_{0.49}Na_{0.19}Ba_{0.01})(Ca_{1.93}Na_{0.04}Mn_{0.03})(Fe^{2+}_{2.49}Mg_{1.35}Fe^{3+}_{0.77}Al_{0.36}Mn_{0.02}Ti_{0.01})(Si_{6.22}Al_{1.78})O_{22}((OH)_{1.47}Cl_{0.45}F_{0.06}O_{0.02})$
QC81-45	incl. in opx	Potassic-hastingsite	$(K_{0.46}Na_{0.17})(Ca_{1.9}Na_{0.05}Mn_{0.04})(Fe^{2+}_{2.5}Mg_{1.27}Fe^{3+}_{0.76}Al_{0.43}Mn_{0.02}\ Cr_{0.01}Ti_{0.01})(Si_{6.21}Al_{1.79})O_{22}((OH)_{1.45}Cl_{0.48}F_{0.06}O_{0.02})$
QC82-44	matrix	Magnesio-ferri-hornblende	$(Na_{0.15}K_{0.14})(Ca_{1.71}Na_{0.14}Fe^{2+}_{0.11}Mn_{0.04})(Mg_{2.09}Fe^{2+}_{1.43}Fe^{3+}_{0.92}Al_{0.54}\ Ti_{0.03})(Si_{6.41}Al_{1.6})O_{22}((OH)_{1.92}O_{0.06}Cl_{0.03})$
QC82-45	matrix	Potassic-hastingsite	$(K_{0.68}Na_{0.19}Ba_{0.02})(Ca_2)(Fe^{2+}_{2.81}Mg_{0.93}Fe^{3+}_{0.84}Al_{0.21}Ti_{0.17}Mn_{0.02}Cr_{0.01})(Si_{6.03}Al_{1.97})O_{22}((OH)_{0.92}Cl_{0.71}O_{0.35}F_{0.03})$
	incl. in opx	Potassic-hastingsite	$(K_{0.67}Na_{0.19}Ba_{0.04})(Ca_2Na_{0.01})(Fe^{2+}_{2.92}Fe^{3+}_{0.88}Mg_{0.77}Al_{0.22}Ti_{0.18}Mn_{0.03})(Si_{5.96}Al_{2.04})O_{22}((OH)_{0.88}Cl_{0.71}O_{0.36}F_{0.06})$
	incl. in grt	Potassic-hastingsite	$(K_{0.48}Na_{0.29}Ba_{0.02})(Ca_{1.96}Na_{0.03}Mn_{0.02})(Fe^{2+}_{2.5}Mg_{1.18}Fe^{3+}_{0.94}Ti_{0.23}Al_{0.14}Mn_{0.01}Cr_{0.01})(Si_{6.12}Al_{1.88})O_{22}((OH)_{0.99}Cl_{0.49}O_{0.46}F_{0.06})$

(Table 4.13 continued)

Sample	Type of Amphibole	Amphibole Species	Structural Formulae for Representative Compositions
QC82-45	alteration	Grunerite	$(K_{0.01})(Fe^{2+}_{1.77}Ca_{0.11}Mn_{0.11})(Fe^{2+}_{2.67}Mg_{2.17}Fe^{3+}_{0.13}Al_{0.03}Ti_{0.01})(Si_{7.84}Al_{0.16})O_{22}((OH)_{1.95}Cl_{0.03}O_{0.01}F_{0.01})$
QC82-46	matrix	Magnesio-ferri-hornblende	$(Na_{0.09}K_{0.09})(Ca_{1.77}Na_{0.1}Fe^{2+}_{0.09}Mn_{0.04})(Mg_{2.44}Fe^{2+}_{1.44}Fe^{3+}_{0.89}Al_{0.2}Ti_{0.04})(Si_{6.82}Al_{1.18})O_{22}((OH)_{1.9}O_{0.07}F_{0.02}Cl_{0.01})$
	alteration	Actinolite	$(Ca_{1.95}Fe^{2+}_{0.03}Mn_{0.02})(Mg_{3.35}Fe^{2+}_{1.46}Fe^{3+}_{0.18})(Si_{7.82}Fe^{3+}_{0.14}Al_{0.05})O_{22}((OH)_{1.97}F_{0.02})$
QC82-47	matrix	Magnesio-ferri-hornblende	$(Na_{0.12}K_{0.05})(Ca_{1.81}Na_{0.1}Fe^{2+}_{0.07}Mn_{0.02})(Mg_{2.43}Fe^{2+}_{1.51}Fe^{3+}_{0.7}Al_{0.35})(Si_{6.88}Al_{1.12})O_{22}((OH)_{1.98}Cl_{0.01}O_{0.01})$
QC82-47	incl. in opx	Magnesio-ferri-hornblende	$(Na_{0.19}K_{0.07})(Ca_{1.89}Na_{0.06}Fe^{2+}_{0.03}Mn_{0.02})(Mg_{2.43}Fe^{2+}_{1.63}Fe^{3+}_{0.6}Al_{0.34})(Si_{6.86}Al_{1.14})O_{22}((OH)_{1.99}Cl_{0.01})$
QC82-48a	matrix	Magnesio-ferri-hornblende	$(Na_{0.22}K_{0.1})(Ca_{1.8}Na_{0.11}Mn_{0.09})(Mg_{2.25}Fe^{2+}_{1.49}Fe^{3+}_{0.81}Al_{0.44}Ti_{0.01})(Si_{6.54}Al_{1.46})O_{22}((OH)_{1.95}O_{0.03}Cl_{0.02})$
QC82-48b	matrix	Magnesio-ferri-hornblende	$(Na_{0.23}K_{0.14})(Ca_{1.85}Na_{0.08}Mn_{0.07})(Mg_{2.12}Fe^{2+}_{1.65}Fe^{3+}_{0.84}Al_{0.36}Ti_{0.02}Mn_{0.01})(Si_{6.5}Al_{1.5})O_{22}((OH)_{1.93}O_{0.04}Cl_{0.04})$
QC82-49a	matrix	Hastingsite	$(Na_{0.25}K_{0.25})(Ca_{1.88}Na_{0.07}Mn_{0.06})(Fe^{2+}_{1.89}Mg_{1.75}Fe^{3+}_{0.85}Al_{0.46}Mn_{0.03}Ti_{0.02})(Si_{6.25}Al_{1.75})O_{22}((OH)_{1.88}Cl_{0.09}O_{0.03})$
QC82-49b	matrix	Ferro-ferri-hornblende	$(K_{0.27}Na_{0.22})(Ca_{1.85}Na_{0.08}Mn_{0.06}Fe^{2+}_{0.01})(Fe^{2+}_{1.98}Mg_{1.75}Fe^{3+}_{0.68}Al_{0.57}\ Ti_{0.02})(Si_{6.34}Al_{1.66})O_{22}((OH)_{1.85}Cl_{0.1}O_{0.04}F_{0.01})$
HP82-59	alteration	Actinolite	$(K_{0.03}Na_{0.02})(Ca_{1.72}Fe^{2+}_{0.24}Mn_{0.03}Na_{0.02})(Mg_{2.62}Fe^{2+}_{2.23}Al_{0.08}Fe^{3+}_{0.07}Ti_{0.01})(Si_{7.83}Al_{0.17})O_{22}((OH)_{1.97}Cl_{0.01}O_{0.01})$
HR02-71	matrix	Ferro-ferri-hornblende	$(Na_{0.18}K_{0.15})(Ca_{1.84}Na_{0.08}Mn_{0.07}Fe^{2+}_{0.01})(Fe^{2+}_{2.26}Mg_{1.74}Fe^{3+}_{0.72}Al_{0.25}Ti_{0.03}Cr_{0.01})(Si_{6.78}Al_{1.22})O_{22}((OH)_{1.92}O_{0.05}Cl_{0.03})$
	alteration	Grunerite	$(Fe^{2+}_{1.46}Mn_{0.33}Ca_{0.08}Na_{0.01})(Fe^{2+}_{2.65}Mg_{2.29}Al_{0.05})(Si_{8.05})O_{22}((OH)_{1.98}F_{0.02})$

is $^{B}\Sigma M^{2+} = {}^{B}Mg + {}^{B}Fe^{2+} + {}^{B}Mn^{2+}$ and the sum of all cations in the B site is $\Sigma B = {}^{B}Li + {}^{B}Na + {}^{B}\Sigma M^{2+} + {}^{B}Ca$ (Hawthorne et al., 2012). The calcic amphiboles are assigned a species name depending on their overall chemistry. Species present in these samples include potassic-hastingsite, magnesio-ferri-hornblende, ferro-ferri-hornblende, ferri-tschermakite, hastingsite and potassic-ferro-pargasite. Grains occurring as inclusions are exclusively potassic-hastingsite (refer to Tables 4.11-4.13 for structural compositions), whereas the matrix amphibole grains occur as various species. Primary amphiboles contain very significant amounts of Cl (up to 2.9 wt%) and also show elevated levels of K (up to 3.46 wt%), Ba (up to 1.09 wt%) and Ti (up to 2.0 wt%).

Trends between Cl and various cations are presented for the primary amphibole data. There is a positive correlation between Cl and X_{Fe}^{2+}, $Al^{[IV]}$, $K^{[XII]}$ and $Ba^{[XII]}$ (Figure 4.26). In addition, increasing the amounts of $X_{Mg}^{[VI]}$, $Si^{[IV]}$ and $Na^{[XII]}$ correlate with decreasing levels of Cl. Only one sample (QC82-45) has chemical data from the three types of primary amphibole (matrix, inclusion in pyroxene, inclusion in garnet). These data show noticeable trends between levels of Cl and the type of amphibole analyzed (Figure 4.27). Amphibole included in garnet are generally lower in wt% Cl (average of ~1.8) than amphibole included in pyroxene and matrix amphibole (averages of ~2.5 wt% Cl).

4.4.4.2 Secondary Amphibole

Secondary replacement amphibole phases (the ones mainly found altering pyroxenes) are actinolite, grunerite and/or cummingtonite. Actinolite falls within the calcic amphibole subgroup. Grunerite and cummingtonite, however, are placed within a

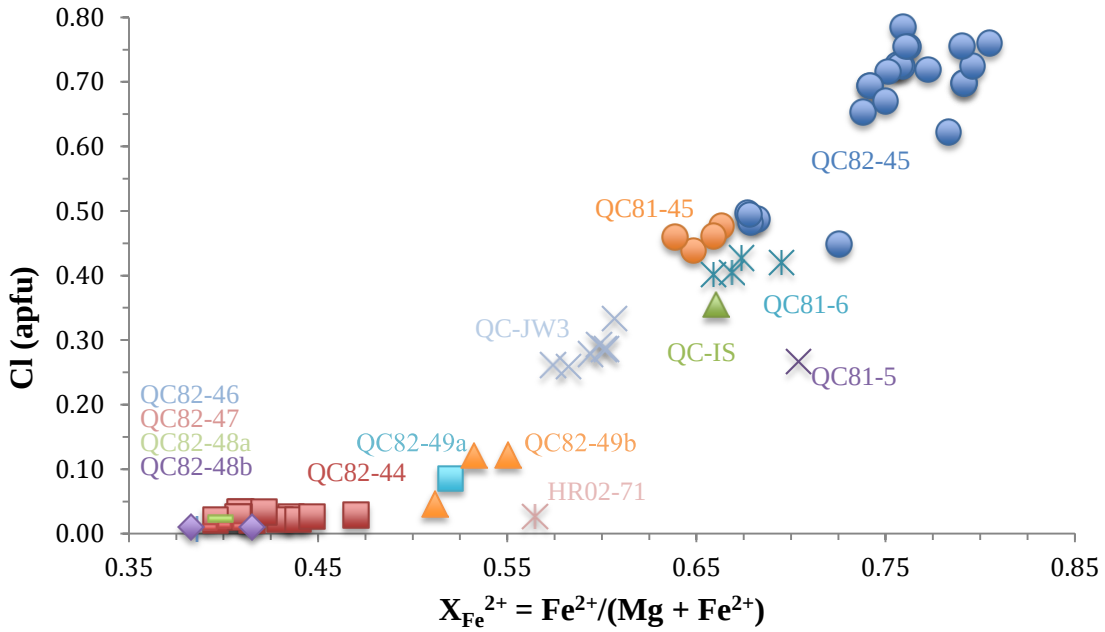

Figure 4.26. Relations between Cl and X_{Fe}^{2+} concentrations found in amphibole from iron-formations in the eastern Beartooth Mountains. Each dot represents a separate analysis. Maximum X_{Fe} and Cl (apfu) values are 0.8 and 0.78, respectively.

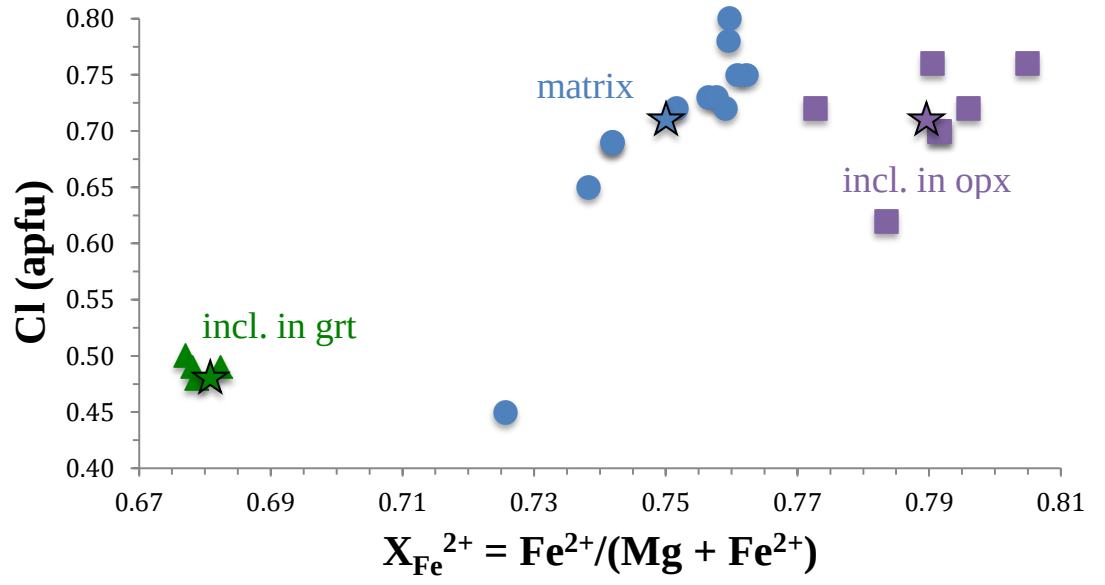

Figure 4.27. Variation in Cl concentration between matrix amphibole and amphibole present as inclusions in orthopyroxene and garnet from one iron-formation sample (QC82-45). Cl concentration in amphibole: matrix grains ≥ inclusions in opx > inclusions in grt. Each point represents an individual analysis. The stars represent averages for each type of amphibole.

separate group known as the magnesium-iron-manganese (Mg-Fe-Mn) subgroup of amphibole, defined as $^{B}(Ca + \Sigma M^{2+})/\Sigma B \geq 0.75$ and $^{B}\Sigma M^{2+}/\Sigma B > {}^{B}Ca/\Sigma B$. The secondary amphiboles contain relatively small amounts of Cl relative to primary amphibole, ranging from 0.01 to 0.39 wt%. They also contain much lower amounts of K_2O, BaO and TiO_2, all of which do not exceed more than 0.07 wt% in any of the analyses.

4.4.5 Biotite

Similar to metamorphic amphibole, the unusual occurrence and chemistry of the biotites in these samples can provide useful information on mineral associations/assemblages as well as on interactions with the metamorphic fluid. The biotite occurs as matrix grains and as inclusions in pyroxene and garnet, and, as with the amphiboles, the chemical composition of biotite differs depending whether or not it is in the matrix or an inclusion. Some biotite analyses from Quad Creek samples contain up to 3.4 wt% Cl. Hellroaring Plateau biotite analyses range from 0.16 to 0.26 wt% Cl. High amounts of BaO (up to 10.5 wt%) and TiO_2 (up to 6.9 wt%) are also present in these samples. Results are summarized in Tables 4.14 and 4.15. Tables showing each analytical point in these samples are provided in Appendix E.

Cl has systematic compositional variations with respect to other crystal chemical features. An increase in Cl in biotite is accompanied with increases in X_{Fe}^{2+}, $Al^{[IV]}$, $K^{[XII]}$ and $Ba^{[XII]}$ (Figure 4.28). Decreasing Cl content correlates with increasing $X_{Mg}^{[VI]}$, $Si^{[IV]}$ and $Na^{[XII]}$ (Figure 4.29). Sample QC82-45 has chemical data from all three types of biotite grains. For this sample, the biotites included in garnet are highest in Cl (~2.6–2.9 wt%), but overlap with matrix biotite (~2.4–2.8 wt%) and biotite included in orthopyroxene (~1.6–2.6 wt%) (Figure 4.30).

Table 4.14. Representative Biotite Compositions in wt%							
Sample	QC82-45*	QC82-45*	QC82-45*	QC81-113*	HR02-72*	HP81-82*	QC81-1*
Type of Biotite	matrix	incl. in grt	incl. in opx	incl. in opx	matrix	matrix	matrix
Analysis #	avg of 16	avg of 9	avg of 9	avg of 3	bt-2	avg of 3	bt-1
SiO_2	29.60	29.06	30.95	33.21	34.84	35.21	33.51
Al_2O_3	13.82	14.07	13.49	15.07	15.19	14.17	15.56
TiO_2	6.00	4.83	5.98	1.04	3.01	4.55	3.85
Cr_2O_3	0.02	-----	0.03	0.02	0.01	0.06	0.01
FeO (measured)	29.13	30.02	29.59	27.15	23.52	24.04	24.38
MnO	0.08	0.13	0.11	0.13	0.05	0.04	0.07
MgO	3.07	3.25	3.45	6.66	8.49	8.56	7.58
NiO	0.02	-----	0.01	0.02	-----	0.01	-----
CaO	0.01	0.04	-----	0.04	0.01	-----	0.01
BaO	8.78	9.60	6.20	2.84	0.64	-----	-----
Na_2O	0.04	0.04	0.05	0.09	0.13	0.05	0.11
K_2O	6.17	5.66	7.14	8.13	9.20	9.83	9.64
F	0.09	0.14	0.11	0.05	-----	0.08	-----
Cl	2.53	2.69	2.18	2.39	0.16	0.25	0.42
H_2O^+ (calculated)	2.83	2.73	2.99	3.02	3.77	3.76	3.66
Total	102.19	102.27	102.28	99.86	99.02	100.61	98.80

* Data from Darrell Henry (personal communication)

Table 4.15. Summary of Representative Biotite Compositions in Table 4.14		
Sample	Type of Biotite	Structural Formulae for Representative Compositions
QC82-45	matrix	$(K_{1.34}Ba_{0.59}\square_{0.06}Na_{0.01})(Fe^{2+}_{4.15}Mg_{0.78}Ti_{0.77}\square_{0.28}Mn_{0.01})(Si_{5.04}Al_{2.78})O_{20}((OH)_{3.22}Cl_{0.73}F_{0.05})$
	incl. in opx	$(K_{1.52}Ba_{0.41}\square_{0.06}Na_{0.02})(Fe^{2+}_{4.13}Mg_{0.86}Ti_{0.75}\square_{0.24}Mn_{0.02})(Si_{5.17}Al_{2.65})O_{20}((OH)_{3.33}Cl_{0.62}F_{0.06})$
	incl. in grt	$(K_{1.24}Ba_{0.65}\square_{0.09}Na_{0.01}Ca_{0.01})(Fe^{2+}_{4.32}Mg_{0.84}Ti_{0.63}\square_{0.2}Mn_{0.02})(Si_5Al_{2.85})O_{20}((OH)_{3.14}Cl_{0.79}F_{0.08})$
QC81-113	incl in opx	$(K_{1.71}Ba_{0.18}\square_{0.08}Na_{0.03}Ca_{0.01})(Fe^{2+}_{3.73}Mg_{1.63}Al_{0.38}Ti_{0.13}\square_{0.11}Mn_{0.02})(Si_{5.46}Al_{2.54})O_{20}((OH)_{3.31}Cl_{0.67}F_{0.03})$
HR02-72	matrix	$(K_{1.85}\square_{0.07}Na_{0.04}Ba_{0.04})(Fe^{2+}_{3.1}Mg_{1.99}Ti_{0.36}Al_{0.31}\square_{0.24}Mn_{0.01})(Si_{5.49}Al_{2.51})O_{20}((OH)_{3.96}Cl_{0.04})$
HP81-82	matrix	$(K_{1.95}\square_{0.04}Na_{0.02})(Fe^{2+}_{3.12}Mg_{1.98}Ti_{0.53}\square_{0.28}Al_{0.07}Cr_{0.01}Mn_{0.01})(Si_{5.47}Al_{2.53})O_{20}((OH)_{3.9}Cl_{0.07}F_{0.04})$
QC81-1	matrix	$(K_{1.96}Na_{0.03}\square_{0.01})(Fe^{2+}_{3.24}Mg_{1.8}Ti_{0.46}Al_{0.25}\square_{0.25}Mn_{0.01})(Si_{5.33}Al_{2.67})O_{20}((OH)_{3.89}Cl_{0.11})$

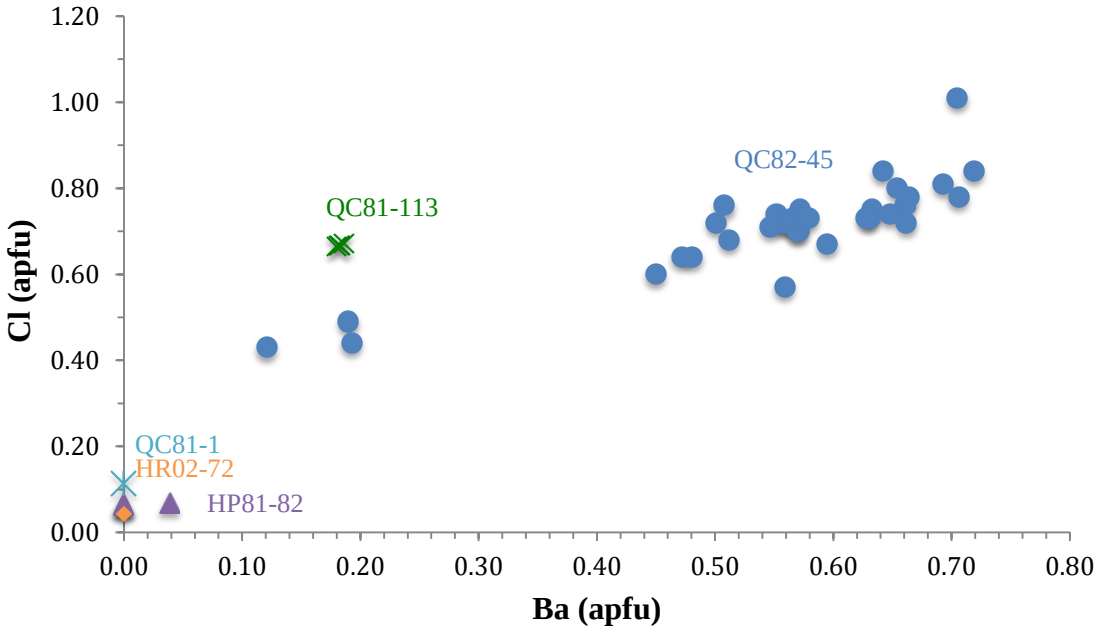

Figure 4.28. Cl and Ba concentrations found in biotite from iron-formation samples in the Beartooth Mountains. Cl concentrations are higher than Ba concentrations.

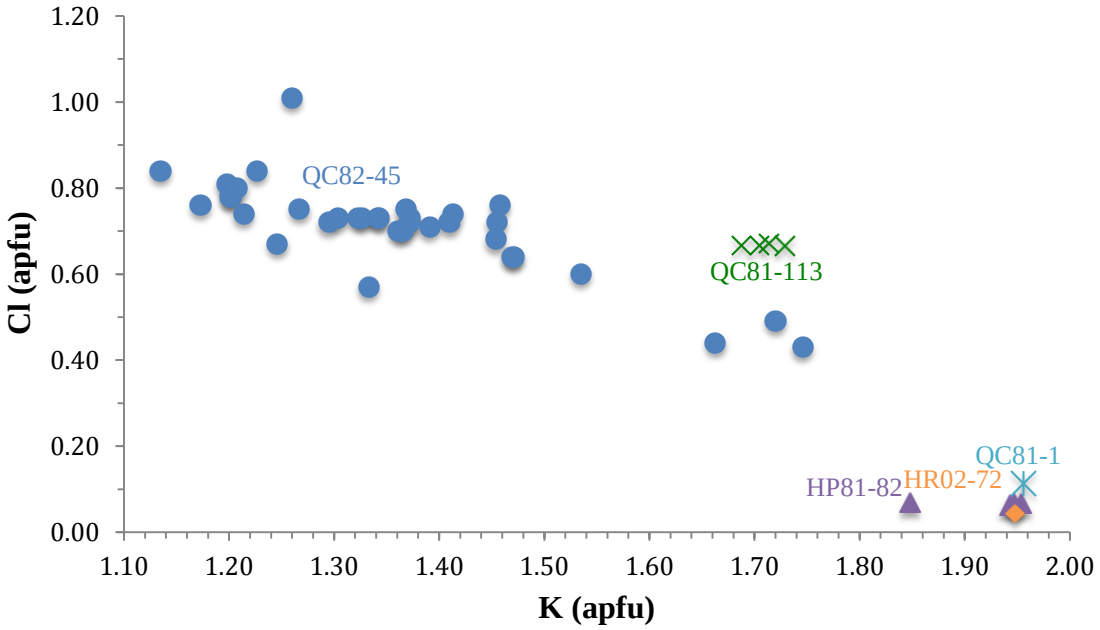

Figure 4.29. Cl and K concentrations found in biotite from iron-formation samples in the Beartooth Mountains. Cl concentrations are lower than K concentrations.

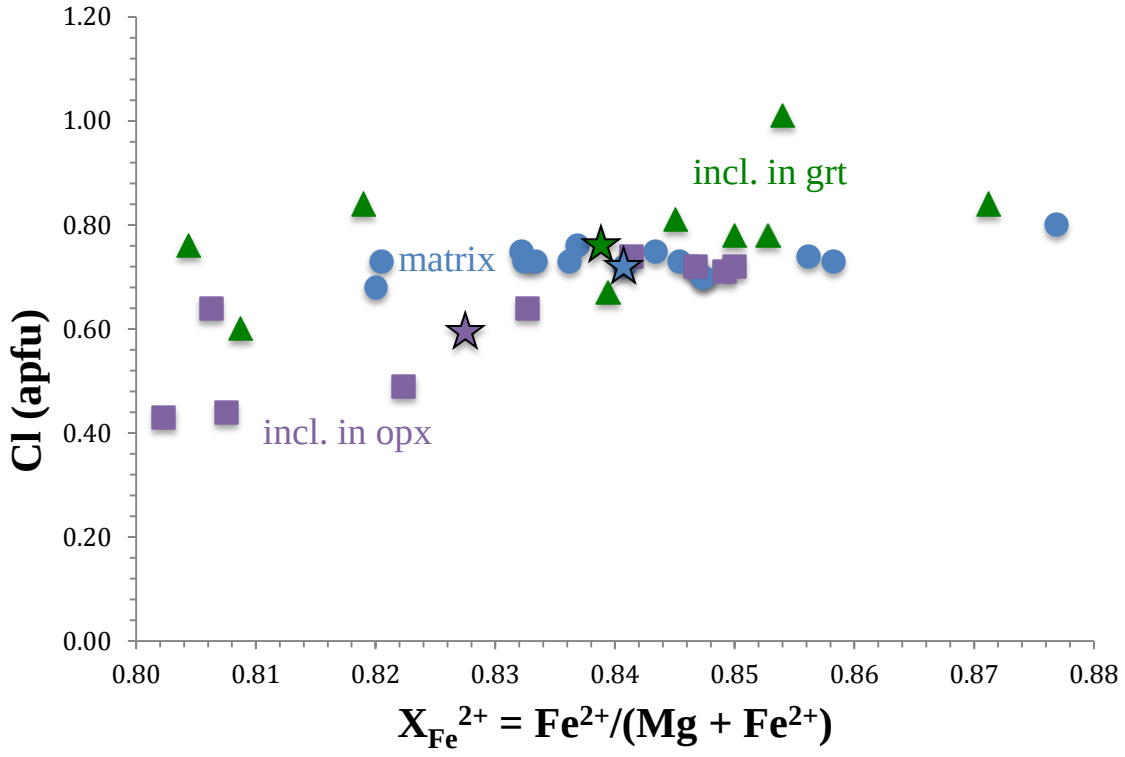

Figure 4.30. Variation in Cl concentration between matrix biotite and biotite present as inclusions in orthopyroxene and garnet from one iron-formation sample (QC82-45). Cl concentration in amphibole: inclusions in grt > matrix grains > inclusions in opx. Each point represents an individual analysis. The stars represent averages for each type of biotite.

4.5 Bulk Rock Chemistry

Bulk compositions for selected iron-formations from the Beartooth Mountains were calculated using a combination of mineral modes and mineral compositions (refer to methods). Because the composition of magnetite rarely changes during metamorphism, two separate bulk composition were calculated for each selected sample: one that incorporates magnetite and one that excludes magnetite (Table 4.16). The values in these tables are converted to moles of each element and are then

subsequently used as the input values for pseudosection calculations in Theriak Domino (de Capitani and Petrakakis, 2010).

Table 4.16. Bulk Compositions in wt% oxides										
With Magnetite										
Sample	SiO_2	Al_2O_3	Fe_2O_3	Cr_2O_3	TiO_2	FeO	MgO	MnO	CaO	Na_2O
QC-IS	44.08	2.17	20.99	-----	-----	24.43	4.63	0.79	2.89	0.01
QC-JW3 (Fe-band)	27.07	3.30	35.45	-----	-----	24.40	3.02	1.41	5.32	0.03
QC-JW3 (Qz-band)	87.59	0.04	6.28	-----	-----	4.21	0.73	0.13	1.01	0.01
QC81-6	39.17	4.78	25.77	0.01	-----	23.99	2.61	1.10	2.57	0.01
QC81-40b	40.30	3.10	25.41	0.01	-----	25.24	3.98	1.04	0.91	-----
QC81-66	42.15	6.45	17.41	0.01	0.01	26.37	4.50	1.80	1.30	-----
QC82-45	58.17	6.12	4.08	0.02	0.03	23.86	4.09	1.34	2.30	-----
HR02-3	55.03	6.63	9.31	0.01	0.01	21.89	4.61	1.04	1.46	0.01
HR02-71	47.88	2.85	21.37	-----	-----	22.59	2.66	1.46	1.18	-----
HP82-59 (Fe-band)	42.39	7.73	14.11	0.01	0.02	29.05	4.32	0.35	2.02	0.01
HP82-59 (Qz-band)	94.94	0.43	1.04	-----	-----	2.84	0.60	0.03	0.12	-----
Without Magnetite										
QC-IS	62.29	3.07	1.18	-----	-----	21.70	6.54	1.12	4.09	0.02
QC-JW3 (Fe-band)	54.54	6.64	1.45	0.01	-----	17.67	6.08	2.84	10.72	0.06
QC-JW3 (Qz-band)	96.23	0.04	0.10	-----	-----	1.57	0.81	0.14	1.11	0.01
QC81-6	62.01	7.56	0.57	0.01	-----	19.89	4.13	1.75	4.06	0.01
QC81-40b	63.54	4.89	0.29	0.02	-----	21.91	6.28	1.64	1.44	-----
QC81-66	55.96	8.56	0.52	0.02	0.02	24.84	5.98	2.38	1.72	-----
QC82-45	61.09	6.43	0.82	0.02	0.03	23.50	4.30	1.40	2.41	-----
HR02-3	62.77	7.41	1.39	0.01	0.01	20.44	5.16	1.16	1.63	0.01
HR02-71	68.32	4.06	1.05	-----	-----	18.98	3.79	2.09	1.69	-----
HP82-59 (Fe-band)	51.91	9.47	1.79	0.02	0.02	28.60	5.29	0.42	2.47	0.01
HP82-59 (Qz-band)	96.13	0.44	0.18	-----	-----	2.48	0.61	0.03	0.13	-----

CHAPTER V. DISCUSSION

The iron-formations investigated in this study are one of many Archean (~3.5 Ga) xenolithic lithologies (e.g. schists, migmatites, quartzites, metabasites) from the Beartooth Mountains, MT that were metamorphosed to peak conditions in the granulite facies (e.g. Mueller et al., 2014). These granulite-facies conditions are well-preserved in the meta-iron-formations as indicated by the dominance of anhydrous minerals (e.g. pyroxenes and garnets). However, the presence of amphibole and biotite associated with pyroxenes and garnets implies that the generally “hydrous” phases are stabilized in these rocks. Therefore, an unusual fluid must have been interacting with these rocks during peak metamorphism. The replacement of amphibole after pyroxene suggests that the meta-iron-formations underwent a subsequent episode of retrograde metamorphism at amphibolite-facies conditions. Evidence for this event is indicated by the late-stage alteration amphiboles rimming or partially/completely replacing pyroxene grains. A likely fluid source for the formation of these amphiboles is the emplacement of the ~2.8 Ga granitic LLMC intrusion (Henry et al., 2014).

The primary amphibole and biotite in this study are among some of the most chlorine-rich ever recorded, reaching up to 2.9 and 3.4 wt% Cl respectively. The maximum Cl observed in these minerals in other studies is 7.24 wt% and 7.45 wt% respectively (Table 1.1). Compositional and structural factors have been shown to have significant influences on the incorporation of Cl into these “hydrous” minerals (e.g. Volfinger et al., 1985; Morrison, 1991; Oberti et al., 1993; Makino et al., 1993). The positive correlations between Cl^- and larger cations like $Fe^{2+\,[VI]}$ (0.78Å), $Al^{[IV]}$ (0.39Å), $K^{[XII]}$ (1.64Å) and $Ba^{\{XII]}$ (1.61Å) suggest that, in sufficient concentrations, these larger

cations may help facilitate Cl incorporation by increasing the size of their respective structural sites in the crystal lattice, thus also expanding the anion site in amphibole and biotite (Figures 5.1 and 5.2). As granulite-facies temperatures are reached and hydrous minerals begin to dehydrate (lose OH^-) and break down, the increased amounts of these larger cations over smaller cations like $Mg^{[VI]}$ (0.72Å), $Si^{[IV]}$ (0.26Å) and $Na^{[XII]}$ (1.18Å) may expand the crystal lattice allowing the larger Cl^- (1.81Å) to replace OH^- (1.53Å) (Figure 5.2; e.g. Henry, 1988). The replacement of OH^- by Cl^- may in turn increase the stability field of these hydrous minerals into higher temperature conditions.

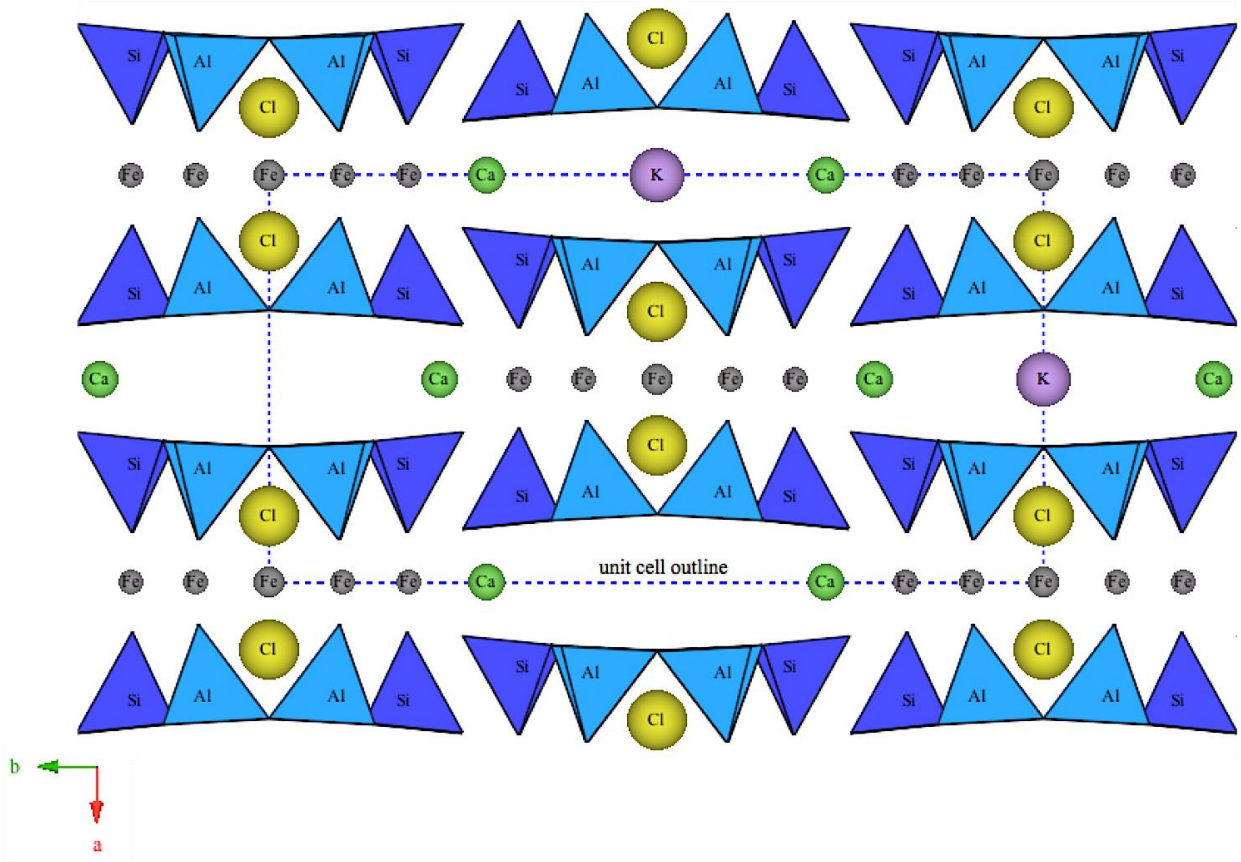

Figure 5.1. Crystal structure of a Cl-rich hastingsite (looking down the c-axis) showing locations and sizes of selected ions: Cl^- (1.81Å), K^+ (1.64Å), Ca^{2+} (1.12Å), Fe^{2+} (0.78Å), Al^{3+} (0.39Å) and Si^{4+} (0.26Å). Ions not pictured in figure include Ba^{2+} (1.61Å), Na^+ (1.18Å), Mg^{2+} (0.72Å), Ti^{4+} (0.61Å), F^- (1.33Å) and OH^- (1.53Å). Ionic radii from Klein et al., 2008. Data from Makino et al. 1993. Image generated using CrystalMaker®.

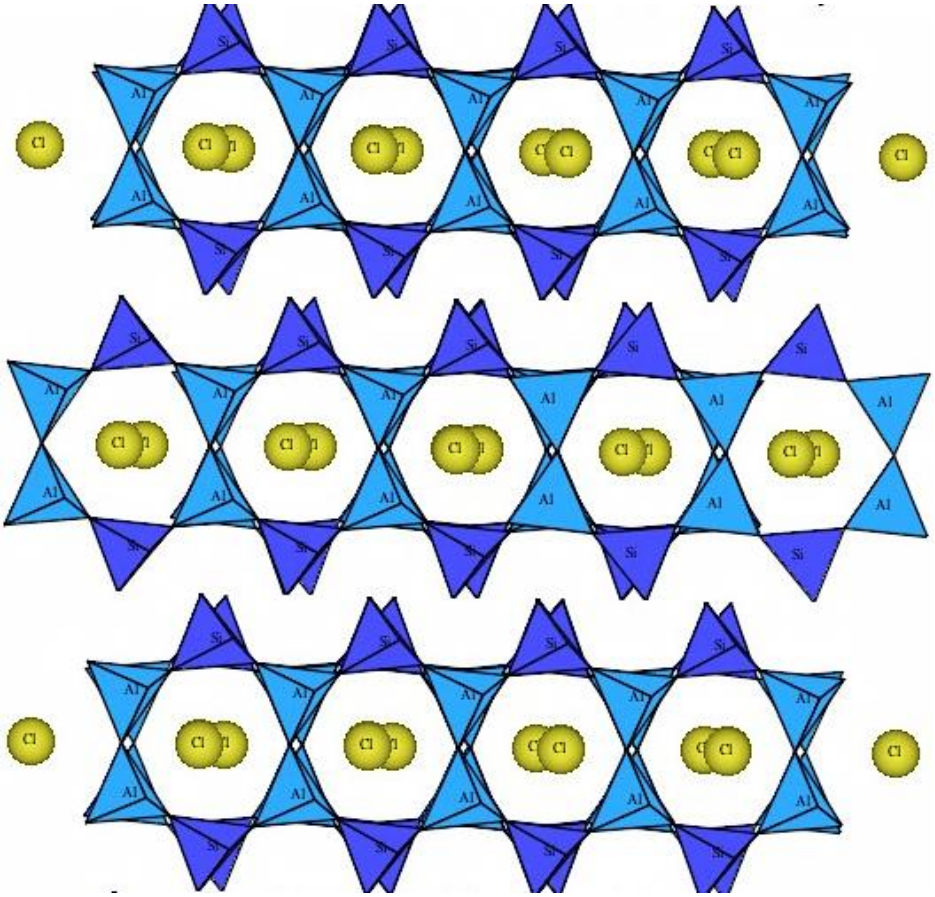

Figure 5.2. Same crystal structure from Figure 5.1 viewed looking down the a-axis to better illustrate the placement of Cl^- in the hydroxyl site in the amphibole structure.

A compilation of previous thermobarometry done on proximal lithologies from the eastern Beartooth Mountains indicates peak metamorphic conditions of 6-8 kbar and 775-850 °C (Figure 5.3; Henry et al., 1982; Maas and Henry, 2002; Will, 2013; Mueller et al., 2014). The garnet-amphibole-plagioclase-quartz barometer of Kohn and Spear (1990) suggests pressure conditions on the lower end of this range (~5-6 kbar), although barometry was only done on a single sample (Table 5.1). Hornblende-plagioclase thermometry and pyroxene-garnet thermometry indicate temperature

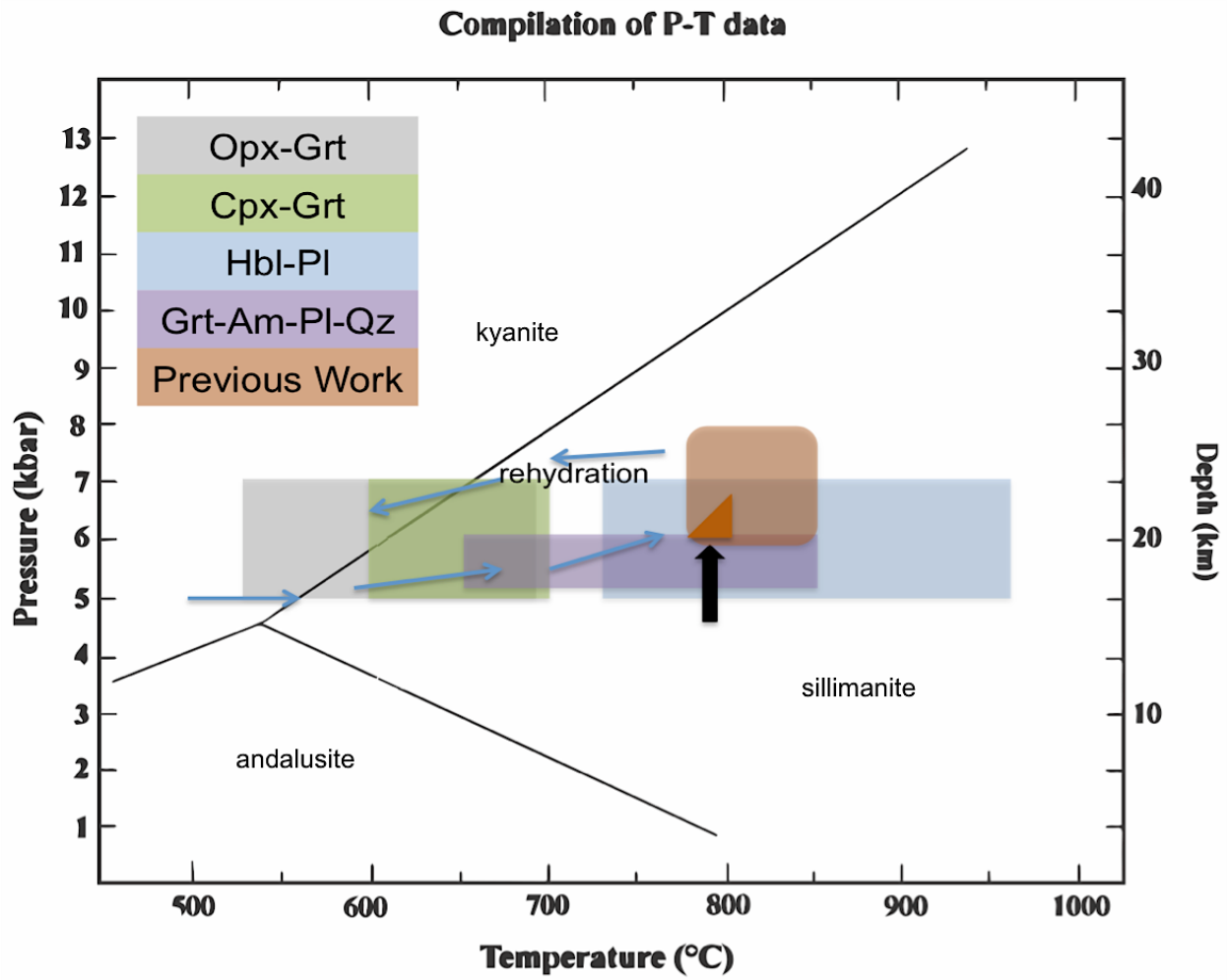

Figure 5.3. Compilation of P-T data from meta-iron-formations in this study and previous work (Henry et al., 1982; Maas and Henry, 2002; Will, 2013; Mueller et al., 2014). The orange triangle represents likely conditions of peak metamorphism based on the convergence of multiple lithologies in the Will (2013) study with previous work. The black arrow points to the bottom area across this triangle, representing the overlap of likely peak conditions determined by Will (2013) with the hbl-pl thermometry and grt-am-pl-qz barometry of the iron-formations in this study. Blue arrows represent the proposed P-T path by Mueller et al., 2014. Stability fields of the aluminosilicate polymorphs are superimposed for reference.

Table 5.1. Results of Garnet-amphibole-plagioclase-quartz Barometry*

Sample	Analyses Used			Pressures (kbar) at assumed temperatures				
	Grt	Am	Pl	650°C	700°C	750°C	800°C	850°C
QC82-49b	grt-12	am-11	avg of pl-10,11	5.14	5.37	5.6	5.83	6.06

* Kohn and Spear (1990) calibration; uncertainty is ±0.5 to ±1 kbar.

ranges of about 740-960 °C and 540-700 °C, respectively (Tables 5.2-5.4). The lower temperature values from pyroxene-garnet thermometry is most likely a result of continued exchange of iron and magnesium between garnet and pyroxenes during slow

Table 5.2. Results of Hornblende-plagioclase Thermometry*

Sample	Analyses Used		Temperatures (°C) at assumed pressures			
	Hbl	Pl	5 kbar	6 kbar	6.5 kbar	7 kbar
QC82-44	avg of 12	avg of pl-12,13,14,15, 20	724	724	724	724
			742	750	754	758
QC82-49b	avg of am-1,3	avg of pl-6,7	962	962	961	961
			930	939	944	949
	am-11	avg of pl-10,11	886	885	884	883
			882	890	895	899

* HB2 ’94 calibration of Holland and Blundy (1994); uncertainty is ± 40°C.

Table 5.3. Results of Garnet-orthopyroxene Thermometry*

Sample	Analyses Used		Temperatures (°C) at assumed pressures			
	Grt	Opx	5 kbar	6 kbar	6.5 kbar	7 kbar
HP82-59	avg of 20	avg of 11	610	616	619	622
HR02-3	avg of 18	avg of 16	619	625	628	631
HR02-71		avg of 12	604	609	612	615
QC-IS	avg of 10	avg of 7	581	586	588	591
QC-JW3	grt-1	opx-1 (core)	582	587	589	592
QC81-1	grt-2	opx-3	531	537	539	542
QC81-5	grt-4	opx-3	677	683	686	689
QC81-6	grt-1	opx-5	648	654	656	659
QC82-45	grt-20	opx-19	612	617	620	623
	grt-8 (traverse 1)	opx-9	666	671	674	677
QC82-49b	avg of grt-1,2,3	avg of opx-6,7,8	669	674	677	680
	avg of grt-11,12	avg of opx-9,10	602	607	610	613
	grt-12	opx-13	613	619	622	624

* Sen and Bhattacharya (1984) calibration; uncertainty is ± 60°C.

Table 5.4. Results of Garnet-clinopyroxene Thermometry*						
Sample	Analyses Used		Temperatures (°C) at assumed pressures			
	Grt	Cpx	5 kbar	6 kbar	6.5 kbar	7 kbar
QC-IS	avg of 10	avg of 19	687	692	694	697
QC-JW3	grt-1	cpx-6 (core)	684	689	691	694
	grt-1	cpx-8 (core)	686	691	693	695
	grt-1	cpx-1 (core)	670	674	677	679
	grt-6	cpx-5	604	608	611	613
	grt-2’	cpx-1’	689	694	696	699
QC81-6	grt-1	cpx-7	691	696	698	701
QC82-45	avg of 68	cpx-16	637	642	645	647
QC82-49b	avg of grt-1,2,3	avg of cpx-4,5	632	637	639	641
	grt-12	cpx-14	628	633	636	638

* Nakamura (2009) calibration; uncertainty is ± 74°C.

cooling of the rocks. Rehydration associated with the amphibolite-facies overprinting event may have also locally reset some of the garnets and pyroxenes, causing them to be out of equilibrium with one another and reflect retrograde metamorphic conditions.

Equilibrium assemblage diagrams were generated using the effective bulk composition (without magnetite) for two samples containing primary amphibole to use as comparisons with thermobarometric calculations (QC-IS and QC82-45). The primary mineral assemblage for both of these samples is grt + opx + cpx + am, resulting in a large stability field ranging from ~3-13 kbar and ~500-760 °C for sample QC-IS (Figure 5.4). Isopleths for the almandine component of garnet and hedenbergite component of clinopyroxene were used to better constrain a probable P-T range. This results in a pressure of ~5 kbar and temperature of ~700 °C. For sample QC82-45 (Figure 5.5), the primary mineral assemblage is only found at ~755 °C from 5-10 kbar. The use of garnet

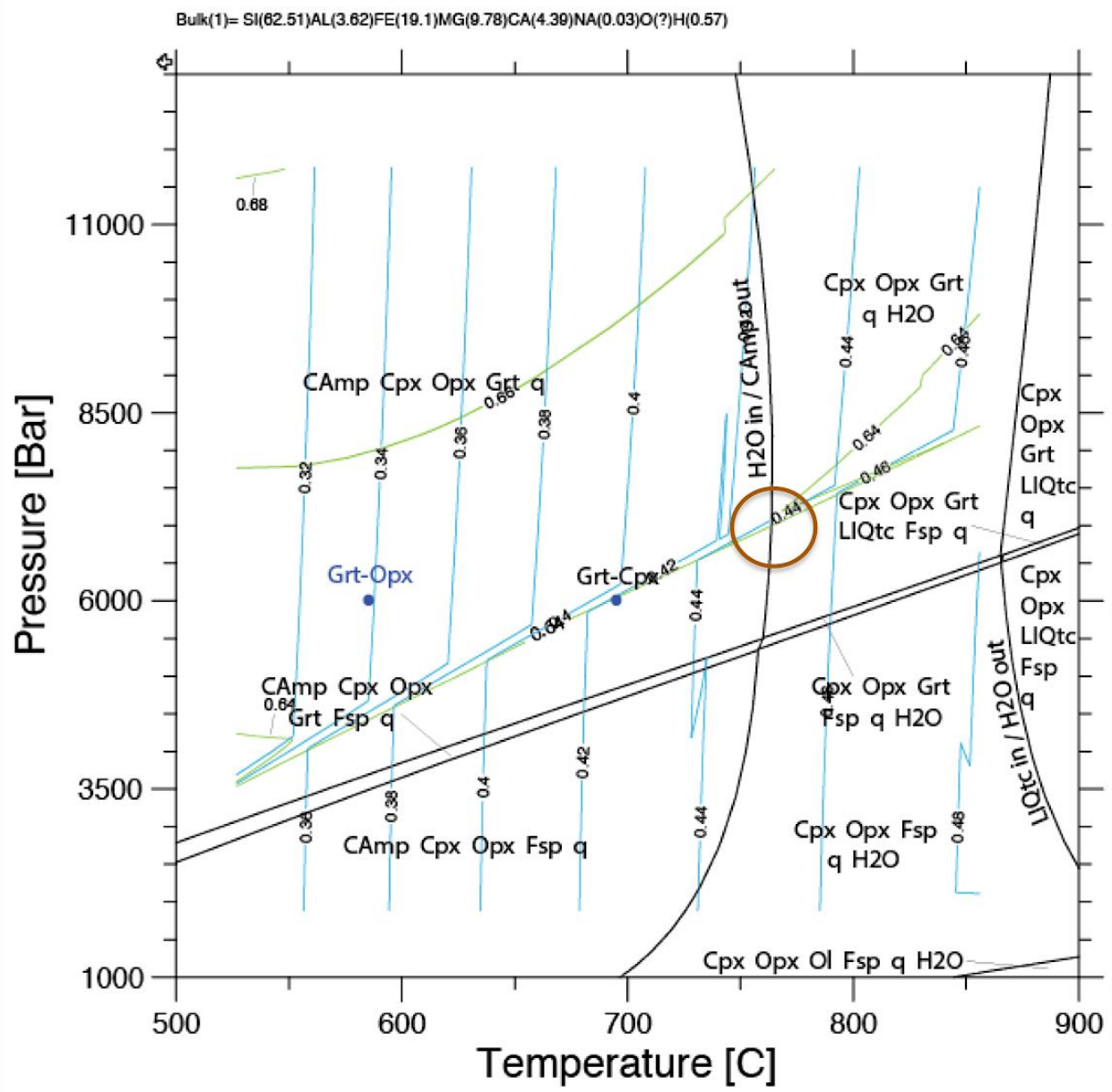

Figure 5.4. Pseudosection for sample QC-IS illustrating area of stability field for the primary mineral assemblage of grt + opx + cpx + am. Garnet isopleths are shown in green (almandine component in this sample is 0.64) and clinopyroxene isopleths are shown in blue (hedenbergite component in this sample is 0.43). Results from grt-opx and grt-cpx thermometry are also plotted (blue dots). Orange circle indicates the likely area of peak metamorphism conditions based on the intersection of the isopleth values with the stability area of the primary mineral assemblage. The circle does not coincide with P-T calculations (explained in text). Non-standard abbreviations are: CAmp = calcic amphibole, q = quartz, Fsp = feldspar, Ol = olivine, LIQtc = melt.

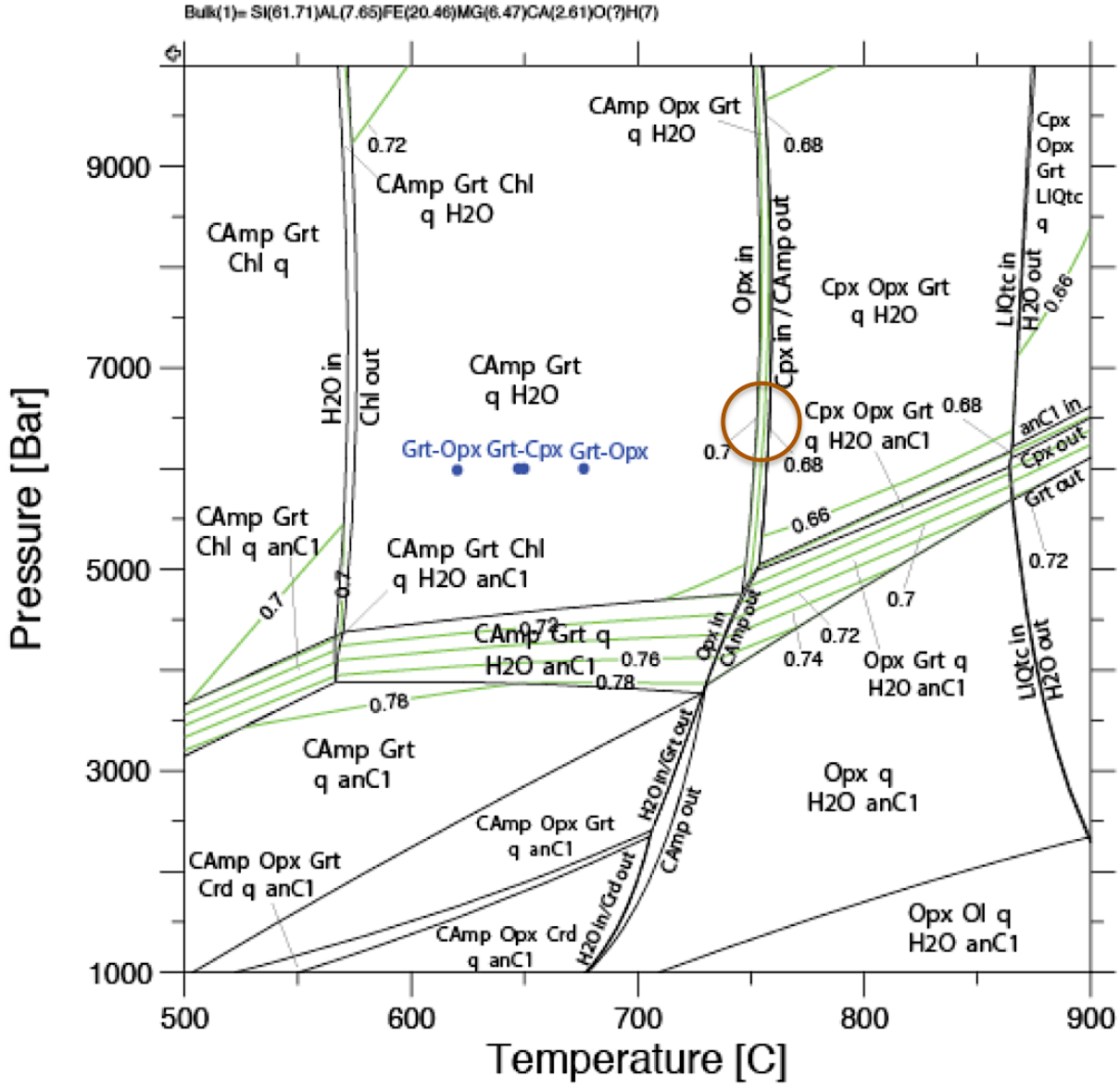

Figure 5.5. Pseudosection for sample QC82-45 illustrating area of stability field for the primary mineral assemblage of grt + opx + cpx + am. Garnet isopleths are shown in green (almandine component in this sample is 0.67). Results from grt-opx and grt-cpx thermometry are also plotted in blue. Orange circle indicates the likely area of peak metamorphic conditions based on the intersection of the isopleth values with the stability area of the primary mineral assemblage. The circle does not coincide with P-T calculations (explained in text). Non-standard abbreviations are: CAmp = calcic amphibole, q = quartz, anC1 = feldspar, Ol = olivine, LIQtc = melt.

isopleths results in a similar stability field. Amphiboles are generally stable up to ~750°C, at which point hydrous minerals tend to dehydrate into more anhydrous minerals. According to these pseudosections, the maximum temperature experienced by both of these samples is close to/right on the upper boundary of amphibole stability. However, the amphiboles from these iron-formations are atypical in that they contain elevated levels of Cl, Ti and Ba. The addition of these components can extend the stability field of the amphiboles and prevent them from breaking down until higher temperatures are reached. Therefore, with additional components, the maximum temperature boundary at which the amphiboles will dehydrate may actually be slightly higher than ~750 °C in these rocks.

Log values of halogen fugacity ratio calculations for coexisting aqueous fluids from biotites indicate samples from the Quad Creek and Hellroaring Plateau areas were in contact with a Cl-rich fluid aqueous phase. Mole fraction of fluorine in selected biotites was relatively low, ranging from 0 to 0.04. Mole fraction of chlorine in these biotites was significantly higher, ranging from 0.01 to 0.25. Fugacity ratios from the meta-iron-formations become increasing negative as temperature rises, with ratios falling between ~ -2.7 and -3.6 at a temperature of 750 °C (Figure 5.6), and between ~ -3.0 and -3.9 at a temperature of 800 °C (Figure 5.7). The numbers calculated for the Beartooth iron-formations are more negative than the values in the Munoz and Swenson study, suggesting the biotites in this study were interacting with a more Cl-rich fluid than the biotites used by Munoz and Swenson (1981).

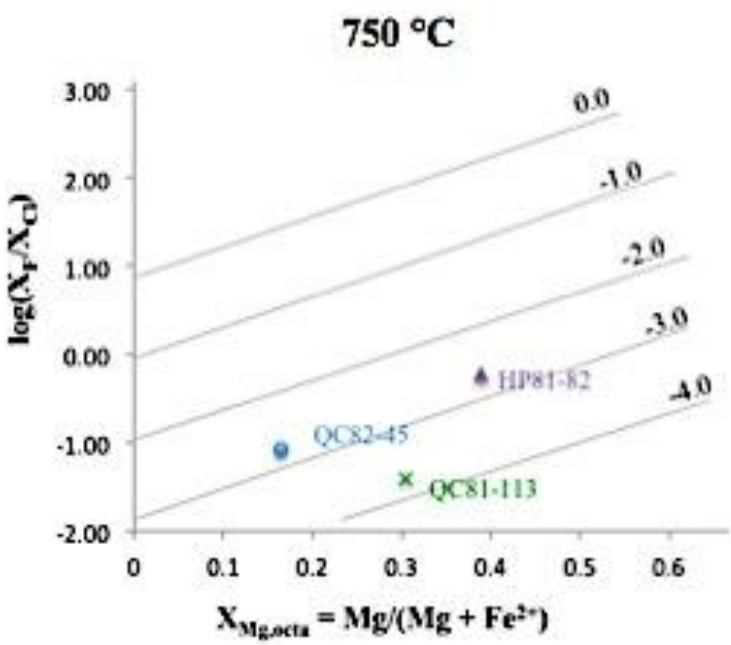

Figure 5.6. adapted from Munoz and Swenson (1981). Relationship between $\log(X_F/X_{Cl})$ vs. X_{Mg} in the octahedral site from multiple suites of biotite-bearing rocks assuming an equilibrium temperature of 750 °C. Diagonal lines represent lines of constant $\log(f_{HF}/f_{HCl})_{fluid}$. Each sample represents the average value from all analysis points in that sample. Biotite analyses containing 0 wt% fluorine were not included.

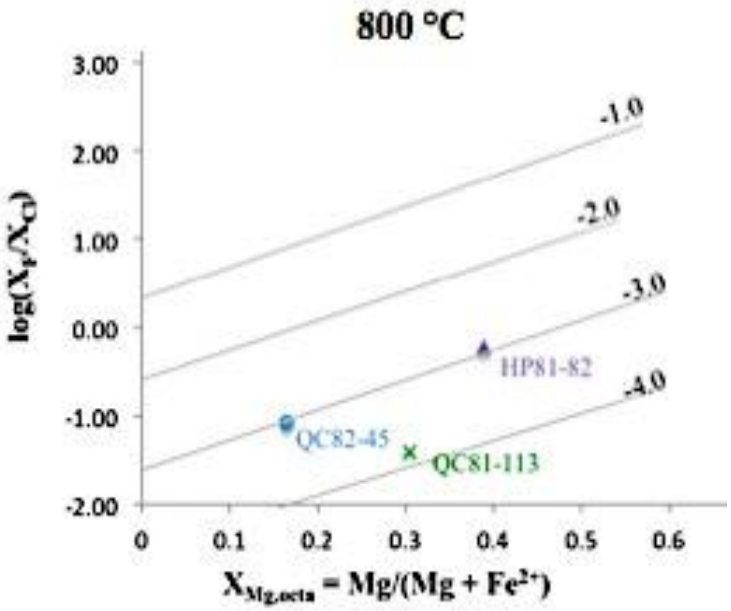

Figure 5.7. adapted from Munoz and Swenson (1981). Relationship between $\log(X_F/X_{Cl})$ vs. X_{Mg} in the octahedral site from multiple suites of biotite-bearing rocks assuming an equilibrium temperature of 800 °C. Diagonal lines represent lines of constant $\log(f_{HF}/f_{HCl})_{fluid}$. Each sample represents the average value from all analysis points in that sample. Biotite analyses containing 0 wt% fluorine were not included.

When the three types of primary biotite analyses are considered from one sample (QC82-45), the matrix grains are generally more enriched in Cl than the biotite inclusions in orthopyroxene and garnet (Figure 5.8). Because mineral inclusions form prior to their host, this trend suggests the composition of the metamorphic fluid became increasingly Cl-rich as the rocks experienced progressive metamorphism (temperature increased). During progressive metamorphism, the hydrous fluid will become increasingly dehydrated and migrate upwards because it is less dense than the surrounding rocks. As the brine becomes more saline, the biotites will partition chlorine from the fluid, causing these later-formed matrix biotites to be more enriched in Cl than earlier biotites. Additionally, increased amounts of Fe^{2+} over Mg (and the distribution of these cations in the octahedral site) correlates with incorporation of Cl into these minerals. This relationship is referred to as the "Mg-Cl avoidance" rule (Munoz and Swenson, 1982; Volfinger et al., 1985; Makino et al., 1993).

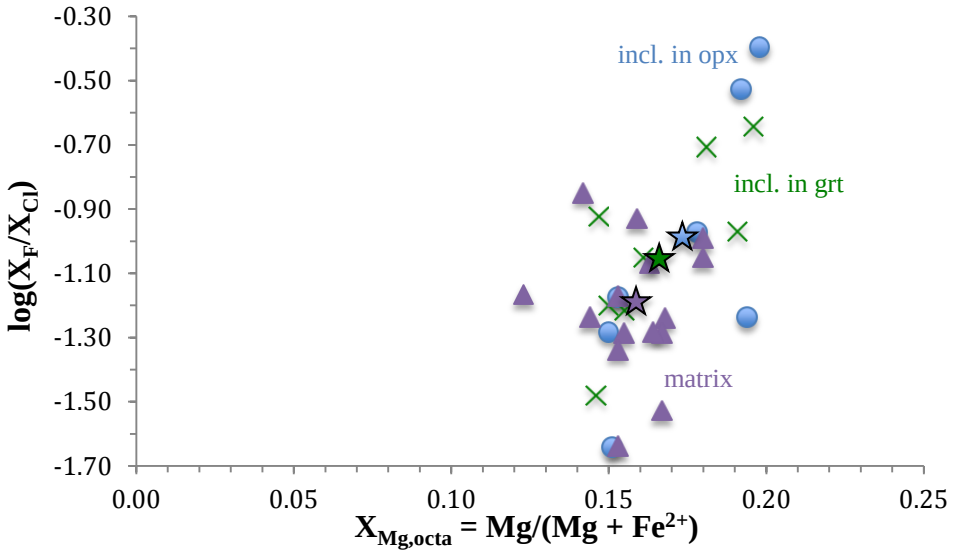

Figure 5.8. Relationship between $\log(X_F/X_{Cl})$ vs. $X_{Mg,\ octa}$ in biotites from sample QC82-45, illustrating how this correlates to changing fluid composition. The stars represent the average values for each type of biotite grain.

CHAPTER VI. CONCLUSION

Chlorine enrichment of hydrous minerals is a function of pressure, temperature, fluid composition and crystal chemistry. The amphibole and biotite present in the Archean granulite-facies iron-formations of the eastern Beartooth Mountains, Montana are some of the most Cl-rich amphibole and biotite recorded, making these samples ideal for investigating the evolving fluid compositions in these rocks. Thermobarometric calculations and equilibrium phase diagrams indicate peak metamorphism at granulite-facies conditions (~775-800 °C and 6 kbar), which falls within the previously determined range of P-T conditions in this area.

Three important conclusions can be determined as a result of this study. (1) The variation in chlorine content in amphibole and biotite in this study is a consequence of the interplay between crystallochemical influences on the incorporation of Cl and changing fluid compositions during progressive metamorphism. While the former is important in facilitating the Cl ←→ OH exchange, the latter is the stronger influence on incorporation of Cl. During progressive metamorphism into granulite-facies conditions, hydrous silicates undergo dehydration and the residual aqueous fluid that is present will become enriched in chlorine, thus producing a more saline brine and lowering the activity of H_2O. (2) The incorporation of Cl into the hydroxyl site of the hydrous minerals will preserve the crystal structure and extend their stability field into high-grade metamorphic conditions. (3) The presence of “hydrous” silicates at these metamorphic conditions indicates that these minerals are extremely sensitive to changing fluid composition and can be used to monitor aqueous fluids in high-grade metamorphic environments.

REFERENCES

Armstrong R.L., Taubeneck, W.H. and Hales, P.O. (1977) Rb–Sr and K-Ar geochronometry of Mesozoic granitic rocks and their Sr isotopic composition, Oregon, Washington, and Idaho. *Geological Society of America Bulletin*, 88, 397–411.

Anderson, J.L., Barth, A.P., Wooden, J.L. and Mazdab, F. (2008) Thermometers and Thermobarometers in Granitic Systems. *Reviews in Mineralogy and Geochemistry*, 69, 121-142.

Baird, G.B., Bhattacharyya, P. Whitney, D.L. and Hudleston, P.J. (2006) Chlorine-bearing fluid flow, deformation, and metamorphism in ductile shear zones of the Seve Nappe, northern Swedish Caledonides. To be submitted to the *Amer. J. Science.*

Bence, A.E. and Albee, A.L. (1968) Empirical correction factors for the electron microanalysis of silicates and oxides, Journal of Geology v.76, 382-403.

Blundy, J. D. and Holland, T. (1990) Calcic Amphibole Equilibria and a New Amphibole-plagioclase Geothermometer. *Contributions to Mineralogy and Petrology* 104.2, 208-224.

Büttner, S. H. (2012) Rock Maker: an MS Excel™ spreadsheet for the calculation of rock compositions from proportional whole rock analyses, mineral compositions, and modal abundance. *Contributions to Mineralogy and Petrology* v.104, 129-135.

Castelli, D. (1988) Chloropotassium ferro-pargasite from Sesia-Lanzo marbles (Western Italian Alps): a record of highly saline fluids. *Rend. Soc. Ital. Mineral. Petrol.* 43, 129-138.

Condie, K. C. (1976) The Wyoming Archean Province in the western United States. In Windley, B. F. (ed.) *The Early History of the Earth.* John Wiley: London, 499-511.

Connolly, J.A.D, and Kerrick, D.M. (1987) An algorithm and computer program for calculating composition phase diagrams. CALPHAD v.11, p. 1-55.

Connor and Harrison (2003) The Laramide Orogeny. *The Traprock*. Vol. 2, 10 – 14.

CrystalMaker® 9.0.4: a crystal and molecular structures program for Mac and Windows. CrystalMaker Software Ltd, Oxford, England (www.crystalmaker.com).

de Capitani, C., and Petrakakis, K. (2010) The computation of equilibrium assemblage diagrams with Theriak/Domino software. American Mineralogist, 95(7), 1006-1016.

Deer, W.A., Howie, R.A., and Zussman, J. (2001) Rock-Forming Minerals, Volume 4A: Framework Silicates – Feldspars. The Geological Society of London, London, United Kingdom, 972 p.

Dick, L.A. and Robinson, G.W. (1979) Chlorine-bearing potassian hastingsite from a sphalerite skarn in southern Yukon. *Cand. Mineral.* 17, 25-26.

Diener, J.F.A., Powell, R., White, R.W. and Holland, T.J.B. (2007) A new thermodynamic model for clino- and orthoamphiboles in the system Na2O-CaO-FeO-MgO-Al2O3-SiO2-H2O-O. *Journal of Metamorphic Geology* 25, 631-56.

Enami, M., Liou, J.G., and Bird, D.K. (1992) Cl-bearing amphibole in the Salton Sea geothermal system, California. *Cand. Mineral.* 30, 1077-1092.

Foster, D. A., Mueller, P. A., Mogk, D. W., Wooden, J. L. and Vogl, J. J. (2006) Proterozoic evolution of the western margin of the Wyoming craton: implications for the tectonic and magmatic evolution of the northern Rocky Mountains. *Canadian Journal of Earth Sciences* 43, 1601-1619.

Green, E., Holland, T., and Powell, R. (2007) An order-disorder model for omphacitic pyroxenes in the system jadeite-diopside-hedenbergite-acmite, with applications to eclogitic rocks. *American Mineralogist* 92, 1181-9.

Hawthorne, F. C., Oberti, R., Harlow, G. E., Maresch, W. V., Martin, R. F., Schumacher, J. C., and Welch, M. D. (2012) Nomenclature of the amphibole supergroup. *American Mineralogist*, 97, 2031-2048.

Henry, D. and Mogk, D. (2003) Selected Features of the Precambrian Rocks of the eastern Beartooth Mountains, Montana and Wyoming. Teaching Petrology in the 21st Century Workbook, section 3, 18 pp.

Henry, D., Mueller, P., and Will, C. (2015) [IN PRESS] Hyalophane from mafic xenoliths within Mesoarchean granitic rocks, Beartooth Mountains, Montana, USA: Indicators for barium metasomatism. Canadian Mineralogist.

Henry, D.J. (1988) Cl-rich minerals in Archean granulite facies ironstones from the Beartooth Mountains, Montana, USA: Implications for fluids involved in granulite metamorphism. p. 67-69.

Henry, D.J., Mogk, D.W., Mueller, D.A., Foster, D.A., and Wooden, J.L. (2014) Upper-to-middle level exposure of a 2.8 Ga continent in the northern Wyoming Province, USA. Geological Society of America Abstracts with Program, 46, 19.

Henry, D. J., Mueller, P. A., Wooden, J. L., Warner, J. L., and Lee-Berman, R. (1982) Granulite facies supracrustal assemblages of the Quad Creek area, eastern Beartooth Mountains, Montana: In Mueller, P. A. and Wooden, J. L., eds., Precambrian Geology of the Beartooth Mountains, Montana and Wyoming, Montana Bureau of Mines and Geology Special Publication, v.84, 147-156.

Holland, T., Baker, J. and Powell, R. (1998) Mixing properties and activity-composition relationships of chlorites in the system MgO-FeO-Al_2O_3-SiO_2-H_2O. *European Journal of Mineralogy* 10, 395-406.

Holland, T. and Blundy, J. (1994) Non-ideal Interactions in Calcic Amphiboles and Their Bearing on Amphibole-Plagioclase Thermometry. *Contributions to Mineralogy and Petrology* 116.4, 433-447.

Holland, T. and Powell, R. (1996) Thermodynamics of order-disorder in minerals. 2. Symmetric formalism applied to solid solutions. *American Mineralogist* 81, 1425-37.

Holland, T. and Powell, R. (2003) Activity-composition relations for phases in petrological calculations: an asymmetric multicomponent formulation. *Contributions to Mineralogy and Petrology* 145, 492-501.

Holland, T.J.B. and Powell, R. (1998) An internally consistent thermodynamic data set for phases of petrological interest. *Journal of Metamorphic Geology* 16, 309-43.

Jacobsen, S.S. (1975) Dashkesanite: High-chlorine amphibole from St. Paul's rocks, Equatorial Atlantic, and Transcaucasia, U.S.S.R. *Min. Sci. Invest., Contrib. Earth Sci., Smithsonian Inst.* 14, 17-20.

James, H.L. (1954) Sedimentary facies of iron-formation. *Economic Geology*, 49, 235-293.

Jiang, S.-Y., Palmer, M.R., Li, Y.-H., and Xue, C.-J. (1996) Ba-rich micas from the Yindongzi-Daxigou Pb-Zn-Ag and Fe deposits, Qinling, northwestern China. *Mineral. Mag.* 60, 433-445.

Jiang, S.-Y., Palmer, M.R., Xue, C.-J., and Li, Y.-H. (1994) Halogen-rich scapolite-biotite rocks from the Tongmugou Pb-Zn deposit, Qinling, north-western China: implications for the ore-forming processes. *Mineral. Mag.* 58, 543-552.

Kamineni, D.C., Bonardi, M., and Rao, A.T. (1982) Halogen-bearing minerals from Airport Hill, Visakpatnam, India. *Amer. Mineral.* 67, 1001-1004.

Klein, C. (2005) Some Precambrian Banded Iron-formations (BIFs) from around the world: Their age, geologic setting, mineralogy, metamorphism, geochemistry, and origins. *American Mineralogist*, 90.10, 1473-1499.

Klein, C., Dutrow, B. and Dana, J. D. (2008) *The 23rd Edition of the Manual of Mineral Science: (after James D. Dana)*. John Wiley.

Kohn, M.J., and Spear, F.S. (1990) 2 new geobarometers for garnet amphibolites, with applications to southeastern Vermont. *American Mineralogist*, v.75, 89-96.

Krogh T, Kamo S, Hanley T, Hess D, Dahl P, Johnson, R. (2011) Geochronology and geochemistry of Precambrian Gneisses, metabasites, and pegmatite from the Tobacco Root Mountains, northwestern Wyoming craton, Montana. Can J Earth Sci 46:161–185.

Krutov, G.A. (1936) Dashkesanite: a new chlorine amphibole of the hastingsite group. *Mineral. Abstr*. 6, 438.

Kullerud, K. (1995) Chlorine, titanium and barium-rich biotites: factors controlling biotite composition and implications for garnet-biotite geothermometry. *Contrib. Minerl. Petrol.* 120, 42-59.

Kullerud, K. (1996) Chlorine-rich amphiboles: interplay between amphibole composition and an evolving fluid. *Eur. J. Mineral.* 8, 355-370.

Kullerud, K. (2000) Occurrence and origin of Cl-rich amphibole and biotite in the Earth's crust – implications for fluid composition and evolution. *In* Stober, I. and Bucher, K. (eds.) Hydrogeology of Crystalline Rocks, 205-225.

Léger, A., Rebbert, C., and Webster, J. (1996) Cl-rich biotite and amphibole from Black Rock Forest, Cornwall, New York. *American Mineralogist*, 81, 495-504.

Liu, J., Liu, W., Ye, K. and Mao, Q. (2009) Chlorine-rich amphibole in Yangkou eclogite, Sulu ultrahigh-pressure metamorphic terrane, China. *Eur. J. Mineral.* 21, 1265-1285.

Locock, A. J. (2014) An Excel spreadsheet to classify chemical analyses of amphiboles following the IMA 2012 recommendations. *Computers and Geosciences* 62, 1-11.

Maas and Henry (2002) Heterogeneous growth and dissolution of sillimanite in migmatites: evidence from cathodoluminescence imaging: GSA Abstracts with Programs 189, p. 17.

Maier, A., Cates, N., Trail, D. and Mojzis, S. (2012) Geology, age and field relations of Hadean zircon-bearing supracrustal rocks from Quad Creek, eastern Beartooth Mountains (Montana-Wyoming). *Chem Geol*. doi: 10 1016/j chemgeo 2012 04 005.

Makino, K., Tomita K. and Suwa, K. (1993) Effect of chlorine on the crystal structure of a chlorine-rich hastingsite. *Mineralogical Magazine*, 57, 677-685.

Manning, C. E. and Aranovich, L. Y. (2014) Brines at High Pressure and Temperature: Thermodynamic, Petrologic and Geochemical Effects. *Precambrian Research* 253, 6-16.

Markl, G. and Piazolo, S. (1998) Halogen-bearing minerals in syenites and high-grade marbles of Dronning Maud Land, Antarctica: monitors of fluid compositional changes during late-magmatic fluid-rock interaction processes. *Contrib. Mineral. Petrol.* 132, 246-268.

McCormick, K.A. and McDonald, A.M. (1999) Chlorine-bearing amphiboles from the Fraser Mine, Sudbury, Ontario, Canada: Description and crystal chemistry. *Cand. Mineral.* 37, 1385-1403.

Mora, C.I. and Valley, J.W. (1989) Halogen-rich scapolite and biotite: Implications for metamorphic fluid-rock interactions. *Amer. Mineral.* 74, 721-737.

Morrison, J. M. (1991) Compositional constraints on the incorporation of Cl into amphiboles. *American Mineralogist* 76, 1920-1930.

Mueller, P. and Frost, C. (2006) The Wyoming Province: A distinctive Archean craton in Laurentian North America. *Can. J. Earth Sci*. 43, 1391–1397.

Mueller, P., Mogk, D., Henry, D., Wooden, J. and Foster, D. (2008) Geologic evolution of the Beartooth Mountains: Insights from petrology and geochemistry. *Northwest Geol*. 37, 5 – 20.

Mueller, P. and Wooden, J. (2012) Trace Element and Lu-Hf Systematics in Hadean-Archean Detrital Zircons: Implications for Crustal Evolution: *Journal of Geology*, v.120, 15-29.

Mueller, P., Wooden, J., Mogk, D., Henry, D. and Bowes, D. (2010) Rapid Growth of an Archean continent by arc magmatism. *Precambrian Res*. 183:70-88.

Mueller, P. A., Mogk, D. W., Henry, D. J., Wooden, J. L. and Foster, D. A. (2014) The Plume to Plate Transition: Hadean and Archean Crustal Evolution in the Northern Wyoming Province, U.S.A. *Modern Approaches in Solid Earth Sciences* 7, 23-54.

Munoz, J. L. and Swenson, A. (1981) Chloride-hydroxyl exchange in biotite and estimation of relative HCl/HF activities in hydrothermal fluids. *Economic Geology* 76, 22 12-222 1.

Munoz, J. L. and Swenson, A. (1982) F-Cl-OH partitioning between biotite and apatite. *Geochimica et Cosmochimica Acta* 56, 3435-3467.

Nakamura, D. (2009) A new formulation of garnet–clinopyroxene geothermometer based on accumulation and statistical analysis of a large experimental data set. *Journal of Metamorphic Geology*, 27: 495–508.

Oberti, R., Ungaretti, L., Cannillo, E., and Hawthorne, F.C. (1993) The mechanism of Cl incorporation in amphibole. *American Mineralogist* 78, 746-752.

Pandey, O.P., Tripathi, P., Parthasarathy, G., Rajagopalan, V. and Sreedhar, B. (2014) Geochemical and Mineralogical Studies of Chlorine-rich Amphibole and Biotite from the 2.5 Ga Mid-crustal Basement Beneath the 1993 Killari Earthquake Region, Maharashtra: Evidence for Mantle Metasomatism Beneath the Deccan Trap. *J. Geol. Soc. India.* 83, 599-612.

Powell, R. and Holland, T.J.B. (1988) An internally consistent thermodynamic dataset with uncertainties and correlations: 3: application methods, worked examples and a computer program. *Journal of Metamorphic Geology*, v.6, 173-204.

Ray, D., Mevel, C. and Banerjee, R. (2009) Hydrothermal alteration studies of gabbros from Northern Central Indian Ridge and their geodynamic implications. *J. Earth Syst. Sci.* 118, 659-676.

Reid, R., McMannis, W., and Palmquist, J. (1975) Precambrian geology of North Snowy Block, Beartooth Mountains, Montana. *In* GSA Special Papers, 157, 1-135.

Sato, H., Yamaguchi, Y. and Makino, K. (1997) Cl incorporation into successively zoned amphiboles from the Ramnes Cauldron, Norway. *Amer. Mineral.* 82, 316-324.

Schneider C.A., Rasband W.S. and Eliceiri K.W. (2012) NIH Image to ImageJ: 25 years of image analysis. *Nat Methods* 9 (7): 671–675.

Sen, S. K. and Bhattacharya, A. (1984) An Orthopyroxene-Garnet Thermometer and Its Application to the Madras Charnockites. *Contributions to Mineralogy and Petrology* 88.1-2, 64-71.

Sharma, R.S., (1981) Mineralogy of a scapolite-bearing rocks from Rajastan, northwest peninsular India. *Lithos*. 14, 165-172.

Sonnenthal, E.L. (1992) Geochemistry of dendritic anorthosites and associated pegmatites in the Skaergaard Intrusion, East Greenland: Evidence for metasomatism by a chlorine-rich fluid. *J. Volc. Geotherm. Res.* 52, 209-230.

Suwa, K., Enami, M. and Horiuchi, T. (1987) Chlorine-rich potassium hastingsite from West Onguil Island, Lützow-Holm Bay, East Antarctica. *Mineral. Mag*. 51, 709-714.

Tracy, R.J. (1991) Ba-rich micas from the Franklin marble, Lime Crest and Sterling Hill, New Jersey. *Amer. Mineral.* 76, 1683-1693.

Trendall, A.F. (1983) Introduction. In A.F. Trendall and R.C. Morris, Eds., Iron-Formation: Facts and Problems, 1-11. Elsevier, Amsterdam.

Uher, P., Kodera, P., Lexa, J. and Bacik, P. (2014) Halogen-rich biotites from the Detva, Biely Vrch Au-porphyry deposit (Slovakia): Compositional variations and genetic aspects. *Central European Mineralogical Conference.* 146-147.

Vanko, D. (1986) High chlorine amphiboles from oceanic rocks: product of highly-saline hydrothermal fluids? *Amer. Mineral.* 71, 51-59.

Vielzeuf, D. (1982) The retrogressive breakdown of orthopyroxene in an intermediate charnockite from Salcix (French Pyrénées). *Bull. Minéral*. 105, 681-690.

Volfinger, M., Robert J. L., Vielzeuf D. and Neiva, A. M. R. (1985) Structural control of the chlorine content of OH-bearing silicates (micas and amphiboles). *Geochimica et Cosmochimica Acta*. 49.1, 37-48.

White, R.W., Powell, R. and Holland, T.J.B. (2007) Progress relating to calculation of partial melting equilibria for metapelites. *Journal Of Metamorphic Geology* 25, 511-27.

Whitney, D. L. and Evans, B. W. (2010) Abbreviations for names of rock-forming minerals. *American Mineralogist* 95, 185-187.

Will, C.N. (2013) Temperature and pressure conditions of Archean amphibolite-granulite facies metamorphic xenoliths from the eastern Beartooth Mountains, Montana and Wyoming, USA Geology and Geophysics, M.S. thesis, 131 pp. Louisiana State University.

Winter, J. D. (2001) An Introduction to Igneous and Metamorphic Petrology: Prentice Hall.

Wooden, J.L., Mueller, P.A., Mogk, D.W., and Bowes, D.R. (1988) A review of the geochemistry and geochronology of Archean rocks of the Beartooth Mountains, Montana-Wyoming. *In* Precambrian and Mesozoic plate margins: Montana, Idaho and Wyoming. *Edited by* S.E. Lewis and R.B. Berg. Montana Bureau of Mines and Geology, Special Publication 96, p. 23-42.

Xiao, Y., Hoefs, J. and Kronz, A. (2005) Compositionally zoned Cl-rich amphiboles from North Dabie Shan, China: Monitor of high-pressure metamorphic fluid/rock interaction processes. *Lithos*. 81, 279-295.

Yardley, B.W.D (1985) Apatite composition and the fugacities of HF and HCI in metamorphic fluids. *Mineralogical Magazine* 49, 77-79.

Zhu, C. and Sverjensky, D. A. (1991) Partitioning of F-Cl-Oh between Minerals and Hydrothermal Fluids. *Geochimica et Cosmochimica Acta* 55(7), 1837-1858.

Zhu, C. and Sverjensky, D. A. (1992) F-Cl-OH partitioning between biotite and apatite. *Geochimica et Cosmochimica Acta* 56, 3435-3467.

APPENDIX A: GARNET EPMA DATA

Sample	QC82-45											
Analysis Type	Traverse 1											
Analysis Pt.	7	8	9	10	11	12	13	14	15	16	17	Avg
Wt%												
SiO_2	37.06	37.20	37.08	37.12	37.18	37.26	37.21	37.31	37.28	37.12	37.34	37.20
Al_2O_3	20.40	20.66	20.64	20.72	20.87	20.33	20.48	20.50	20.48	20.85	20.73	20.61
TiO_2	0.02	0.02	0.01	0.02	0.03	0.05	0.01	0.03	0.01	0.01	0.02	0.02
Cr_2O_3	0.06	0.05	0.08	0.03	0.04	0.05	0.04	0.00	0.02	0.02	0.06	0.04
Fe_2O_3	1.85	1.55	1.52	1.27	1.37	1.78	1.87	1.84	1.83	1.57	0.84	1.57
FeO	29.35	29.31	29.17	29.26	29.24	29.08	28.88	29.10	29.21	29.09	29.46	29.19
MnO	3.09	3.02	2.94	2.87	2.91	2.79	2.87	2.87	2.83	2.91	2.85	2.90
MgO	1.45	1.71	1.79	1.81	1.80	1.79	1.81	1.79	1.80	1.80	1.73	1.75
CaO	7.25	7.10	7.03	7.03	7.11	7.41	7.42	7.37	7.27	7.14	7.21	7.21
Total	100.51	100.62	100.24	100.12	100.55	100.53	100.57	100.81	100.72	100.52	100.23	100.49
Structural formula (in apfu) based on 12 oxygens												
Z (iv) site:												
Si	2.976	2.977	2.975	2.979	2.972	2.983	2.977	2.979	2.979	2.969	2.993	2.978
Fe^{3+}	0.001	0.001	0.000	0.001	0.002	0.003	0.000	0.002	0.001	0.000	0.001	0.001
Al	0.023	0.022	0.024	0.019	0.026	0.015	0.023	0.020	0.020	0.031	0.006	0.021
Site total	3.000	3.000	3.000	3.000	3.000	3.000	3.000	3.000	3.000	3.000	3.000	3.000
Al (total)	1.940	1.955	1.959	1.967	1.973	1.927	1.940	1.938	1.938	1.973	1.962	1.952
Fe^{3+}(total)	0.112	0.093	0.091	0.077	0.082	0.107	0.112	0.111	0.110	0.095	0.051	0.095
Y (vi) site:												
Al	1.908	1.926	1.928	1.941	1.941	1.904	1.908	1.909	1.909	1.935	1.952	1.924
Ti	0.001	0.001	0.000	0.001	0.002	0.003	0.000	0.002	0.001	0.000	0.001	0.001
Cr^{3+}	0.004	0.003	0.005	0.002	0.003	0.003	0.003	0.000	0.001	0.001	0.003	0.003
Fe^{3+}	0.111	0.092	0.091	0.076	0.081	0.104	0.112	0.109	0.109	0.094	0.050	0.094
Site total	2.023	2.022	2.024	2.019	2.026	2.015	2.023	2.020	2.020	2.031	2.006	2.021

X (viii) site:												
Fe^{2+}	1.971	1.961	1.958	1.964	1.955	1.947	1.932	1.943	1.952	1.945	1.975	1.955
Mn^{2+}	0.210	0.204	0.200	0.195	0.197	0.189	0.194	0.194	0.191	0.197	0.193	0.197
Mg	0.173	0.204	0.214	0.217	0.214	0.214	0.215	0.213	0.214	0.215	0.207	0.209
Ca	0.623	0.608	0.605	0.605	0.609	0.636	0.636	0.630	0.623	0.612	0.619	0.619
Site total	2.977	2.978	2.976	2.981	2.974	2.985	2.977	2.980	2.980	2.969	2.994	2.979
Molecular percentages of endmembers												
Almandine	66.20	65.87	65.79	65.90	65.73	65.21	64.89	65.19	65.50	65.52	65.97	65.61
Pyrope	5.81	6.85	7.18	7.28	7.19	7.15	7.24	7.15	7.18	7.24	6.90	7.02
Spessartine	7.05	6.86	6.71	6.54	6.61	6.34	6.52	6.51	6.42	6.63	6.46	6.60
Grossular	18.21	18.54	18.72	18.94	19.64	17.70	18.64	18.24	18.01	19.91	18.77	18.66
Andradite	2.48	1.67	1.33	1.19	0.60	3.29	2.55	2.83	2.80	0.62	1.68	1.91
Schorlomite	0.07	0.06	0.02	0.05	0.08	0.14	0.02	0.08	0.04	0.02	0.05	0.06
Uvarovite	0.18	0.16	0.26	0.10	0.14	0.17	0.14	0.00	0.05	0.07	0.17	0.13

Sample	QC82-45											
Analysis Type	Traverse 2											
Analysis Pt.	18	19	20	21	22	23	24	25	26	27	28	Avg
Wt%												
SiO_2	37.59	37.25	37.20	36.91	37.17	37.24	37.13	37.05	37.17	37.27	37.10	37.19
Al_2O_3	20.62	20.65	20.56	20.81	20.82	20.78	20.71	20.92	20.86	20.71	20.56	20.72
TiO_2	0.02	0.03	0.02	0.02	0.00	0.04	0.00	0.04	0.03	0.03	0.03	0.02
Cr_2O_3	0.11	0.06	0.11	0.03	0.04	0.03	0.04	0.03	0.06	0.10	0.11	0.07
Fe_2O_3	1.21	1.40	1.74	1.47	1.73	1.55	1.80	1.78	1.59	1.31	1.68	1.57
FeO	30.09	29.56	29.31	29.05	29.04	29.21	29.19	29.28	29.39	29.43	29.45	29.36
MnO	3.22	2.94	2.93	2.93	2.87	2.98	2.85	2.94	2.86	2.97	3.16	2.97
MgO	1.39	1.68	1.78	1.74	1.74	1.75	1.73	1.73	1.73	1.60	1.37	1.66
CaO	7.14	7.06	7.07	7.06	7.34	7.19	7.20	7.02	7.11	7.26	7.27	7.16

Total	101.38	100.62	100.72	100.01	100.75	100.78	100.66	100.78	100.80	100.69	100.72	100.72
Structural formula (in apfu) based on 12 oxygens												
Z (iv) site:												
Si	2.992	2.981	2.974	2.968	2.967	2.973	2.969	2.959	2.967	2.980	2.973	2.973
Fe^{3+}	0.001	0.002	0.001	0.001	0.000	0.002	0.000	0.002	0.002	0.002	0.002	0.001
Al	0.007	0.018	0.024	0.031	0.033	0.025	0.031	0.039	0.031	0.018	0.025	0.026
Site total	3.000	3.000	3.000	3.000	3.000	3.000	3.000	3.000	3.000	3.000	3.000	3.000
Al (total)	1.940	1.954	1.945	1.979	1.967	1.962	1.960	1.978	1.970	1.958	1.950	1.960
Fe^{3+}(total)	0.072	0.084	0.105	0.089	0.104	0.093	0.108	0.107	0.095	0.079	0.101	0.094
Y (vi) site:												
Al	1.928	1.929	1.912	1.940	1.926	1.930	1.920	1.930	1.932	1.933	1.917	1.927
Ti	0.001	0.002	0.001	0.001	0.00	0.002	0.00	0.002	0.002	0.002	0.002	0.001
Cr^{3+}	0.007	0.004	0.007	0.002	0.003	0.002	0.003	0.002	0.004	0.007	0.007	0.004
Fe^{3+}	0.071	0.083	0.104	0.088	0.104	0.091	0.108	0.105	0.094	0.077	0.099	0.093
Site total	2.007	2.018	2.024	2.031	2.033	2.025	2.031	2.039	2.031	2.018	2.025	2.026
X (viii) site:												
Fe^{2+}	2.003	1.978	1.959	1.953	1.939	1.950	1.952	1.955	1.962	1.968	1.973	1.963
Mn^{2+}	0.217	0.199	0.199	0.200	0.194	0.201	0.193	0.199	0.193	0.201	0.214	0.201
Mg	0.164	0.200	0.212	0.208	0.207	0.208	0.207	0.206	0.206	0.191	0.164	0.198
Ca	0.609	0.605	0.605	0.608	0.628	0.615	0.617	0.601	0.608	0.622	0.624	0.613
Site total	2.993	2.982	2.976	2.969	2.967	2.975	2.969	2.961	2.969	2.982	2.975	2.974
Molecular percentages of endmembers												
Almandine	66.91	66.34	65.85	65.78	65.34	65.55	65.74	66.03	66.08	66.00	66.33	66.00
Pyrope	5.49	6.70	7.13	7.00	6.97	7.00	6.96	6.97	6.92	6.41	5.50	6.64
Spessartine	7.26	6.68	6.67	6.72	6.54	6.77	6.51	6.71	6.51	6.73	7.20	6.76
Grossular	17.28	18.22	17.98	20.09	20.14	19.24	19.38	20.02	19.64	19.01	18.87	19.08
Andradite	2.67	1.77	1.94	0.25	0.88	1.23	1.26	0.08	0.56	1.42	1.66	1.25
Schorlomite	0.04	0.08	0.07	0.06	0.00	0.11	0.00	0.11	0.08	0.10	0.09	0.07
Uvarovite	0.34	0.20	0.36	0.09	0.13	0.11	0.13	0.09	0.20	0.33	0.35	0.21

Sample	QC82-45												
Analysis Type	Traverse 3												
Analysis Pt.	29	30	31	32	33	34	35	36	37	38	39	40	Avg
Wt%													
SiO_2	36.96	37.17	37.06	36.83	37.06	37.09	37.09	37.08	37.10	37.10	37.18	37.31	37.09
Al_2O_3	20.60	20.76	20.49	20.63	20.91	20.79	20.57	20.52	20.65	20.77	20.42	20.46	20.63
TiO_2	0.05	0.02	0.00	0.01	0.01	0.01	0.00	0.02	0.03	0.03	0.00	0.03	0.02
Cr_2O_3	0.04	0.03	0.04	0.01	0.01	0.00	0.05	0.04	0.03	0.06	0.03	0.05	0.03
Fe_2O_3	1.51	1.45	1.83	2.01	1.72	1.47	1.63	2.18	1.66	1.62	1.85	1.26	1.68
FeO	29.61	29.48	29.24	29.06	29.33	29.45	29.24	29.16	29.42	29.48	29.31	29.50	29.36
MnO	3.33	3.36	3.29	3.30	3.32	3.30	3.33	3.35	3.22	3.26	3.29	3.17	3.29
MgO	1.39	1.55	1.57	1.61	1.61	1.68	1.68	1.65	1.64	1.63	1.63	1.57	1.60
CaO	6.84	6.88	6.99	6.85	6.84	6.69	6.83	6.92	6.85	6.79	6.96	7.13	6.88
Total	100.34	100.69	100.49	100.32	100.80	100.48	100.43	100.92	100.60	100.73	100.67	100.48	100.58
Structural formula (in apfu) based on 12 oxygens													
Z (iv) site:													
Si	2.973	2.975	2.975	2.961	2.963	2.973	2.976	2.965	2.973	2.969	2.979	2.992	2.973
Fe^{3+}	0.003	0.001	0.000	0.001	0.000	0.000	0.000	0.001	0.002	0.002	0.000	0.002	0.001
Al	0.023	0.024	0.025	0.038	0.037	0.026	0.024	0.034	0.026	0.030	0.021	0.006	0.026
Site total	3.000	3.000	3.000	3.000	3.000	3.000	3.000	3.000	3.000	3.000	3.000	3.000	3.000
Al (total)	1.960	1.966	1.947	1.964	1.979	1.971	1.953	1.944	1.958	1.966	1.938	1.940	1.957
Fe^{3+}(total)	0.091	0.088	0.110	0.121	0.104	0.089	0.099	0.131	0.100	0.097	0.112	0.076	0.102
Y (vi) site:													
Al	1.930	1.935	1.913	1.916	1.933	1.938	1.922	1.900	1.924	1.929	1.908	1.927	1.923
Ti	0.003	0.001	0.000	0.001	0.000	0.000	0.000	0.001	0.002	0.002	0.000	0.002	0.001
Cr^{3+}	0.003	0.002	0.002	0.001	0.000	0.000	0.003	0.003	0.002	0.004	0.002	0.003	0.002
Fe^{3+}	0.088	0.086	0.110	0.121	0.103	0.088	0.098	0.130	0.099	0.096	0.112	0.074	0.101
Site total	2.023	2.024	2.025	2.038	2.037	2.026	2.024	2.034	2.026	2.030	2.021	2.006	2.026
X (viii) site:													
Fe^{2+}	1.992	1.973	1.963	1.954	1.961	1.974	1.962	1.950	1.971	1.973	1.964	1.978	1.968
Mn^{2+}	0.227	0.228	0.223	0.225	0.225	0.224	0.226	0.227	0.219	0.221	0.223	0.215	0.224

Mg	0.167	0.185	0.188	0.193	0.192	0.201	0.201	0.196	0.196	0.195	0.195	0.188	0.191
Ca	0.590	0.590	0.601	0.590	0.585	0.575	0.587	0.593	0.588	0.582	0.597	0.613	0.591
Site total	2.977	2.976	2.975	2.962	2.963	2.974	2.976	2.966	2.974	2.970	2.979	2.994	2.974
Molecular percentages of endmembers													
Almandine	66.94	66.30	65.98	65.97	66.17	66.39	65.93	65.74	66.29	66.41	65.91	66.09	66.18
Pyrope	5.62	6.22	6.32	6.53	6.49	6.76	6.74	6.61	6.60	6.55	6.55	6.27	6.44
Spessartine	7.63	7.65	7.51	7.59	7.58	7.53	7.61	7.65	7.35	7.43	7.48	7.18	7.52
Grossular	18.23	18.54	17.92	18.90	19.49	18.39	17.75	17.78	18.09	18.50	17.16	17.35	18.17
Andradite	1.29	1.15	2.16	0.93	0.23	0.91	1.79	2.02	1.50	0.84	2.82	2.87	1.54
Schorlomite	0.16	0.05	0.00	0.04	0.02	0.02	0.01	0.05	0.08	0.08	0.00	0.08	0.05
Uvarovite	0.13	0.09	0.12	0.04	0.02	0.00	0.16	0.14	0.09	0.19	0.08	0.17	0.10

Sample	QC82-45													
Analysis Type	Traverse 4													
Analysis Pt.	8	9	10	11	12	13	14	15	16	17	18	19	20	21
Wt%														
SiO_2	37.29	37.29	37.29	37.33	37.32	37.39	37.35	37.39	37.14	37.47	37.22	37.38	37.26	37.43
Al_2O_3	20.24	20.42	20.25	20.39	20.44	20.46	20.48	20.53	20.50	20.59	20.56	20.62	20.55	20.58
TiO_2	0.04	0.00	0.01	0.00	0.02	0.04	0.01	0.00	0.00	0.02	0.00	0.02	0.01	0.00
Cr_2O_3	0.07	0.06	0.10	0.08	0.07	0.04	0.06	0.00	0.03	0.02	0.00	0.00	0.02	0.01
Fe_2O_3	0.86	0.44	0.83	0.58	1.16	0.81	0.64	0.60	0.98	0.31	0.46	0.25	0.82	0.83
FeO	29.82	29.93	29.50	29.63	29.51	29.52	29.63	29.80	29.58	30.12	29.84	29.89	29.43	29.55
MnO	3.03	2.87	2.95	2.78	2.85	2.78	2.83	2.83	2.83	2.72	2.62	2.71	2.81	2.71
MgO	1.54	1.58	1.69	1.77	1.77	1.79	1.86	1.85	1.84	1.88	1.82	1.81	1.83	1.80
CaO	7.02	6.97	7.11	7.06	7.10	7.19	6.92	6.83	6.77	6.71	6.84	6.91	7.04	7.23
Total	99.89	99.58	99.73	99.63	100.23	100.02	99.76	99.84	99.67	99.84	99.38	99.59	99.77	100.15
Structural formula (in apfu) based on 12 oxygens														

Z (iv) site:														
Si	3.008	3.012	3.008	3.011	2.995	3.003	3.007	3.008	2.995	3.013	3.007	3.012	2.999	3.002
Fe^{3+}	0.000	0.000	0.000	0.000	0.001	0.000	0.000	0.000	0.000	0.000	0.000	0.000	0.000	0.000
Al	0.000	0.000	0.000	0.000	0.004	0.000	0.000	0.000	0.005	0.000	0.000	0.000	0.000	0.000
Site total	3.008	3.012	3.008	3.011	3.000	3.003	3.007	3.008	3.000	3.013	3.007	3.012	3.000	3.002
Al (total)	1.928	1.946	1.930	1.941	1.939	1.941	1.946	1.950	1.953	1.953	1.960	1.960	1.954	1.949
Fe^{3+}(total)	0.052	0.027	0.050	0.035	0.070	0.049	0.039	0.037	0.060	0.019	0.028	0.015	0.050	0.050
Y (vi) site:														
Al	1.924	1.944	1.926	1.938	1.929	1.937	1.943	1.947	1.943	1.951	1.958	1.959	1.949	1.945
Ti	0.002	0.000	0.000	0.000	0.001	0.002	0.000	0.000	0.000	0.001	0.000	0.001	0.000	0.000
Cr^{3+}	0.005	0.004	0.007	0.005	0.005	0.002	0.004	0.000	0.002	0.001	0.000	0.000	0.001	0.000
Fe^{3+}	0.052	0.027	0.050	0.035	0.068	0.049	0.039	0.037	0.060	0.019	0.028	0.015	0.049	0.050
Site total	1.983	1.975	1.983	1.979	2.004	1.991	1.986	1.983	2.005	1.972	1.986	1.974	2.000	1.996
X (viii) site:														
Fe^{2+}	2.011	2.022	1.990	1.998	1.980	1.983	1.995	2.005	1.995	2.026	2.016	2.014	1.981	1.982
Mn^{2+}	0.207	0.196	0.202	0.190	0.194	0.189	0.193	0.193	0.194	0.185	0.180	0.185	0.191	0.184
Mg	0.185	0.191	0.203	0.213	0.212	0.215	0.223	0.222	0.221	0.225	0.219	0.217	0.220	0.215
Ca	0.607	0.603	0.614	0.610	0.610	0.619	0.597	0.588	0.585	0.578	0.592	0.597	0.607	0.621
Site total	3.010	3.013	3.009	3.011	2.996	3.006	3.007	3.008	2.995	3.014	3.007	3.013	3.000	3.002
Molecular percentages of endmembers														
Almandine	67.63	68.26	66.92	67.32	66.10	66.41	66.96	67.38	66.62	68.47	67.67	68.02	66.04	66.19
Pyrope	6.21	6.43	6.81	7.18	7.06	7.19	7.49	7.47	7.39	7.62	7.37	7.34	7.34	7.17
Spessartine	6.96	6.63	6.78	6.39	6.47	6.32	6.47	6.48	6.46	6.27	6.03	6.24	6.38	6.15
Grossular	16.23	17.11	16.60	17.07	17.15	17.39	16.92	16.83	17.11	16.57	17.52	17.60	17.74	17.94
Andradite	2.62	1.36	2.53	1.79	2.92	2.46	1.95	1.84	2.31	0.94	1.42	0.76	2.41	2.52
Schorlomite	0.11	0.01	0.02	0.01	0.07	0.12	0.02	0.00	0.00	0.07	0.00	0.05	0.02	0.01
Uvarovite	0.23	0.20	0.33	0.26	0.23	0.12	0.18	0.00	0.11	0.06	0.00	0.00	0.07	0.02

Sample	QC82-45														
Analysis Type	Traverse 4 (continued)														
Analysis Pt.	22	23	28	29	30	31	32	33	34	35	36	37	38	39	Avg
Wt%															
SiO_2	37.38	37.86	37.41	37.27	37.25	37.38	37.48	37.45	37.03	37.34	37.37	37.12	37.33	37.36	37.34
Al_2O_3	20.57	19.44	20.14	20.28	20.12	20.23	20.26	20.30	20.44	20.19	20.35	20.16	20.36	20.26	20.35
TiO_2	0.00	0.03	0.02	0.08	0.02	0.05	0.00	0.01	0.02	0.03	0.01	0.04	0.04	0.07	0.02
Cr_2O_3	0.05	0.06	0.05	0.02	0.01	0.00	0.00	0.01	0.00	0.02	0.00	0.00	0.02	0.03	0.03
Fe_2O_3	0.00	0.36	0.86	0.73	1.29	0.92	0.78	0.81	1.39	0.50	0.49	1.28	0.61	0.93	0.40
FeO	30.29	30.15	29.91	29.79	29.35	29.56	29.42	29.59	29.04	29.78	29.69	29.14	29.60	29.61	29.97
MnO	2.90	2.68	2.75	2.76	2.86	2.77	2.88	2.79	2.82	2.65	2.73	2.83	2.67	2.70	2.79
MgO	1.72	1.91	1.63	1.69	1.80	1.79	1.76	1.85	1.85	1.80	1.84	1.86	1.86	1.86	1.79
CaO	0.00	7.05	7.15	7.05	7.11	7.16	7.30	7.07	7.11	7.03	7.00	7.11	7.07	7.07	6.78
Total	92.91	99.52	99.93	99.66	99.80	99.86	99.88	99.88	99.70	99.34	99.47	99.53	99.57	99.90	99.47
Structural formula (in apfu) based on 12 oxygens															
Z (iv) site:															
Si	3.250	3.060	3.014	3.008	3.003	3.009	3.016	3.012	2.986	3.020	3.017	2.999	3.011	3.006	3.017
Fe^{3+}	0.000	0.000	0.000	0.000	0.000	0.000	0.000	0.000	0.001	0.000	0.000	0.001	0.000	0.000	0.000
Al	0.000	0.000	0.000	0.000	0.000	0.000	0.000	0.000	0.013	0.000	0.000	0.000	0.000	0.000	0.000
Site total	3.250	3.060	3.014	3.008	3.003	3.009	3.016	3.012	3.000	3.020	3.017	3.000	3.011	3.006	3.017
Al (total)	2.056	1.853	1.917	1.933	1.918	1.924	1.925	1.928	1.949	1.927	1.939	1.925	1.938	1.926	1.939
Fe^{3+}(total)	0.000	0.022	0.052	0.044	0.078	0.056	0.047	0.049	0.084	0.030	0.029	0.078	0.037	0.056	0.024
Y (vi) site:															
Al	2.108	1.852	1.913	1.929	1.912	1.920	1.921	1.924	1.929	1.925	1.936	1.919	1.936	1.921	1.937
Ti	0.000	0.002	0.001	0.005	0.001	0.003	0.000	0.001	0.001	0.002	0.000	0.002	0.002	0.004	0.001
Cr^{3+}	0.004	0.004	0.003	0.001	0.001	0.000	0.000	0.000	0.000	0.001	0.000	0.000	0.001	0.002	0.002
Fe^{3+}	0.000	0.022	0.052	0.044	0.078	0.056	0.047	0.049	0.083	0.030	0.029	0.077	0.037	0.056	0.024
Site total	2.111	1.879	1.970	1.980	1.992	1.979	1.968	1.974	2.013	1.958	1.966	1.998	1.976	1.984	1.965
X (viii) site:															
Fe^{2+}	2.203	2.038	2.015	2.011	1.979	1.990	1.979	1.991	1.958	2.014	2.005	1.969	1.996	1.993	2.025

Mn^{2+}	0.213	0.184	0.188	0.188	0.196	0.189	0.196	0.190	0.193	0.182	0.186	0.194	0.183	0.184	0.191
Mg	0.223	0.230	0.196	0.204	0.216	0.215	0.211	0.222	0.222	0.217	0.221	0.224	0.224	0.223	0.215
Ca	0.000	0.610	0.617	0.609	0.614	0.618	0.629	0.609	0.614	0.609	0.605	0.615	0.611	0.610	0.587
Site total	2.639	3.061	3.016	3.013	3.005	3.012	3.016	3.013	2.987	3.022	3.017	3.002	3.013	3.010	3.018
Molecular percentages of endmembers															
Almandine	83.48	72.32	68.21	67.73	66.24	67.07	67.04	67.23	65.55	68.58	67.96	65.66	67.34	66.98	68.70
Pyrope	8.44	8.14	6.63	6.86	7.23	7.25	7.16	7.51	7.43	7.39	7.49	7.46	7.54	7.51	7.30
Spessartine	8.08	6.51	6.36	6.34	6.55	6.36	6.65	6.43	6.45	6.18	6.32	6.45	6.16	6.19	6.48
Grossular	0.00	11.57	15.91	16.53	15.96	16.37	16.75	16.30	18.08	16.15	16.70	16.42	16.90	16.17	16.12
Andradite	0.00	1.16	2.66	2.24	3.93	2.82	2.39	2.48	2.42	1.55	1.50	3.89	1.87	2.84	1.23
Schorlomite	0.00	0.10	0.07	0.24	0.06	0.14	0.01	0.04	0.06	0.10	0.02	0.12	0.12	0.21	0.06
Uvarovite	0.00	0.20	0.17	0.06	0.04	0.00	0.00	0.02	0.00	0.05	0.00	0.00	0.06	0.09	0.10

Sample	QC82-45						QC81-40b		QC81-66	QC81-1	QC-IS	QC81-5
Analysis Type	In opx	In biot-7	w/ biot inc.	Rim	By opx 19	Near biot-2	Typical	Typical	Core	Typical	Avg of 10	Typical
Analysis Pt.	grt-5	grt-8	grt-13	grt-15	grt-20	grt-25	grt-1	grt-1	grt-1	grt-2	grt-1	grt-4
Wt%												
SiO_2	37.32	37.33	37.41	37.78	37.58	37.64	37.73	37.65	37.78	37.17	37.20	36.85
Al_2O_3	19.95	20.11	19.90	20.43	19.72	19.92	20.61	20.59	21.31	20.32	20.72	20.44
TiO_2	0.00	0.04	0.04	0.02	0.05	0.00	0.00	0.00	0.00	0.04	0.01	0.00
Cr_2O_3	0.13	0.05	0.04	0.03	0.06	0.02	0.03	0.04	0.03	0.07	0.01	0.08
Fe_2O_3	0.94	1.70	1.11	0.50	0.85	0.70	1.31	1.27	0.00	0.09	1.91	2.76
FeO	30.56	29.84	29.93	30.16	29.94	29.85	28.94	28.81	30.63	34.24	28.00	29.82
MnO	3.84	3.45	3.25	3.33	3.11	3.73	4.16	4.64	4.67	1.87	3.43	1.88
MgO	1.34	1.49	1.64	1.57	1.68	1.46	2.44	2.70	2.54	3.23	1.87	2.96
CaO	6.08	6.77	6.73	6.91	6.94	6.86	5.94	5.23	4.08	2.02	7.56	5.51
Total	100.16	100.78	100.04	100.73	99.93	100.17	101.16	100.93	101.04	99.05	100.71	100.31

Structural formula (in apfu) based on 12 oxygens												
Z (iv) site:												
Si	3.017	2.994	3.017	3.020	3.032	3.032	2.996	2.995	3.003	3.020	2.968	2.950
Fe^{3+}	0.000	0.002	0.000	0.000	0.000	0.000	0.000	0.000	0.000	0.000	0.001	0.000
Al	0.000	0.004	0.000	0.000	0.000	0.000	0.004	0.005	0.000	0.000	0.032	0.050
Site total	3.017	3.000	3.017	3.020	3.032	3.032	3.000	3.000	3.003	3.020	3.000	3.000
Al (total)	1.906	1.909	1.897	1.927	1.879	1.895	1.935	1.937	1.996	1.946	1.957	1.942
Fe^{3+}(total)	0.057	0.103	0.067	0.030	0.052	0.042	0.078	0.076	0.000	0.005	0.115	0.166
Y (vi) site:												
Al	1.901	1.898	1.892	1.925	1.875	1.891	1.924	1.926	1.996	1.946	1.916	1.879
Ti	0.000	0.002	0.002	0.001	0.003	0.000	0.000	0.000	0.000	0.002	0.001	0.000
Cr^{3+}	0.008	0.003	0.003	0.002	0.004	0.001	0.002	0.003	0.002	0.004	0.001	0.005
Fe^{3+}	0.057	0.101	0.067	0.030	0.052	0.042	0.078	0.076	0.000	0.005	0.114	0.166
Site total	1.966	2.004	1.964	1.958	1.934	1.935	2.004	2.005	1.998	1.958	2.032	2.050
X (viii) site:												
Fe^{2+}	2.066	2.002	2.019	2.017	2.020	2.011	1.922	1.917	2.036	2.327	1.868	1.997
Mn^{2+}	0.263	0.234	0.222	0.226	0.212	0.254	0.280	0.313	0.314	0.129	0.232	0.127
Mg	0.162	0.178	0.197	0.187	0.202	0.175	0.289	0.320	0.301	0.391	0.222	0.353
Ca	0.526	0.582	0.581	0.592	0.600	0.592	0.505	0.446	0.347	0.176	0.646	0.473
Site total	3.017	2.996	3.019	3.021	3.035	3.032	2.996	2.995	2.999	3.022	2.968	2.950
Molecular percentages of endmembers												
Almandine	70.04	66.81	68.53	68.65	69.64	69.28	64.15	63.99	67.93	79.22	62.93	67.68
Pyrope	5.49	5.95	6.67	6.37	6.97	6.04	9.64	10.69	10.04	13.32	7.49	11.97
Spessartine	8.90	7.82	7.55	7.68	7.32	8.76	9.34	10.44	10.49	4.38	7.81	4.32
Grossular	12.24	14.61	13.58	15.59	13.04	13.66	13.44	11.56	11.44	2.45	20.22	14.08
Andradite	2.91	4.55	3.42	1.55	2.68	2.19	3.34	3.19	0.00	0.27	1.49	1.68
Schorlomite	0.00	0.11	0.12	0.05	0.15	0.00	0.00	0.00	0.00	0.12	0.03	0.00
Uvarovite	0.42	0.17	0.14	0.11	0.19	0.07	0.09	0.13	0.09	0.23	0.03	0.26

Sample	HP82-59									
Analysis Type	Small garnet core			Small garnet rim			Large garnet traverse			
Analysis Pt.	17	18	19	20	21	22	26	27	28	29
Wt%										
SiO_2	37.37	37.01	37.81	36.52	37.67	36.32	37.35	37.20	37.54	37.73
Al_2O_3	21.12	20.95	20.88	20.88	20.80	20.54	20.59	20.65	21.01	20.58
TiO_2	0.04	0.04	0.05	0.00	0.02	0.00	0.00	0.03	0.04	0.00
Cr_2O_3	0.00	0.02	0.01	0.00	0.00	0.03	0.04	0.02	0.05	0.00
Fe_2O_3	0.92	2.07	0.00	2.31	0.16	3.25	0.38	1.64	0.63	0.00
FeO	32.85	32.81	33.86	31.91	33.19	31.69	32.96	32.84	33.54	33.52
MnO	0.66	0.66	0.67	0.70	0.61	0.67	0.68	0.69	0.76	0.61
MgO	2.38	2.33	2.28	2.44	2.39	2.28	2.31	2.25	2.17	2.19
CaO	5.43	5.20	5.11	5.23	5.46	5.46	5.38	5.43	5.27	5.22
Total	100.77	101.09	100.67	99.99	100.30	100.25	99.69	100.75	101.00	99.85
Structural formula (in apfu) based on 12 oxygens										
Z (iv) site:										
Si	2.978	2.951	3.018	2.940	3.014	2.925	3.010	2.975	2.991	3.037
Fe^{3+}	0.002	0.002	0.000	0.000	0.000	0.000	0.000	0.002	0.002	0.000
Al	0.019	0.047	0.000	0.060	0.000	0.075	0.000	0.023	0.007	0.000
Site total	3.000	3.000	3.018	3.000	3.014	3.000	3.010	3.000	3.000	3.037
Al (total)	1.988	1.979	1.964	1.992	1.962	1.966	1.957	1.954	1.976	1.950
Fe^{3+}(total)	0.055	0.124	0.000	0.140	0.009	0.197	0.023	0.099	0.038	0.000
Y (vi) site:										
Al	1.964	1.922	1.964	1.920	1.961	1.875	1.955	1.923	1.966	1.952
Ti	0.002	0.002	0.003	0.000	0.001	0.000	0.000	0.002	0.002	0.000
Cr^{3+}	0.000	0.001	0.001	0.000	0.000	0.002	0.003	0.001	0.003	0.000
Fe^{3+}	0.053	0.122	0.000	0.140	0.009	0.197	0.023	0.097	0.035	0.000
Site total	2.019	2.047	1.968	2.060	1.972	2.075	1.981	2.023	2.007	1.952
X (viii) site:										
Fe^{2+}	2.190	2.187	2.260	2.148	2.220	2.135	2.221	2.197	2.234	2.256
Mn^{2+}	0.045	0.045	0.045	0.048	0.041	0.046	0.046	0.047	0.051	0.042

Mg	0.283	0.277	0.271	0.293	0.285	0.274	0.277	0.268	0.258	0.263
Ca	0.464	0.444	0.437	0.451	0.468	0.471	0.464	0.465	0.450	0.450
Site total	2.981	2.953	3.014	2.940	3.015	2.925	3.010	2.977	2.993	3.011
Molecular percentages of endmembers										
Almandine	73.46	74.07	76.57	73.07	75.07	72.97	74.76	73.79	74.65	77.05
Pyrope	9.49	9.38	9.19	9.96	9.64	9.36	9.34	9.01	8.61	8.97
Spessartine	1.49	1.51	1.53	1.62	1.40	1.56	1.56	1.57	1.71	1.42
Grossular	15.39	14.86	12.52	15.34	13.35	16.01	13.06	13.71	13.89	12.56
Andradite	0.05	0.00	0.00	0.00	0.48	0.00	1.15	1.77	0.86	0.00
Schorlomite	0.12	0.12	0.15	0.00	0.06	0.00	0.00	0.09	0.12	0.00
Uvarovite	0.00	0.06	0.03	0.00	0.00	0.10	0.13	0.06	0.16	0.00

Sample	HP82-59									
Analysis Type	Large garnet traverse (continued)									
Analysis Pt.	30	31	32	33	34	35	36	37	38	39
Wt%										
SiO_2	37.14	36.72	36.75	37.15	37.34	37.02	36.98	36.93	36.37	36.89
Al_2O_3	20.27	20.75	20.56	21.14	20.95	20.93	20.70	20.80	20.48	20.74
TiO_2	0.01	0.02	0.02	0.00	0.00	0.03	0.03	0.03	0.02	0.00
Cr_2O_3	0.00	0.01	0.02	0.03	0.07	0.03	0.05	0.05	0.05	0.05
Fe_2O_3	1.13	1.25	2.90	0.83	2.95	2.92	0.00	1.96	1.55	1.60
FeO	33.57	32.75	33.37	33.45	33.79	33.02	33.25	33.11	32.27	32.46
MnO	0.75	0.68	0.60	0.77	0.75	0.64	0.74	0.64	0.82	0.61
MgO	2.13	2.29	2.21	2.27	2.30	2.30	2.20	2.28	2.29	2.35
CaO	4.91	5.00	4.72	4.80	4.68	5.09	4.71	4.97	4.94	5.34
Total	99.91	99.46	101.15	100.43	102.84	101.98	98.66	100.77	98.79	100.04
Structural formula (in apfu) based on 12 oxygens										
Z (iv) site:										

Si	3.000	2.971	2.941	2.976	2.939	2.933	3.013	2.956	2.966	2.967
Fe^{3+}	0.000	0.001	0.001	0.000	0.000	0.002	0.000	0.002	0.001	0.000
Al	0.000	0.028	0.058	0.024	0.061	0.065	0.000	0.042	0.033	0.033
Site total	3.000	3.000	3.000	3.000	3.000	3.000	3.013	3.000	3.000	3.000
Al (total)	1.935	1.985	1.953	2.000	1.958	1.969	1.986	1.972	1.976	1.974
Fe^{3+}(total)	0.069	0.076	0.175	0.050	0.175	0.174	0.000	0.118	0.095	0.097
Y (vi) site:										
Al	1.930	1.951	1.882	1.972	1.882	1.889	1.988	1.921	1.935	1.933
Ti	0.001	0.001	0.001	0.000	0.000	0.002	0.002	0.002	0.001	0.000
Cr^{3+}	0.000	0.001	0.001	0.002	0.004	0.002	0.003	0.003	0.003	0.003
Fe^{3+}	0.069	0.075	0.174	0.050	0.175	0.172	0.000	0.116	0.094	0.097
Site total	1.999	2.028	2.058	2.024	2.061	2.065	1.993	2.042	2.033	2.033
X (viii) site:										
Fe^{2+}	2.268	2.216	2.233	2.241	2.224	2.188	2.265	2.216	2.200	2.184
Mn^{2+}	0.051	0.047	0.041	0.052	0.050	0.043	0.051	0.043	0.057	0.042
Mg	0.256	0.276	0.264	0.271	0.270	0.272	0.267	0.272	0.278	0.282
Ca	0.425	0.433	0.405	0.412	0.395	0.432	0.411	0.426	0.432	0.460
Site total	3.001	2.972	2.942	2.976	2.939	2.935	2.995	2.958	2.967	2.967
Molecular percentages of endmembers										
Almandine	75.63	74.56	75.90	75.29	75.69	74.56	75.79	74.92	74.16	73.59
Pyrope	8.55	9.29	8.96	9.11	9.18	9.26	8.94	9.20	9.38	9.50
Spessartine	1.71	1.57	1.38	1.76	1.70	1.46	1.71	1.47	1.91	1.40
Grossular	10.63	14.44	12.62	13.75	12.62	14.53	13.31	13.92	14.05	14.90
Andradite	3.44	0.05	1.01	0.00	0.59	0.00	0.00	0.24	0.27	0.45
Schorlomite	0.03	0.06	0.06	0.00	0.00	0.09	0.09	0.09	0.06	0.00
Uvarovite	0.00	0.03	0.06	0.10	0.22	0.10	0.16	0.16	0.16	0.16

Sample	HR02-3								
Analysis Type	Cores								
Analysis Pt.	42	43	44	45	46	47	48	49	50
Wt%									
SiO_2	36.41	37.43	36.61	37.66	37.21	37.50	36.86	37.88	37.08
Al_2O_3	21.24	20.97	20.89	20.84	20.56	20.92	20.48	20.98	20.79
TiO_2	0.00	0.03	0.00	0.00	0.02	0.00	0.00	0.02	0.04
Cr_2O_3	0.00	0.00	0.00	0.00	0.00	0.00	0.03	0.04	0.01
Fe_2O_3	2.41	1.07	1.48	0.13	0.52	1.33	1.50	0.42	0.37
FeO	30.02	30.89	30.11	31.43	30.89	30.90	30.59	31.58	30.93
MnO	2.55	2.63	2.51	2.57	2.49	2.53	2.71	2.64	2.60
MgO	2.95	3.15	2.92	2.97	3.00	3.05	2.94	3.09	2.94
CaO	4.43	4.38	4.62	4.45	4.49	4.64	4.29	4.33	4.35
Total	100.01	100.56	99.14	100.05	99.18	100.86	99.40	100.98	99.11
Structural formula (in apfu) based on 12 oxygens									
Z (iv) site:									
Si	2.923	2.982	2.960	3.013	3.005	2.981	2.978	3.004	2.996
Fe^{3+}	0.000	0.002	0.000	0.000	0.000	0.000	0.000	0.000	0.002
Al	0.077	0.017	0.040	0.000	0.000	0.019	0.022	0.000	0.001
Site total	3.000	3.000	3.000	3.013	3.005	3.000	3.000	3.004	3.000
Al (total)	2.022	1.974	1.998	1.966	1.959	1.966	1.958	1.963	1.982
Fe^{3+}(total)	0.146	0.064	0.090	0.008	0.032	0.079	0.091	0.025	0.022
Y (vi) site:									
Al	1.932	1.952	1.950	1.965	1.957	1.940	1.929	1.961	1.978
Ti	0.000	0.002	0.000	0.000	0.001	0.000	0.000	0.001	0.002
Cr^{3+}	0.000	0.000	0.000	0.000	0.000	0.000	0.002	0.003	0.001
Fe^{3+}	0.146	0.063	0.090	0.008	0.032	0.079	0.091	0.025	0.020
Site total	2.077	2.017	2.040	1.973	1.990	2.019	2.022	1.990	2.001
X (viii) site:									
Fe^{2+}	2.015	2.058	2.036	2.103	2.086	2.054	2.067	2.095	2.090
Mn^{2+}	0.173	0.177	0.172	0.174	0.170	0.170	0.185	0.177	0.178

Mg	0.353	0.374	0.352	0.354	0.361	0.361	0.354	0.365	0.354
Ca	0.381	0.374	0.400	0.382	0.388	0.395	0.371	0.368	0.377
Site total	2.923	2.983	2.960	3.013	3.006	2.981	2.978	3.006	2.999
Molecular percentages of endmembers									
Almandine	68.95	68.98	68.78	71.07	69.90	68.90	69.41	70.19	69.70
Pyrope	12.08	12.54	11.89	11.97	12.10	12.12	11.89	12.24	11.81
Spessartine	5.93	5.95	5.81	5.89	5.71	5.71	6.23	5.94	5.93
Grossular	13.04	11.51	13.52	10.68	10.64	11.88	10.69	10.19	11.60
Andradite	0.00	0.93	0.00	0.39	1.59	1.38	1.68	1.25	0.81
Schorlomite	0.00	0.09	0.00	0.00	0.06	0.00	0.00	0.06	0.12
Uvarovite	0.00	0.00	0.00	0.00	0.00	0.00	0.10	0.13	0.03

Sample	HR02-3								
Analysis Type	Cores								
Analysis Pt.	54	55	56	57	58	59	60	61	62
Wt%									
SiO_2	37.05	37.68	37.22	36.88	37.23	37.19	36.93	37.02	36.74
Al_2O_3	20.52	20.97	20.74	21.03	20.81	20.83	21.14	20.65	20.48
TiO_2	0.04	0.00	0.01	0.02	0.00	0.00	0.01	0.03	0.00
Cr_2O_3	0.00	0.03	0.00	0.02	0.01	0.00	0.00	0.00	0.02
Fe_2O_3	2.47	0.00	1.37	2.96	2.31	1.34	2.96	1.75	2.28
FeO	30.00	30.90	30.48	30.01	30.73	30.31	30.29	30.30	30.32
MnO	2.74	2.79	2.85	2.76	2.71	2.75	2.86	2.95	2.87
MgO	3.14	3.18	3.05	3.07	3.04	3.21	2.96	3.00	2.88
CaO	4.66	4.40	4.46	4.56	4.39	4.41	4.45	4.42	4.35
Total	100.62	99.95	100.18	101.31	101.23	100.04	101.61	100.12	99.94
Structural formula (in apfu) based on 12 oxygens									

Z (iv) site:									
Si	2.958	3.012	2.980	2.926	2.957	2.977	2.925	2.969	2.958
Fe^{3+}	0.002	0.000	0.001	0.001	0.000	0.000	0.001	0.002	0.000
Al	0.040	0.000	0.020	0.072	0.043	0.023	0.075	0.029	0.042
Site total	3.000	3.012	3.000	3.000	3.000	3.000	3.000	3.000	3.000
Al (total)	1.943	1.976	1.964	1.981	1.959	1.972	1.988	1.961	1.955
Fe^{3+}(total)	0.148	0.000	0.082	0.177	0.138	0.081	0.177	0.106	0.138
Y (vi) site:									
Al	1.891	1.976	1.937	1.894	1.905	1.942	1.898	1.923	1.902
Ti	0.002	0.000	0.001	0.001	0.000	0.000	0.001	0.002	0.000
Cr^{3+}	0.000	0.002	0.000	0.001	0.001	0.000	0.000	0.000	0.001
Fe^{3+}	0.146	0.000	0.082	0.175	0.138	0.081	0.176	0.104	0.138
Site total	2.040	1.978	2.020	2.072	2.043	2.023	2.075	2.029	2.042
X (viii) site:									
Fe^{2+}	2.003	2.066	2.041	1.991	2.041	2.029	2.006	2.032	2.042
Mn^{2+}	0.185	0.189	0.193	0.186	0.182	0.186	0.192	0.200	0.196
Mg	0.374	0.379	0.364	0.363	0.360	0.383	0.349	0.359	0.346
Ca	0.399	0.377	0.383	0.388	0.374	0.378	0.378	0.380	0.375
Site total	2.960	3.010	2.980	2.928	2.957	2.977	2.925	2.971	2.958
Molecular percentages of endmembers									
Almandine	67.65	69.64	68.47	68.02	69.03	68.16	68.59	68.40	69.01
Pyrope	12.62	12.78	12.21	12.40	12.17	12.87	11.95	12.07	11.69
Spessartine	6.26	6.37	6.48	6.34	6.17	6.26	6.56	6.75	6.62
Grossular	11.30	11.12	11.33	13.12	11.45	11.72	12.88	11.34	11.23
Andradite	2.05	0.00	1.48	0.00	1.15	0.98	0.00	1.36	1.39
Schorlomite	0.12	0.00	0.03	0.06	0.00	0.00	0.03	0.09	0.00
Uvarovite	0.00	0.10	0.00	0.06	0.03	0.00	0.00	0.00	0.06

Sample	QC82-49b						QC-JW3					QC81-6		HR02-71
Analysis Type	area 1					area 4	core					core	rim	
Analysis Pt.	grt-1	grt-2	grt-3	grt-11	grt-12	grt-12	grt-1	grt-8	grt-6	grt-2'	grt-7'	grt-1	grt-2	
Wt%														
SiO_2	37.60	37.57	37.52	37.41	37.14	37.97	37.29	37.35	37.05	37.36	36.87	37.66	37.52	36.94
Al_2O_3	20.73	20.61	20.54	20.47	20.12	20.54	20.18	21.02	20.85	20.81	20.48	20.61	20.52	20.38
TiO_2	0.00	0.00	0.00	0.01	0.01	0.02	0.00	0.00	0.02	0.02	0.01	0.01	0.00	0.00
Cr_2O_3	0.03	0.01	0.00	0.00	0.01	0.00	0.02	0.00	0.00	0.00	0.00	0.00	0.02	0.00
Fe_2O_3	2.61	1.92	1.55	1.78	2.21	0.52	2.18	1.20	2.68	2.73	3.59	1.48	1.47	1.89
FeO	25.69	26.20	25.98	26.47	26.88	27.58	24.96	25.29	24.64	24.68	24.41	28.12	27.50	26.50
MnO	3.95	3.61	3.68	3.85	4.37	3.77	6.30	6.14	6.53	6.52	6.53	3.87	3.69	5.70
MgO	2.96	2.68	2.69	2.68	2.23	2.62	2.04	2.01	2.25	2.18	2.15	2.17	2.11	1.46
CaO	7.80	8.03	8.09	7.49	7.13	7.30	7.50	7.47	7.07	7.43	7.21	7.13	7.70	7.25
Total	101.37	100.63	100.04	100.16	100.10	100.32	100.48	100.48	101.09	101.73	101.25	101.05	100.53	100.12
Structural formula (in apfu) based on 12 oxygens														
Z (iv) site:														
Si	2.960	2.979	2.989	2.984	2.981	3.020	2.982	2.977	2.943	2.950	2.932	2.991	2.991	2.975
Fe^{3+}	0.000	0.000	0.000	0.001	0.001	0.000	0.000	0.000	0.001	0.001	0.001	0.001	0.000	0.000
Al	0.040	0.021	0.011	0.016	0.019	0.000	0.018	0.023	0.056	0.049	0.067	0.009	0.009	0.025
Site total	3.000	3.000	3.000	3.000	3.000	3.020	3.000	3.000	3.000	3.000	3.000	3.000	3.000	3.000
Al (total)	1.936	1.935	1.936	1.933	1.914	1.928	1.913	1.980	1.965	1.949	1.937	1.936	1.935	1.944
Fe^{3+}(total)	0.155	0.115	0.093	0.107	0.133	0.031	0.132	0.072	0.160	0.162	0.215	0.088	0.088	0.114
Y (vi) site:														
Al	1.883	1.906	1.918	1.909	1.885	1.926	1.885	1.951	1.896	1.887	1.853	1.920	1.919	1.910
Ti	0.000	0.000	0.000	0.001	0.001	0.001	0.000	0.000	0.001	0.001	0.001	0.001	0.000	0.000
Cr^{3+}	0.002	0.001	0.000	0.000	0.001	0.000	0.001	0.000	0.000	0.000	0.000	0.000	0.001	0.000
Fe^{3+}	0.155	0.115	0.093	0.106	0.133	0.031	0.132	0.072	0.159	0.161	0.214	0.088	0.088	0.114
Site total	2.040	2.021	2.011	2.016	2.019	1.958	2.018	2.023	2.056	2.049	2.067	2.009	2.009	2.025
X (viii) site:														

Fe^{2+}	1.691	1.738	1.731	1.766	1.804	1.835	1.670	1.686	1.637	1.630	1.624	1.867	1.834	1.785
Mn^{2+}	0.263	0.242	0.248	0.260	0.297	0.254	0.427	0.414	0.439	0.436	0.440	0.260	0.249	0.389
Mg	0.347	0.317	0.319	0.319	0.267	0.311	0.243	0.239	0.266	0.257	0.255	0.257	0.251	0.176
Ca	0.658	0.682	0.691	0.640	0.613	0.622	0.643	0.638	0.602	0.628	0.614	0.607	0.658	0.626
Site total	2.960	2.979	2.989	2.984	2.981	3.022	2.982	2.977	2.944	2.951	2.933	2.991	2.991	2.975
Molecular percentages of endmembers														
Almandine	57.14	58.33	57.90	59.16	60.52	62.47	55.99	56.63	55.59	55.23	55.36	62.43	61.30	59.99
Pyrope	11.74	10.63	10.69	10.68	8.95	10.58	8.16	8.02	9.05	8.70	8.69	8.59	8.38	5.91
Spessartine	8.90	8.14	8.31	8.72	9.96	8.65	14.31	13.92	14.92	14.78	15.00	8.70	8.33	13.07
Grossular	19.69	19.88	19.88	18.16	16.32	16.65	17.22	20.92	19.88	19.73	19.13	17.01	18.67	18.56
Andradite	2.44	2.99	3.22	3.26	4.19	1.60	4.27	0.51	0.49	1.51	1.79	3.24	3.25	2.47
Schorlomite	0.00	0.00	0.00	0.03	0.03	0.06	0.00	0.00	0.06	0.06	0.03	0.03	0.00	0.00
Uvarovite	0.09	0.03	0.00	0.00	0.03	0.00	0.06	0.00	0.00	0.00	0.00	0.00	0.06	0.00

APPENDIX B: PYROXENE EPMA DATA

Sample	QC82-45											
Analysis Type	opx incl.	opx incl.	opx incl.	w/ biot incl.	by grt-8	by biot-18	grt incl.	opx	opx	opx	opx	opx
Analysis Pt.	4/24	4/25	4/26	opx-4	opx-9	opx-19	opx-24	1	2	3	4	5
Wt%												
SiO_2	49.04	48.92	48.83	48.49	48.88	48.44	48.69	48.25	48.13	48.20	48.32	48.22
Al_2O_3	0.33	0.38	0.34	0.37	0.33	0.48	0.42	0.41	0.42	0.42	0.46	0.44
TiO_2	0.07	0.08	0.04	0.07	0.03	0.07	0.00	0.07	0.05	0.06	0.07	0.09
Cr_2O_3	0.01	0.00	0.02	0.00	0.02	0.01	0.01	0.00	0.03	0.00	0.04	0.03
Fe_2O_3	0.57	0.60	0.76	0.37	0.94	1.50	1.11	2.15	1.89	2.06	2.00	2.05
FeO	37.01	37.27	36.94	40.59	39.55	38.24	39.07	37.43	37.28	37.46	37.63	37.48
MnO	0.85	0.84	0.94	1.50	1.32	1.20	1.28	1.07	1.08	1.03	0.97	1.04
MgO	11.22	11.00	11.02	8.39	9.37	9.81	9.52	10.20	10.20	10.17	10.19	10.19
CaO	0.65	0.65	0.69	0.77	0.68	0.82	0.70	0.82	0.82	0.84	0.84	0.80
Total	99.75	99.74	99.57	100.53	101.11	100.57	100.78	100.40	99.90	100.23	100.50	100.34
Structural formula (in apfu) based on 6 oxygens												
T (iv) site:												
Si	1.981	1.979	1.979	1.983	1.977	1.963	1.973	1.956	1.959	1.957	1.956	1.955
Al	0.016	0.018	0.016	0.017	0.016	0.023	0.020	0.019	0.020	0.020	0.022	0.021
Fe^{3+}	0.003	0.002	0.005	0.000	0.007	0.014	0.007	0.025	0.021	0.023	0.022	0.024
Site total	2.000	2.000	2.000	2.000	2.000	2.000	2.000	2.000	2.000	2.000	2.000	2.000
Al (total)	0.016	0.018	0.016	0.018	0.016	0.023	0.020	0.019	0.020	0.020	0.022	0.021
Fe^{3+}(total)	0.017	0.018	0.023	0.011	0.029	0.046	0.034	0.065	0.058	0.063	0.061	0.063
M (vi) site:												
Al	0.000	0.000	0.000	0.001	0.000	0.000	0.000	0.000	0.000	0.000	0.000	0.000
Ti	0.002	0.002	0.001	0.002	0.001	0.002	0.000	0.002	0.002	0.002	0.002	0.003
Fe^{3+}	0.014	0.016	0.018	0.011	0.021	0.032	0.027	0.040	0.037	0.040	0.039	0.039
Fe^{2+}	1.250	1.261	1.252	1.388	1.338	1.296	1.324	1.269	1.269	1.272	1.274	1.271

Mn^{2+}	0.029	0.029	0.032	0.052	0.045	0.041	0.044	0.037	0.037	0.035	0.033	0.036
Mg	0.676	0.664	0.666	0.511	0.565	0.593	0.575	0.616	0.619	0.615	0.615	0.616
Ca	0.028	0.028	0.030	0.034	0.030	0.036	0.030	0.036	0.036	0.036	0.036	0.035
Site total	2.000	2.000	2.000	2.000	1.999	2.000	2.000	2.000	1.999	2.000	1.999	1.999
Molecular percentages of major components												
Diopside	0.99	0.97	1.05	0.91	0.88	1.13	0.92	1.18	1.18	1.20	1.19	1.15
Hedenbergite	1.83	1.85	1.97	2.46	2.09	2.47	2.12	2.43	2.41	2.48	2.47	2.38
Enstatite	31.63	30.97	30.94	22.28	25.40	26.84	25.89	28.42	28.48	28.41	28.44	28.46
Ferrosilite	61.08	61.49	61.19	67.51	65.49	63.12	64.67	62.26	62.13	62.31	62.31	62.29
Kanoite	2.90	2.89	3.25	5.18	4.55	4.14	4.40	3.73	3.75	3.57	3.37	3.60

Sample	QC82-45				QC-IS						QC81-1	QC81-5
Analysis Type	opx	opx	opx	cpx in amph	core	rim	core	rim	core			
Analysis Pt.	1	2	3	cpx-16	opx-1	opx-2	opx-3	cpx-4	cpx-5	opx-1	opx-3	opx-3
Wt%												
SiO_2	48.45	48.51	48.69	50.53	49.46	49.91	49.66	50.75	50.91	48.79	49.81	49.15
Al_2O_3	0.42	0.43	0.42	0.62	0.49	0.51	0.48	0.73	0.88	0.45	0.78	0.64
TiO_2	0.04	0.06	0.06	0.08	0.00	0.00	0.00	0.00	0.00	0.05	0.02	0.00
Cr_2O_3	0.00	0.03	0.00	0.01	0.00	0.00	0.00	0.00	0.00	0.00	0.01	0.00
Fe_2O_3	1.06	1.08	0.31	0.72	0.00	0.00	0.00	0.83	0.72	1.32	1.34	1.05
FeO	37.74	37.88	38.09	17.22	37.25	36.82	37.36	16.63	17.33	35.95	33.29	34.64
MnO	1.00	1.07	1.05	0.46	1.34	1.41	1.39	0.61	0.60	1.50	0.44	0.58
MgO	10.18	10.14	10.12	8.59	10.73	10.95	10.45	8.54	8.37	11.18	14.42	12.80
CaO	0.83	0.81	0.85	21.46	0.75	0.60	0.69	21.41	21.18	0.70	0.11	0.42
Na_2O	0.00	0.00	0.00	0.00	0.02	0.05	0.02	0.17	0.19	0.02	0.00	0.04
Total	99.71	99.99	99.59	99.69	100.04	100.25	100.05	99.66	100.18	99.96	100.21	99.33
Structural formula (in apfu) based on 6 oxygens												

T (iv) site:												
Si	1.973	1.971	1.983	1.973	1.995	2.005	2.006	1.978	1.976	1.969	1.961	1.971
Al	0.020	0.020	0.017	0.027	0.005	0.000	0.000	0.022	0.024	0.021	0.036	0.029
Fe^{3+}	0.007	0.008	0.000	0.000	0.000	0.000	0.000	0.000	0.000	0.010	0.002	0.000
Site total	2.000	2.000	2.000	2.000	2.000	2.005	2.006	2.000	2.000	2.000	2.000	2.000
Al (total)	0.020	0.020	0.020	0.029	0.023	0.024	0.023	0.034	0.040	0.021	0.036	0.030
Fe^{3+}(total)	0.032	0.033	0.010	0.021	0.000	0.000	0.000	0.024	0.021	0.040	0.040	0.032
M (vi) site:												
Al	0.000	0.000	0.003	0.001	0.018	0.024	0.023	0.011	0.017	0.000	0.000	0.001
Ti	0.001	0.002	0.002	0.002	0.000	0.000	0.000	0.000	0.000	0.002	0.001	0.000
Fe^{3+}	0.025	0.025	0.010	0.021	0.000	0.000	0.000	0.024	0.021	0.030	0.037	0.032
Fe^{2+}	1.285	1.287	1.297	0.562	1.257	1.237	1.262	0.542	0.563	1.213	1.096	1.162
Mn^{2+}	0.034	0.037	0.036	0.015	0.046	0.048	0.048	0.020	0.020	0.051	0.015	0.020
Mg	0.618	0.614	0.614	0.500	0.645	0.656	0.629	0.496	0.484	0.672	0.846	0.765
Ca	0.036	0.035	0.037	0.898	0.032	0.026	0.030	0.894	0.881	0.030	0.005	0.018
Na	0.000	0.000	0.000	0.000	0.002	0.004	0.002	0.013	0.014	0.002	0.000	0.003
Site total	2.000	1.999	2.000	2.000	2.000	1.995	1.994	2.000	2.000	2.000	2.000	2.000
Molecular percentages of major components												
Diopside	1.17	1.14	1.19	40.24	1.10	0.90	1.00	40.69	38.76	1.08	0.20	0.72
Hedenbergite	2.44	2.39	2.51	45.26	2.15	1.70	2.01	44.44	45.02	1.96	0.26	1.09
Enstatite	28.38	28.08	28.01	4.82	29.33	30.00	28.66	4.46	4.84	30.29	40.75	36.32
Ferrosilite	62.53	62.66	62.98	5.42	61.58	61.15	62.30	4.87	5.63	59.21	53.69	56.65
Jadeite	0.00	0.00	0.00	0.00	0.16	0.39	0.16	0.00	0.00	0.00	0.00	0.00
Aegerine	0.00	0.00	0.00	0.00	0.00	0.00	0.00	1.28	1.43	0.16	0.00	0.31
Esseneite	0.00	0.00	0.00	2.12	0.00	0.00	0.00	1.14	0.67	0.00	0.00	0.00
Johannsenite	0.00	0.00	0.00	1.52	0.00	0.00	0.00	2.01	1.97	0.00	0.00	0.00
Kanoite	3.45	3.68	3.63	0.00	4.59	4.84	4.80	0.00	0.00	5.15	1.47	1.97

Sample	QC82-44										QC81-40b	
Analysis Type	opx-1	opx-1	opx-1	opx-1	opx-1	opx-1	opx-1	opx-2	opx-2	opx-2	opx	opx
Analysis Pt.	10	11	12	13	14	15	16	17	18	19	opx-2	opx-3
Wt%												
SiO_2	49.43	49.01	48.61	49.06	49.55	49.06	49.58	49.52	48.95	50.07	50.39	50.06
Al_2O_3	0.72	0.77	0.76	0.82	0.79	0.80	0.75	0.72	0.88	0.81	0.71	0.69
TiO_2	0.00	0.00	0.02	0.00	0.02	0.00	0.00	0.03	0.00	0.00	0.00	0.00
Cr_2O_3	0.02	0.00	0.00	0.02	0.00	0.00	0.01	0.03	0.07	0.00	0.02	0.02
Fe_2O_3	1.01	0.48	1.72	1.58	1.35	0.87	2.81	2.88	2.26	1.37	0.00	0.00
FeO	31.67	30.12	30.00	29.97	30.61	30.36	30.33	30.42	30.26	31.02	34.36	34.79
MnO	1.08	1.13	1.17	1.36	1.15	1.15	1.17	1.12	1.15	1.17	1.33	1.58
MgO	14.43	14.96	14.75	15.03	15.12	14.85	15.29	15.21	14.90	15.13	13.10	12.49
CaO	0.48	0.45	0.41	0.24	0.40	0.39	0.32	0.28	0.40	0.47	0.43	0.39
Na_2O	0.00	0.00	0.03	0.04	0.00	0.03	0.01	0.02	0.00	0.02	0.00	0.02
K_2O	0.00	0.03	0.00	0.01	0.01	0.01	0.02	0.04	0.01	0.00	0.00	0.00
Total	98.84	96.96	97.47	98.13	99.00	97.52	100.29	100.27	98.89	100.06	100.34	100.04
Structural formula (in apfu) based on 6 oxygens												
T (iv) site:												
Si	1.968	1.975	1.956	1.959	1.961	1.969	1.942	1.941	1.945	1.962	1.994	1.994
Al	0.032	0.025	0.036	0.039	0.037	0.031	0.035	0.033	0.041	0.037	0.006	0.006
Fe^{3+}	0.000	0.000	0.007	0.003	0.002	0.000	0.023	0.025	0.014	0.001	0.000	0.000
Site total	2.000	2.000	2.000	2.000	2.000	2.000	2.000	2.000	2.000	2.000	2.000	2.000
Al (total)	0.034	0.037	0.036	0.039	0.037	0.038	0.035	0.033	0.041	0.037	0.033	0.032
Fe^{3+}(total)	0.030	0.015	0.052	0.047	0.040	0.026	0.083	0.085	0.068	0.040	0.000	0.000
M (vi) site:												
Al	0.002	0.012	0.000	0.000	0.000	0.007	0.000	0.000	0.000	0.000	0.027	0.027
Ti	0.000	0.000	0.001	0.000	0.001	0.000	0.000	0.001	0.000	0.000	0.000	0.000
Fe^{3+}	0.030	0.015	0.045	0.044	0.038	0.026	0.060	0.060	0.054	0.040	0.000	0.000
Fe^{2+}	1.055	1.015	1.010	1.001	1.013	1.019	0.993	0.997	1.006	1.017	1.137	1.159
Mn^{2+}	0.036	0.039	0.040	0.046	0.039	0.039	0.039	0.037	0.039	0.039	0.045	0.053
Mg	0.856	0.899	0.885	0.894	0.892	0.889	0.893	0.889	0.882	0.884	0.773	0.742

Ca	0.020	0.019	0.018	0.010	0.017	0.017	0.013	0.012	0.017	0.020	0.018	0.017
Na	0.000	0.000	0.002	0.003	0.000	0.002	0.001	0.002	0.000	0.002	0.000	0.002
K	0.000	0.002	0.000	0.001	0.001	0.001	0.001	0.002	0.001	0.000	0.000	0.000
Site total	1.999	2.000	2.000	1.999	2.000	2.000	2.000	1.999	1.998	2.000	1.999	1.999
Molecular percentages of major components												
Diopside	0.92	0.91	0.83	0.49	0.80	0.78	0.64	0.56	0.80	0.92	0.74	0.65
Hedenbergite	1.13	1.03	0.95	0.54	0.90	0.90	0.72	0.63	0.91	1.06	1.09	1.02
Enstatite	39.81	42.00	41.15	41.35	41.47	41.38	42.10	42.13	41.14	40.93	35.89	33.97
Ferrosilite	51.27	49.63	49.21	48.84	49.28	49.70	49.03	49.38	49.10	49.32	56.10	57.26
Jadeite	0.00	0.00	0.00	0.00	0.00	0.00	0.00	0.00	0.00	0.00	0.00	0.09
Aegerine	0.00	0.00	0.23	0.31	0.00	0.23	0.08	0.15	0.00	0.15	0.00	0.00
Kanoite	3.64	3.86	4.00	4.61	3.86	3.91	3.93	3.77	3.90	3.88	4.48	5.36

Sample	QC81-40b		QC81-66	QC81-6								
Analysis Type	opx	opx	core	core	rim	cpx	opx	opx	opx	opx	cpx	cpx
Analysis Pt.	opx-4	opx-6	opx-1	opx-1	opx-2	cpx-3	opx-3	opx-4	opx-5	opx-6	cpx-6	cpx-7
Wt%												
SiO_2	50.61	50.12	49.86	49.74	50.10	50.68	50.11	50.01	49.88	50.29	51.53	51.14
Al_2O_3	0.72	0.73	0.59	0.52	0.53	0.79	0.49	0.52	0.54	0.56	0.78	0.77
TiO_2	0.00	0.02	0.04	0.00	0.00	0.00	0.00	0.00	0.00	0.01	0.00	0.00
Cr_2O_3	0.02	0.00	0.02	0.02	0.02	0.01	0.01	0.02	0.04	0.04	0.00	0.02
Fe_2O_3	0.00	0.12	1.38	0.00	0.00	1.01	0.00	0.00	0.00	0.00	0.45	1.06
FeO	34.63	35.19	34.14	35.98	35.96	15.83	36.14	36.05	35.84	36.03	16.24	16.25
MnO	1.40	1.61	1.48	1.45	1.44	0.61	1.41	1.35	1.45	1.46	0.59	0.54
MgO	13.04	12.56	13.23	11.42	11.53	8.88	11.59	11.32	11.40	11.46	9.00	9.08
CaO	0.44	0.54	0.34	0.82	0.70	21.49	0.74	0.78	0.75	0.75	21.89	21.44
Na_2O	0.01	0.01	0.00	0.00	0.00	0.17	0.00	0.00	0.00	0.00	0.15	0.15

Total	100.87	100.90	101.08	99.95	100.28	99.47	100.49	100.05	99.90	100.60	100.62	100.46
Structural formula (in apfu) based on 6 oxygens												
T (iv) site:												
Si	1.993	1.981	1.964	1.998	2.005	1.973	2.001	2.008	2.004	2.007	1.981	1.972
Al	0.007	0.019	0.027	0.002	0.000	0.027	0.000	0.000	0.000	0.000	0.019	0.028
Fe^{3+}	0.000	0.000	0.008	0.000	0.000	0.000	0.000	0.000	0.000	0.000	0.000	0.000
Site total	2.000	2.000	2.000	2.000	2.005	2.000	2.001	2.008	2.004	2.007	2.000	2.000
Al (total)	0.033	0.034	0.027	0.025	0.025	0.036	0.023	0.025	0.026	0.026	0.035	0.035
Fe^{3+}(total)	0.000	0.004	0.041	0.000	0.000	0.030	0.000	0.000	0.000	0.000	0.013	0.031
M (vi) site:												
Al	0.027	0.015	0.000	0.022	0.025	0.010	0.023	0.025	0.026	0.026	0.017	0.007
Ti	0.000	0.001	0.001	0.000	0.000	0.000	0.000	0.000	0.000	0.000	0.000	0.000
Fe^{3+}	0.000	0.004	0.033	0.000	0.000	0.030	0.000	0.000	0.000	0.000	0.013	0.031
Fe^{2+}	1.141	1.163	1.125	1.209	1.203	0.516	1.207	1.210	1.204	1.202	0.522	0.524
Mn^{2+}	0.047	0.054	0.049	0.049	0.049	0.020	0.048	0.046	0.049	0.049	0.019	0.018
Mg	0.766	0.740	0.777	0.684	0.688	0.515	0.690	0.677	0.683	0.682	0.516	0.522
Ca	0.019	0.023	0.014	0.035	0.030	0.897	0.032	0.034	0.032	0.032	0.902	0.886
Na	0.001	0.001	0.000	0.000	0.000	0.013	0.000	0.000	0.000	0.000	0.011	0.011
Site total	1.999	2.000	1.999	1.999	1.995	2.000	1.999	1.992	1.994	1.992	2.000	1.999
Molecular percentages of major components												
Diopside	0.75	0.89	0.59	1.28	1.10	42.48	1.16	1.22	1.18	1.17	42.94	41.95
Hedenbergite	1.12	1.40	0.85	2.27	1.93	42.50	2.03	2.17	2.08	2.07	43.46	42.13
Enstatite	35.42	33.48	35.68	31.02	31.44	4.53	31.52	31.06	31.12	31.10	4.32	5.13
Ferrosilite	56.27	56.86	55.17	59.21	59.32	4.53	59.33	59.64	59.28	59.25	4.37	5.15
Jadeite	0.01	0.00	0.00	0.00	0.00	0.00	0.00	0.00	0.00	0.00	0.00	0.00
Aegerine	0.00	0.08	0.00	0.00	0.00	1.28	0.00	0.00	0.00	0.00	1.12	1.12
Esseneite	0.00	0.00	0.00	0.00	0.00	1.67	0.00	0.00	0.00	0.00	0.18	1.96
Johannsenite	0.00	0.00	0.00	0.00	0.00	2.01	0.00	0.00	0.00	0.00	1.92	1.76
Kanoite	4.69	5.39	4.96	4.96	4.92	0.00	4.80	4.64	4.98	4.99	0.00	0.00

Sample	HR02-3											
Analysis Type	opx	opx	opx	opx	opx	opx	opx	opx	opx	opx	opx	opx
Analysis Pt.	5	6	7	8	9	10	11	12	13	14	18	19
Wt%												
SiO_2	48.77	49.23	49.38	49.22	50.03	49.78	49.21	49.32	50.09	49.27	49.48	49.16
Al_2O_3	0.92	0.94	0.98	0.88	0.82	0.86	0.82	0.86	0.82	0.83	0.77	0.84
TiO_2	0.01	0.00	0.03	0.02	0.03	0.02	0.01	0.00	0.00	0.03	0.00	0.01
Cr_2O_3	0.04	0.05	0.03	0.00	0.01	0.02	0.00	0.00	0.01	0.00	0.00	0.00
Fe_2O_3	3.93	3.09	2.00	2.93	1.53	3.33	2.90	2.99	1.66	3.67	3.22	1.61
FeO	32.82	32.34	33.50	32.60	34.25	32.90	33.17	33.48	34.27	33.64	33.38	32.94
MnO	0.74	0.74	0.82	0.85	0.74	0.77	0.80	0.71	0.73	0.83	0.84	0.78
MgO	13.65	13.87	13.60	13.82	13.72	14.27	13.69	13.45	13.55	13.36	13.68	13.82
CaO	0.33	0.39	0.33	0.38	0.31	0.33	0.34	0.37	0.33	0.36	0.32	0.31
Na_2O	0.00	0.12	0.01	0.05	0.00	0.00	0.00	0.07	0.06	0.04	0.03	0.00
K_2O	0.00	0.00	0.01	0.02	0.00	0.00	0.01	0.00	0.01	0.00	0.00	0.01
Total	101.21	100.77	100.69	100.76	101.43	102.28	100.95	101.25	101.53	102.03	101.72	99.48
Structural formula (in apfu) based on 6 oxygens												
T (iv) site:												
Si	1.920	1.936	1.947	1.938	1.958	1.931	1.938	1.939	1.959	1.928	1.936	1.956
Al	0.043	0.044	0.046	0.041	0.038	0.039	0.038	0.040	0.038	0.038	0.036	0.039
Fe^{3+}	0.038	0.020	0.008	0.021	0.005	0.030	0.024	0.022	0.003	0.034	0.029	0.004
Site total	2.000	2.000	2.000	2.000	2.000	2.000	2.000	2.000	2.000	2.000	2.000	2.000
Al (total)	0.043	0.044	0.046	0.041	0.038	0.039	0.038	0.040	0.038	0.038	0.036	0.039
Fe^{3+}(total)	0.116	0.092	0.059	0.087	0.045	0.097	0.086	0.088	0.049	0.108	0.095	0.048
M (vi) site:												
Ti	0.000	0.000	0.001	0.001	0.001	0.001	0.000	0.000	0.000	0.001	0.000	0.000
Fe^{3+}	0.079	0.071	0.052	0.066	0.040	0.067	0.062	0.067	0.046	0.074	0.066	0.044
Fe^{2+}	1.080	1.064	1.105	1.073	1.121	1.067	1.093	1.101	1.121	1.101	1.092	1.096
Mn^{2+}	0.025	0.025	0.027	0.028	0.025	0.025	0.027	0.024	0.024	0.028	0.028	0.026
Mg	0.801	0.813	0.799	0.811	0.800	0.825	0.804	0.788	0.790	0.779	0.798	0.820
Ca	0.014	0.016	0.014	0.016	0.013	0.014	0.014	0.016	0.014	0.015	0.013	0.013

Na	0.000	0.009	0.001	0.004	0.000	0.000	0.000	0.005	0.005	0.003	0.002	0.000
K	0.000	0.000	0.001	0.001	0.000	0.000	0.001	0.000	0.000	0.000	0.000	0.001
Site total	1.999	1.998	1.999	2.000	2.000	1.999	2.000	2.000	2.000	2.000	2.000	2.000
Molecular percentages of major components												
Diopside	0.60	0.72	0.59	0.70	0.54	0.61	0.62	0.66	0.57	0.64	0.57	0.57
Hedenbergite	0.81	0.94	0.81	0.92	0.76	0.79	0.84	0.92	0.81	0.90	0.79	0.76
Enstatite	38.33	38.52	37.49	38.35	37.82	39.42	38.21	37.47	37.30	37.11	38.01	38.65
Ferrosilite	53.39	52.01	53.71	52.64	54.63	52.63	53.78	54.00	54.65	54.35	53.97	53.44
Aegerine	0.00	0.92	0.08	0.39	0.00	0.00	0.00	0.54	0.46	0.31	0.23	0.00
Kanoite	2.51	2.49	2.75	2.87	2.46	2.57	2.70	2.39	2.42	2.80	2.82	2.64

Sample	HR02-3				HR02-71							
Analysis Type	opx	opx	opx	opx	opx	opx	opx	opx	opx	opx	opx	opx
Analysis Pt.	20	21	22	23	28	29	30	31	32	33	34	35
Wt%												
SiO_2	49.06	48.99	48.95	48.95	48.34	48.03	48.61	47.57	47.27	47.12	47.72	47.36
Al_2O_3	0.68	0.80	0.83	0.92	0.35	0.22	0.38	0.28	0.30	0.35	0.37	0.35
TiO_2	0.00	0.02	0.00	0.01	0.00	0.00	0.00	0.00	0.00	0.02	0.00	0.02
Cr_2O_3	0.00	0.00	0.00	0.00	0.00	0.01	0.00	0.03	0.00	0.01	0.03	0.03
Fe_2O_3	4.10	3.61	3.81	2.75	1.66	2.06	0.58	1.17	1.95	2.45	0.86	0.52
FeO	32.98	32.66	31.43	33.07	36.93	36.62	37.55	36.34	36.41	36.05	37.33	37.00
MnO	0.86	0.75	0.82	0.82	2.63	2.67	2.56	2.57	2.53	2.63	2.67	2.53
MgO	13.66	13.90	14.31	13.53	9.64	9.67	9.53	9.46	9.28	9.34	8.99	8.88
CaO	0.30	0.31	0.38	0.38	0.80	0.68	0.78	0.74	0.74	0.78	0.67	0.91
Na_2O	0.01	0.00	0.06	0.00	0.00	0.00	0.00	0.02	0.00	0.00	0.03	0.02
K_2O	0.01	0.00	0.00	0.01	0.00	0.00	0.00	0.01	0.02	0.00	0.00	0.00
Total	101.66	101.04	100.59	100.45	100.35	99.96	99.99	98.20	98.49	98.75	98.68	97.62

Structural formula (in apfu) based on 6 oxygens												
T (iv) site:												
Si	1.924	1.927	1.927	1.938	1.966	1.963	1.982	1.975	1.963	1.953	1.978	1.983
Al	0.031	0.037	0.038	0.043	0.017	0.011	0.018	0.014	0.015	0.017	0.018	0.017
Fe^{3+}	0.044	0.035	0.035	0.020	0.017	0.026	0.000	0.011	0.023	0.030	0.004	0.000
Site total	2.000	2.000	2.000	2.000	2.000	2.000	2.000	2.000	2.000	2.000	2.000	2.000
Al (total)	0.031	0.037	0.038	0.043	0.017	0.011	0.018	0.014	0.015	0.017	0.018	0.017
Fe^{3+}(total)	0.121	0.107	0.113	0.082	0.051	0.063	0.018	0.037	0.061	0.076	0.027	0.017
M (vi) site:												
Ti	0.000	0.001	0.000	0.000	0.000	0.000	0.000	0.000	0.000	0.001	0.000	0.001
Fe^{3+}	0.077	0.071	0.078	0.062	0.034	0.037	0.018	0.026	0.038	0.046	0.023	0.017
Fe^{2+}	1.082	1.075	1.034	1.095	1.256	1.252	1.280	1.262	1.264	1.249	1.294	1.295
Mn^{2+}	0.029	0.025	0.027	0.027	0.091	0.092	0.088	0.090	0.089	0.092	0.094	0.090
Mg	0.799	0.815	0.840	0.798	0.585	0.589	0.579	0.586	0.574	0.577	0.556	0.554
Ca	0.013	0.013	0.016	0.016	0.035	0.030	0.034	0.033	0.033	0.035	0.030	0.041
Na	0.001	0.000	0.005	0.000	0.000	0.000	0.000	0.002	0.000	0.000	0.002	0.002
K	0.001	0.000	0.000	0.001	0.000	0.000	0.000	0.001	0.001	0.000	0.000	0.000
Site total	2.000	2.000	2.000	2.000	2.000	2.000	2.000	1.999	2.000	2.000	1.999	1.999
Molecular percentages of major components												
Diopside	0.55	0.57	0.73	0.69	1.12	0.97	1.06	1.05	1.04	1.11	0.90	1.22
Hedenbergite	0.74	0.76	0.90	0.94	2.40	2.05	2.35	2.26	2.29	2.41	2.09	2.86
Enstatite	38.44	39.12	40.09	37.68	24.08	24.51	23.73	24.17	23.82	23.78	22.41	22.35
Ferrosilite	54.05	53.22	51.11	53.58	61.57	62.03	62.22	61.89	62.35	61.60	63.16	62.72
Aegerine	0.08	0.00	0.47	0.00	0.00	0.00	0.00	0.16	0.00	0.00	0.24	0.16
Kanoite	2.92	2.54	2.78	2.78	9.14	9.37	8.84	9.09	9.01	9.37	9.39	8.97

Sample	HR02-71						HP82-59					
Analysis Type	opx	opx	opx	opx	opx	opx	opx	opx	opx	opx	opx	opx
Analysis Pt.	36	37	38	39	opx-1	opx-2	46	47	48	49	50	51
Wt%												
SiO_2	47.57	47.41	46.98	46.99	48.41	48.53	50.09	49.15	49.58	48.84	49.55	48.47
Al_2O_3	0.28	0.30	0.36	0.28	0.27	0.24	0.92	0.67	0.69	0.73	0.71	0.96
TiO_2	0.01	0.00	0.00	0.00	0.02	0.01	0.02	0.02	0.03	0.00	0.04	0.07
Cr_2O_3	0.00	0.01	0.00	0.03	0.00	0.02	0.02	0.00	0.02	0.00	0.01	0.00
Fe_2O_3	3.00	2.29	1.58	3.65	1.16	1.11	2.86	3.55	2.44	2.14	0.85	3.68
FeO	36.76	36.70	36.34	35.78	37.57	37.57	36.22	36.50	37.72	35.98	37.69	35.82
MnO	2.58	2.63	2.60	2.61	2.52	2.32	0.26	0.30	0.27	0.21	0.26	0.17
MgO	9.26	9.05	9.11	9.30	9.46	9.58	12.73	11.98	11.55	12.08	11.54	11.79
CaO	0.74	0.79	0.68	0.76	0.69	0.65	0.48	0.47	0.52	0.50	0.56	0.49
Na_2O	0.00	0.04	0.02	0.04	0.00	0.04	0.02	0.00	0.00	0.00	0.01	0.07
K_2O	0.02	0.00	0.00	0.01	0.01	0.00	0.01	0.01	0.02	0.01	0.00	0.02
Total	100.22	99.22	97.67	99.45	100.10	100.08	103.63	102.65	102.84	100.49	101.21	101.54
Structural formula (in apfu) based on 6 oxygens												
T (iv) site:												
Si	1.947	1.958	1.967	1.938	1.975	1.978	1.938	1.932	1.947	1.951	1.970	1.924
Al	0.014	0.015	0.018	0.014	0.013	0.012	0.042	0.031	0.032	0.034	0.030	0.045
Fe^{3+}	0.039	0.027	0.015	0.048	0.011	0.010	0.020	0.037	0.021	0.015	0.000	0.031
Site total	2.000	2.000	2.000	2.000	2.000	2.000	2.000	2.000	2.000	2.000	2.000	2.000
Al (total)	0.014	0.015	0.018	0.014	0.013	0.012	0.042	0.031	0.032	0.034	0.033	0.045
Fe^{3+}(total)	0.092	0.071	0.050	0.113	0.036	0.034	0.083	0.105	0.072	0.064	0.025	0.110
M (vi) site:												
Al	0.000	0.000	0.000	0.000	0.000	0.000	0.000	0.000	0.000	0.000	0.003	0.000
Ti	0.000	0.000	0.000	0.000	0.001	0.000	0.001	0.001	0.001	0.000	0.001	0.002
Fe^{3+}	0.053	0.044	0.035	0.065	0.024	0.024	0.063	0.068	0.051	0.050	0.025	0.079
Fe^{2+}	1.259	1.268	1.272	1.234	1.282	1.281	1.172	1.200	1.239	1.202	1.253	1.189
Mn^{2+}	0.089	0.092	0.092	0.091	0.087	0.080	0.009	0.010	0.009	0.007	0.009	0.006
Mg	0.565	0.557	0.569	0.572	0.575	0.582	0.734	0.702	0.676	0.719	0.684	0.698

Ca	0.032	0.035	0.031	0.034	0.030	0.029	0.020	0.020	0.022	0.021	0.024	0.021
Na	0.000	0.003	0.002	0.003	0.000	0.003	0.001	0.000	0.000	0.000	0.001	0.005
K	0.001	0.000	0.000	0.001	0.000	0.000	0.000	0.001	0.001	0.001	0.000	0.001
Site total	2.000	2.000	2.000	1.999	2.000	1.999	1.999	2.000	1.999	2.000	2.000	2.000
Molecular percentages of major components												
Diopside	1.03	1.08	0.95	1.09	0.94	0.90	0.77	0.74	0.78	0.81	0.84	0.78
Hedenbergite	2.29	2.46	2.12	2.35	2.09	1.97	1.24	1.27	1.43	1.35	1.54	1.33
Enstatite	23.55	22.81	23.25	23.87	23.88	24.60	35.46	34.30	32.77	34.84	32.78	33.91
Ferrosilite	62.62	62.51	62.43	61.61	62.97	62.96	57.28	59.50	60.88	58.82	60.86	58.28
Aegerine	0.00	0.32	0.16	0.33	0.03	0.34	0.15	0.00	0.00	0.00	0.08	0.55
Kanoite	9.13	9.33	9.29	9.35	8.76	8.05	0.86	1.02	0.91	0.72	0.88	0.58

Sample	HP82-59					QC82-49b						
Analysis Type	opx	opx	opx	opx	opx	opx incl. – area 1	opx incl. – area 1	near cpx – area 1	near cpx – area 1	near cpx – area 1	near grt – area 1	near grt – area 1
Analysis Pt.	52	53	54	55	56	cpx-4	cpx-5	opx-6	opx-7	opx-8	opx-9	opx-10
Wt%												
SiO_2	48.83	48.37	48.46	48.24	47.84	50.69	50.76	49.55	49.50	49.57	49.64	49.34
Al_2O_3	0.92	0.59	0.69	0.71	0.69	0.88	0.88	0.51	0.56	0.51	0.55	0.58
TiO_2	0.07	0.00	0.03	0.01	0.04	0.03	0.02	0.01	0.01	0.04	0.01	0.00
Cr_2O_3	0.00	0.00	0.01	0.01	0.00	0.00	0.02	0.00	0.00	0.01	0.02	0.00
Fe_2O_3	4.49	2.75	4.16	3.71	3.75	1.54	1.90	1.55	1.73	1.32	1.27	2.08
FeO	36.26	37.82	38.04	38.20	37.75	12.45	12.03	31.90	31.83	32.05	32.21	31.84
MnO	0.22	0.46	0.49	0.46	0.46	0.54	0.59	1.32	1.26	1.32	1.38	1.43
MgO	11.81	10.52	10.42	10.20	10.23	10.94	10.92	14.14	14.22	14.14	13.99	14.02
CaO	0.64	0.59	0.60	0.62	0.58	21.95	22.34	0.64	0.58	0.56	0.64	0.56
Na_2O	0.02	0.01	0.02	0.01	0.01	0.00	0.00	0.00	0.00	0.00	0.00	0.00

Total	103.26	101.11	102.92	102.17	101.35	99.03	99.46	99.62	99.69	99.52	99.71	99.85
Structural formula (in apfu) based on 6 oxygens												
T (iv) site:												
Si	1.911	1.945	1.922	1.927	1.926	1.957	1.952	1.965	1.961	1.967	1.968	1.955
Al	0.042	0.028	0.032	0.033	0.033	0.040	0.040	0.024	0.026	0.024	0.026	0.027
Fe^{3+}	0.046	0.027	0.046	0.039	0.041	0.003	0.008	0.011	0.013	0.009	0.007	0.017
Site total	2.000	2.000	2.000	2.000	2.000	2.000	2.000	2.000	2.000	2.000	2.000	2.000
Al (total)	0.042	0.028	0.032	0.033	0.033	0.040	0.040	0.024	0.026	0.024	0.026	0.027
Fe^{3+}(total)	0.132	0.083	0.124	0.111	0.113	0.045	0.055	0.046	0.052	0.040	0.038	0.062
M (vi) site:												
Ti	0.002	0.000	0.001	0.000	0.001	0.001	0.001	0.000	0.000	0.001	0.000	0.000
Fe^{3+}	0.086	0.056	0.078	0.072	0.072	0.042	0.047	0.035	0.039	0.030	0.031	0.045
Fe^{2+}	1.187	1.272	1.262	1.277	1.271	0.402	0.387	1.058	1.055	1.064	1.068	1.055
Mn^{2+}	0.007	0.016	0.016	0.016	0.016	0.018	0.019	0.044	0.042	0.044	0.046	0.048
Mg	0.689	0.631	0.616	0.608	0.614	0.630	0.626	0.836	0.840	0.836	0.827	0.828
Ca	0.027	0.025	0.025	0.027	0.025	0.908	0.920	0.027	0.025	0.024	0.027	0.024
Na	0.002	0.001	0.002	0.001	0.001	0.000	0.000	0.000	0.000	0.000	0.000	0.000
Site total	2.000	2.000	2.000	2.000	2.000	2.000	1.999	2.000	2.000	2.000	1.999	2.000
Molecular percentages of major components												
Diopside	1.01	0.85	0.86	0.87	0.83	51.96	53.45	1.21	1.10	1.05	1.19	1.05
Hedenbergite	1.74	1.72	1.75	1.83	1.72	33.17	33.03	1.53	1.38	1.34	1.54	1.34
Enstatite	33.60	30.27	29.71	29.20	29.58	5.53	4.68	38.67	39.00	38.73	37.99	38.23
Ferrosilite	58.41	62.65	62.53	63.01	62.84	3.53	2.89	51.74	51.63	52.02	52.06	51.79
Aegerine	0.16	0.08	0.16	0.08	0.08	0.00	0.00	0.00	0.00	0.00	0.00	0.00
Esseneite	0.00	0.00	0.00	0.00	0.00	4.03	4.00	0.00	0.00	0.00	0.00	0.00
Johannsenite	0.00	0.00	0.00	0.00	0.00	1.78	1.93	0.00	0.00	0.00	0.00	0.00
Kanoite	0.75	1.59	1.68	1.59	1.60	0.00	0.00	4.46	4.26	4.46	4.65	4.84

Sample	QC82-49b					QC-JW3						
Analysis Type	near opx - area 7	near opx - area 7	near pl-6, am-3 - area 6	near gar-12, opx-13, pl-16, am-11 - area 4	near gar-12, cpx-14, pl-16, am-11 - area 4	opx	cpx	cpx	opx	cpx	opx	opx
Analysis Pt.	cpx-26	cpx-27	opx-5	opx-13	cpx-14	opx-1	cpx-2	cpx-3	opx-4	cpx-5	opx-7	opx-1'
Wt%												
SiO_2	49.54	49.63	50.23	50.48	51.52	48.93	50.99	50.29	51.82	50.29	48.72	49.91
Al_2O_3	0.63	0.75	0.76	0.63	1.08	0.39	0.39	0.56	0.66	0.80	0.51	0.78
TiO_2	0.00	0.00	0.00	0.00	0.04	0.00	0.00	0.00	0.00	0.00	0.03	0.00
Cr_2O_3	0.00	0.00	0.00	0.00	0.02	0.00	0.00	0.00	0.00	0.00	0.00	0.00
Fe_2O_3	0.53	0.00	0.66	0.24	0.88	2.26	3.70	4.26	0.00	3.94	4.46	3.88
FeO	22.78	22.43	33.08	33.09	13.11	31.58	11.98	12.59	30.34	11.60	30.68	12.39
MnO	0.65	0.70	2.26	1.44	0.56	4.07	1.72	1.74	2.04	1.01	2.65	1.13
MgO	4.06	4.29	13.37	14.07	10.54	12.45	10.27	9.91	15.18	10.09	13.39	10.14
NiO	0.00	0.00	0.05	0.00	0.00	0.00	0.00	0.00	0.00	0.00	0.00	0.00
CaO	21.50	21.51	0.62	0.55	21.74	0.37	21.90	21.26	0.46	22.25	0.75	21.26
Na_2O	0.22	0.19	0.00	0.00	0.29	0.03	0.19	0.19	0.05	0.22	0.02	0.18
K_2O	0.00	0.00	0.00	0.00	0.00	0.00	0.00	0.00	0.02	0.00	0.00	0.00
Total	99.90	99.50	101.04	100.52	99.76	100.08	101.14	100.80	100.59	100.19	101.21	99.67
Structural formula (in apfu) based on 6 oxygens												
T (iv) site:												
Si	1.986	1.992	1.973	1.982	1.972	1.958	1.945	1.933	2.013	1.933	1.922	1.932
Al	0.014	0.008	0.027	0.018	0.028	0.018	0.018	0.025	0.000	0.036	0.024	0.036
Fe^{3+}	0.000	0.000	0.000	0.000	0.000	0.024	0.037	0.042	0.000	0.031	0.054	0.032
Site total	2.000	2.000	2.000	2.000	2.000	2.000	2.000	2.000	2.013	2.000	2.000	2.000
Al (total)	0.030	0.035	0.035	0.029	0.049	0.018	0.018	0.025	0.030	0.036	0.024	0.036
Fe^{3+}(total)	0.016		0.020	0.007	0.025	0.068	0.106	0.123	0.000	0.114	0.132	0.113
M (vi) site:												

Al	0.000	0.000	0.000	0.000	0.021	0.000	0.000	0.000	0.030	0.000	0.000	0.000
Ti	0.000	0.000	0.000	0.000	0.001	0.000	0.000	0.000	0.001	0.000	0.001	0.000
Fe^{3+}	0.016	0.000	0.020	0.007	0.025	0.044	0.069	0.081	0.000	0.083	0.078	0.081
Fe^{2+}	0.764	0.753	1.087	1.087	0.420	1.057	0.382	0.405	0.986	0.373	1.012	0.401
Mn^{2+}	0.022	0.024	0.075	0.048	0.018	0.138	0.056	0.057	0.067	0.033	0.089	0.037
Mg	0.243	0.257	0.783	0.824	0.601	0.743	0.584	0.568	0.879	0.578	0.787	0.585
Ni	0.000	0.000	0.002	0.000	0.000	0.000	0.000	0.000	0.000	0.000	0.000	0.000
Ca	0.923	0.925	0.026	0.023	0.892	0.016	0.895	0.875	0.019	0.916	0.032	0.882
Na	0.017	0.015	0.000	0.000	0.021	0.002	0.014	0.014	0.004	0.016	0.002	0.014
K	0.000	0.000	0.000	0.000	0.000	0.000	0.000	0.000	0.001	0.000	0.000	0.000
Site total	2.000	2.000	2.000	2.000	2.000	2.000	2.000	2.000	1.987	2.000	2.000	2.000
Molecular percentages of major components												
Diopside	21.39	22.67	1.09	1.00	49.82	0.66	50.62	47.32	0.92	52.31	1.43	48.80
Hedenbergite	67.31	66.49	1.51	1.33	34.78	0.94	33.14	33.72	1.03	33.73	1.83	33.45
Enstatite	1.44	1.51	34.28	37.89	5.12	29.88	4.44	5.34	40.41	3.20	34.67	5.34
Ferrosilite	4.52	4.43	52.83	53.15	3.58	52.46	2.91	3.80	49.12	2.07	50.37	3.66
Jadeite	0.12	1.48	0.00	0.00	0.00	0.00	0.00	0.00	0.32	0.00	0.00	0.00
Aegerine	1.59	0.00	0.00	0.00	2.14	0.00	1.43	1.45	0.00	1.67	0.16	1.37
Esseneite	0.00	0.00	0.00	0.00	0.40	0.00	1.79	2.59	0.00	3.68	0.00	3.62
Johannsenite	2.21	2.38	0.00	0.00	1.81	0.00	5.66	5.79	0.00	3.34	0.00	3.77
Kanoite	0.00	0.00	7.54	4.80	0.00	13.96	0.00	0.00	6.81	0.00	9.10	0.00

Sample	QC-JW3											
Analysis Type	opx	cpx	opx	opx	circle 1	circle 1	circle 3	circle 3	cpx	cpx	core	rim
Analysis Pt.	opx-3'	cpx-4'	opx-5'	opx-6'	cpx-3	opx-4	opx-5	opx-8	cpx-1	cpx-2	opx-1	opx-1
Wt%												
SiO_2	48.34	49.79	48.84	48.83	51.68	50.04	49.90	49.60	51.03	51.36	49.93	50.07
Al_2O_3	0.45	0.72	0.48	0.40	0.72	0.58	0.58	0.64	0.65	0.64	0.48	0.50
TiO_2	0.00	0.03	0.00	0.00	0.01	0.01	0.00	0.00	0.00	0.00	0.02	0.01
Cr_2O_3	0.00	0.00	0.00	0.00	0.01	0.00	0.00	0.02	0.00	0.00	0.01	0.00

Fe_2O_3	3.98	4.50	4.14	4.39	1.54	1.00	0.08	1.79	1.27	0.99	0.00	0.00
FeO	29.71	11.14	29.63	29.98	14.19	33.58	32.97	32.96	14.77	14.38	34.39	33.85
MnO	2.45	1.08	2.49	2.50	0.86	2.26	3.09	3.38	1.09	0.99	2.51	2.53
MgO	13.85	10.42	14.17	14.12	10.27	12.93	12.78	12.52	9.50	9.57	11.91	12.46
CaO	0.72	21.72	0.75	0.55	21.62	0.73	0.61	0.47	21.51	22.11	0.83	0.60
Na_2O	0.00	0.18	0.00	0.00	0.16	0.00	0.00	0.00	0.14	0.14	0.00	0.00
K_2O	0.00	0.03	0.01	0.00	0.01	0.00	0.00	0.00	0.00	0.00	0.00	0.00
Total	99.50	99.61	100.50	100.77	101.06	101.12	100.01	101.38	99.97	100.18	100.08	100.02
Structural formula (in apfu) based on 6 oxygens												
T (iv) site:												
Si	1.930	1.925	1.928	1.926	1.967	1.971	1.985	1.958	1.972	1.976	1.996	1.996
Al	0.021	0.033	0.022	0.019	0.032	0.027	0.015	0.030	0.028	0.024	0.004	0.004
Fe^{3+}	0.049	0.042	0.050	0.056	0.000	0.002	0.000	0.012	0.000	0.000	0.000	0.000
Site total	2.000	2.000	2.000	2.000	2.000	2.000	2.000	2.000	2.000	2.000	2.000	2.000
Al (total)	0.021	0.033	0.022	0.019	0.032	0.027	0.027	0.030	0.030	0.029	0.023	0.023
Fe^{3+}(total)	0.120	0.131	0.123	0.130	0.044	0.030	0.003	0.053	0.037	0.029	0.000	0.000
M (vi) site:												
Al	0.000	0.000	0.000	0.000	0.000	0.000	0.012	0.000	0.002	0.005	0.019	0.020
Ti	0.000	0.001	0.000	0.000	0.000	0.000	0.000	0.000	0.000	0.000	0.001	0.000
Fe^{3+}	0.070	0.088	0.073	0.074	0.044	0.028	0.003	0.041	0.037	0.029	0.000	0.000
Fe^{2+}	0.992	0.360	0.978	0.989	0.452	1.106	1.097	1.088	0.477	0.463	1.150	1.129
Mn^{2+}	0.083	0.035	0.083	0.084	0.028	0.075	0.104	0.113	0.036	0.032	0.085	0.085
Mg	0.824	0.600	0.834	0.830	0.582	0.759	0.758	0.737	0.547	0.549	0.710	0.740
Ca	0.031	0.900	0.032	0.023	0.882	0.031	0.026	0.020	0.891	0.912	0.036	0.026
Na	0.000	0.013	0.000	0.000	0.012	0.000	0.000	0.000	0.010	0.010	0.000	0.000
K	0.000	0.001	0.001	0.000	0.000	0.000	0.000	0.000	0.000	0.000	0.000	0.000
Site total	2.000	2.000	2.000	2.000	2.000	2.000	2.000	1.999	2.000	2.000	2.000	2.000
Molecular percentages of major components												
Diopside	1.43	53.15	1.50	1.09	46.30	1.25	1.06	0.81	44.16	46.43	1.36	1.02
Hedenbergite	1.72	31.89	1.76	1.30	35.90	1.82	1.53	1.20	38.52	39.13	2.21	1.55
Enstatite	36.79	4.13	37.23	37.42	5.98	33.05	31.87	30.39	5.28	4.23	30.45	32.13
Ferrosilite	49.39	2.48	48.68	49.69	4.64	53.65	53.65	53.26	4.61	3.57	56.23	55.51
Aegerine	0.00	1.38	0.00	0.00	1.17	0.00	0.00	0.00	1.05	1.04	0.00	0.00
Esseneite	0.00	3.36	0.00	0.00	3.23	0.00	0.00	0.00	2.66	1.83	0.00	0.00
Johannsenite	0.00	3.62	0.00	0.00	2.77	0.00	0.00	0.00	3.57	3.23	0.00	0.00

Kanoite	8.49	0.00	8.54	8.59	0.00	7.55	10.40	11.36	0.00	0.00	8.54	8.58

Sample	QC-JW3											
Analysis Type	core	rim	opx	cpx	cpx	rim	incl. in grt	cpx	in qz band	opx	opx	cpx
Analysis Pt.	cpx-4	cpx-4	opx-5	cpx-6	cpx-7	cpx-8	cpx-9	cpx-10	opx-11	opx-12	opx-13	cpx-14
Wt%												
SiO_2	51.16	51.49	50.03	50.92	51.05	50.96	51.02	50.91	50.40	50.42	49.72	51.39
Al_2O_3	0.68	0.58	0.52	0.73	0.66	0.75	0.68	0.69	0.37	0.36	0.34	0.33
TiO_2	0.00	0.00	0.00	0.00	0.00	0.00	0.03	0.00	0.02	0.00	0.00	0.00
Cr_2O_3	0.00	0.00	0.00	0.00	0.00	0.00	0.00	0.00	0.00	0.02	0.00	0.00
Fe_2O_3	0.62	0.69	0.00	1.24	0.66	1.03	0.75	1.02	0.00	0.00	0.00	0.59
FeO	15.41	13.93	34.02	15.05	14.70	15.08	16.12	15.88	32.88	33.42	33.27	14.99
MnO	1.11	0.93	2.38	1.08	1.01	1.11	1.18	1.13	3.46	3.41	3.38	1.23
MgO	9.04	9.76	12.39	9.25	9.53	9.22	9.30	9.23	12.40	12.18	11.80	9.43
CaO	21.65	22.36	0.60	21.55	21.64	21.58	20.64	20.77	0.72	0.73	0.70	21.70
Na_2O	0.17	0.14	0.00	0.14	0.13	0.14	0.15	0.17	0.00	0.00	0.04	0.13
Total	99.84	99.88	99.96	99.95	99.39	99.87	99.88	99.80	100.25	100.54	99.25	99.79
Structural formula (in apfu) based on 6 oxygens												
T (iv) site:												
Si	1.982	1.982	1.996	1.971	1.980	1.973	1.978	1.976	2.005	2.004	2.004	1.989
Al	0.018	0.018	0.004	0.029	0.020	0.027	0.022	0.024	0.000	0.000	0.000	0.011
Site total	2.000	2.000	2.000	2.000	2.000	2.000	2.000	2.000	2.005	2.004	2.004	2.000
Al (total)	0.031	0.026	0.024	0.033	0.030	0.034	0.031	0.032	0.017	0.017	0.016	0.015
Fe^{3+}(total)	0.018	0.020	0.000	0.036	0.019	0.030	0.022	0.030	0.000	0.000	0.000	0.017
M (vi) site:												
Al	0.013	0.008	0.021	0.004	0.010	0.007	0.009	0.007	0.017	0.017	0.016	0.004
Ti	0.000	0.000	0.001	0.000	0.000	0.000	0.001	0.000	0.001	0.000	0.000	0.000

Fe^{3+}	0.018	0.020	0.000	0.036	0.019	0.030	0.022	0.030	0.000	0.000	0.000	0.017
Fe^{2+}	0.499	0.449	1.135	0.487	0.477	0.488	0.523	0.515	1.094	1.111	1.122	0.485
Mn^{2+}	0.036	0.030	0.080	0.035	0.033	0.036	0.039	0.037	0.117	0.115	0.115	0.040
Mg	0.522	0.560	0.737	0.534	0.551	0.532	0.538	0.534	0.735	0.722	0.709	0.544
Ca	0.899	0.922	0.026	0.894	0.899	0.895	0.857	0.864	0.031	0.031	0.030	0.900
Na	0.013	0.010	0.000	0.011	0.010	0.011	0.011	0.013	0.000	0.000	0.003	0.010
Site total	2.000	2.000	2.000	2.000	2.000	2.000	2.000	2.000	1.995	1.995	1.996	2.000
Molecular percentages of major components												
Diopside	43.14	48.54	1.01	43.33	45.36	43.38	40.40	40.82	1.24	1.23	1.18	44.84
Hedenbergite	41.26	38.87	1.56	39.54	39.27	39.81	39.29	39.40	1.85	1.90	1.86	39.99
Enstatite	4.53	3.74	32.21	5.02	4.87	4.92	6.65	6.29	30.35	29.75	29.13	4.78
Ferrosilite	4.33	2.99	55.84	4.58	4.22	4.51	6.47	6.07	53.88	54.69	55.26	4.26
Jadeite	0.00	0.00	0.00	0.00	0.00	0.00	0.00	0.00	0.00	0.00	0.31	0.00
Aegerine	1.28	1.04	0.00	1.05	0.98	1.05	1.13	1.28	0.00	0.00	0.00	0.98
Esseneite	0.54	0.94	0.00	2.55	0.95	1.96	1.07	1.71	0.00	0.00	0.00	0.74
Johannsenite	3.64	3.03	0.00	3.54	3.32	3.64	3.88	3.71	0.00	0.00	0.00	4.03
Kanoite	0.00	0.00	8.08	0.00	0.00	0.00	0.00	0.00	11.75	11.55	11.60	0.00

Sample	QC-JW3								
Analysis Type	cpx	opx	opx	cpx	opx	cpx	opx	opx	cpx
Analysis Pt.	cpx-15	opx-16	opx-17	cpx-18	opx-19	cpx-20	opx-21	opx-22	cpx-23
Wt%									
SiO_2	51.27	50.25	50.18	51.37	50.06	51.34	49.77	49.81	51.11
Al_2O_3	0.35	0.29	0.27	0.33	0.27	0.43	0.37	0.44	0.58
TiO_2	0.00	0.00	0.00	0.00	0.04	0.00	0.02	0.04	0.00
Cr_2O_3	0.00	0.00	0.03	0.00	0.01	0.00	0.01	0.02	0.00
Fe_2O_3	0.78	0.00	0.00	0.19	0.00	0.56	0.00	0.00	0.49
FeO	15.61	32.68	33.27	15.26	32.84	15.28	34.21	33.75	15.74
MnO	1.29	3.84	3.45	1.23	3.78	1.37	3.59	3.80	1.48

MgO	9.14	12.25	12.05	9.38	11.89	9.18	11.18	11.52	9.00
CaO	21.39	0.65	0.82	21.58	0.76	21.63	0.57	0.88	21.22
Na_2O	0.15	0.00	0.00	0.12	0.00	0.14	0.00	0.02	0.14
Total	99.98	100.00	100.07	99.46	99.65	99.93	99.72	100.28	99.76
Structural formula (in apfu) based on 6 oxygens									
T (iv) site:									
Si	1.986	2.007	2.005	1.994	2.010	1.987	2.008	1.993	1.985
Al	0.014	0.000	0.000	0.006	0.000	0.013	0.000	0.007	0.015
Site total	2.000	2.007	2.005	2.000	2.010	2.000	2.008	2.000	2.000
Al (total)	0.016	0.014	0.013	0.015	0.013	0.020	0.018	0.021	0.027
Fe^{3+}(total)	0.023	0.000	0.000	0.006	0.000	0.016	0.000	0.000	0.014
M (vi) site:									
Al	0.002	0.014	0.013	0.009	0.013	0.007	0.018	0.014	0.011
Ti	0.000	0.001	0.000	0.000	0.001	0.000	0.001	0.001	0.000
Fe^{3+}	0.023	0.000	0.000	0.006	0.000	0.016	0.000	0.000	0.014
Fe^{2+}	0.506	1.091	1.112	0.495	1.103	0.495	1.154	1.129	0.511
Mn^{2+}	0.042	0.130	0.117	0.040	0.129	0.045	0.123	0.129	0.049
Mg	0.528	0.729	0.718	0.543	0.712	0.530	0.672	0.687	0.521
Ca	0.888	0.028	0.035	0.898	0.033	0.897	0.025	0.038	0.883
Na	0.011	0.000	0.000	0.009	0.000	0.011	0.000	0.002	0.011
Site total	2.000	1.993	1.994	2.000	1.990	2.000	1.992	1.999	2.000
Molecular percentages of major components									
Diopside	42.48	1.12	1.39	44.51	1.29	43.42	0.91	1.43	41.35
Hedenbergite	40.70	1.68	2.15	40.61	2.00	40.53	1.57	2.35	40.56
Enstatite	5.15	29.45	29.40	4.88	28.59	4.78	27.08	27.06	5.38
Ferrosilite	4.93	53.86	54.64	4.46	54.35	4.46	57.10	55.08	5.28
Jadeite	0.00	0.00	0.00	0.34	0.00	0.00	0.00	0.00	0.00
Aegerine	1.13	0.00	0.00	0.57	0.00	1.05	0.00	0.00	1.05
Esseneite	1.15	0.00	0.00	0.00	0.00	0.58	0.00	0.00	0.38
Johannsenite	4.23	0.00	0.00	4.04	0.00	4.49	0.00	0.00	4.87
Kanoite	0.00	13.09	11.75	0.00	12.97	0.00	12.37	12.90	0.00

APPENDIX C: FELDSPAR EPMA DATA

Sample	QC82-44												
Analysis Pt.	7	8	9	10	11	12	13	14	15	19	20	21	22
Wt%													
SiO_2	55.54	57.35	56.74	57.04	57.29	55.62	56.62	56.57	57.57	57.30	57.30	57.66	56.84
Al_2O_3	28.00	27.67	27.26	27.30	26.99	25.76	28.85	28.00	27.60	27.26	27.49	27.80	27.40
FeO	0.17	0.22	0.13	0.38	0.68	0.09	0.08	0.07	0.05	0.12	0.11	0.39	0.06
MgO	0.00	0.02	0.00	0.00	0.00	0.01	0.00	0.00	0.00	0.00	0.00	0.00	0.02
CaO	9.79	9.22	9.54	9.80	9.03	11.58	10.64	10.06	9.57	9.03	9.31	9.44	9.30
BaO	0.05	0.09	0.13	0.15	0.08	0.08	0.09	0.11	0.07	0.12	0.12	0.08	0.10
Na_2O	5.36	5.91	5.86	6.14	6.13	5.78	4.92	5.21	5.59	6.45	6.25	5.82	5.74
K_2O	0.08	0.06	0.13	0.32	0.24	0.15	0.15	0.25	0.10	0.14	0.16	0.07	0.18
Total	98.99	100.54	99.79	101.13	100.44	99.07	101.35	100.27	100.55	100.42	100.74	101.26	99.64
Structural formula (in apfu) based on 8 oxygens													
T (iv) site:													
Si	2.518	2.556	2.553	2.544	2.565	2.543	2.508	2.532	2.562	2.562	2.554	2.554	2.556
Al	1.496	1.453	1.445	1.435	1.424	1.388	1.506	1.477	1.448	1.436	1.444	1.451	1.452
Site total	4.014	4.009	3.998	3.979	3.990	3.930	4.014	4.009	4.010	3.998	3.998	4.005	4.009
M site:													
Fe^{2+}	0.006	0.008	0.005	0.014	0.025	0.003	0.003	0.003	0.002	0.004	0.004	0.014	0.002
Mg	0.000	0.001	0.000	0.000	0.000	0.001	0.000	0.000	0.000	0.000	0.000	0.000	0.001
Ca	0.475	0.440	0.460	0.468	0.433	0.567	0.505	0.482	0.456	0.433	0.445	0.448	0.448
Ba	0.001	0.002	0.002	0.003	0.001	0.001	0.002	0.002	0.001	0.002	0.002	0.001	0.002
Na	0.471	0.511	0.511	0.531	0.532	0.512	0.423	0.452	0.482	0.559	0.540	0.500	0.501
K	0.005	0.003	0.007	0.018	0.014	0.009	0.008	0.014	0.006	0.008	0.009	0.004	0.010
Site total	0.952	0.956	0.981	1.020	0.981	1.090	0.938	0.951	0.946	1.002	0.996	0.953	0.961
Main feldspar components (mol %)													
Albite	49.48	53.42	52.12	52.05	54.28	47.01	45.07	47.55	51.01	55.81	54.23	52.44	52.10
Anorthite	49.94	46.06	46.89	45.91	44.18	52.05	53.86	50.74	48.26	43.18	44.64	47.00	46.65

Orthoclase	0.49	0.36	0.76	1.78	1.40	0.80	0.90	1.50	0.60	0.80	0.91	0.41	1.07
Celsian	0.09	0.16	0.23	0.26	0.14	0.13	0.17	0.20	0.13	0.21	0.21	0.15	0.18

Sample	QC82-44					QC82-49b							
Analysis Type						hyal-area 4					pl-area 4		
Analysis Pt.	23	24	25	26	27	1	2	3	4	5	6	7	8
Wt%													
SiO_2	57.48	56.71	55.67	56.07	56.77	61.43	61.33	61.23	60.97	61.33	47.72	47.70	47.76
Al_2O_3	27.00	27.06	27.82	26.94	26.92	19.45	19.61	20.06	19.76	19.65	32.91	32.90	32.79
FeO	0.09	0.33	0.09	0.04	0.07	0.03	0.05	0.02	0.04	0.03	0.08	0.06	0.12
MnO	0.00	0.00	0.00	0.00	0.00	0.00	0.01	0.02	0.00	0.00	0.01	0.00	0.00
MgO	0.00	0.01	0.00	0.01	0.00	0.01	0.00	0.00	0.01	0.01	0.00	0.00	0.00
CaO	9.19	9.00	10.14	9.12	9.05	0.09	0.11	0.45	0.17	0.13	16.42	16.41	16.41
BaO	0.20	0.07	0.10	0.11	0.05	5.55	5.67	5.68	5.71	5.63	0.02	0.00	0.00
SrO	0.00	0.00	0.00	0.00	0.00	0.03	0.11	0.12	0.09	0.11	0.20	0.11	0.15
Na_2O	5.86	5.84	5.26	5.42	5.57	1.05	1.07	1.09	1.04	0.97	1.93	2.00	2.01
K_2O	0.20	0.27	0.23	0.41	0.21	12.56	12.39	12.53	12.59	12.62	0.03	0.01	0.03
Total	100.02	99.29	99.31	98.12	98.64	100.21	100.33	101.19	100.37	100.48	99.32	99.20	99.26
Structural formula (in apfu) based on 8 oxygens													
T (iv) site:													
Si	2.576	2.562	2.520	2.561	2.574	2.915	2.908	2.885	2.896	2.906	2.203	2.203	2.206
Al	1.426	1.441	1.484	1.450	1.439	1.087	1.096	1.114	1.106	1.097	1.791	1.791	1.785
Site total	4.002	4.003	4.004	4.011	4.013	4.002	4.004	3.999	4.002	4.003	3.993	3.994	3.991
M site:													
Fe^{2+}	0.003	0.012	0.003	0.002	0.003	0.001	0.002	0.001	0.002	0.001	0.003	0.002	0.005
Mn	0.000	0.000	0.000	0.000	0.000	0.000	0.000	0.001	0.000	0.000	0.000	0.000	0.000
Mg	0.000	0.001	0.000	0.001	0.000	0.001	0.000	0.000	0.000	0.001	0.000	0.000	0.000

Ca	0.441	0.436	0.492	0.446	0.440	0.005	0.006	0.023	0.009	0.006	0.812	0.812	0.812
Ba	0.004	0.001	0.002	0.002	0.001	0.103	0.105	0.105	0.106	0.105	0.000	0.000	0.000
Sr	0.000	0.000	0.000	0.000	0.000	0.001	0.003	0.003	0.002	0.003	0.005	0.003	0.004
Na	0.509	0.512	0.462	0.480	0.490	0.097	0.098	0.099	0.096	0.089	0.173	0.179	0.180
K	0.011	0.016	0.013	0.024	0.012	0.761	0.749	0.753	0.763	0.763	0.002	0.001	0.002
Site total	0.965	0.964	0.968	0.952	0.942	0.966	0.961	0.983	0.976	0.966	0.992	0.995	0.997
Main feldspar components (mol %)													
Albite	52.74	53.06	47.67	50.41	51.96	10.02	10.23	10.12	9.81	9.28	17.50	18.07	18.08
Anorthite	45.71	45.19	50.78	46.87	46.66	0.48	0.58	2.32	0.88	0.67	82.31	81.88	81.73
Orthoclase	1.18	1.61	1.37	2.51	1.29	78.81	78.20	76.86	78.39	79.19	0.16	0.05	0.20
Celsian	0.36	0.13	0.18	0.21	0.09	10.69	10.99	10.70	10.92	10.86	0.03	0.00	0.00

Sample	QC82-49b												
Analysis Type	pl-area 4			hyal-area 4	pl-area 4			incl. in am-2	near opx-5, kfs-8 (area 6)		near opx-5, pl-6,7 (area 6)	near pl-16 (area 6)	near hyal-15 (area 6)
Analysis Pt.	9	10	11	12	13	14	15	pl-4	pl-6	pl-7	hyal-8	hyal-15	pl-16
Wt%													
SiO_2	47.86	48.11	48.03	62.21	52.47	48.59	48.39	46.90	46.24	46.21	58.55	60.06	47.69
Al_2O_3	32.72	32.54	32.38	19.00	29.58	32.06	32.45	32.82	33.05	33.03	20.71	19.73	32.27
FeO	0.05	0.09	0.09	0.02	0.04	0.07	0.13	0.69	0.31	0.34	0.32	0.02	0.04
MnO	0.01	0.00	0.00	0.00	0.00	0.01	0.02	0.01	0.03	0.03	0.01	0.00	0.00
MgO	0.00	0.00	0.00	0.01	0.01	0.00	0.00	0.02	0.00	0.00	0.00	0.00	0.00
CaO	16.44	16.30	16.33	0.16	13.17	15.86	16.15	16.92	17.33	17.42	1.06	0.47	16.56
BaO	0.05	0.00	0.04	3.79	0.14	0.04	0.00	0.02	0.02	0.00	6.81	5.60	0.02
SrO	0.15	0.07	0.06	0.09	0.09	0.07	0.11	0.00	0.00	0.00	0.00	0.00	0.00
Na_2O	2.00	2.19	2.08	1.03	3.66	2.41	2.21	1.86	1.57	1.63	1.07	1.10	1.62

K_2O	0.01	0.03	0.05	13.41	0.48	0.06	0.03	0.06	0.03	0.03	11.62	12.55	0.00
Total	99.29	99.33	99.06	99.72	99.65	99.17	99.49	99.30	98.57	98.69	100.14	99.53	98.22
Structural formula (in apfu) based on 8 oxygens													
T (iv) site:													
Si	2.210	2.219	2.221	2.940	2.394	2.243	2.228	2.176	2.159	2.157	2.818	2.881	2.221
Al	1.780	1.769	1.765	1.058	1.591	1.744	1.760	1.795	1.819	1.817	1.175	1.115	1.771
Site total	3.990	3.987	3.986	3.998	3.984	3.986	3.988	3.971	3.978	3.974	3.992	3.996	3.992
M site:													
Fe^{2+}	0.002	0.003	0.004	0.001	0.002	0.003	0.005	0.027	0.012	0.013	0.013	0.001	0.002
Mn	0.000	0.000	0.000	0.000	0.000	0.000	0.001	0.000	0.001	0.001	0.000	0.000	0.000
Mg	0.000	0.000	0.000	0.000	0.001	0.000	0.000	0.001	0.000	0.000	0.000	0.000	0.000
Ca	0.813	0.805	0.809	0.008	0.644	0.784	0.796	0.841	0.867	0.871	0.055	0.024	0.826
Ba	0.001	0.000	0.001	0.070	0.003	0.001	0.000	0.000	0.000	0.000	0.128	0.105	0.000
Sr	0.004	0.002	0.002	0.002	0.002	0.002	0.003	0.000	0.000	0.000	0.000	0.000	0.000
Na	0.179	0.196	0.187	0.095	0.323	0.216	0.197	0.167	0.142	0.148	0.100	0.102	0.146
K	0.001	0.002	0.003	0.808	0.028	0.003	0.002	0.004	0.001	0.002	0.714	0.768	0.000
Site total	0.997	1.004	1.001	0.984	1.000	1.006	0.998	1.013	1.011	1.021	0.996	0.999	0.973
Main feldspar components (mol %)													
Albite	17.98	19.51	18.69	9.66	32.41	21.48	19.78	16.51	14.06	14.48	10.00	10.21	15.03
Anorthite	81.86	80.31	80.94	0.82	64.51	78.09	80.03	83.07	85.77	85.33	5.47	2.41	84.90
Orthoclase	0.07	0.18	0.30	82.37	2.82	0.35	0.18	0.37	0.15	0.20	71.64	76.86	0.02
Celsian	0.09	0.00	0.07	7.16	0.25	0.08	0.00	0.04	0.03	0.00	12.89	10.52	0.04

APPENDIX D: AMPHIBOLE EPMA DATA

Sample	QC-IS												
Analysis Type	Traverse of matrix grain												
Analysis Pt.	1	2	3	4	5	6	7	8	9	10	11	12	13
Wt%													
SiO_2	40.01	39.72	39.71	39.71	39.81	39.90	39.69	39.46	39.72	39.51	39.80	39.66	39.43
TiO_2	0.15	0.12	0.12	0.12	0.12	0.12	0.11	0.10	0.11	0.12	0.09	0.12	0.12
Al_2O_3	12.07	11.97	12.06	11.75	11.77	11.72	11.73	11.71	11.70	11.70	11.68	11.66	11.64
Cr_2O_3	0.01	0.01	0.01	0.00	0.01	0.00	0.00	0.01	0.00	0.02	0.02	0.00	0.01
MnO	0.25	0.23	0.28	0.23	0.26	0.31	0.27	0.28	0.24	0.21	0.26	0.26	0.31
FeO	20.08	19.64	19.51	19.88	19.88	19.89	19.67	19.72	19.71	19.55	19.61	19.81	19.67
Fe_2O_3	4.97	5.66	6.33	5.70	5.46	5.59	6.20	5.90	5.89	5.99	6.47	5.75	5.53
NiO	0.05	0.00	0.01	0.00	0.03	0.01	0.01	0.00	0.01	0.01	0.00	0.02	0.02
MgO	5.50	5.71	5.67	5.68	5.71	5.73	5.75	5.69	5.79	5.76	5.79	5.66	5.69
CaO	11.48	11.30	11.47	11.52	11.53	11.59	11.50	11.59	11.58	11.42	11.58	11.44	11.52
Na_2O	0.58	0.62	0.61	0.60	0.63	0.62	0.62	0.64	0.60	0.62	0.62	0.60	0.62
BaO	0.17	0.22	0.23	0.22	0.18	0.19	0.20	0.18	0.15	0.14	0.19	0.16	0.19
K_2O	2.84	2.94	2.92	2.98	2.96	2.98	3.03	3.00	3.04	3.01	2.95	3.02	2.99
H_2O (calc)	1.43	1.43	1.42	1.42	1.43	1.46	1.42	1.44	1.44	1.44	1.45	1.44	1.44
F	0.21	0.21	0.21	0.22	0.23	0.17	0.25	0.22	0.22	0.21	0.22	0.20	0.22
Cl	1.37	1.36	1.42	1.38	1.33	1.34	1.32	1.31	1.31	1.31	1.30	1.33	1.29
O=F,Cl (calc)	*-0.40*	*-0.39*	*-0.41*	*-0.40*	*-0.40*	*-0.37*	*-0.40*	*-0.39*	*-0.39*	*-0.39*	*-0.39*	*-0.38*	*-0.38*
Total	100.75	100.74	101.55	101.01	100.93	101.24	101.38	100.85	101.11	100.62	101.64	100.75	100.30
Normalization procedure(s)	Si–Ca&Li=15 Si–Mg&Li=13												
T site (ideally 8 apfu):													
Si	6.259	6.221	6.180	6.217	6.230	6.229	6.194	6.192	6.208	6.204	6.192	6.224	6.216

Al	1.741	1.779	1.820	1.783	1.770	1.771	1.806	1.808	1.792	1.796	1.808	1.776	1.784
T subtotal	**8.000**	**8.000**	**8.000**	**8.000**	**8.000**	**8.000**	**8.000**	**8.000**	**8.000**	**8.000**	**8.000**	**8.000**	**8.000**
C site (ideally 5 apfu):													
Ti	0.017	0.014	0.014	0.014	0.014	0.014	0.013	0.012	0.013	0.014	0.010	0.015	0.014
Al	0.483	0.429	0.392	0.386	0.401	0.385	0.352	0.357	0.364	0.369	0.334	0.381	0.379
Cr	0.001	0.001	0.001	0.000	0.001	0.000	0.000	0.002	0.000	0.002	0.002	0.000	0.002
Fe^{3+}	0.585	0.667	0.740	0.672	0.642	0.658	0.730	0.697	0.694	0.707	0.758	0.678	0.657
Ni	0.006	0.000	0.001	0.000	0.004	0.002	0.002	0.000	0.001	0.001	0.000	0.003	0.002
Mn^{2+}	0.000	0.000	0.000	0.000	0.003	0.013	0.000	0.014	0.004	0.000	0.002	0.000	0.016
Fe^{2+}	2.626	2.556	2.537	2.602	2.603	2.596	2.566	2.588	2.575	2.560	2.551	2.600	2.593
Mg	1.283	1.333	1.315	1.326	1.332	1.333	1.338	1.331	1.349	1.348	1.343	1.324	1.337
C subtotal	**5.001**	**5.000**	**5.000**	**5.000**	**5.000**	**5.001**	**5.001**	**5.001**	**5.000**	**5.001**	**5.000**	**5.001**	**5.000**
B site (ideally 2 apfu):													
Mn^{2+}	0.033	0.031	0.037	0.031	0.031	0.028	0.036	0.024	0.028	0.028	0.032	0.035	0.025
Fe^{2+}	0.002	0.018	0.004	0.001	0.000	0.000	0.000	0.000	0.000	0.009	0.000	0.001	0.000
Ca	1.924	1.895	1.913	1.933	1.933	1.939	1.923	1.949	1.939	1.921	1.930	1.924	1.946
Na	0.041	0.056	0.047	0.036	0.036	0.033	0.041	0.028	0.033	0.042	0.037	0.041	0.029
B subtotal	**2.000**	**2.000**	**2.001**	**2.001**	**2.000**	**2.000**	**2.000**	**2.001**	**2.000**	**2.000**	**1.999**	**2.001**	**2.000**
A site (from 0 to 1 apfu):													
Na	0.134	0.133	0.136	0.147	0.155	0.154	0.146	0.166	0.148	0.146	0.148	0.141	0.159
Ba	0.007	0.009	0.010	0.009	0.008	0.008	0.008	0.007	0.006	0.006	0.008	0.007	0.008
K	0.566	0.586	0.579	0.596	0.591	0.592	0.604	0.600	0.606	0.604	0.586	0.604	0.601
A subtotal	**0.707**	**0.728**	**0.725**	**0.752**	**0.754**	**0.754**	**0.758**	**0.773**	**0.760**	**0.756**	**0.742**	**0.752**	**0.768**
W site (ideally 2 apfu):													
OH	1.500	1.507	1.498	1.499	1.506	1.535	1.500	1.519	1.518	1.517	1.525	1.519	1.519
F	0.102	0.102	0.101	0.108	0.112	0.083	0.123	0.110	0.110	0.107	0.110	0.098	0.109
Cl	0.363	0.362	0.374	0.366	0.353	0.353	0.350	0.348	0.346	0.349	0.344	0.353	0.345
O	0.034	0.028	0.027	0.028	0.028	0.028	0.027	0.024	0.025	0.028	0.021	0.029	0.028
W subtotal	**1.999**	**1.999**	**2.000**	**2.001**	**1.999**	**1.999**	**2.000**	**2.001**	**1.999**	**2.001**	**2.000**	**1.999**	**2.001**
Sum T,C,B,A	**15.708**	**15.728**	**15.726**	**15.753**	**15.754**	**15.755**	**15.759**	**15.775**	**15.760**	**15.757**	**15.741**	**15.754**	**15.768**
Species	potassic-hastingsite												

Sample	QC82-44												QC81-1
Analysis Type	Matrix												Secon. am
Analysis Pt.	28	29	30	31	32	33	34	35	36	37	38	39	am-4
Wt%													
SiO_2	43.66	43.09	43.53	44.22	42.70	43.60	43.84	42.57	43.36	43.84	43.32	43.02	52.96
TiO_2	0.24	0.28	0.28	0.26	0.28	0.27	0.26	0.28	0.29	0.24	0.25	0.26	0.01
Al_2O_3	12.60	12.51	11.84	12.37	12.08	11.93	12.01	12.49	12.85	12.14	12.19	12.04	0.26
Cr_2O_3	0.01	0.01	0.01	0.01	0.03	0.01	0.05	0.01	0.03	0.03	0.02	0.02	0.00
MnO	0.26	0.33	0.34	0.30	0.31	0.28	0.28	0.31	0.32	0.31	0.31	0.31	0.24
FeO	12.95	11.87	14.39	13.04	13.03	12.23	13.39	11.60	12.23	12.12	11.34	11.38	27.66
Fe_2O_3	6.53	7.88	7.59	7.17	7.66	8.80	7.20	9.61	8.36	8.43	10.10	9.74	0.00
MgO	9.40	9.61	9.10	9.70	9.33	9.65	9.30	9.40	9.41	9.83	9.24	9.74	15.27
CaO	11.02	11.07	10.02	10.82	10.17	10.95	10.80	11.11	11.00	11.02	10.69	11.01	0.15
Na_2O	1.07	1.01	1.01	0.88	0.95	0.98	0.97	1.00	0.97	1.08	1.15	1.03	0.01
K_2O	0.64	0.73	0.79	0.67	0.82	0.73	0.72	0.75	0.72	0.72	0.67	0.71	0.00
H_2O (calc)	1.94	1.92	1.91	1.94	1.92	1.93	1.93	1.91	1.92	1.93	1.93	1.93	2.01
F	0.00	0.00	0.00	0.00	0.00	0.00	0.00	0.00	0.00	0.00	0.00	0.00	0.01
Cl	0.10	0.13	0.11	0.09	0.09	0.08	0.10	0.13	0.13	0.10	0.10	0.08	0.00
O=F,Cl (calc)	*-0.02*	*-0.03*	*-0.02*	*-0.02*	*-0.02*	*-0.02*	*-0.02*	*-0.03*	*-0.03*	*-0.02*	*-0.02*	*-0.02*	*0.00*
Total	100.39	100.41	100.90	101.45	99.34	101.43	100.82	101.14	101.57	101.76	101.29	101.25	98.58
Normalization procedure(s)	Si–Ca&Li=15 Si–Mg&Li=13		Si–Ca&Li=15 Si–Na=15					Si–Ca&Li=15 Si–Mg&Li=13	Si–Ca&Li=15 Si–Na=15	Si–Ca&Li=15 Si–Mg&Li=13	Si–Ca&Li=15 Si–Mg&Li=13 Si–Na=15	Si–Ca&Li=15 Si–Mg&Li=13	Si–Ca&Li=15 Si–Na=15
T site (ideally 8 apfu):													
Si	6.459	6.384	6.464	6.474	6.417	6.410	6.482	6.292	6.358	6.413	6.374	6.339	7.979

Al	1.541	1.616	1.536	1.526	1.583	1.590	1.518	1.708	1.642	1.587	1.626	1.661	0.021
T subtotal	**8.000**	**8.000**	**8.000**	**8.000**	**8.000**	**8.000**	**8.000**	**8.000**	**8.000**	**8.000**	**8.000**	**8.000**	**8.000**
C site (ideally 5 apfu):													
Ti	0.027	0.031	0.031	0.029	0.031	0.030	0.029	0.031	0.031	0.026	0.028	0.029	0.001
Al	0.656	0.568	0.536	0.608	0.557	0.477	0.575	0.467	0.579	0.506	0.488	0.431	0.025
Cr	0.001	0.001	0.001	0.002	0.003	0.002	0.006	0.001	0.003	0.004	0.002	0.002	0.000
Fe^{3+}	0.726	0.879	0.848	0.791	0.865	0.974	0.800	1.068	0.923	0.928	1.119	1.081	0.000
Fe^{2+}	1.517	1.398	1.569	1.455	1.453	1.401	1.540	1.361	1.405	1.392	1.337	1.319	1.544
Mg	2.073	2.122	2.014	2.116	2.090	2.116	2.050	2.072	2.058	2.144	2.026	2.139	3.430
C subtotal	**5.000**	**4.999**	**4.999**	**5.001**	**4.999**	**5.000**	**5.000**	**5.000**	**4.999**	**5.000**	**5.000**	**5.001**	**5.000**
B site (ideally 2 apfu):													
Mn^{2+}	0.033	0.041	0.043	0.037	0.040	0.034	0.034	0.039	0.040	0.038	0.038	0.039	0.031
Fe^{2+}	0.085	0.072	0.218	0.141	0.185	0.102	0.116	0.073	0.094	0.089	0.058	0.083	1.941
Ca	1.747	1.757	1.594	1.697	1.638	1.725	1.711	1.759	1.728	1.727	1.685	1.738	0.024
Na	0.135	0.130	0.145	0.125	0.137	0.139	0.138	0.129	0.138	0.145	0.218	0.140	0.003
B subtotal	**2.000**	**2.000**	**2.000**	**2.000**	**2.000**	**2.000**	**1.999**	**2.000**	**2.000**	**1.999**	**1.999**	**2.000**	**1.999**
A site (from 0 to 1 apfu):													
Na	0.172	0.160	0.146	0.125	0.138	0.140	0.140	0.159	0.139	0.161	0.109	0.153	0.000
K	0.121	0.138	0.150	0.125	0.157	0.136	0.135	0.141	0.135	0.134	0.126	0.134	0.000
A subtotal	**0.293**	**0.298**	**0.296**	**0.250**	**0.295**	**0.276**	**0.275**	**0.300**	**0.274**	**0.295**	**0.235**	**0.287**	0.000
W site (ideally 2 apfu):													
OH	1.921	1.905	1.910	1.920	1.915	1.919	1.916	1.905	1.904	1.922	1.918	1.921	1.993
F	0.000	0.000	0.000	0.000	0.000	0.000	0.000	0.000	0.000	0.000	0.000	0.000	0.005
Cl	0.025	0.033	0.028	0.022	0.022	0.021	0.026	0.034	0.033	0.025	0.026	0.021	0.000
O	0.054	0.063	0.063	0.058	0.063	0.060	0.058	0.062	0.063	0.053	0.056	0.059	0.002
W subtotal	**2.000**	**2.001**	**2.001**	**2.000**	**2.000**	**2.000**	**2.000**	**2.001**	**2.000**	**2.000**	**2.000**	**2.001**	**2.000**
Sum T,C,B,A	**15.293**	**15.297**	**15.295**	**15.251**	**15.294**	**15.276**	**15.274**	**15.300**	**15.273**	**15.294**	**15.234**	**15.288**	**14.999**
Species	magnesio-ferri-hornblende							ferri-tschermakite		magnesio-ferri-hornblende	ferri-tschermakite		grunerite

Sample	QC82-45												
Analysis Type	alt. am	alt. am	matrix core	matrix core	matrix core	matrix rim	alt. am	matrix rim	matrix rim	incl in grt	incl in grt	incl in grt	alt. am
Analysis Pt.	am-4	am-5	am-7	am-8	am-9	am-10	am-10	am-11	am-12	am-13	am-14	am-15	am-17
Wt%													
SiO_2	48.95	51.23	36.92	36.80	36.94	36.79	41.89	36.67	36.77	38.07	38.45	38.25	50.93
TiO_2	0.02	0.05	1.39	1.43	1.45	1.41	0.04	1.44	1.46	2.00	1.90	1.93	0.07
Al_2O_3	0.14	0.22	11.06	11.03	11.01	10.98	3.61	11.12	11.39	10.65	10.60	10.70	0.69
Cr_2O_3	0.00	0.00	0.05	0.01	0.02	0.00	0.04	0.03	0.03	0.01	0.05	0.05	0.02
MnO	1.03	0.86	0.15	0.15	0.16	0.19	0.91	0.17	0.16	0.16	0.19	0.15	0.66
FeO	32.98	35.44	23.37	23.40	23.57	23.40	32.23	23.29	23.54	22.12	22.32	22.15	33.00
Fe_2O_3	3.89	0.00	3.48	3.45	3.37	3.85	3.24	4.11	3.53	3.64	3.51	4.17	0.11
NiO	0.00	0.00	0.01	0.05	0.03	0.01	0.00	0.03	0.02	0.03	0.00	0.02	0.00
MgO	9.42	9.35	3.76	3.69	3.72	3.73	5.14	3.67	3.65	4.94	4.92	4.94	9.70
CaO	0.14	0.36	11.37	11.26	11.35	11.37	0.89	11.39	11.35	11.38	11.19	11.34	1.75
Na_2O	0.00	0.00	0.54	0.56	0.56	0.57	0.01	0.59	0.55	0.98	1.01	1.03	0.00
BaO	0.00	0.00	0.56	0.54	0.56	0.64	0.02	0.61	0.65	0.53	0.61	0.57	0.00
K_2O	0.00	0.03	3.27	3.27	3.30	3.30	0.07	3.24	3.37	2.39	2.33	2.36	0.05
H_2O (calc)	1.92	1.93	1.15	1.08	1.15	1.13	1.77	1.11	1.13	1.38	1.37	1.38	1.89
F	0.00	0.00	0.04	0.05	0.04	0.08	0.02	0.01	0.02	0.05	0.09	0.07	0.04
Cl	0.00	0.00	2.60	2.86	2.59	2.60	0.39	2.82	2.71	1.82	1.79	1.78	0.13
O=F,Cl (calc)	*0.00*	*0.00*	*-0.60*	*-0.67*	*-0.60*	*-0.62*	*-0.10*	*-0.64*	*-0.62*	*-0.43*	*-0.44*	*-0.43*	*-0.05*
Total	98.49	99.47	99.12	98.96	99.22	99.44	90.18	99.66	99.71	99.72	99.89	100.46	99.04
Normalization procedure(s) used for apfu	Si–Ca&Li=15 Si–Na=15		Si–Ca&Li=15 Si–Mg&Li=13				Si–Ca&Li=15 Si–Na=15	Si–Ca&Li=15 Si–Mg&Li=13					Si–Ca&Li=15 Si–Na=15
T site (ideally 8 apfu):													
Si	7.753	7.981	6.079	6.079	6.080	6.054	7.392	6.026	6.032	6.126	6.171	6.112	7.920
Al	0.026	0.019	1.921	1.921	1.920	1.946	0.608	1.974	1.968	1.874	1.829	1.888	0.080

T subtotal	**7.999**	**8.000**	**8.000**	**8.000**	**8.000**	**8.000**	**8.000**	**8.000**	**8.000**	**8.000**	**8.000**	**8.000**	**8.000**
C site (ideally 5 apfu):													
Ti	0.000	0.006	0.172	0.178	0.180	0.175	0.005	0.178	0.180	0.242	0.229	0.232	0.008
Al	0.000	0.021	0.225	0.227	0.216	0.183	0.143	0.180	0.235	0.146	0.176	0.128	0.046
Cr	0.000	0.000	0.007	0.001	0.003	0.000	0.006	0.004	0.004	0.001	0.006	0.006	0.002
Fe^{3+}	0.000	0.000	0.431	0.428	0.419	0.478	0.430	0.507	0.436	0.440	0.424	0.503	0.012
Ni	0.000	0.000	0.001	0.007	0.004	0.001	0.000	0.004	0.003	0.004	0.000	0.003	0.000
Mn^{2+}	0.000	0.000	0.021	0.018	0.022	0.026	0.000	0.024	0.020	0.004	0.000	0.000	0.000
Fe^{2+}	2.531	2.801	3.218	3.233	3.243	3.219	3.063	3.202	3.230	2.977	2.987	2.952	2.682
Mg	2.224	2.171	0.923	0.909	0.913	0.915	1.352	0.899	0.893	1.185	1.177	1.177	2.249
C subtotal	**5.000**	**4.999**	**4.998**	**5.001**	**5.000**	**4.997**	**4.999**	**4.998**	**5.001**	**4.999**	**4.999**	**5.001**	**4.999**
B site (ideally 2 apfu):													
Mn^{2+}	0.138	0.113	0.000	0.003	0.000	0.000	0.136	0.000	0.002	0.018	0.026	0.020	0.087
Fe^{2+}	1.838	1.816	0.000	0.000	0.000	0.000	1.694	0.000	0.000	0.000	0.009	0.007	1.610
Ca	0.024	0.060	2.000	1.993	2.000	2.000	0.168	2.000	1.995	1.962	1.924	1.942	0.292
Na	0.000	0.000	0.000	0.004	0.000	0.000	0.002	0.000	0.003	0.020	0.040	0.031	0.011
B subtotal	**2.000**	**1.989**	**2.000**	**2.000**	**2.000**	**2.000**	**2.000**	**2.000**	**2.000**	**2.000**	**1.999**	**2.000**	**2.000**
A site (from 0 to 1 apfu):													
Ca	0.000	0.000	0.006	0.000	0.002	0.005	0.000	0.005	0.000	0.000	0.000	0.000	0.000
Na	0.000	0.000	0.172	0.176	0.179	0.182	0.002	0.188	0.172	0.286	0.274	0.288	0.004
Ba	0.000	0.000	0.025	0.024	0.025	0.028	0.001	0.027	0.029	0.023	0.026	0.025	0.000
K	0.000	0.006	0.687	0.689	0.693	0.693	0.016	0.679	0.705	0.491	0.477	0.481	0.010
A subtotal	0.000	**0.006**	**0.890**	**0.889**	**0.899**	**0.908**	**0.019**	**0.899**	**0.906**	**0.800**	**0.777**	**0.794**	**0.014**
W site (ideally 2 apfu):													
OH	2.000	2.000	1.253	1.173	1.256	1.233	1.872	1.209	1.236	1.478	1.467	1.482	1.946
F	0.000	0.000	0.021	0.026	0.021	0.042	0.011	0.005	0.010	0.025	0.046	0.035	0.020
Cl	0.000	0.000	0.726	0.801	0.723	0.725	0.117	0.786	0.754	0.497	0.487	0.482	0.034
W subtotal	**2.000**	**2.000**	**2.000**	**2.000**	**2.000**	**2.000**	**2.000**	**2.000**	**2.000**	**2.000**	**2.000**	**1.999**	**2.000**
Sum T,C,B,A	**14.999**	**14.994**	**15.888**	**15.890**	**15.899**	**15.905**	**15.018**	**15.897**	**15.907**	**15.799**	**15.775**	**15.795**	**15.013**
Species	grunerite		potassic-hastingsite				grunerite	potassic-hastingsite					grunerite

Sample	QC82-45												
Analysis Type	alt. am	matrix	incl. in gar	incl. in opx	incl. in opx	incl. in opx	incl. in opx	incl. in opx	incl. in opx	matrix	by biot 45	incl. in opx	matrix
Analysis Pt.	am-18	28	29	30	am-32	33	34	am-35	am-41	am-43	am-46	am-47	48
Wt%													
SiO_2	52.79	37.11	37.97	36.84	36.84	36.73	37.05	36.73	36.16	37.55	36.61	36.77	36.88
TiO_2	0.05	1.40	1.84	1.53	1.53	1.37	1.70	1.44	1.29	1.53	1.29	1.35	1.34
Al_2O_3	0.28	11.38	10.86	11.94	11.94	12.05	11.90	11.85	11.75	12.08	11.70	11.49	11.59
Cr_2O_3	0.00	0.04	0.04	0.02	0.02	0.02	0.03	0.02	0.00	0.05	0.04	0.01	0.04
MnO	0.70	0.17	0.17	0.21	0.21	0.18	0.19	0.20	0.18	0.18	0.10	0.18	0.14
FeO	31.05	23.22	22.04	24.41	24.41	24.37	24.17	24.33	23.74	22.51	23.16	23.66	22.74
Fe_2O_3	0.00	4.52	4.12	4.02	4.02	4.26	4.48	3.93	4.69	3.54	4.51	4.28	4.57
NiO	0.04	0.00	0.00	0.00	0.00	0.00	0.00	0.00	0.00	0.00	0.00	0.00	0.00
MgO	12.02	3.83	4.96	3.19	3.19	2.97	3.27	3.12	3.18	4.18	3.67	3.49	3.97
CaO	0.20	11.50	11.62	11.48	11.48	11.41	11.54	11.43	11.42	11.47	11.48	11.59	11.60
Na_2O	0.03	0.65	1.06	0.63	0.63	0.59	0.76	0.54	0.53	0.54	0.52	0.58	0.62
BaO	0.00	0.55	0.53	1.07	1.07	1.09	0.84	0.65	1.03	0.63	0.70	0.61	0.36
K_2O	0.01	3.20	2.39	3.26	3.26	3.15	2.93	3.46	3.37	3.02	3.40	3.30	3.30
H_2O (calc)	1.96	1.14	1.29	1.11	1.11	1.13	1.22	1.13	1.06	1.45	1.09	1.13	1.17
F	0.03	0.08	0.25	0.17	0.17	0.00	0.10	0.07	0.16	0.00	0.11	0.10	0.06
Cl	0.04	2.61	1.82	2.55	2.55	2.76	2.28	2.62	2.71	1.64	2.73	2.60	2.53
O=F,Cl (calc)	*-0.02*	*-0.62*	*-0.52*	*-0.65*	*-0.65*	*-0.62*	*-0.56*	*-0.62*	*-0.68*	*-0.37*	*-0.66*	*-0.63*	*-0.60*
Total	99.18	100.77	100.44	101.78	101.78	101.46	101.90	100.91	100.59	100.01	100.45	100.51	100.31
Normalization procedure(s) used for apfu	Si–Ca&Li=15 Si–Na=15	Si–Ca&Li=15 Si–Mg&Li=13											
T site (ideally 8 apfu):													
Si	8.046	6.011	6.076	5.955	5.955	5.961	5.950	5.976	5.930	6.042	5.969	5.993	5.984
Al	0.000	1.989	1.924	2.045	2.045	2.039	2.050	2.024	2.070	1.958	2.031	2.007	2.016

T subtotal	**8.046**	**8.000**	**8.000**	**8.000**	**8.000**	**8.000**	**8.000**	**8.000**	**8.000**	**8.000**	**8.000**	**8.000**	**8.000**
C site (ideally 5 apfu):													
Ti	0.006	0.171	0.222	0.186	0.186	0.167	0.205	0.176	0.159	0.185	0.158	0.166	0.164
Al	0.050	0.183	0.124	0.230	0.230	0.266	0.202	0.248	0.201	0.333	0.217	0.200	0.200
Cr	0.000	0.005	0.005	0.003	0.003	0.003	0.004	0.003	0.000	0.006	0.005	0.001	0.005
Fe^{3+}	0.000	0.551	0.497	0.490	0.490	0.519	0.540	0.483	0.580	0.429	0.554	0.527	0.556
Ni	0.005	0.000	0.000	0.000	0.000	0.000	0.000	0.000	0.000	0.000	0.000	0.000	0.000
Mn^{2+}	0.000	0.021	0.020	0.023	0.023	0.017	0.019	0.024	0.025	0.014	0.014	0.025	0.019
Fe^{2+}	2.208	3.144	2.949	3.300	3.300	3.309	3.247	3.309	3.255	3.030	3.157	3.223	3.088
Mg	2.731	0.925	1.183	0.769	0.769	0.719	0.783	0.757	0.777	1.003	0.892	0.848	0.960
C subtotal	**5.000**	**5.000**	**5.000**	**5.001**	**5.001**	**5.000**	**5.000**	**5.000**	**4.997**	**5.000**	**4.997**	**4.990**	**4.992**
B site (ideally 2 apfu):													
Mn^{2+}	0.090	0.002	0.004	0.005	0.005	0.007	0.007	0.003	0.000	0.010	0.000	0.000	0.000
Fe^{2+}	1.750	0.000	0.000	0.000	0.000	0.000	0.000	0.000	0.000	0.000	0.000	0.000	0.000
Ca	0.033	1.996	1.992	1.988	1.988	1.984	1.986	1.993	2.000	1.978	2.000	2.000	2.000
Na	0.009	0.002	0.004	0.006	0.006	0.008	0.008	0.004	0.000	0.012	0.000	0.000	
B subtotal	**1.882**	**2.000**	**2.000**	**1.999**	**1.999**	**1.999**	**2.001**	**2.000**	**2.000**	**2.000**	**2.000**	**2.000**	**2.000**
A site (from 0 to 1 apfu):													
Ca	0.000	0.000	0.000	0.000	0.000	0.000	0.000	0.000	0.007	0.000	0.005	0.024	0.017
Na	0.000	0.202	0.325	0.191	0.191	0.177	0.229	0.166	0.169	0.156	0.164	0.183	0.195
Ba	0.000	0.024	0.023	0.047	0.047	0.048	0.036	0.028	0.045	0.027	0.031	0.027	0.016
K	0.002	0.661	0.488	0.672	0.672	0.652	0.600	0.718	0.705	0.620	0.707	0.686	0.683
A subtotal	**0.002**	**0.887**	**0.836**	**0.910**	**0.910**	**0.877**	**0.865**	**0.912**	**0.926**	**0.803**	**0.907**	**0.920**	**0.911**
W site (ideally 2 apfu):													
OH	1.975	1.242	1.380	1.214	1.214	1.240	1.328	1.241	1.163	1.553	1.188	1.230	1.273
F	0.014	0.041	0.127	0.087	0.087	0.000	0.051	0.036	0.083	0.000	0.057	0.052	0.031
Cl	0.010	0.717	0.494	0.699	0.699	0.760	0.621	0.723	0.754	0.447	0.755	0.719	0.696
W subtotal	**1.999**	**2.000**	**2.001**	**2.000**	**2.000**	**2.000**	**2.000**	**2.000**	**2.000**	**2.000**	**2.000**	**2.001**	**2.000**
Sum T,C,B,A	**14.930**	**15.887**	**15.836**	**15.910**	**15.910**	**15.876**	**15.866**	**15.912**	**15.923**	**15.803**	**15.904**	**15.910**	**15.903**
Species	grunerite	potassic-hastingsite											

Sample	QC82-45		HP82-59										
Analysis Type	matrix	matrix	alt. am	alt. am	alt. am	alt. am	alt. am	alt. am	alt. am	alt. am	alt. am	alt. am	am
Analysis Pt.	am-49	am-50	33	34	35	39	40	41	42	43	44	70	71
Wt%													
SiO_2	36.88	37.80	52.35	52.76	52.74	55.16	54.01	55.07	54.70	54.48	55.00	55.49	40.37
TiO_2	1.34	1.44	0.00	0.00	0.04	0.03	0.03	0.02	0.05	0.06	0.06	0.07	0.52
Al_2O_3	11.59	11.27	0.63	0.56	0.66	0.46	0.67	0.58	0.54	0.59	0.42	0.60	14.27
Cr_2O_3	0.04	0.06	0.05	0.00	0.00	0.00	0.00	0.00	0.00	0.00	0.02	0.02	0.00
MnO	0.14	0.17	0.24	0.18	0.26	0.27	0.33	0.29	0.19	0.24	0.22	0.44	0.13
FeO	22.74	23.29	18.35	17.25	16.33	20.77	19.39	20.03	20.22	20.74	19.70	21.57	20.83
Fe_2O_3	4.57	4.18	3.24	3.04	4.31	0.50	0.42	0.00	0.00	0.00	0.00	0.00	4.67
MgO	3.97	4.11	12.66	12.21	12.72	12.11	11.87	11.81	11.37	11.44	12.18	13.14	4.95
CaO	11.60	11.76	10.43	12.33	12.17	11.68	12.13	11.47	11.25	11.65	12.25	8.23	11.48
Na_2O	0.62	0.69	0.09	0.06	0.06	0.09	0.07	0.07	0.08	0.03	0.05	0.09	1.09
BaO	0.36	0.30	0.00	0.04	0.01	0.02	0.00	0.04	0.00	0.00	0.01	0.00	0.09
K_2O	3.30	3.15	0.07	0.05	0.02	0.03	0.03	0.03	0.03	0.03	0.01	0.07	1.78
H_2O (calc)	1.17	1.21	2.02	2.02	2.03	2.02	2.03	2.03	2.03	2.02	2.03	2.04	1.69
F	0.06	0.07	0.00	0.00	0.00	0.00	0.00	0.00	0.00	0.00	0.00	0.00	0.00
Cl	2.53	2.41	0.02	0.01	0.00	0.00	0.00	0.00	0.00	0.00	0.00	0.00	0.93
O=F,Cl (calc)	*-0.60*	*-0.57*	*0.00*	*0.00*	*0.00*	*0.00*	*0.00*	*0.00*	*0.00*	*0.00*	*0.00*	*0.00*	*-0.21*
Total	100.31	101.34	100.14	100.51	101.34	103.13	100.97	101.43	100.47	101.27	101.95	101.78	102.59
Normalization procedure(s) used for apfu	Si–Ca&Li=15 Si–Mg&Li=13		Si–Ca&Li=15 Si–Na=15										Si–Ca&Li=15 Si–Mg&Li=13
T site (ideally 8 apfu):													
Si	5.984	6.055	7.755	7.776	7.700	7.928	7.913	8.007	8.033	7.970	7.963	8.020	6.131
Al	2.016	1.945	0.109	0.098	0.113	0.072	0.087	0.000	0.000	0.030	0.037	0.000	1.869

Ti	0.000	0.000	0.000	0.000	0.004	0.000	0.000	0.000	0.000	0.000	0.000	0.000	0.000
Fe^{3+}	0.000	0.000	0.135	0.126	0.182	0.000	0.000	0.000	0.000	0.000	0.000	0.000	0.000
T subtotal	**8.000**	**8.000**	**7.999**	**8.000**	**7.999**	**8.000**	**8.000**	**8.007**	**8.033**	**8.000**	**8.000**	**8.020**	**8.000**
C site (ideally 5 apfu):													
Ti	0.164	0.174	0.000	0.000	0.000	0.003	0.003	0.002	0.005	0.006	0.006	0.008	0.060
Al	0.200	0.182	0.000	0.000	0.000	0.006	0.029	0.099	0.094	0.072	0.035	0.102	0.685
Cr	0.005	0.008	0.006	0.000	0.000	0.000	0.000	0.000	0.000	0.000	0.002	0.003	0.000
Fe^{3+}	0.556	0.505	0.225	0.212	0.291	0.053	0.045	0.000	0.000	0.000	0.000	0.000	0.533
Mn^{2+}	0.019	0.023	0.000	0.000	0.000	0.000	0.000	0.000	0.000	0.000	0.000	0.000	0.000
Fe^{2+}	3.088	3.119	1.973	2.105	1.940	2.343	2.330	2.339	2.412	2.427	2.328	2.056	2.602
Mg	0.960	0.981	2.796	2.683	2.769	2.595	2.593	2.560	2.489	2.495	2.629	2.831	1.121
C subtotal	**4.992**	**4.992**	**5.000**	**5.000**	**5.000**	**5.000**	**5.000**	**5.000**	**5.000**	**5.000**	**5.000**	**5.000**	**5.001**
B site (ideally 2 apfu):													
Mn^{2+}	0.000	0.000	0.030	0.022	0.032	0.033	0.041	0.035	0.024	0.029	0.027	0.054	0.017
Fe^{2+}	0.000	0.000	0.301	0.021	0.055	0.155	0.046	0.097	0.072	0.111	0.058	0.551	0.045
Ca	2.000	2.000	1.656	1.947	1.904	1.799	1.904	1.787	1.770	1.826	1.900	1.274	1.868
Na	0.000	0.000	0.013	0.009	0.009	0.013	0.009	0.021	0.024	0.008	0.015	0.026	0.070
B subtotal	**2.000**	**2.000**	**2.000**	**1.999**	**2.000**	**2.000**	**2.000**	**1.940**	**1.890**	**1.974**	**2.000**	**1.905**	**2.000**
A site (from 0 to 1 apfu):													
Ca	0.017	0.018	0.000	0.000	0.000	0.000	0.000	0.000	0.000	0.000	0.000	0.000	0.000
Na	0.195	0.214	0.013	0.009	0.009	0.013	0.009	0.000	0.000	0.000	0.000	0.000	0.250
Ba	0.016	0.013	0.000	0.001	0.000	0.001	0.000	0.001	0.000	0.000	0.000	0.000	0.004
K	0.683	0.644	0.014	0.009	0.003	0.005	0.006	0.005	0.006	0.006	0.002	0.013	0.345
A subtotal	**0.911**	**0.889**	**0.027**	**0.019**	**0.012**	**0.019**	**0.015**	**0.006**	**0.006**	**0.006**	**0.002**	**0.013**	**0.599**
W site (ideally 2 apfu):													
OH	1.273	1.310	1.995	1.998	2.000	1.999	2.000	1.999	2.000	2.000	1.999	2.000	1.762
F	0.031	0.035	0.000	0.000	0.000	0.000	0.000	0.000	0.000	0.000	0.000	0.000	0.000
Cl	0.696	0.654	0.005	0.002	0.000	0.001	0.000	0.001	0.000	0.000	0.001	0.000	0.238
W subtotal	**2.000**	**1.999**	**2.000**	**2.000**	**2.000**	**2.000**	**2.000**	**2.000**	**2.000**	**2.000**	**2.000**	**2.000**	**2.000**
Sum T,C,B,A	**15.903**	**15.881**	**15.026**	**15.018**	**15.011**	**15.019**	**15.015**	**14.953**	**14.929**	**14.980**	**15.002**	**14.938**	**15.600**
Species	potassic-hastingsite		actinolite										potassic-ferro-pargasite

Sample	HP82-59							QC81-5		QC81-6			
Analysis Type	alt. am	alt. am	alt. am	alt. am	alt. am	alt. am	alt. am	incl. in opx	alt. am	core	rim	incl. in opx	matrix
Analysis Pt.	72	73	74	75	76	77	78	am-1	am-3	am-1	am-2	am-3	am-4
Wt%													
SiO_2	52.52	53.95	53.10	55.32	55.59	55.15	54.72	37.51	53.02	39.55	39.47	39.42	38.54
TiO_2	0.01	0.10	0.04	0.03	0.00	0.06	0.04	0.52	0.01	0.08	0.12	0.10	0.08
Al_2O_3	0.38	0.60	0.55	2.87	0.66	0.47	0.46	12.81	0.16	11.56	12.16	12.12	11.48
Cr_2O_3	0.00	0.00	0.02	0.00	0.00	0.01	0.00	0.01	0.00	0.00	0.00	0.00	0.00
MnO	0.22	0.24	0.25	0.20	0.23	0.26	0.27	0.05	0.46	0.26	0.23	0.26	0.27
FeO	19.10	19.25	19.68	20.27	19.57	20.24	20.92	19.37	29.36	19.81	19.36	20.65	19.43
Fe_2O_3	0.00	1.68	2.35	0.00	0.00	0.00	0.07	7.02	0.00	5.47	5.21	4.24	6.20
NiO	0.00	0.00	0.00	0.01	0.00	0.00	0.00	0.00	0.00	0.00	0.00	0.01	0.02
MgO	11.50	12.03	12.01	16.35	12.99	12.13	12.13	4.57	13.55	5.50	5.62	5.09	5.28
CaO	11.23	12.02	10.97	3.70	10.93	11.64	11.17	11.23	0.07	11.47	11.54	11.46	11.22
Na_2O	0.07	0.09	0.07	0.14	0.14	0.06	0.04	1.04	0.00	0.71	0.68	0.82	0.73
BaO	0.00	0.00	0.01	0.06	0.01	0.00	0.00	0.00	0.00	0.07	0.12	0.11	0.13
K_2O	0.03	0.04	0.04	0.23	0.02	0.01	0.01	2.30	0.00	2.55	2.53	2.51	2.62
H_2O (calc)	2.03	2.02	2.01	2.08	2.04	2.03	2.02	1.52	2.00	1.44	1.44	1.42	1.41
F	0.00	0.00	0.00	0.00	0.00	0.00	0.00	0.00	0.00	0.13	0.12	0.12	0.13
Cl	0.00	0.01	0.02	0.00	0.00	0.01	0.02	0.98	0.00	1.51	1.50	1.56	1.57
O=F,Cl (calc)	*0.00*	*0.00*	*-0.01*	*0.00*	*0.00*	*0.00*	*-0.01*	*-0.22*	*0.00*	*-0.40*	*-0.39*	*-0.40*	*-0.41*
Total	97.09	102.03	101.11	101.27	102.18	102.06	101.87	98.71	98.63	99.71	99.71	99.50	98.69
Normalization procedure(s) used for apfu	Si–Ca&Li=15 Si–Na=15							Si–Ca&Li=15 Si–Mg&Li=13	Si–Ca&Li=15 Si–Na=15	Si–Ca&Li=15 Si–Mg&Li=13			
T site (ideally 8 apfu):													
Si	7.992	7.842	7.813	7.877	7.984	7.977	7.955	6.009	8.047	6.257	6.225	6.256	6.189

Al	0.008	0.103	0.096	0.123	0.016	0.023	0.045	1.991	0.000	1.743	1.775	1.744	1.811
Ti	0.000	0.010	0.005	0.000	0.000	0.000	0.000	0.000	0.000	0.000	0.000	0.000	0.000
Fe^{3+}	0.000	0.045	0.087	0.000	0.000	0.000	0.000	0.000	0.000	0.000	0.000	0.000	0.000
T subtotal	**8.000**	**8.000**	**8.001**	**8.000**	**8.000**	**8.000**	**8.000**	**8.000**	**8.047**	**8.000**	**8.000**	**8.000**	**8.000**
C site (ideally 5 apfu):													
Ti	0.001	0.000	0.000	0.004	0.000	0.007	0.005	0.063	0.001	0.010	0.014	0.012	0.010
Al	0.060	0.000	0.000	0.359	0.096	0.058	0.034	0.428	0.029	0.412	0.485	0.523	0.362
Cr	0.000	0.000	0.002	0.000	0.000	0.001	0.000	0.001	0.000	0.000	0.000	0.000	0.000
Fe^{3+}	0.000	0.140	0.172	0.000	0.000	0.000	0.007	0.848	0.000	0.652	0.618	0.506	0.749
Ni	0.000	0.000	0.000	0.001	0.000	0.000	0.000	0.000	0.000	0.000	0.000	0.001	0.003
Mn^{2+}	0.000	0.000	0.000	0.000	0.000	0.000	0.000	0.000	0.000	0.009	0.008	0.011	0.005
Fe^{2+}	2.331	2.253	2.191	1.166	2.123	2.318	2.326	2.568	1.905	2.620	2.554	2.742	2.609
Mg	2.609	2.607	2.634	3.470	2.781	2.616	2.629	1.091	3.066	1.297	1.321	1.204	1.264
C subtotal	**5.001**	**5.000**	**4.999**	**5.000**	**5.000**	**5.000**	**5.001**	**4.999**	**5.001**	**5.000**	**5.000**	**4.999**	**5.002**
B site (ideally 2 apfu):													
Mn^{2+}	0.029	0.029	0.031	0.024	0.028	0.031	0.033	0.007	0.059	0.026	0.023	0.024	0.032
Fe^{2+}	0.100	0.086	0.230	1.248	0.228	0.130	0.218	0.026	1.822	0.000	0.000	0.000	0.000
Ca	1.831	1.872	1.729	0.564	1.682	1.804	1.740	1.928	0.011	1.944	1.950	1.949	1.931
Na	0.021	0.013	0.010	0.038	0.039	0.017	0.009	0.040	0.000	0.030	0.027	0.028	0.037
B subtotal	**1.981**	**2.000**	**2.000**	**1.874**	**1.977**	**1.982**	**2.000**	**2.001**	**1.892**	**2.000**	**2.000**	**2.001**	**2.000**
A site (from 0 to 1 apfu):													
Na	0.000	0.013	0.010	0.000	0.000	0.000	0.002	0.283	0.000	0.188	0.181	0.225	0.190
Ba	0.000	0.000	0.000	0.002	0.000	0.000	0.000	0.000	0.000	0.003	0.005	0.005	0.006
K	0.006	0.008	0.007	0.042	0.004	0.001	0.002	0.470	0.000	0.515	0.509	0.508	0.537
A subtotal	**0.006**	**0.021**	**0.017**	**0.044**	**0.004**	**0.001**	**0.004**	**0.753**	0.000	**0.706**	**0.695**	**0.738**	**0.733**
W site (ideally 2 apfu):													
OH	1.999	1.997	1.994	2.000	2.000	1.999	1.994	1.608	1.998	1.511	1.511	1.496	1.487
F	0.000	0.000	0.000	0.000	0.000	0.000	0.000	0.000	0.000	0.065	0.060	0.060	0.066
Cl	0.001	0.003	0.006	0.000	0.000	0.001	0.006	0.266	0.000	0.405	0.401	0.420	0.427
O	0.000	0.000	0.000	0.000	0.000	0.000	0.000	0.126	0.002	0.019	0.029	0.024	0.019
W subtotal	**2.000**	**2.000**	**2.000**	**2.000**	**2.000**	**2.000**	**2.000**	**2.000**	**2.000**	**2.000**	**2.001**	**2.000**	**1.999**
Sum T,C,B,A	**14.988**	**15.021**	**15.017**	**14.918**	**14.981**	**14.983**	**15.005**	**15.753**	**14.940**	**15.706**	**15.695**	**15.738**	**15.735**
Species	actinolite			cummingtonite	actinolite			potassic-hastingsite	gruneri te	potassic-hastingsite		potassic-ferro-pargasite	potassic-hastingsite

Sample	QC82-46		QC82-47			QC82-48a	QC82-48b		QC82-49a	QC82-49b			
Analysis Type	matrix	alt. am	avg of 2	am	avg of 2	matrix	core	rim	matrix	core	core	core	near grt 12, opx-13, cpx-14 (area 4)
Analysis Pt.	hbl circle 2	act circle 2	matrix	incl. in opx	matrix	am-26	am-1	am-2	am-2	am-1	am-3	am-9	am-11
Wt%													
SiO_2	46.83	55.04	46.37	46.70	46.86	43.74	44.78	44.78	41.34	41.49	41.55	42.08	42.15
TiO_2	0.32	0.02	0.04	0.00	0.04	0.12	0.16	0.22	0.14	0.03	0.00	0.50	0.43
Al_2O_3	8.04	0.28	8.35	8.59	8.52	10.82	10.41	8.89	12.42	12.40	12.69	12.40	11.75
Cr_2O_3	0.00	0.00	0.00	0.00	0.01	0.01	0.01	0.01	0.01	0.00	0.01	0.01	0.00
MnO	0.36	0.19	0.19	0.15	0.16	0.72	0.69	0.57	0.68	0.53	0.58	0.33	0.29
FeO	12.58	12.55	12.85	13.51	12.73	11.89	12.76	11.89	14.96	16.16	15.61	15.12	15.72
Fe_2O_3	8.11	2.98	6.38	5.39	6.30	7.21	7.08	7.99	7.50	6.05	6.16	5.66	5.79
NiO	0.00	0.00	0.00	0.00	0.00	0.00	0.00	0.00	0.00	0.01	0.00	0.00	0.00
MgO	11.23	15.84	10.93	11.12	11.18	10.08	10.08	10.74	7.75	7.40	7.68	8.11	7.85
CaO	11.32	12.80	11.43	12.03	11.42	11.23	11.57	11.62	11.60	11.29	11.31	11.40	11.38
Na_2O	0.67	0.02	0.78	0.88	0.79	1.12	1.07	1.04	1.07	1.02	1.02	1.03	0.98
BaO	0.00	0.03	0.03	0.00	0.02	0.02	0.00	0.00	0.08	0.03	0.04	0.00	0.00
K_2O	0.50	0.00	0.24	0.37	0.25	0.50	0.49	0.46	1.28	1.42	1.44	1.37	1.30
H_2O (calc)	1.92	2.04	2.01	2.01	2.01	1.97	1.97	1.95	1.85	1.83	1.84	1.79	1.84
F	0.04	0.05	0.00	0.00	0.00	0.00	0.00	0.00	0.00	0.01	0.03	0.05	0.00
Cl	0.03	0.01	0.05	0.05	0.04	0.09	0.04	0.04	0.33	0.47	0.47	0.22	0.17
O=F,Cl (calc)	*-0.02*	*-0.02*	*-0.01*	*-0.01*	*-0.01*	*-0.02*	*-0.01*	*-0.01*	*-0.07*	*-0.11*	*-0.12*	*-0.07*	*-0.04*
Total	101.93	101.83	99.64	100.79	100.32	99.50	101.10	100.19	100.94	100.03	100.31	99.98	99.60

Normalization procedure(s) used for apfu	Si–Ca&Li=15 Si–Na=15		Si–Ca&Li=15 Si–Mg&Li=13										
T site (ideally 8 apfu):													
Si	6.820	7.816	6.876	6.857	6.884	6.538	6.597	6.659	6.249	6.330	6.307	6.370	6.420
Al	1.180	0.047	1.124	1.143	1.116	1.462	1.403	1.341	1.751	1.670	1.693	1.630	1.580
Ti	0.000	0.002	0.000	0.000	0.000	0.000	0.000	0.000	0.000	0.000	0.000	0.000	0.000
Fe^{3+}	0.000	0.135	0.000	0.000	0.000	0.000	0.000	0.000	0.000	0.000	0.000	0.000	0.000
T subtotal	**8.000**	**8.000**	**8.000**	**8.000**	**8.000**	**8.000**	**8.000**	**8.000**	**8.000**	**8.000**	**8.000**	**8.000**	**8.000**
C site (ideally 5 apfu):													
Ti	0.035	0.000	0.004	0.000	0.004	0.013	0.018	0.025	0.016	0.003	0.000	0.057	0.049
Al	0.200	0.000	0.336	0.343	0.360	0.444	0.405	0.217	0.461	0.560	0.577	0.582	0.530
Cr	0.000	0.000	0.000	0.000	0.001	0.001	0.001	0.001	0.001	0.000	0.001	0.001	0.000
Fe^{3+}	0.888	0.184	0.712	0.595	0.697	0.810	0.785	0.895	0.852	0.694	0.704	0.645	0.664
Ni	0.000	0.000	0.000	0.000	0.000	0.000	0.000	0.000	0.000	0.000	0.000	0.000	0.000
Mn^{2+}	0.000	0.000	0.000	0.000	0.000	0.000	0.005	0.003	0.031	0.000	0.000	0.000	0.000
Fe^{2+}	1.439	1.463	1.532	1.628	1.489	1.485	1.572	1.478	1.892	2.058	1.980	1.885	1.974
Mg	2.438	3.353	2.416	2.434	2.449	2.246	2.214	2.381	1.746	1.683	1.738	1.829	1.782
C subtotal	**5.000**	**5.000**	**5.000**	**5.000**	**5.000**	**4.999**	**5.000**	**5.000**	**4.999**	**4.999**	**5.000**	**4.999**	**4.999**
B site (ideally 2 apfu):													
Mn^{2+}	0.044	0.023	0.024	0.019	0.020	0.091	0.081	0.069	0.056	0.068	0.075	0.042	0.037
Fe^{2+}	0.094	0.027	0.062	0.031	0.075	0.003	0.000	0.000	0.000	0.004	0.000	0.028	0.028
Ca	1.766	1.948	1.816	1.892	1.798	1.799	1.826	1.851	1.879	1.846	1.839	1.848	1.857
Na	0.095	0.003	0.098	0.057	0.108	0.108	0.093	0.080	0.065	0.082	0.086	0.082	0.078
B subtotal	**1.999**	**2.001**	**2.000**	**1.999**	**2.001**	**2.001**	**2.000**	**2.000**	**2.000**	**2.000**	**2.000**	**2.000**	**2.000**
A site (from 0 to 1 apfu):													
Na	0.094	0.003	0.126	0.193	0.117	0.217	0.213	0.220	0.248	0.219	0.215	0.219	0.210
Ba	0.000	0.001	0.001	0.000	0.001	0.001	0.000	0.000	0.003	0.001	0.002	0.000	0.000
K	0.093	0.000	0.045	0.069	0.047	0.095	0.092	0.087	0.247	0.276	0.279	0.265	0.253
A subtotal	**0.187**	**0.004**	**0.172**	**0.262**	**0.165**	**0.313**	**0.305**	**0.307**	**0.498**	**0.496**	**0.496**	**0.484**	**0.463**
W site (ideally 2 apfu):													
OH	1.904	1.971	1.978	1.988	1.981	1.950	1.954	1.941	1.884	1.867	1.865	1.806	1.858
F	0.018	0.022	0.000	0.000	0.000	0.000	0.000	0.000	0.000	0.005	0.014	0.023	0.000
Cl	0.007	0.002	0.013	0.012	0.010	0.023	0.010	0.010	0.085	0.122	0.121	0.056	0.043
O	0.070	0.004	0.009	0.000	0.009	0.027	0.036	0.049	0.032	0.007	0.000	0.115	0.098
W subtotal	**1.999**	**1.999**	**2.000**	**2.000**	**2.000**	**2.000**	**2.000**	**2.000**	**2.001**	**2.001**	**2.000**	**2.000**	**1.999**
Sum T,C,B,A	**15.186**	**15.005**	**15.172**	**15.261**	**15.166**	**15.313**	**15.305**	**15.307**	**15.497**	**15.495**	**15.496**	**15.483**	**15.462**

Species	magnesio-ferri-hornblende	actinolite	magnesio-ferri-hornblende	hastingsite	ferro-ferri-hornblende

Sample	QC-JW								QC81-45			
Analysis Type	matrix	am	am	Alt. am	matrix	matrix	matrix	am	incl. in opx	core	rim	core
Analysis Pt.	am-7	am-1	am-2	am-2	am-3	am-4	am-6	am-3	am in opx	am-1	am-2	am-3
Wt%												
SiO_2	41.08	40.96	41.43	52.37	41.42	41.06	41.16	41.25	40.05	39.45	39.14	39.42
TiO_2	0.00	0.04	0.02	0.00	0.00	0.01	0.03	0.01	0.08	0.08	0.05	0.10
Al_2O_3	12.62	12.12	12.25	1.45	11.58	12.09	12.61	11.94	12.14	11.50	11.54	11.54
Cr_2O_3	0.00	0.00	0.00	0.02	0.00	0.01	0.01	0.00	0.08	0.00	0.00	0.00
MnO	0.67	0.48	0.47	0.78	0.71	0.62	0.68	0.54	0.46	0.35	0.36	0.40
FeO	17.30	16.57	17.48	15.74	17.37	17.06	17.01	16.92	19.28	18.89	19.06	18.64
Fe_2O_3	6.34	6.30	5.35	3.02	6.64	6.91	6.89	6.57	6.55	6.74	6.08	6.47
NiO	0.00	0.00	0.00	0.04	0.00	0.06	0.01	0.01	0.00	0.01	0.01	0.03
MgO	6.40	6.90	6.71	12.95	6.32	6.36	6.40	6.81	5.49	5.74	5.53	5.91
CaO	11.29	11.55	11.63	11.57	10.94	10.92	11.36	11.43	11.46	11.46	11.39	11.38
Na_2O	1.06	0.87	0.93	0.07	1.01	1.05	1.00	0.90	0.74	0.77	0.71	0.77
BaO	0.04	0.00	0.03	0.00	0.03	0.03	0.04	0.06	0.09	0.14	0.11	0.14
K_2O	1.23	1.37	1.31	0.05	0.99	1.10	1.16	1.37	2.31	2.36	2.38	2.50
H_2O (calc)	1.64	1.66	1.65	2.02	1.61	1.66	1.64	1.67	1.38	1.40	1.40	1.38
F	0.07	0.06	0.05	0.00	0.02	0.01	0.03	0.06	0.12	0.14	0.10	0.13
Cl	1.10	1.00	1.07	0.06	1.27	1.09	1.13	0.99	1.81	1.64	1.71	1.72

O=F,Cl (calc)	*-0.28*	*-0.25*	*-0.26*	*-0.01*	*-0.30*	*-0.25*	*-0.27*	*-0.25*	*-0.46*	*-0.43*	*-0.43*	*-0.44*
Total	100.56	99.62	100.10	100.13	99.61	99.78	100.88	100.28	101.58	100.24	99.14	100.09
Normalization procedure(s) used for apfu	Si–Ca&Li=15 Si–Mg&Li=13			Si–Ca&Li=15 Si–Na=15	Si–Ca&Li=15 Si–Mg&Li=13							
T site (ideally 8 apfu):												
Si	6.294	6.317	6.361	7.702	6.407	6.336	6.283	6.333	6.212	6.209	6.229	6.212
Al	1.706	1.683	1.639	0.252	1.593	1.664	1.717	1.667	1.788	1.791	1.771	1.788
Fe^{3+}	0.000	0.000	0.000	0.046	0.000	0.000	0.000	0.000	0.000	0.000	0.000	0.000
T subtotal	**8.000**	**8.000**	**8.000**	**8.000**	**8.000**	**8.000**	**8.000**	**8.000**	**8.000**	**8.000**	**8.000**	**8.000**
C site (ideally 5 apfu):												
Ti	0.000	0.004	0.002	0.000	0.000	0.001	0.004	0.001	0.009	0.009	0.006	0.012
Al	0.573	0.520	0.579	0.000	0.519	0.535	0.552	0.493	0.431	0.343	0.394	0.355
Cr	0.000	0.000	0.000	0.002	0.000	0.001	0.001	0.000	0.010	0.000	0.000	0.000
Fe^{3+}	0.731	0.731	0.617	0.287	0.773	0.801	0.790	0.761	0.763	0.800	0.727	0.767
Ni	0.000	0.000	0.000	0.005	0.000	0.007	0.002	0.002	0.000	0.001	0.001	0.004
Mn^{2+}	0.018	0.020	0.020	0.000	0.006	0.000	0.021	0.014	0.016	0.015	0.022	0.017
Fe^{2+}	2.216	2.139	2.246	1.867	2.247	2.193	2.173	2.172	2.501	2.485	2.538	2.456
Mg	1.462	1.586	1.536	2.838	1.456	1.462	1.457	1.557	1.269	1.347	1.312	1.388
C subtotal	**5.000**	**5.000**	**5.000**	**4.999**	**5.001**	**5.000**	**5.000**	**5.000**	**4.999**	**5.000**	**5.000**	**4.999**
B site (ideally 2 apfu):												
Mn^{2+}	0.068	0.042	0.040	0.097	0.088	0.081	0.066	0.056	0.044	0.031	0.027	0.036
Fe^{2+}	0.000	0.000	0.000	0.070	0.000	0.010	0.000	0.000	0.000	0.000	0.000	0.000
Ca	1.853	1.909	1.913	1.823	1.812	1.806	1.858	1.880	1.904	1.933	1.942	1.921
Na	0.078	0.049	0.046	0.010	0.100	0.103	0.076	0.064	0.051	0.036	0.031	0.042
B subtotal	**1.999**	**2.000**	**1.999**	**2.000**	**2.000**	**2.000**	**2.000**	**2.000**	**1.999**	**2.000**	**2.000**	**1.999**
A site (from 0 to 1 apfu):												
Na	0.237	0.210	0.230	0.010	0.204	0.211	0.221	0.204	0.171	0.199	0.188	0.193
Ba	0.002	0.000	0.001	0.000	0.001	0.001	0.002	0.002	0.004	0.006	0.005	0.006
K	0.240	0.270	0.256	0.009	0.195	0.217	0.225	0.269	0.457	0.474	0.483	0.503
A subtotal	**0.479**	**0.480**	**0.487**	**0.019**	**0.400**	**0.429**	**0.448**	**0.475**	**0.632**	**0.679**	**0.676**	**0.702**
W site (ideally 2 apfu):												
OH	1.680	1.699	1.696	1.984	1.657	1.705	1.685	1.711	1.447	1.474	1.476	1.452
F	0.034	0.031	0.022	0.000	0.011	0.007	0.014	0.030	0.059	0.070	0.050	0.065
Cl	0.286	0.261	0.278	0.016	0.333	0.286	0.293	0.258	0.476	0.438	0.461	0.459

O	0.000	0.009	0.004	0.000	0.000	0.002	0.007	0.002	0.019	0.019	0.012	0.024
W subtotal	**2.000**	**2.000**	**2.000**	**2.000**	**2.001**	**2.000**	**1.999**	**2.001**	**2.001**	**2.001**	**1.999**	**2.000**
Sum T,C,B,A	**15.478**	**15.480**	**15.486**	**15.018**	**15.401**	**15.429**	**15.448**	**15.475**	**15.630**	**15.679**	**15.676**	**15.700**
Species	ferro-ferri-hornblende			actinolite			ferro-ferri-hornblende			potassic-hastingsite		

Sample	HR02-71			
Analysis Type	matrix	alt. am	matrix	alt. am
Analysis Pt.	am-1	am-2	am-1	am-2
		Wt%		
SiO_2	43.82	51.82	45.57	52.89
TiO_2	0.22	0.00	0.23	0.00
Al_2O_3	8.07	0.25	8.39	0.26
Cr_2O_3	0.05	0.00	0.05	0.00
MnO	0.52	2.82	0.54	2.87
FeO	17.49	32.25	18.59	32.91
Fe_2O_3	6.17	0.00	5.97	0.00
MgO	7.56	9.99	7.86	10.20
CaO	11.12	0.73	11.56	0.74
Na_2O	0.88	0.06	0.91	0.06
BaO	0.03	0.04	0.03	0.04
K_2O	0.76	0.00	0.79	0.00
H_2O (calc)	1.89	1.94	1.94	1.94
Cl	0.10	0.02	0.11	0.02
O=F,Cl (calc)	*-0.02*	*0.00*	*-0.02*	*0.00*
Total	98.66	99.92	102.52	101.93
Normalization	Si–Ca&Li=15 Si–	Si–Ca&Li=15 Si–	Si–Ca&Li=15 Si–	Si–Ca&Li=15 Si–

procedure(s) used for apfu	Mg&Li=13	Na=15	Mg&Li=13	Na=15
T site (ideally 8 apfu):				
Si	6.778	7.989	6.779	7.989
Al	1.222	0.011	1.221	0.011
T subtotal	**8.000**	**8.000**	**8.000**	**8.000**
C site (ideally 5 apfu):				
Ti	0.026	0.000	0.026	0.000
Al	0.249	0.035	0.250	0.035
Cr	0.006	0.000	0.006	0.000
Fe^{3+}	0.719	0.000	0.667	0.000
Fe^{2+}	2.257	2.669	2.309	2.668
Mg	1.743	2.296	1.743	2.297
C subtotal	**5.000**	**5.000**	**5.001**	**5.000**
B site (ideally 2 apfu):				
Mn^{2+}	0.068	0.368	0.068	0.367
Fe^{2+}	0.005	1.489	0.005	1.489
Ca	1.843	0.121	1.843	0.120
Na	0.084	0.018	0.084	0.019
B subtotal	**2.000**	**1.996**	**2.000**	**1.995**
A site (from 0 to 1 apfu):				
Na	0.180	0.000	0.179	0.000
Ba	0.001	0.002	0.001	0.001
K	0.150	0.000	0.150	0.000
A subtotal	**0.331**	**0.002**	**0.330**	**0.001**
W site (ideally 2 apfu):				
OH	1.922	1.995	1.973	1.995
Cl	0.026	0.005	0.027	0.005
O	0.051	0.000	0.000	0.000
W subtotal	**1.999**	**2.000**	**2.000**	**2.000**
Sum T,C,B,A	**15.331**	**14.998**	**15.331**	**14.996**
Species	ferro-ferri-hornblende	grunerite	ferro-ferri-hornblende	grunerite

APPENDIX E: BIOTITE EPMA DATA

Sample	QC82-45											
Analysis Type	opx incl	opx incl	opx incl	grt incl	grt incl	grt incl	grt incl	grt incl	grt incl	matrix	matrix	matrix
Analysis Pt.	biot-1	biot-2	biot-3	biot 7	biot 11	biot 12	biot 14	biot-16	biot 17	biot 18	biot 21	biot 22
Wt%												
SiO_2	32.53	33.32	32.73	29.04	29.50	28.83	29.07	28.76	28.96	29.32	29.32	28.79
Al_2O_3	13.25	13.18	13.39	13.98	14.17	13.94	14.23	14.12	14.30	14.06	14.22	14.12
TiO_2	4.80	4.93	4.92	4.53	4.98	4.62	5.08	5.04	5.16	5.58	6.27	6.29
Cr_2O_3	0.03	0.09	0.15	0.00	0.00	0.00	0.00	0.00	0.00	0.00	0.00	0.00
FeO	30.70	30.74	30.08	29.91	30.29	30.42	29.04	30.26	29.80	29.29	29.41	29.08
MnO	0.14	0.14	0.13	0.12	0.14	0.11	0.20	0.16	0.10	0.09	0.10	0.11
MgO	3.72	4.25	4.02	3.71	3.25	3.13	3.96	2.93	2.95	3.05	2.77	2.29
CaO	0.00	0.00	0.00	0.03	0.03	0.04	0.11	0.06	0.01	0.00	0.01	0.02
BaO	2.95	1.90	3.00	9.50	8.90	10.21	9.88	9.81	10.49	9.44	9.74	9.65
Na_2O	0.06	0.05	0.09	0.05	0.04	0.03	0.05	0.02	0.03	0.03	0.03	0.00
K_2O	8.18	8.45	7.96	5.58	5.73	5.42	5.38	5.45	5.48	5.80	5.60	5.47
F	0.10	0.34	0.28	0.30	0.11	0.09	0.32	0.17	0.09	0.00	0.08	0.10
Cl	1.75	1.58	1.76	2.86	2.32	2.76	2.64	2.66	2.66	2.58	2.58	2.74
H_2O (calculated)	3.15	3.14	3.08	2.61	2.88	2.72	2.69	2.71	2.77	2.85	2.83	2.72
Subtotal	101.36	102.11	101.59	102.22	102.34	102.32	102.65	102.15	102.80	102.09	102.96	101.38
O=F,Cl	0.44	0.50	0.52	0.77	0.57	0.66	0.73	0.67	0.64	0.58	0.62	0.66
Total	100.92	101.61	101.08	101.45	101.77	101.66	101.92	101.48	102.16	101.50	102.35	100.72
Structural formula (in apfu) based on 24 anions												
T (iv) site:												
Si	5.360	5.398	5.361	5.006	5.029	4.995	4.967	4.971	4.977	5.022	4.983	4.983
Al	2.573	2.516	2.585	2.840	2.847	2.846	2.865	2.877	2.896	2.838	2.848	2.880
Site total	7.934	7.914	7.946	7.847	7.876	7.841	7.832	7.848	7.874	7.861	7.831	7.863

Al (total)	2.573	2.516	2.585	2.840	2.847	2.846	2.865	2.877	2.896	2.838	2.848	2.880
R (vi) site:												
Ti	0.595	0.601	0.606	0.587	0.638	0.602	0.653	0.655	0.667	0.719	0.801	0.819
Cr	0.004	0.012	0.019	0.000	0.000	0.000	0.000	0.000	0.000	0.000	0.000	0.000
Fe^{2+}	4.231	4.164	4.121	4.312	4.318	4.408	4.149	4.374	4.283	4.196	4.180	4.209
Mn^{2+}	0.020	0.019	0.018	0.018	0.020	0.016	0.029	0.023	0.015	0.013	0.014	0.016
Mg	0.914	1.026	0.982	0.953	0.826	0.808	1.009	0.755	0.756	0.779	0.702	0.591
Vacancy	0.237	0.178	0.254	0.130	0.197	0.166	0.160	0.192	0.280	0.293	0.302	0.366
Site total	6.000	6.000	6.000	6.000	6.000	6.000	6.000	6.000	6.000	6.000	6.000	6.000
A (xii) site:												
Ca	0.000	0.000	0.000	0.006	0.005	0.007	0.020	0.011	0.002	0.000	0.002	0.004
Ba	0.190	0.121	0.193	0.642	0.595	0.693	0.661	0.664	0.706	0.634	0.649	0.654
Na	0.019	0.016	0.029	0.017	0.013	0.010	0.017	0.007	0.010	0.010	0.010	0.000
K	1.720	1.746	1.663	1.227	1.246	1.198	1.173	1.202	1.201	1.267	1.214	1.208
Vacancy	0.071	0.117	0.115	0.109	0.141	0.091	0.129	0.116	0.080	0.089	0.125	0.134
Site total	2.000	2.000	2.000	2.000	2.000	2.000	2.000	2.000	2.000	2.000	2.000	2.000
X (anion) site:												
OH	3.459	3.392	3.366	3.001	3.270	3.140	3.063	3.128	3.176	3.251	3.214	3.142
F	0.052	0.174	0.145	0.164	0.059	0.049	0.173	0.093	0.049	0.000	0.043	0.055
Cl	0.489	0.434	0.489	0.836	0.670	0.810	0.764	0.779	0.775	0.749	0.743	0.804
Site total	4.000	4.000	4.000	4.000	4.000	4.000	4.000	4.000	4.000	4.000	4.000	4.000

Sample	QC82-45											
Analysis Type	grt incl	opx incl	matrix	matrix	opx incl	qz incl	matrix	matrix	matrix	grt incl	opx incl	grt incl
Analysis Pt.	biot 23	biot 26	biot 27	biot 30	biot 31	biot 36	biot 37	biot 38	biot 39	biot 40	biot 42	biot 44
Wt%												
SiO_2	28.28	29.82	29.60	30.16	30.58	29.85	29.13	29.03	29.24	28.46	30.13	30.64
Al_2O_3	14.43	13.91	13.90	13.93	13.88	14.29	14.05	14.04	14.08	13.96	13.91	13.47
TiO_2	4.69	6.45	5.99	6.53	5.84	5.82	5.66	5.71	5.52	4.05	6.28	5.36
FeO	30.64	29.30	28.55	29.17	29.37	28.10	30.22	29.63	28.83	30.55	28.92	29.24

MnO	0.11	0.09	0.10	0.11	0.10	0.14	0.10	0.09	0.10	0.16	0.11	0.08
MgO	2.54	3.10	3.23	3.10	3.96	3.65	2.80	3.01	3.54	2.93	3.26	3.88
NiO	0.00	0.00	0.00	0.06	0.00	0.06	0.03	0.00	0.00	0.00	0.00	0.00
CaO	0.03	0.01	0.01	0.01	0.01	0.01	0.02	0.01	0.02	0.04	0.01	0.03
BaO	10.52	8.38	8.56	7.64	7.25	8.44	9.44	9.88	9.38	10.27	7.30	6.84
Na_2O	0.04	0.04	0.07	0.05	0.05	0.05	0.03	0.05	0.04	0.03	0.03	0.03
K_2O	5.10	6.58	6.29	6.81	6.93	6.18	6.07	5.93	5.98	5.63	6.85	7.15
F	0.00	0.00	0.08	0.16	0.07	0.17	0.19	0.09	0.12	0.06	0.00	0.12
Cl	2.85	2.58	2.59	2.54	2.26	1.98	2.51	2.49	2.52	3.39	2.25	2.10
H_2O (calculated)	2.71	2.91	2.82	2.86	3.00	2.96	2.78	2.83	2.81	2.53	2.99	2.97
Subtotal	101.94	103.17	101.79	103.13	103.30	101.70	103.03	102.79	102.18	102.06	102.04	101.91
O=F,Cl	0.64	0.58	0.62	0.64	0.54	0.52	0.65	0.60	0.62	0.79	0.51	0.52
Total	101.30	102.58	101.17	102.49	102.76	101.19	102.39	102.19	101.56	101.27	101.53	101.39
Structural formula (in apfu) based on 24 anions												
T (iv) site:												
Si	4.935	5.021	5.048	5.053	5.083	5.046	4.976	4.969	4.998	4.992	5.071	5.155
Al	2.968	2.760	2.794	2.750	2.719	2.847	2.829	2.832	2.837	2.886	2.759	2.671
Site total	7.903	7.781	7.842	7.803	7.802	7.894	7.805	7.802	7.835	7.878	7.831	7.826
Al (total)	2.968	2.760	2.794	2.750	2.719	2.847	2.829	2.832	2.837	2.886	2.759	2.671
R (vi) site:												
Ti	0.615	0.817	0.768	0.823	0.730	0.740	0.727	0.735	0.710	0.534	0.795	0.678
Fe^{2+}	4.471	4.126	4.072	4.087	4.083	3.973	4.317	4.242	4.122	4.481	4.071	4.114
Mn^{2+}	0.016	0.013	0.014	0.016	0.014	0.020	0.014	0.013	0.014	0.024	0.016	0.011
Mg	0.661	0.778	0.821	0.774	0.981	0.920	0.713	0.768	0.902	0.766	0.818	0.973
Ni	0.000	0.000	0.000	0.008	0.000	0.008	0.004	0.000	0.000	0.000	0.000	0.000
Vacancy	0.236	0.267	0.324	0.293	0.192	0.339	0.224	0.242	0.252	0.195	0.301	0.223
Site total	6.000	6.000	6.000	6.000	6.000	6.000	6.000	6.000	6.000	6.000	6.000	6.000
A (xii) site:												
Ca	0.006	0.002	0.002	0.002	0.002	0.002	0.004	0.002	0.004	0.008	0.002	0.005
Ba	0.719	0.553	0.572	0.502	0.472	0.559	0.632	0.663	0.628	0.706	0.481	0.451
Na	0.014	0.013	0.023	0.016	0.016	0.016	0.010	0.017	0.013	0.010	0.010	0.010
K	1.135	1.413	1.368	1.455	1.470	1.333	1.323	1.295	1.304	1.260	1.471	1.535
Vacancy	0.126	0.019	0.035	0.025	0.040	0.090	0.032	0.024	0.051	0.017	0.036	0.000

Site total	2.000	2.000	2.000	2.000	2.000	2.000	2.000	2.000	2.000	2.000	2.000	2.001
X (anion) site:												
OH	3.157	3.264	3.208	3.194	3.327	3.342	3.171	3.229	3.205	2.959	3.358	3.337
F	0.000	0.000	0.043	0.085	0.037	0.091	0.103	0.049	0.065	0.033	0.000	0.064
Cl	0.843	0.736	0.749	0.721	0.637	0.567	0.727	0.722	0.730	1.008	0.642	0.599
Site total	4.000	4.000	4.000	4.000	4.000	4.000	4.000	4.000	4.000	4.000	4.000	4.000

Sample	QC82-45										
Analysis Type	by amph	matrix	opx incl	opx incl	opx incl	matrix	matrix	matrix	matrix	matrix	matrix
Analysis Pt.	biot 45	biot 48	biot 1	biot 2	biot 3	biot 4	biot 5	biot 6	biot 19	biot 20	biot 21
Wt%											
SiO_2	30.15	30.14	29.80	29.69	29.94	29.98	29.88	29.72	29.84	29.75	29.52
Al_2O_3	13.68	13.79	13.31	13.24	13.36	13.40	13.42	13.37	13.63	13.66	13.72
TiO_2	4.93	5.50	6.83	6.85	6.88	6.33	6.36	6.51	6.23	6.24	6.29
Cr_2O_3	0.00	0.00	0.00	0.00	0.00	0.01	0.04	0.01	0.07	0.11	0.12
FeO	29.71	29.16	29.15	29.08	29.00	29.18	29.44	29.21	28.45	28.26	28.48
MnO	0.08	0.05	0.08	0.12	0.09	0.07	0.07	0.07	0.08	0.06	0.07
MgO	3.25	3.59	2.96	2.90	2.87	2.95	3.02	2.95	3.21	3.17	3.13
NiO	0.00	0.00	0.03	0.02	0.04	0.04	0.05	0.02	0.06	0.03	0.00
CaO	0.04	0.01	0.00	0.00	0.00	0.00	0.00	0.02	0.00	0.00	0.00
BaO	7.61	7.73	8.40	8.20	8.46	8.59	8.60	8.54	8.49	8.55	8.66
Na_2O	0.03	0.04	0.06	0.03	0.05	0.05	0.04	0.03	0.04	0.08	0.07
K_2O	6.70	6.74	6.52	6.40	6.35	6.28	6.13	6.29	6.18	6.17	6.30
F	0.12	0.13	0.09	0.03	0.07	0.03	0.07	0.06	0.04	0.07	0.07
Cl	2.63	2.38	2.51	2.46	2.51	2.44	2.53	2.44	2.52	2.52	2.51
H_2O (calculated)	2.79	2.88	2.86	2.88	2.87	2.90	2.86	2.87	2.86	2.84	2.84

Subtotal	101.72	102.14	102.60	101.90	102.49	102.25	102.51	102.11	101.70	101.51	101.78
O=F,Cl	0.64	0.59	0.60	0.57	0.60	0.56	0.60	0.58	0.59	0.60	0.60
Total	101.08	101.55	101.99	101.33	101.89	101.68	101.91	101.54	101.12	100.91	101.19
Structural formula (in apfu) based on 24 anions											
T (iv) site:											
Si	5.142	5.097	5.051	5.057	5.071	5.093	5.071	5.061	5.080	5.075	5.038
Al	2.750	2.749	2.659	2.658	2.667	2.683	2.684	2.683	2.735	2.746	2.759
Site total	7.892	7.846	7.710	7.714	7.737	7.776	7.755	7.744	7.815	7.822	7.797
Al (total)	2.750	2.749	2.659	2.658	2.667	2.683	2.684	2.683	2.735	2.746	2.759
R (vi) site:											
Ti	0.632	0.699	0.871	0.877	0.876	0.809	0.812	0.834	0.798	0.801	0.807
Cr	0.000	0.000	0.000	0.000	0.000	0.001	0.005	0.001	0.009	0.015	0.016
Fe^{2+}	4.238	4.124	4.132	4.142	4.107	4.146	4.178	4.160	4.050	4.032	4.064
Mn^{2+}	0.012	0.007	0.011	0.017	0.013	0.010	0.010	0.010	0.012	0.009	0.010
Mg	0.826	0.905	0.748	0.736	0.725	0.747	0.764	0.749	0.815	0.806	0.796
Ni	0.000	0.000	0.004	0.003	0.005	0.005	0.007	0.003	0.008	0.004	0.000
Vacancy	0.292	0.264	0.234	0.224	0.273	0.281	0.224	0.243	0.308	0.334	0.306
Site total	6.000	6.000	6.000	6.000	6.000	6.000	6.000	6.000	6.000	6.000	6.000
A (xii) site:											
Ca	0.007	0.002	0.000	0.000	0.000	0.000	0.000	0.004	0.000	0.000	0.000
Ba	0.509	0.512	0.558	0.547	0.561	0.572	0.572	0.570	0.566	0.572	0.579
Na	0.010	0.013	0.020	0.010	0.016	0.016	0.013	0.010	0.013	0.026	0.023
K	1.458	1.454	1.410	1.391	1.372	1.361	1.327	1.366	1.342	1.343	1.372
Vacancy	0.016	0.019	0.012	0.052	0.050	0.051	0.088	0.050	0.078	0.059	0.026
Site total	2.000	2.000	2.000	2.000	2.000	2.000	2.000	2.000	2.000	2.000	2.000
X (anion) site:											
OH	3.175	3.248	3.231	3.274	3.242	3.281	3.235	3.263	3.251	3.234	3.236
F	0.065	0.070	0.048	0.016	0.037	0.016	0.038	0.032	0.022	0.038	0.038
Cl	0.760	0.682	0.721	0.710	0.720	0.703	0.728	0.704	0.727	0.729	0.726
Site total	4.000	4.000	4.000	4.000	4.000	4.000	4.000	4.000	4.000	4.000	4.000

Sample	QC81-113			HP81-82			QC81-1	HR02-72
Analysis Type	opx incl	opx incl	opx incl	core	rim	matrix	biot	matrix
Analysis Pt.	biot-1	biot-2	biot-3	biot-1	biot-2	biot-3	1	biot-2
Wt%								
SiO_2	32.98	33.28	33.37	35.24	35.29	35.11	33.51	34.84
Al_2O_3	15.05	15.05	15.11	14.34	14.25	13.93	15.56	15.19
TiO_2	1.07	1.02	0.00	4.67	4.53	4.44	3.85	3.01
Cr_2O_3	0.02	0.02	0.02	0.10	0.04	0.03	0.01	0.01
FeO	27.18	27.14	27.14	24.21	24.29	23.62	24.38	23.52
MnO	0.13	0.13	0.13	0.02	0.04	0.05	0.07	0.05
MgO	6.56	6.66	6.76	8.72	8.41	8.56	7.58	8.49
NiO	0.03	0.02	0.00	0.00	0.02	0.01	0.00	0.00
CaO	0.05	0.03	0.03	0.00	0.00	0.00	0.01	0.01
BaO	2.83	2.90	2.78	0.00	0.00	0.00	0.00	0.64
Na_2O	0.09	0.08	0.09	0.05	0.06	0.04	0.11	0.13
K_2O	8.01	8.18	8.18	9.87	9.88	9.74	9.64	9.20
F	0.02	0.07	0.05	0.08	0.06	0.10	0.00	0.00
Cl	2.38	2.41	2.37	0.26	0.24	0.25	0.42	0.16
H_2O (calculated)	3.02	3.01	2.99	3.78	3.78	3.72	3.66	3.77
Subtotal	99.42	100.00	99.02	101.34	100.89	99.60	98.80	99.02
O=F,Cl	0.55	0.57	0.56	0.09	0.08	0.10	0.09	0.04
Total	98.87	99.42	98.47	101.25	100.81	99.50	98.71	98.98
Structural formula (in apfu) based on 24 anions								
T (iv) site:								
Si	5.447	5.466	5.529	5.437	5.472	5.503	5.329	5.487
Al	2.553	2.534	2.471	2.563	2.528	2.497	2.671	2.513
Site total	8.000	8.000	8.000	8.000	8.000	8.000	8.000	8.000
Al (total)	2.930	2.913	2.950	2.608	2.604	2.573	2.916	2.819
R (vi) site:								

Al	0.377	0.380	0.479	0.045	0.076	0.076	0.245	0.306
Ti	0.133	0.126	0.000	0.542	0.528	0.523	0.460	0.356
Cr	0.003	0.003	0.003	0.012	0.005	0.004	0.001	0.001
Fe^{2+}	3.754	3.728	3.760	3.124	3.150	3.096	3.242	3.098
Mn^{2+}	0.018	0.018	0.018	0.003	0.005	0.007	0.009	0.007
Mg	1.615	1.631	1.670	2.006	1.944	2.000	1.797	1.993
Ni	0.004	0.003	0.000	0.000	0.002	0.001	0.000	0.000
Vacancy	0.096	0.112	0.070	0.268	0.290	0.294	0.245	0.238
Site total	6.000	6.000	6.000	6.000	6.000	6.000	6.000	6.000
A (xii) site:								
Ca	0.009	0.005	0.005	0.000	0.000	0.000	0.002	0.001
Ba	0.183	0.187	0.180	0.000	0.000	0.000	0.000	0.039
Na	0.029	0.025	0.029	0.015	0.018	0.012	0.034	0.041
K	1.688	1.714	1.729	1.943	1.954	1.947	1.956	1.848
Vacancy	0.091	0.069	0.056	0.042	0.028	0.040	0.009	0.071
Site total	2.000	2.000	2.000	2.000	2.000	2.000	2.000	2.000
X (anion) site:								
OH	3.323	3.293	3.308	3.893	3.908	3.884	3.887	3.957
F	0.010	0.036	0.026	0.039	0.029	0.050	0.000	0.000
Cl	0.666	0.671	0.665	0.068	0.063	0.066	0.113	0.043
Site total	4.000	4.000	4.000	4.000	4.000	4.000	4.000	4.000

VITA

Nicholas Daigle was born and raised in Metairie, Louisiana and graduated from Jesuit High School in 2009 before beginning his undergraduate career at Louisiana State University. Initially accepted as an anthropology major, he fell in love with the geosciences and decided to switch majors in his third semester after completing the first two introductory courses. Three years later he graduated with a B.S. from LSU and immediately began working on his M.S. degree in metamorphic petrology with Dr. Darrell Henry.

During his time at LSU, Nick was a member of the Geological Society of America (GSA), Mineralogical Society of America (MSA), LSU AAPG Student Chapter, Volunteer LSU and International Student Volunteers (ISV). While acquiring his M.S., he held a research assistantship position for which he served as the technician for the microprobe at LSU. In his spare time, he enjoys long distance running and biking, volunteering, eating, drinking and binge-watching Netflix.